Histochemical characterization of inputs to motoneurons of extraocular muscles subserving different functions. An immunohistochemical study in primate.

Dissertation zur Erlangung des Grades eines Doktors der Naturwissenschaften
der Fakultät für Biologie
der Ludwig-Maximilians-Universität München

vorgelegt von Christina Zeeh geb. Schulze

aus München

1. Gutachter: Prof. Dr. Anja Horn-Bochtler
2. Gutachter: Prof. Dr. Hans Straka

Eingereicht: 18.08.2015
Tag der mündlichen Prüfung: 02.03.2016


„Die Sonne sank,
bevor es Abend wurde."
Martina
1972–2015

Eidesstattliche Erklärung

Ich erkläre hiermit an Eides statt, dass ich die vorliegende Dissertation selbstständig und ohne unerlaubte Beihilfe angefertigt habe. Die aus fremden Quellen direkt oder indirekt übernommenen Gedanken sind als solche kenntlich gemacht und nach ihrer Herkunft unter Bezeichnung der Fundstelle einzeln nachgewiesen.

Die Arbeit wurde bisher keiner anderen Prüfungsbehörde vorgelegt.

München, den 17.08.2015

List of Publications

- Horn AKE, **Schulze C**, Radtke-Schuller S. 2009.
  The Edinger-Westphal nucleus represents different functional cell groups in different species. Ann N Y Acad Sci 1164:45-50.

- **Zeeh C** and Horn AKE. 2012.
  Der Okulomotoriuskern und seine Subnuclei beim Menschen. Kli Monatsbl Augenheilkd 229:1-7.

- **Zeeh C**, Hess BJM, Horn AKE. 2013.
  Calretinin inputs are confined to motoneurons for upward eye movements in Monkey. J Comp Neurol 521:3154-3166.

- Che-Ngwa E, **Zeeh C**, Messoudi A, Büttner-Ennever JA, Horn AKE. 2014.
  Delineation of motoneuron subgroups supplying individual eye muscles in the human oculomotor nucleus. Front Neuroanat, 8:2,
  DOI: 10.3389/fnana.2014.00002.

- **Zeeh C**, Mustari MJ, Hess BJM, Horn AKE. 2015.
  Transmitter input to different motoneuron subgroups in the oculomotor and trochlear nucleus in monkey. Front Neuroanat,
  DOI:10.3389/fnana.2015.00095.

List of Conference Contributions

- **Schulze C** and Horn AKE. 2007.
  Functional cell groups of the oculomotor nucleus complex in the rat.
  Neuroforum, Februar Vol. XIII (1), Neurowissenschaftliche Gesellschaft.

- **Schulze C**, Rothermel M, Lienbacher K, Curie T, Klupp BG, Mettenleiter TC, Distler C, Hatt H, Hoffmann K-P, Horn AKE. 2009.
  Transsynaptic retrograde labelling in the oculomotor system in rodent using tetanus toxin fragment C and Pseudorabies virus: opportunities and limitations. Neuroforum, Februar Vol. XV (1), Neurowissenschaftliche Gesellschaft.

- **Schulze C**, Mustari MJ, Holstein GR, Horn AKE. 2009.
  Transmitter inputs to different motoneuron subgroups in the oculomotor and trochlear nucleus in monkey. Soc Neurosci Abstr 356.9 Z19, Society for Neuroscience, Annual Meeting.

- **Zeeh C**, Hess BJM, Chen-Ngwa E, Feige JM, Horn AKE. 2013.
  Calretinin inputs are confined to motoneurons for upward eye movements in primates. Neuroforum, Februar Vol. XIX (1), Neurowissenschaftliche Gesellschaft.

- Feige JM, **Zeeh C**, Roeber G, Arzberger T, Kretzschmar H, Horn AKE. 2013.
  Tau pathology in motoneurons of extraocular muscles in progressive supranuclear palsy (PSP). Anatomentagung in Magdeburg.

- **Zeeh C**, Ahlfeld J, Mustari MJ, Horn AKE. 2013.
  Calretinin as a marker for upgaze pathways in the oculomotor system. Anatomische Gesellschaft, Würzburg.

List of Contributions

The Edinger-Westphal nucleus represents different functional cell groups in different species.

Horn AKE, **Schulze C**, Radtke-Schuller S. 2009.

Ann N Y Acad Sci 1164:45-50.

Contribution of Christina Zeeh (formerly Schulze):

- Acquisition, analysis and interpretation of rat data.
- Immunolabelling of rat sections (choline acetyltransferase, urocortin).
- Preparation of Fig. 1 A, B: "Transverse sections through the nIII of rat stained for choline acetyltransferase (ChAT) or urocortin (UCN)."
- Preparation of Fig. 3 A: "Plots of transverse sections through the oculomotor (nIII) and Edinger-Westphal nucleus of rat."
- Writing and revising, together with all other authors.
- Conception of the work together with AKE Horn.

Date, place:

Signature of Christina Zeeh: Signature of Prof. Dr. Anja Horn-Bochtler (Supervisor):

Contribution of S. Radtke-Schuller and AKE. Horn:

Acquisition, analysis and interpretation of ferret data, immunolabelling of ferret sections and preparation of figures were performed by S. Radtke-Schuller. Acquisition, analysis and interpretation of human and monkey data, immunolabelling of human and monkey sections and preparation of figures were performed by AKE. Horn. Writing and revising, together with all other authors.

Calretinin inputs are confined to motoneurons for upward eye movements in Monkey.

Zeeh C, Hess BJM, Horn AKE. 2013.

J Comp Neurol 521:3154-3166.

Constribution of Christina Zeeh:

- Acquisition (including tracer injections), analysis and interpretation of data.
- Immunolabelling of all sections.
- Quantification of the Calretinin input to all motoneuron subgroups.
- Counting of Calretinin-immunoreactive puncta of all motoneuron subgroups.
- Performance of the statistical analysis, evaluation and interpretation of the data.
- Preparation of all figures and tables.
- Writing and revising, together with all other authors.
- Conception of the work together with AKE Horn.

Contribution of BJM. Hess and AKE. Horn:

Animals have been operated in the facilities of BJM. Hess, who participated in the surgery. Writing and revising, together with all other authors.

Transmitter input to different motoneuron subgroups in the oculomotor and trochlear nucleus in monkey.

Zeeh C, Mustari MJ, Hess BJM, Horn AKE. 2015.

Front Neuroanat, DOI:10.3389/fnana.2015.00095.

Constribution of Christina Zeeh:

- Acquisition (including tracer injections), analysis and interpretation of data.
- Immunolabelling of all sections.
- Quantification of the transmitter input to all motoneuron subgroups.
- Counting of Calretinin-immunoreactive puncta of all motoneuron subgroups.
- Performance of the statistical analysis, evaluation and interpretation of the data.
- Preparation of all figures and tables.
- Writing and revising, together with all other authors.
- Conception of the work together with AKE. Horn.

Contribution of BJM. Hess, MJ. Mustari and AKE. Horn:

Animals have been operated in the facilities of BJM. Hess and MJ. Mustari. BJM. Hess participated in the surgery, and MJ. Mustari performed the surgery and injection of one animal. Writing and revising, together with all other authors.

Delineation of motoneuron subgroups supplying individual eye muscles in the human oculomotor nucleus.

Che-Ngwa E, **Zeeh C**, Messoudi A, Büttner-Ennever JA, Horn AKE. 2014.

Front Neuroanat, 8:2, DOI: 10.3389/fnana.2014.00002.

Contribution of Christina Zeeh:

- Quantification of the transmitter input to all motoneuron subgroups.
- Counting of immunoreactive puncta of all motoneuron subgroups.
- Performance of the statistical analysis, evaluation and interpretation of the data.
- Preparation of figure 7: "Histogram of the quantitative analysis of GABAergic and calretinin (CR) input to motoneurons in the oculomotor and trochlear nucleus."
- Preparation of table 3: "Quantification of calretinin and GABAergic input to nIV and nIII subgroups."
- Writing and revising, together with all other authors.

Date, place:

Signature of Christina Zeeh: Signature of Prof. Dr. Anja Horn-Bochtler (Supervisor):

Contribution of E. Che-Ngwa, A. Messoudi, JA. Büttner-Ennever and AKE: Horn:

Acquisition and analysis of data was done by E. Che-Ngwa. Immunolabelling of human sections was done by E. Che-Ngwa and A. Messoudi. Conception of the work was done by AKE. Horn and JA. Büttner-Ennever. All authors contributed to the interpretation of data, preparation of figures, writing of the manuscript and approved the final version.

Table of contents

Abbreviations

AchR	acetylcholine receptor
AD	averaged density
AMPA	alpha-amino-3-hydroxy-5-methyl-4-isoxazolepropionic acid
ATD	ascending tract of Deiters
CCN	central caudal nucleus
CEN	central group
ChAT	choline acetyltransferase
cMRF	central mesencephalic reticular formation
CR	calretinin
CTB	Cholera toxin subunit B
CVTT	ventral tegmental tract
DAB	3, 3` Diaminobenzidine
DL	dorsolateral group
DM	dorsomedial group
DR	dorsal raphe nucleus
EAP	extravidin-peroxidase
EBN	excitatory burst neuron
EOM	extraocular muscle
EPSP	excitatory postsynaptic potential
EW	Edinger-Westphal nucleus
EWcp	non-preganglionic centrally projecting EW
EWpg	EW preganglionic
GABA	gamma-aminobutyric acid
GABA-A	GABA-A receptor
GAD	glutamate decarboxylase
GLU	glutamate

Gly	glycine
GlyR	glycine receptor
HRP	horseradish peroxidase
IBN	inhibitory burst neuron
IC	inferior colliculus
INT	internuclear neuron
INC	interstitial nucleus of Cajal
IO	inferior oblique muscle
IPN	interpeduncular nucleus
IR	inferior rectus muscle
LP	levator palpebrae muscle
LR	lateral rectus muscle
MGB	medial geniculate body
MIF	multiply innervated muscle fiber
ML	medial lemniscus
MLF	medial longitudinal fascicle
MR	medial rectus muscle
MVN	medial vestibular nucleus
MVNm	MVN magocellular part
MVNp	MVN parvocellular part
NIII	oculomotor nerve
nIII	oculomotor nucleus
NIV	trochlear nerve
nIV	trochlear nucleus
NVI	abducens nerve
nVI	abducens nucleus

NVIII	facial nerve
NMDA	N-methyl-$_D$-aspartate
NOT	nucleus of the optic tract
NP	nucleus of Perlia
NP-NF	non-phosphorylated neurofilament
NPC	Niemann-Pick disease type C
NPO	pretectal olivary nucleus
OKR	optokinetic response
pIII	perioculomotor region
$pIII_{PG}$	preganglionic neurons in the pIII
$pIII_{UCN}$	UCN-positive neurons in the pIII
PAG	periaqueductal gray
PV	parvalbumin
PB	phosphate buffer
PG	preganglionic neurons
PN	pontine nuclei
PPH	nucleus prepositus hypoglossi
PPRF	paramedian pontine reticular formation
PSP	progressive supranuclear palsy
RIMLF	rostral interstitial nucleus of the medial longitudinal fascicle
RN	red nucleus
SC	superior colliculus
SCP	superior cerebellar peduncle
SEM	standard error of the mean
SIF	singly innervated muscle fiber
SNc	substantia nigra pars compacta

SNr	substantia nigra pars reticulata
SO	superior oblique muscle
SOA	supraoculomotor area
SPEM	smooth pursuit eye movements
SR	superior rectus muscle
SVN	superior vestibular nucleus
SVNm	SVN magnocellular part
TBS	tris buffer
UCN	urocortin
VEN	ventral group
vGlut	vesicular glutamate transporter
vLVN	ventral part of the lateral vestibular nucleus
VOR	vestibulo-ocular reflex
WGA	wheat germ agglutinin
WGA-HRP	WGA conjugated to horseradish peroxidase

1 Abstract

Eye movements are important to aid vision, and they serve two main functions: to stabilize a moving visual target on the retina and to stabilize gaze during own body movements. Six types of eye movements have been evolved fulfilling this function: saccades, smooth pursuit, vestibulo-ocular reflex, optokinetic response, convergence and gaze holding. In all vertebrates the eyes are moved by six pairs of extraocular muscles that enable horizontal, vertical and rotatory eye movements. The motoneurons of these muscles are located in the oculomotor (nIII), trochlear (nIV) and abducens (nVI) nucleus in the brainstem. Motoneurons of the lateral rectus muscle (LR) in nVI and of the medial rectus muscle (MR) in nIII provide horizontal eye movements, those of inferior oblique (IO) and superior rectus muscle (SR) in nIII upward eye movements. Motoneurons of the superior oblique (SO) and the inferior rectus muscle (IR) in nIII convey downward eye movements. Recently, it was shown that each extraocular muscle is controlled by two motoneuronal groups:

1. Motoneurons of singly innervated muscle fibers (SIF) that lie within the boundaries of motonuclei providing a fast muscle contraction (twitch) and 2. motoneurons of multiply innervated muscle fibers (MIF) in the periphery of motonuclei providing a tonic muscle contraction (non-twitch). Tract-tracing studies indicate that both motoneuronal groups receive premotor inputs from different brainstem areas. A current hypothesis suggests that pathways controlling twitch motoneurons serve to generate eye movements, whereas the non-twitch system is involved in gaze holding. Lesions of inputs to the twitch motoneuron system may lead to supranuclear gaze palsies, whereas impairment of the non-twitch motoneuron system may result in gaze holding deficits, like nystagmus, or strabismus. Up to date only limited data are available about the histochemical characteristics including transmitters to the SIF- (twitch) and MIF (non-twitch) motoneurons.

The present study was undertaken to investigate the histochemical profile of inputs to motoneuronal groups of individual eye muscles mediating horizontal and vertical eye movements including the inputs to MIF- and SIF motoneurons. The MIF motoneurons of the IR and MR are located in the periphery dorsolateral to nIII, close to the Edinger-Westphal nucleus (EW), which is known to contain preganglionic cholinergic neurons. Other scientists have found that the EW is composed of urocortin-positive neurons involved in food intake or stress. In order to delineate these different cell

populations within the supraoculomotor area dorsal to nIII, a comparative study in different mammals was conducted to locate the cholinergic preganglionic neurons and urocortin-positive neurons. Only then, it became obvious that the cytoarchitecturally defined EW labels different cell populations in different species. In rat, ferret and human the cytoarchitecturally defined EW is composed of urocortin-positive neurons. Only in monkey the EW contains cholinergic preganglionic neurons, which lie close to the MIF-motoneurons of MR and IR in the C-group.

In monkey, I performed a systematic study on the histochemical profile and transmitter inputs to the different motoneuron subgroups, including MIF- and SIF motoneurons. Brainstem sections containing prelabelled motoneurons were immunostained for the calcium-binding protein calretinin (CR), gamma-aminobutyric acid (GABA) or glutamate decarboxylase (GAD), glycine transporter 2, glycine receptor 1, and the vesicular glutamate transporters (vGlut) 1 and 2.

The study on the histochemical profile of the motoneuron inputs revealed three main results: 1.The inhibitory control of SIF motoneurons for horizontal and vertical eye movements differs. Unlike previous studies in the primate a considerable GABAergic input was found to all SIF motoneuronal groups, but a glycinergic input was confined to motoneurons of the MR mediating horizontal eye movements. 2. The excitatory inputs to motoneurons for upgaze and downgaze differ in their histochemistry. A striking finding was that CR-positive nerve endings were confined to the motoneurons of muscles involved in upgaze, e.g. SR, IO and the levator palpebrae, which elevates the upper eyelid and acts in synchrony with the SR. Since double-immunoflourescence labelling with anti-GAD did not reveal any colocalization of GAD and CR, the CR-input to upgaze motoneurons is considered as excitatory. 3. The histochemistry of MIF- and SIF motoneurons differs only for vGlut1. Whereas SIF- and MIF motoneurons of individual eye muscles do not differ in their GABAergic, glycinergic and vGlut2 input, vGlut1 containing terminals were covering the supraoculomotor area and targeting only MR MIF motoneurons. It is reasonable to assume that the vGlut1 input affects the near response system in the supraoculomotor area, which houses the preganglionic neurons in the EW mediating pupillary constriction and accommodation and the MR MIF motoneurones involved in vergence.

The histochemical data in monkey enabled the localization of the corresponding motoneuronal subgroups of individual eye muscles in human with the development of an updated nIII map.

Taken together the present work provides new data on the histochemical properties of premotor inputs to motoneuronal groups of the twitch- and non-twitch eye muscle systems in primates. Especially the selective association of CR in premotor upgaze pathways may open the possibility for a targeted research of this system in human post-mortem studies of clinical cases with impairment of upward eye movements, such as progressive supranuclear palsy (PSP) or Niemann-Pick disease (NPC).

1.1 Zusammenfassung

Augenbewegungen sind essenziell um ein ungestörtes Sehen zu garantieren. Dabei sind zwei Hauptfunktionen entscheidend: Die Stabilisierung eines sich bewegenden Objekts auf der Retina und das Stabilisieren des Blickes während einer Bewegung. Zur Erfüllung dieser Aufgaben dienen sechs verschiedene Augenbewegungstypen: Sakkaden, smooth pursuit, vestibulookulärer Reflex, optokinetische Augenbewegungen, Konvergenz und Fixation.

Um die dafür benötigten horizontalen, vertikalen und rotatorischen Bewegungen des Auges ausführen zu können, besitzen Vertebraten sechs Augenmuskelpaare.

Die Motoneurone der Augenmuskeln liegen in drei Kerngebieten des Hirnstamms: im Nucleus oculomotorius (nIII), im Nucleus trochlearis (nIV) und im Nucleus abducens (nVI).

Der nIII enthält die Motoneurone des Musculus rectus medialis (MR), des Musculus rectus superior (SR), des Musculus inferior obliquus (IO) sowie des Musculus rectus inferior (IR). Die Motoneurone des Musculus obliquus superior (SO) liegen im nIV und die des Musculus rectus lateralis (LR) im nVI. MR und LR führen gemeinsam horizontale Augenbewegungen aus. IO und SR sind in Blickbewegungen nach oben involviert, wohingegen SO und IR die Blickbewegungen nach unten steuern.

Kürzlich wurde gezeigt, dass jeder extraokuläre Muskel durch zwei Gruppen von Motoneuronen kontrolliert wird: 1. Durch Motoneurone der einfach innervierten Muskelfasern (singly innervated muscle fibers, SIF). Sie antworten auf elektrische Stimulierung mit fortgeleiteten Aktionspotentialen und einer schnellen Muskelkontraktion (twitch). 2. Durch Motoneurone der multipel-innervierten Muskelfasern (multiply innervated muscle fibers, MIF). Diese reagieren auf elektrische Reizung nur lokal, ohne fortgeleitete Aktionspotentiale, mit einer langsamen tonischen Kontraktion (non-twitch).

An Primaten konnte gezeigt werden, dass die Motoneurone von SIFs und MIFs räumlich voneinander getrennt liegen. MIF Motoneurone liegen außerhalb der Motokerne in der Peripherie, während sich SIF Motoneurone innerhalb der klassischen Augenmuskelkerne befinden.

Trakt-tracing Studien deuten auch darauf hin, dass diese beiden Motoneuronengruppen prämotorische Eingänge aus unterschiedlichen Hirnstammregionen erhalten.

Eine derzeitige Hypothese besagt, dass Bahnen, welche die twitch Motoneurone kontrollieren für die Generierung der Augenbewegungen verantwortlich sind. Das non-twitch System hingegen ist in die Blickstabilisierung involviert. Läsionen des twitch-Systems können zu supranukleären Blickparesen führen, Beeinträchtigungen des non-twitch Systems wiederum zu Blickstabilisierungsdefiziten, wie Nystagmus oder Strabismus.

Bisher sind nur wenige Daten über die Histochemie, sowie über die Transmittereingänge der SIF- (twitch) und MIF (non-twitch) Motoneurone bekannt.

In der vorliegenden Arbeit wurden die prämotorischen Eingänge auf die Motoneurone, die vertikale und horizontale Augenbewegungen vermitteln, histochemisch untersucht und verglichen, sowie die prämotorischen Eingänge auf die MIF- und SIF Motoneuronen individueller Augenmuskeln.

Die MIF Motoneurone des IR und MR liegen gemeinsam in der C-Gruppe, peripher, dorsolateral zum nIII, nahe des Edinger-Westphal Kerns (EW). Traditionell wird der EW als Sitz der cholinergen präganglionären Neurone angesehen, jedoch wurde gezeigt, dass der EW auch urocortin-positive Neurone enthält. Urocortin ist ein Peptid, das in Verbindung mit Nahrungsaufnahme und Stress steht.

Dorsal zum nIII liegt das supraokulomotorische Areal (SOA), in dem verschiedene Zellgruppen mit unterschiedlichen Funktionen zu finden sind. Um diese Zellpopulationen im SOA lokalisieren und gegeneinander abgrenzen zu können, wurde eine vergleichende Studie in unterschiedlichen Säugetieren durchgeführt. Hier wird deutlich, dass der zytoarchitektonisch definierte EW in verschiedenen Spezies unterschiedliche Zellpopulationen enthält: In der Ratte, dem Frettchen und dem Menschen enthält der zytoarchitektonisch definierte EW urocortin-positive Neurone. Im Affen hingegen finden sich cholinerge präganglionäre Neurone im EW, nahe der C-Gruppe, in der die MIF-Motoneurone des MR und IR liegen.

Auf Grund der räumlichen Nähe wurden im Affen systematisch die histochemischen Profile und Transmittereingänge aller unterschiedlichen Motoneuronensubgruppen, einschließlich MIF- und SIF Motoneurone individueller Augenmuskeln, untersucht. Hierfür wurden Hirnstammschnitte mit vormarkierten Motoneuronen auf folgende Marker histochemisch angefärbt: auf das Calcium-bindende Protein Calretinin (CR), auf Gamma-Aminobuttersäure (GABA) oder Glutamatdecarboxylase (GAD), auf den Glyzintransporter 2, den Glyzinrezeptor 1 sowie auf die vesikulären Glutamat-transporter (vGlut) 1 und 2.

Die Untersuchung der histochemischen Eigenschaften der prämotorischen Eingänge auf die unterschiedlichen Motoneuronengruppen zeigten drei wichtige Ergebnisse:

1. Motoneurone, die bei horizontalen und vertikalen Augenbewegungen involviert sind, werden unterschiedlich inhibitorisch kontrolliert.

2. Motoneurone, die an Blickbewegungen nach oben beteiligt sind, haben andere histochemische Eigenschaften im Vergleich zu Motoneuonen, die bei Blickbewegungen nach unten involviert sind. Hierbei war auffällig, dass CR-positive Nervenendigungen ausschließlich an Motoneuronen zu finden sind, die an Blickbewegungen nach oben beteiligt sind, wie z.B. SR, IO und an Motoneuronen des Musculus levator palpebrae, welcher das Augenlid anhebt und synchron mit dem SR agiert. Nachdem eine Doppelimmunfluoreszenzfärbung mit anti-GAD keine Colokalisation von CR und GAD gezeigt hat, wird davon ausgegangen, dass der CR-Eingang der Motoneurone für Blickbewegungen nach oben exzitatorisch ist.

3. Eine unterschiedliche Histochemie der SIF- und MIF Motoneurone zeigt sich bisher nur in einem vesikulären Glutamattransporter. Die Ergebnisse zeigen: 1. SIF- und MIF Motoneurone individueller Augenmuskeln unterscheiden sich nicht in ihren GABAergen, glyzinergen und vGlut2 Eingängen. 2. VGlut1-positive Terminalen findet man nur im SOA, wo sie ausschließlich die MIF Motoneurone des MR kontaktieren. Man nimmt an, dass die vGlut1 Eingänge auf das Nah-Antwort-Zentrum, das im SOA liegt, Einfluss haben. Im SOA liegen auch die im EW lokalisierten präganglionären Neurone, die Linsenakkomodation und Pupillenreflex vermitteln, sowie die MIF Motoneurone des MR, die bei Vergenzbewegungen beteiligt sind.

Basierend auf den histochemischen Daten des Affens, ist im Menschen eine Lokalisation der korrespondierenden Motoneuronengruppen der einzelnen Augenmuskeln und dadurch auch eine Aktualisierung der bestehenden Karte des menschlichen nIII möglich.

Zusammenfassend liefert die vorliegende Arbeit neue Erkenntnisse über die histochemischen Eigenschaften der prämotorischen Eingänge der Motoneurone des twitch- und non-twitch Augenmuskelsystems im Primaten.

Für weitere Untersuchungen ist besonders der selektive Zusammenhang von CR mit den prämotorischen Bahnen für Blickbewegungen nach oben interessant. Im Menschen können anhand von post-mortem Studien gezielt klinische Fälle, die eine Beeinträchtigung des Blickaufwärtssystems aufweisen, wie z.B. eine progressive

supranukleäre Blickparese (PSP) oder die Niemann-Pick-Krankheit (NPC), untersucht werden.

2 Introduction

2.1 Eye Movements

The basic requirement for clear and accurate visual perception is to hold images steady on the retina and to bring them to the center of the fovea. If we had no eye movements, images would move across the retina during head movement and would cause blurred and unclear vision.

In primates it is possible to distinguish six types of eye movements: The vestibulo-ocular reflex (VOR), the optokinetic response (OKR), smooth pursuit eye movements (SPEM), vergence, saccades and visual fixation (Horn and Leigh, 2011).

The VOR is a slow, compensatory eye movement that stabilizes images during head movements by moving the eye in the opposite direction of the head movement. The VOR is mainly generated by signals arising in the semicircular canals (Büttner and Büttner-Ennever, 2006). Large moving visual fields lead to slow, conjugated eye movements, the optokinetic response. It complements the VOR particularly in the low frequency range, where its gain is low (Robinson, 1981; Büttner and Büttner-Ennever, 2006).

In animals without fovea (e.g. rabbit) eye movements are dominated by the VOR and OKR, which are sufficient to stabilize vision. These two types of eye movements are phylogenetically old and can be found in all vertebrates investigated so far (Highstein and Reisine, 1979; Graf and Baker, 1985; Baker et al., 1998; Fritzsch, 1998; Straka and Dieringer, 2004).

With the evolution of foveal vision, it became necessary to change the line of sight independently of head movements. This has been achieved by saccadic eye movements. Saccades move both eyes rapidly in a conjugate fashion to a new eye position - without movement of the head (Büttner and Büttner-Ennever, 2006). In primate, saccades last between 15 and 100 ms and their velocity can reach 700^{o}/s (Becker, 1989; Büttner and Büttner-Ennever, 2006). They include voluntary and involuntary changes in fixation: Voluntary saccades are made purposefully by the subject. Often they are made in response to an instruction to direct focus towards an object already present in the person's visual environment. An involuntary or reflexive saccade is triggered by the appearance of a new stimulus in the subject's environment.

In afoveal animals, saccades usually occur together with head movements (Leigh and Zee, 2006).

With the evolution of the fovea it became necessary to follow a moving object smoothly. This is possible to a limited degree with saccadic movements; however, the image of the moving target will slide off eventually, with the consequent decline in visual acuity (Leigh and Zee, 2006). The smooth pursuit system however, allows to track small moving targets with the fovea in a fixed visual environment. Smooth pursuit eye movements (SPEM) are voluntary eye movements requiring motivation and attention. Although SPEMs are considered as slow eye movements, they can reach velocities above 100^{o}/s (Lisberger et al., 1981; Simons and Büttner, 1985). Not only the eyes also the head is involved in tracking moving objects. The VOR normally brings the eye to the opposite direction of the head movements, and for this reason has to be suppressed under the condition of SPEMs. One suggested possibility is that smooth pursuit signals cancel and consequently suppress the VOR (Leigh and Zee, 2006; Akao et al, 2007).

Gaze holding or visual fixation allows to hold a stationary object on the fovea when the observer is stationary too, and permits a stable eye position between the eye movements (Büttner and Büttner-Ennever, 2006). With the development of frontal vision it became possible to keep a target in focus on both foveae simultaneously. This requires disconjugated or vergence eye movements. Vergence eye movements are generally small (less than 5^{o}) and slow (latency 150-200ms) (Büttner and Büttner-Ennever, 2006). During natural visual search, vergence eye movements are accompanied by saccades (because in our environment most targets differ in horizontal and vertical direction and in distance), and are much faster (Leigh and Zee, 2006). Vergence eye movements play also an important role in near triad.

2.1.1 Near Triad

The near triad consists of three actions of inner and extraocular muscles: lens accommodation, pupillary constriction and the concomitant activation of vergence. This is helpful to focus on near objects clearer. This action involves the contraction of the medial rectus muscle and the relaxation of the lateral rectus muscle. Lens

accommodation and pupillary constriction is under control of the Edinger-Westphal nucleus (EW).
In order to meet all these different requirements of eye movements – from fast eye movements to accurate visual fixation - it is essential to have eye muscles with a very complex architecture.

2.2 Extraocular muscles

2.2.1 Arrangement and function

The eye of vertebrates is rotated by six extraocular muscles (EOM), four recti (superior-, inferior-, medial- and lateral muscles) and two oblique muscles (superior- and inferior muscles). An additional EOM, the levator palpeprae muscle (LP), is present only in mammals and elevates the upper eye lid (Spencer and Porter, 2006).
Among all vertebrate classes, the presence of the four recti and two oblique muscles is rather constant, but the EOMs vary in innervation-pattern and arrangement (Isomura, 1981; Evinger, 1988; Spencer and Porter, 2006).
In mammals the eyeball is embedded in orbital fat and connective tissue within the bony orbit and is attached by the EOMs. The recti muscles and the superior oblique muscles have their origin from the annulus of Zinn, a tendinous ring which surrounds the optic foramen and a portion of the superior orbital fissure (Sevel, 1986). The inferior oblique muscle (IO) arises from the maxillary bone in the medial wall of the orbit, and the LP has its origin at the sphenoid bone above the optic foramen. The medial rectus (MR) lies medial to the globe and inserts posterior to the corneoscleral junction. The lateral rectus (LR) lies lateral to the globe, inserts on the sclera via a long and broad tendon. The two vertical muscles, the superior rectus (SR) and inferior rectus (IR), insert dorsally and ventrally on the globe and anterior to the equator (Spencer and Porter, 2006). The superior oblique muscle (SO) passes through the trochlea, a chondral ring at the upper edge of the medial orbit, turns laterally to insert on the superior aspect of the globe. The insertion of this muscle is posterolateral to the central point of the globe in frontal-eyed mammals and anterolateral in lateral-eyed mammals (Spencer and Porter, 2006).

The IO passes ventral to the tendon of the IR and inserts on the lateral aspect of the globe medial to the tendon of the LR (Miller, 1998) (Fig.1).

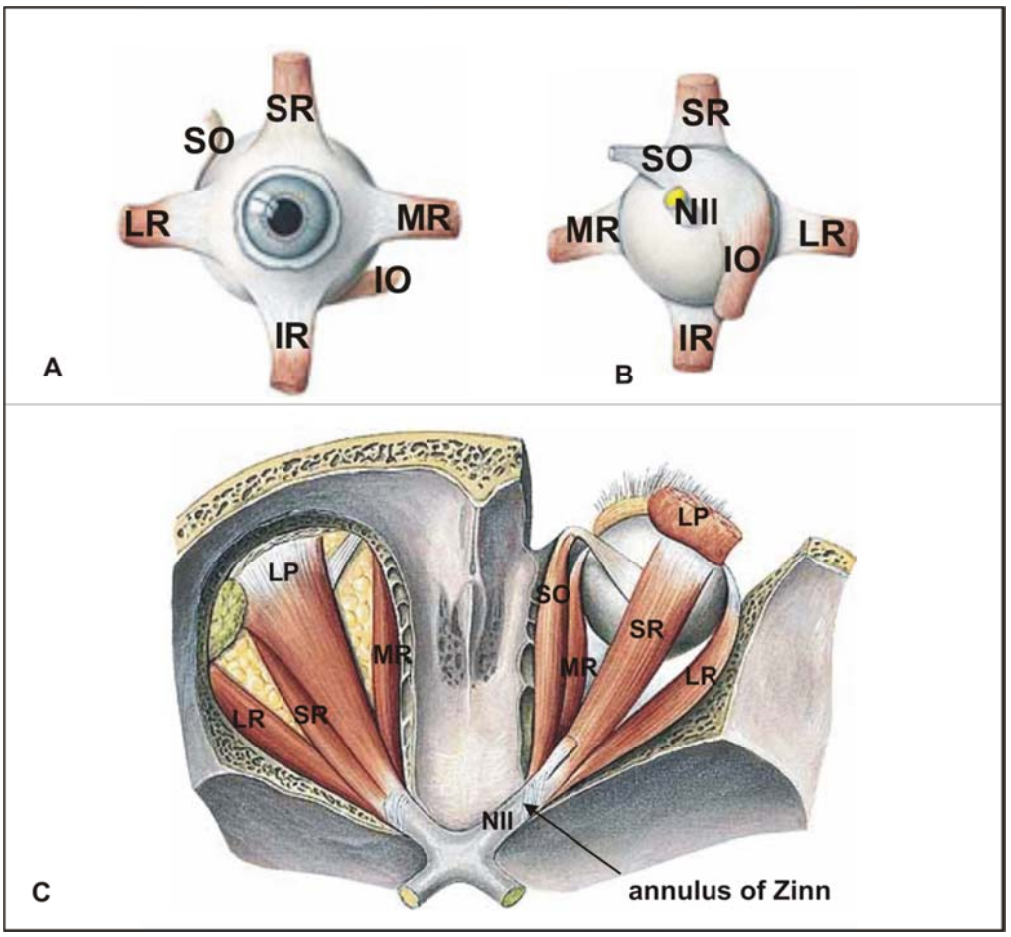

Fig.1: Arrangement of the extraocular muscles: A, B: Schematic drawing of the right eye viewed from the front (A) and back (B) side. The levator palpebrae muscle (LP) is cut at its origin. C: The arrangement of eye muscles within the orbit viewed from dorsal. The surrounding tissue is removed to better visualize the extraocular muscles. The inferior oblique (IO) and inferior rectus (IR) muscle are covered by the overlying eye muscles and are not visible in C. All muscles, except the LP and IO, originate from the annulus of Zinn.

NII - optic nerve; SO - superior oblique muscle; SR - superior rectus muscle; LR - lateral rectus muscle; MR - medial rectus muscle

According to their location and insertion at the globe, the EOMs have different functions in eye movements (Tab.1). The MR and LR, the horizontal eye muscles,

insert on the opposite sides of the globe, and therefore these muscles are functional antagonists that serve as the principle adductor (MR) and abductor (LR) of the eye. Up to date these two are referred to as the only muscles with no secondary function.
Recent studies report of compartmentalized innervations of horizontal EOMs. The results show that LR and MR motor nerves divide into superior and inferior branches of approximately equal size, innervating similar proportioned compartments of EOM fibers (Peng et al., 2010; da Silva Costa et al., 2011; Clark and Demer, 2014). Da Silva Costa et al. suggest that differential innervations in horizontal rectus EOM compartments can potentially mediate previously unrecognized vertical oculorotary actions for these EOM (da Silva Costa et al., 2011; Clark and Demer, 2014).
Since the optic axis of the eye forms an angle of 23° with the vertical recti and 51° with the oblique muscles, all other EOMs show different functions depending on their actual eye position: Only in 23° abduction the SR and IR function as pure elevator and depressor, respectively. The intorsional (SR) and extorsional (IR) component increases with adduction for both muscles. Similarly, the primary function of the SO is intorsion with contribution to depression and abduction of the globe. The primary action of the IO is extorsion with contribution to elevation and abduction (Horn and Leigh, 2011).

Muscle	Primary Function	Secondary Function	Tertiary Function
Superior oblique	intorsion	depression	abduction
Inferior oblique	extorsion	elevation	abduction
Medial rectus	adduction	none	none
Lateral rectus	abduction	none	none
Superior rectus	elevation	intorsion	adduction
Inferior rectus	depression	extorsion	adduction

Tab. 1: The different function of the six extraocular muscles in eye movements.

2.2.2 Gross and fine anatomy

The EOMs are among the fastest muscles in mammals, with contraction speeds obtained from experiments on cats as fast as about 7.5 ms for MR (twitch contraction time: onset to peak force; see Li et al., 2011; Cooper and Eccles, 1930; Denny-Brown, 1929). However, they also possess slow, non-twitch fibers that are characteristic of phylogenetically older avian or amphibian skeletal muscles (Morgan and Proske, 1984; Spencer and Porter, 1988; Ruff et al., 1989; Spencer and Porter, 2006).

It has long been recognized that EOMs have two distinct layers: an outer orbital and an inner global layer (Kato, 1938).The outer orbital layer is adjacent to the periorbita and orbital bone and the inner global layer lies close to the optic nerve and eye bulb (Spencer and Porter, 1988; Porter et al., 1995; Demer et al., 2000). A thin muscle fiber layer external to the orbital layer has been documented in sheep and human, and has been termed the peripheral layer (Harker, 1972) and marginal zone, respectively (Wasicky et al., 2000).

The global layer extends through the full muscle length inserting into the sclera via a well-defined tendon, whereas the orbital layer ends before the muscle becomes tendinous (Spencer and Porter, 2006). Recent studies have shown that this early termination of the orbital layer is a consequence of its insertion into the collagenous tissue of the pulleys formed by the Tenon's capsule at approximately the equator of the globe (Demer et al., 2000).

Extraocular muscle fibers can be classified in different ways. Initially the EOM fibers were distinguished according to their histological appearance into "Felderstruktur" and "Fibrillenstruktur" fibers (Siebeck and Kruger, 1955). Later, the classification was based on the content and distribution of mitochondria or it was differentiated between "coarse", "fine" and "granular" fibers (Durston, 1974).

Mayr and collegues were the first, who described six fiber types in rat, characterized on the basis of their location in the orbital or global layer, muscle fiber diameter, innervation pattern, histochemical features and ultrastructure (Mayr et al., 1975). Further investigations of EOMs in different mammals confirmed the concept of six EOM fiber types (Spencer and Porter, 1988). A categorization of the human EOM is based on histochemical properties and expression of different myosin heavy-chain isoforms (Kjiellgren et al., 2003; Spencer and Porter, 2006).

Accordingly, all EOM consist of at least 6 different muscle fiber types, which can be divided into two main categories based on their innervation (Spencer and Porter, 2006). The singly innervated muscle fibers (SIF) correspond to the twitch fibers (type IIA) of a mammalian skeletal muscle. This fiber type responds with an “all-or-nothing” potential to electrical stimulation (Lennerstrand, 1974; Chiarandini and Stefani, 1979; Nelson et al., 1986; Jacoby et al., 1989; Lynch et al., 1994).

The multiply innervated muscle fibers (MIF) are rare in vertebrate, besides the EOMs they are found in the tensor tympani muscle of the middle ear and in the laryngeal muscles (Fernand and Hess, 1969; Mascarello et al., 1982; Veggetti et al., 1982; Han et al., 1999). The two types of MIFs in the EOMs resemble the multiply innervated fibers found in avian skeletal muscles (correspond to orbital layer MIFs) and in amphibian skeletal muscles (correspond to global layer MIFs) (Morgan and Proske, 1984). After electrical stimulation they respond with local potentials resulting in a slow tonic contraction (Lennerstrand, 1974; Chiarandini and Stefani, 1979) and are called non-twitch muscle fibers (Siebeck and Kruger, 1955). Physiological studies identified two types of MIFs in the EOM: the MIFs of the orbital layer are contacted by an additional “en plaque” ending at the middle of the muscle fiber, which is reflected in their capability to propagate action potentials, whereas global MIFs lack these additional “en plaque” endings (Hess and Pilar, 1963; Bach-y-Rita and Ito, 1966; Pilar and Hess, 1966; Pilar, 1967).

The orbital layer consists of two fiber types, one MIF type and one SIF type, the global layer consists of one MIF type and three SIF types. This arrangement is a common pattern seen across different species (Spencer and Porter, 2006).

Orbital layer:

80 % of muscle fibers in the orbital layer represent SIFs. The orbital SIFs contain small myofibrils (myofibril volume is low (60 %)) in comparison to skeletal muscles (70-85 %), have a high percentage of mitochondria (20 % volume of the orbital SIFs), and accordingly a high oxidative enzyme content (Hoppeler and Fluck, 2002).

These qualities implicate, that orbital SIFs are fast-twitch and fatigue resistant muscles, with the capacity for anaerobic metabolism (Spencer and Porter, 1988).

SIFs of the orbital layer show an unique expression of the myosin gene, only seen in EOMs and laryngeal muscle and a developmental myosin isoform (associated with

developing skeletal muscles) (Wieczorek et al., 1985; Jacoby et al., 1990; Brueckner et al., 1996). The isoforms are specialized to provide specific contractile force/velocity at a specific energy cost. The unique myosin expression profile suggests a highly specialized role in eye movements (Spencer and Porter, 2006).

Orbital MIFs make up 20 % of the fibers. Their myofibrils are larger than those of the orbital SIFs and multiple nerve terminals are distributed along the myofiber length. In contrast to the SIFs, orbital MIFs express an embryonic myosin (Rubinstein and Hoh, 2000; Briggs and Schachat, 2002) and a neonatal myosin heavy chain isoform (Wieczorek et al., 1985; McLoon et al., 1999). The heterogeneous features of this fiber type are unlike anything that had been described for a skeletal muscles before and, it is difficult to draw a conclusion regarding the function (Spencer and Porter, 2006).

Global layer:

The global layer contains three different types of SIFs, red-, intermediate- and white SIFs, all of them with characteristics of fast twitch muscle fibers.

Global red SIFs represent about one-third of the fibers, predominantly in the intermediate zone between orbital and global layers. The global red SIFs have a high mitochondrial volume (< 20 %) and a very low myofibril volume (55 %) (Spencer and Porter, 2006). They are suggested to be highly fatigue resistant and furthermore they express the type IIA myosin isoform (Brueckner et al., 1996; Rubinstein and Hoh, 2000).

Global intermediate SIFs comprise one-fourth of the global fibers. Numerous medium-sized mitochondria are distributed singly or in small clusters, myofibrillar size is between the other two types of global SIFs and the myosin isoform content is likely type IIX (Rubinstein and Hoh, 2000). With their intermediate contraction speed and intermediate fatigue resistance, global intermediate SIFs are classified into red and the white global SIFs (Spencer and Porter, 2006).

The global white SIFs incorporate one-third of the fibers of the global layer. They have few small mitochondria that are singly arranged between the myofibrils and this fiber type likely express type IIB myosin heavy chain (Rubinstein and Hoh, 2000).

The fiber profile is consistent with a fast-twitch and low fatigue resistance fiber (Spencer and Porter, 1988).

MIFs constitute the remaining 10 % of the global fibers. These fibers contain very few small mitochondria arranged singly between the very large myofibrils. The ultra-structural profile is similar to slow, tonic muscle fibers of amphibian. This fiber type exhibits a slow graded, local contraction with non-propagated response to an electrical stimulation (Chiarandini and Stefani, 1979). The finding of a phylo-genetically primitive muscle fiber type in one of the fastest skeletal muscle is difficult to reconstruct. One assumption is that they play a potential role in either very fine foveating movements of the eye or they are part of a specialized proprioceptive apparatus (Ruskell, 1978).

2.2.3 Neuromuscular junction

The twitch fibers, or SIFs, respond to electrical excitation with an “all-or-nothing” contraction that propagates along the whole length of the fiber. They are innervated by relatively large nerves (7-11 µm), which terminate as large “en plaque” motor endplates in an endplate zone in the middle of the fiber (Namba et al., 1968; Spencer and Porter, 2006). The neuromuscular junction of twitch fibers in orbital and global layer is morphologically identical, but only the “en plaque” terminals of the intermediate SIFs of the global layer show clusters of large nerve endings (Spencer and Porter, 1988).
The non-twitch fibers, or MIFs, are multiply innervated by a myelinated and fine (3-5 µm) nerve fiber. These fibers respond to electrical stimulation with a slow tonic contraction, which is not propagated along the muscle fiber (Bondi and Chiarandini, 1983). The motor endplates “en grappe” endings are typically small and distributed along the length of the muscle fiber but have a higher density in the distal half of the muscle (Porter et al., 1985; Spencer and Porter, 1988) (Fig. 2).

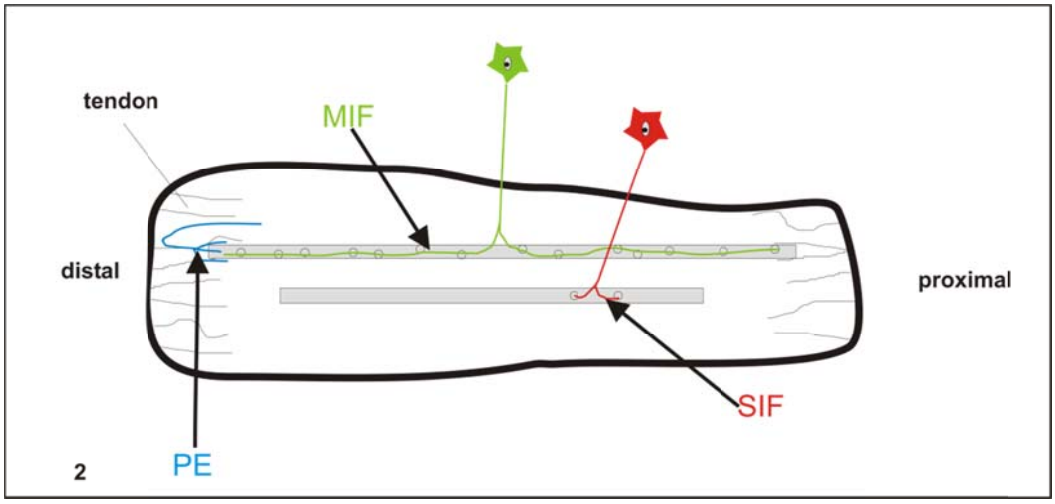

Fig. 2: Illustration of an eye muscle and its different fiber types.
Singly innervated muscle fibers (SIFs) are innervated by one single "en plaque" ending per fiber (in red). Multiply innervated muscle fibers (MIFs) are innervated by multiple "en grappe" endings throughout their whole extent (in green). Upon electrical stimulation SIFs respond in an "all or nothing" fashion, whereas MIFs respond with a slow contraction and local potential. The MIFs extend proximal and distal into the tendon, where the palisade endings (PEs) are located.
SIF - singly innervated muscle fiber; MIF - multiply innervated muscle fiber; PE - Palisade ending
With permission from Elsevier. Modified from: The extraocular motor nuclei: organization and functional neuroanatomy. Büttner-Ennever JA, Prog. Brain.Res. 151, 1-42, © 2006, Elsevier.

2.2.4. *Acetylcholine receptor (AchR) subunits are differentially expressed in SIF- and MIF of EOMs*

The acetylcholine receptor is a pentameric protein with different adult and fetal isoforms. The fetal isoform consists of two alpha subunits, a beta, a delta, and a gamma. During the development of the acetylcholine receptors, the gamma-subunit, is replaced by an epsilon-subunit (Kaminski et al., 1996; Missias et al., 1996).
Recent studies have shown that "en plaque" endings of SIFs express the adult epsilon-subunit, whereas the "en grappe" endings of MIFs express only the fetal subunit gamma and not the adult subunit (Fraterman et al., 2006). Currently it is not clear why the fetal gamma-subunit is still expressed in the "en grappe" endings of MIFs, but this finding has consequences for the understanding of ocular myasthenia. In myasthenia gravis weakness of the EOMs is often an initial and persisting symptom.

It has been proposed that the presence of antibodies to fetal AChR expressed in EOM causes their weakness (Oda, 1993; MacLennan et al., 1997).

2.2.5 Palisade endings (specialty of global MIFs)

The global layer possesses an unusual feature, unique to eye muscles, it has palisade endings (PE) at the myotendinous junction (Dogiel, 1906; Cilimbaris, 1910; Ruskell, 1999). PEs have been found in almost all species that have been investigated (Eberhorn et al., 2005b). PEs form a cuff of nerve branches around the muscle fiber tip. They contact only one type of muscle fiber, the MIFs of the global layer (Mayr, 1977; Alvarado-Mallart and Pincon Raymond, 1979; Richmond et al., 1984; Ruskell, 1999). The palisade terminals arise from nerve fibers that enter the tendon from the central nerve entry zone, then turn back 180^{o}, to contact the tip of the muscle fibers. PEs may function as proprioceptors and are unique to eye muscles (Dogiel, 1906).

Since their first description (Huber, 1900; Dogiel, 1906) the location, histochemistry, structure, and connectivity of PEs have been well studied, but their function is much discussed (Ruskell, 1999; Donaldson, 2000). Some of their properties are typical of sensory endings, for example terminals in the collagen tendon, and other properties are typical of motor structures, for example their cholinergic transmitter and the location of their somata.

Recent studies in monkeys indicated that the cell bodies of PEs are located within the peripheral groups around the motonuclei of EOM (Lienbacher et al., 2011; Zimmermann et al., 2011). From these findings two hypothesis are suggested for the function of the peripheral cell groups: In the first hypothesis one homogenous neuron population gives rise to multiple nerve endings supplying non-twitch MIFs that terminate as PEs at the myotendinous junction. In the second hypothesis, the peripheral motoneurons around the oculomotor nucleus may consist of two different neuron populations: Sensory neurons giving rise to PEs and motoneurons providing the multiple innervation of non-twitch muscle fibers (Lienbacher and Horn, 2012) (Fig. 3).

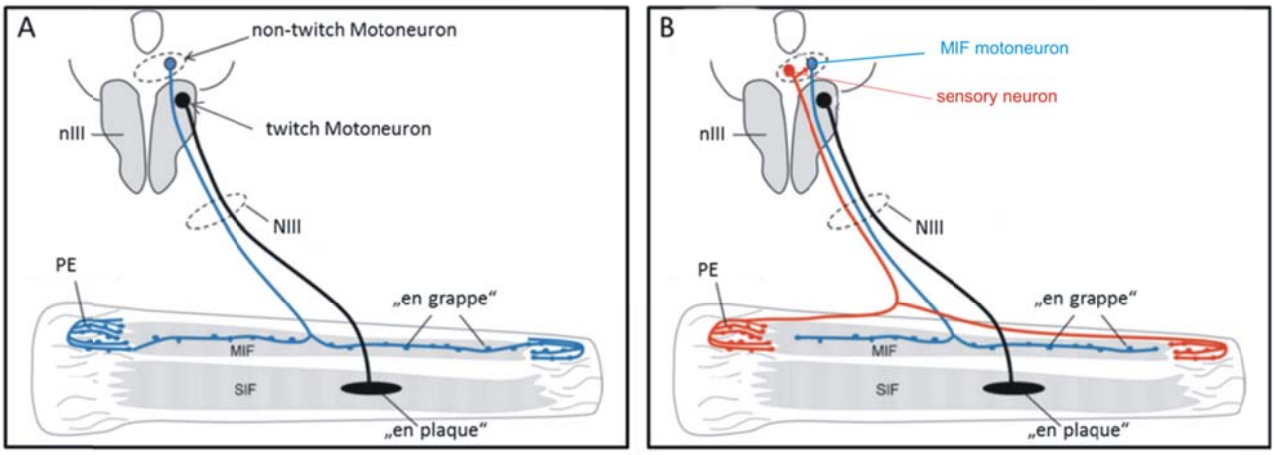

Fig. 3: Schematically illustration of the two hypothesis of the origin of Palisade endings (PEs).
A: Schema proposed hypothesis one: one cell body, located in the peripheral group, gives rise to PE and the multiply "en grappe" endings of non-twitch muscle fibers (in black).
B: Schema proposed hypothesis two: Two sets of neurons are located in the peripheral group.
MIF motoneurons providing the multiply innervation of non-twitch muscle fibers (in blue) and a sensory neuron giving rise to sensory terminals, the PE (in red).
nIII - oculomotor nucleus; NIII - oculomotor nerve; MIF - multiply innervated muscle fiber;
SIF - singly innervated muscle fiber; PE - Palisade endings
With permission from Springer Science and Business Media: Illustration assumed from: Palisade endings and proprioception in extraocular muscles: a comparison with skeletal muscles. Lienbacher K and Horn AKE. Biol Cybern 106, 643-655, Fig. 9, 10. © 2012, Springer.

2.3 Motor innervation of extraocular eye muscles

2.3.1 Organization of motor neurons

The motoneurons innervating the eye muscles lie in three distinct nuclei within the brainstem: the oculomotor nucleus (nIII) and the trochlear nucleus (nIV) in the mesencephalon, and further caudal, the abducens nucleus (nVI) at the pontomedullary junction (Fig. 4).

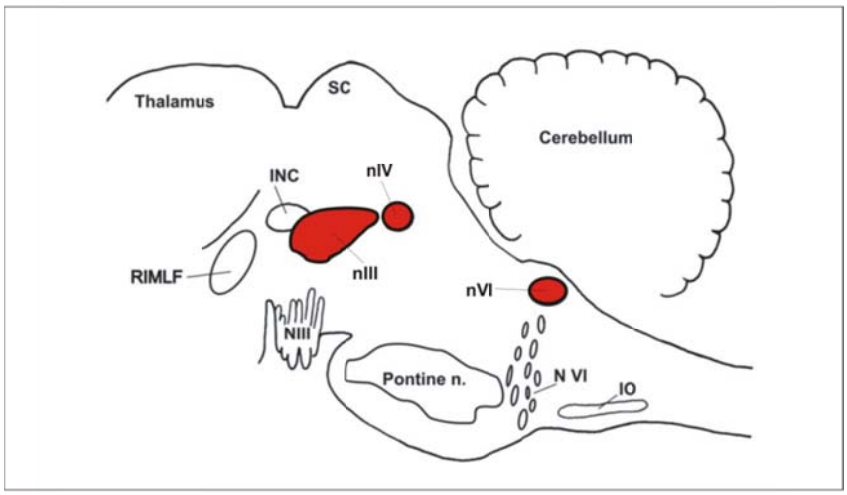

Fig. 4: Sagittal section through the brainstem of monkey, showing the location of the oculomotor (nIII), the trochlear (nIV) and the abducens nucleus (nVI). The nIII and nIV are located in the mesencephalon, the nVI lies more caudal in the pontomedullary brainstem underneath the genu of the facial nerve.
RIMLF - rostral interstitial nucleus of the medial longitudinal fasciculus; INC - interstitial nucleus of Cajal; nIII - oculomotor nucleus; nIV - trochlear nucleus; nVI - abducens nucleus; IO - inferior olive; NVI - abducens nerve; NIII - oculomotor nerve; SC - superior colliculus
With permission from Elsevier. Modified from: Present concepts of the oculomotor system. Büttner U and Büttner-Ennever JA. Rev Oculomot Res, Vol 2, 3-32. © 1988, Elsevier.

The nVI lies in the pontomedullary brainstem beneath the fourth ventricle, underneath the genu of the facial nerve. The majority of abducens motoneurons innervate the ipsilateral LR via the abducens nerve. Some species, for example cats, contain motoneurons of accessory eye muscles, the retractor bulbi muscles (Spencer et al., 1980) controlling the nictitating membrane, and therefore participating in the retraction reflex of the eye. In primates the nictitating membrane is degenerated to a vestigial plica semilunaris, the retractor bulbi is reduced to a single homologous slip, the accessory lateral rectus muscle. This accessory muscle is innervated by the abducens nerve (NVI) (Spencer and Porter, 1981; Schnyder, 1984). Motoneurons that innervate the accessory lateral rectus muscle are located in the accessory abducens nucleus, which lies ventral to the rostral half of the abducens nucleus (Schnyder, 1984).

An additional population within the nVI is formed by the internuclear neurons (INTs), which project rostrally via the medial longitudinal fasciculus (MLF) to the MR motoneurons in the contralateral nIII (Büttner-Ennever and Akert, 1981; McCrea et

al., 1986) and provide the neuroanatomical basis for conjugate horizontal eye movements (Glicksman, 1980; Evinger et al., 1987; Straka and Dieringer, 1991).

The trochlear nucleus (nIV) is located in the mesencephalic tegmentum and adjoins the oculomotor nucleus caudally. It contains mainly motoneurons innervating the contralateral SO via the trochlear nerve (NIV). Only a few project to the ipsilateral SO muscle (Porter et al., 1983; Miyazaki, 1985a; Evinger et al., 1987).

The nIII is located in the tegmentum of the midbrain, ventral to the aqueduct and dorsal to the fibers of the medial longitudinal fascicle (MLF). This compact paired nucleus contains the motoneurons of the ipsilateral MR, IR and IO and the motoneurons of the contralateral SR (Büttner-Ennever, 2006).

The first systematic study of individual motoneuron subgroups of the nIII was performed at the end of the 19th century using neuroanatomical and electrophysiological methods and clinical observations (Edinger, 1885; Bernheimer, 1897; Brouwer, 1918). In 1953 Warwick established the presently accepted topographical map of nIII by retrograde degeneration techniques in non-human primates (Warwick, 1953).

After introduction and development of retrograde tract-tracing methods with horseradish peroxidase (HRP) more detailed information about the organization of the motoneuons in the nIII was obtained in different species including primates (cat: Gacek, 1977; Miyazaki, 1985b; cat and rabbit: Akagi, 1978, rabbit: Murphy et al., 1986; rat: Glicksman, 1980; monkey: Büttner-Ennever et al., 2001).

The motoneuron subgroups within nIII show a topographical arrangement. From rostral to caudal, the motoneuron subgroups in all investigated vertebrate species follow an IR, MR, IO and SR sequence. In mammals, nIII also includes motoneurons which innervate the levator palpeprae muscle (LP). In rodents the LP motoneurons primarily occupied the caudal aspects of the contralateral oculomotor nucleus (Evinger et al., 1987), whereas in cat and primates the motoneurons lie in an unpaired separate group caudal to nIII, called the central caudal nucleus (CCN) (Evinger, 1988).

One main difference in the organization of the nIII between primate and non-primate is the existence of two subpopulations of the MR motoneurons in primates (Büttner-Ennever and Akert, 1981). The A-group contains the main part of MR motoneurons and lies at the ventral portion of nIII. The B-group is located dorsolateral within nIII and forms a circular group. A third additional MR-subgroup in the so-called C-group

at the dorsomedial peripheral border of nIII belongs to a separate set of motoneurons described in figure 6 C and D (Büttner-Ennever and Akert, 1981; Porter et al., 1983) (Fig. 5).

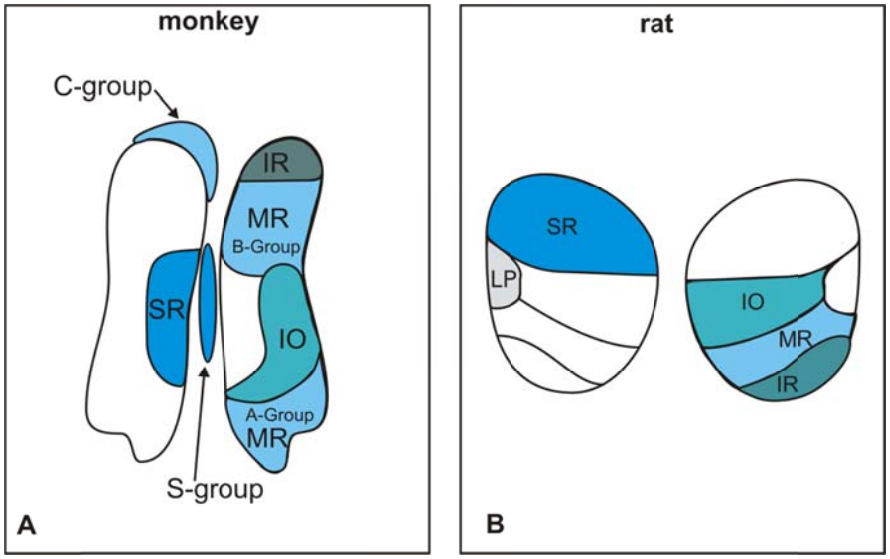

Fig. 5: Frontal section illustrating the location of motoneurons in the oculomotor nucleus (nIII) in monkey (A) and rat (B). All muscles are innervated ipsilaterally, except the SR, the motoneurons of SR lie contralaterally. Motoneurons of singly innervated muscle fibers (SIFs) are found only within the boundaries of the classical nIII, whereas the motoneurons of multiply innervated muscle fibers (MIFs) are located in the periphery of nIII. This is most clearly found in primate, where the MIF motoneurons are located in the C-group and S-group (A).

SR - superior rectus muscle; IR - inferior rectus muscle; MR - medial rectus muscle; IO - inferior oblique muscle

2.3.2 Twitch- and non-twitch motoneurons

Tracer injection into the belly or distal myotendinous junctions of EOMs in monkey revealed that MIF motoneurons lie separately from the SIF motoneurons for all six EOM, which formed the basis for a new concept of a dual innervation of EOM (Büttner-Ennever et al., 2001; Büttner-Ennever and Horn, 2002).

A distal tracer injection, enclosing exclusively the endplates of the MIFs, results in retrograde labelling of only the motoneurons in the periphery around the motonuclei (a belly injection labels both, motoneurons of MIFs and SIFs). These peripheral motoneurons tend to be smaller in diameter and are considered to be the motoneurons of tonic MIFs, whereas the “classical” motoneurons within the boundaries of the motonuclei are considered to be SIF motoneurons (for review: Büttner-Ennever, 2006).

2.3.3 C-group and S-group

The MIF motoneurons of individual EOMs are organized in the following way: The MIF motoneurons of MR and IR form a group at the dorsomedial border of nIII termed C-group (Büttner-Ennever and Akert, 1981; Büttner-Ennever et al., 2001). Recent studies have shown that both motoneuronal groups are separated from each other, with the IR MIF motoneurons adjacent to the dorsal nIII and the MR MIF motoneurons more medially reaching up to the Edinger-Westphal nucleus (Tang et al., 2015). The MIF motoneurons of SR and IO are located at the midline, sandwiched between the two nIII, in the so called S-group. MIF motoneurons of the SO lay as a cap dorsal to the nIV. LR MIF motoneurons are found in a shell around the medial borders of nVI, intermingled between the fascicles of the NVI, or located around the facial genu (Büttner-Ennever et al., 2001) (Fig. 6).

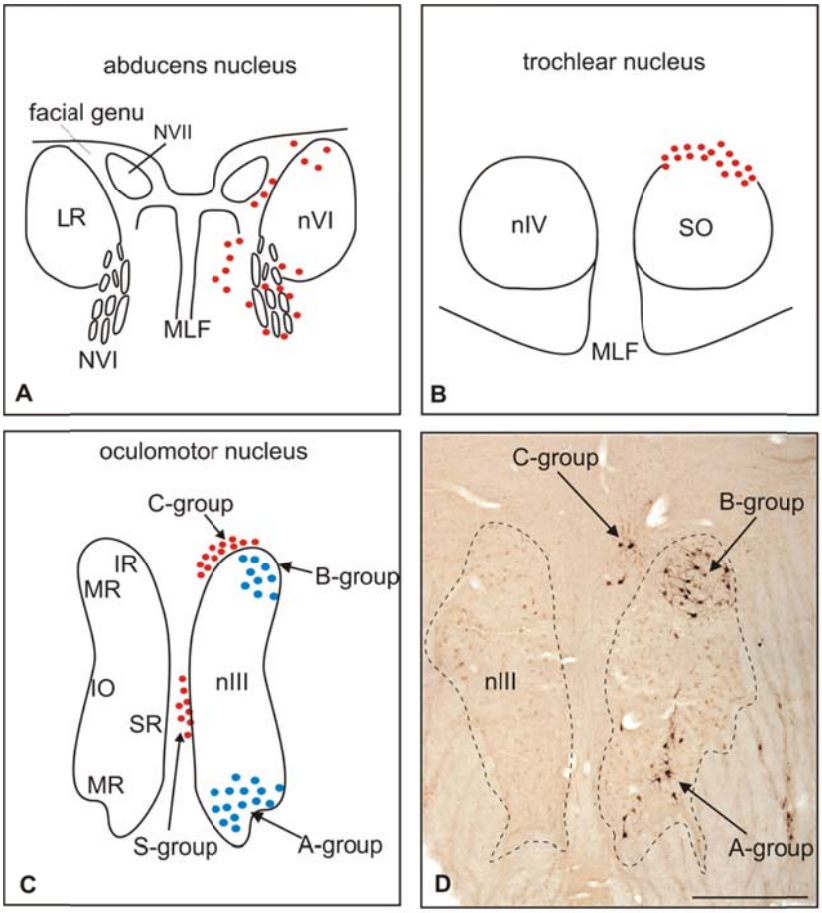

Fig. 6: Frontal section through the abducens nucleus (nVI) (A), trochlear nucleus (nIV) (B) and oculomotor nucleus (nIII) (C, D) of monkey, demonstrating the distribution of singly- (SIF) and multiply innervated (MIF) muscle fiber neurons. The SIF motoneurons (blue dots) lay within the boundaries of the classical motonuclei, whereas MIF motoneurons (red dots) appear in subgroups in the periphery of the nuclei borders. Lateral rectus (LR) MIF motoneurons are located at the midline borders and between the rootlets of the NVI, or around the facial genu (A). MIF motoneurons of the superior oblique (SO) lay like a cap at the dorsal borders of nIV (B). The C-group is located at the dorsomedial border of nIII and contains the MIF motoneurons of medial rectus (MR) and inferior rectus (IR) (C). The S-group is found at the midline, sandwiched between the two parts of nIII, containing the MIF motoneurons of superior rectus (SR) and inferior oblique (IO) (C). In the monkey and other primates the MR motoneurons are arranged in three distinct clusters. The A group (blue dots) is found at the ventral portion of the nIII, dorsolateral the motoneurons of the B group (blue dots) and dorsomedially at the peripheral border of the nIII the C-group, containing the MIF motoneurons (C). (D) Frontal section through the monkey nIII demonstrating retrogradly labeled neurons after a tracer injection into MR. All three distinct clusters of MR motoneurons are labeled.

NVII - facial nerve; NVI - abducens nerve; nVI - abducens nucleus; nIV - trochlear nucleus; nIII - oculomotor nucleus; MLF - medial longitudinal fasciculus; LR - lateral rectus muscle; SO - superior oblique muscle; IR - inferior rectus muscle; MR - medial rectus muscle; IO - inferior oblique muscle; SR - superior rectus muscle; Scale bar = 500 µm in D (applies to D).

With permission from Elsevier. Modified from: The extraocular motor nuclei: organization and functional neuroanatomy. Büttner-Ennever JA. Prog Brain. Res 151, 1-42, © 2006, Elsevier.

2.3.4 Delineation from other perioculomotor nuclei: Edinger-Westphal nucleus

The Edinger-Westphal nucleus (EW) is located in the midbrain dorsal to the nIII, mediating lens accommodation and pupillary constriction (Edinger, 1885; Westphal, 1887) via their projection to the ciliary ganglion.

The EW sends preganglionic axons along the oculomotor nerve (NIII) to the ipsilateral ciliary ganglion. The ciliary ganglion sends postganglionic parasympathetic fibers either to the sphincter pupillae muscle or the ciliary muscle. Activation of the sphincter pupillae muscles of the iris results in pupil constriction. Contractiion of the ciliaris muscle releases the tension on the Zonular fibers, making the lens more convex, known as accommodation. In all vertebrates, including human, the EW forms a circumscribed cell group, with primarily small basophil neurons, located dorsomedial to the nIII. Traditionally the EW is considered as the location for the parasympathetic preganglionic neurons of the ciliary ganglion controlling the lens and the sphincter pupillae muscle (Edinger, 1885; Westphal, 1887). However, tract-tracing studies revealed a considerable variation in the location of the preganglionic neurons across species in particular to the location to the cytoarchitecturally defined EW (Büttner-Ennever, 2006). Only in monkey and bird, the preganglionic neurons are located in the EW (Akert et al., 1980; Gamlin and Reiner, 1991; Sun and May, 1993), in all other species studied so far, the preganglionic neurons are located around the EW or at the medial borders of nIII (mouse: Vann and Atherton, 1991, hamster: Pickard et al., 2002). Recently, an additional group containing the neuropeptide urocortin 1 has been associated with the EW in several species (Vaughan et al., 1995; Yamamoto et al., 1998; Ryabinin et al., 2005; May et al., 2008).

In conclusion the EW is the location of the preganglionic neurons in some species or contains the neuropeptide urocortin and not the preganglionic neurons (Fig. 7).

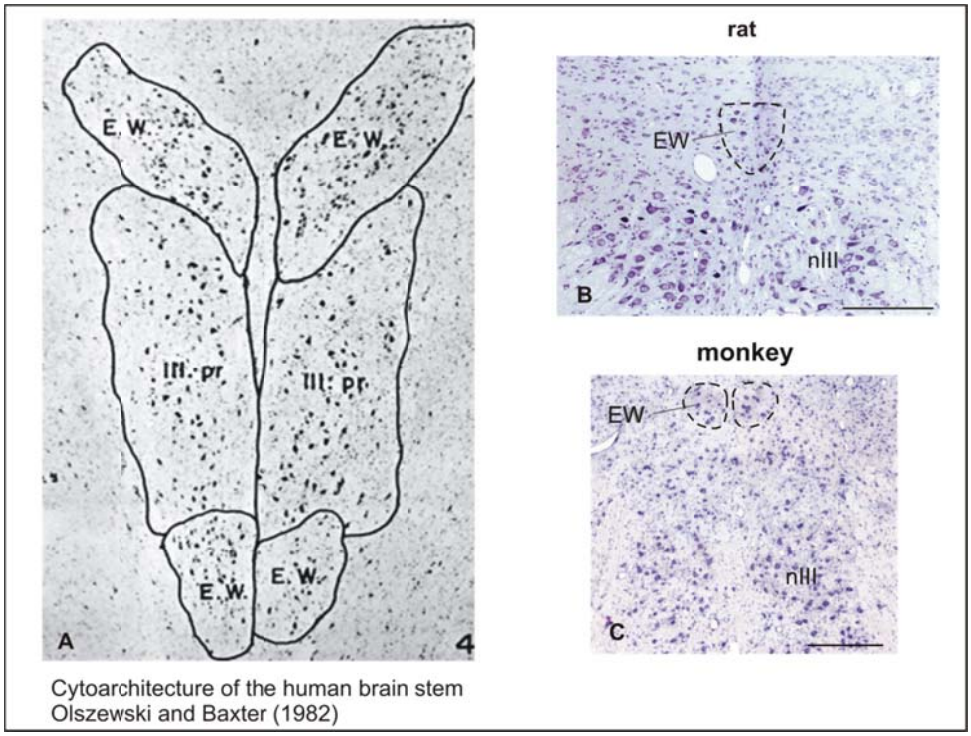

Fig. 7: Frontal section through the brain stem of human (A), rat (B) and monkey (C), showing the location of the Edinger-Westphal nucleus (EW) and the oculomotor nucleus (nIII).
EW - Edinger-Westphal nucleus; nIII - oculomotor nucleus;
Scale bar = 100 µm in B (applies to B); Scale bar = 250 µm in C (applies to C).
Fig. A: with permission from S. Karger AG. Adopted from: Cytoarchitecture of the Human Brain Stem, 2nd Edition, Olszewski J and Baxter D, Fig. 4, p 97, © 1982, Karger.

2.4 Different histochemical properties of MIF- and SIF motoneurons

It has been shown in monkey and rat, that SIF- and MIF motoneurons have different histochemical staining properties (Eberhorn et al., 2005a; Eberhorn et al., 2006). These experiments revealed that MIF motoneurons in the periphery of the motor nuclei do not contain non-phosphorylated neurofilaments (NP-NF) and lack perineuronal nets, whereas SIF motoneurons express these two markers at high intensity.

The function of the perineuronal nets is still unclear (Hockfield et al., 1990; Okamoto et al., 1994; Brückner et al., 1999). One hypothesis suggests that perineuronal nets are associated with highly active neurons (Brückner et al., 1993), such as those found in the rat medial septum and in neurons of the primate saccadic system (up to

1000 Hz) (Henn and Hepp, 1984; Morris and Henderson, 2000; Horn et al., 2003), whereas slow modulatory neurons – like serotoninergic neurons in the raphe nuclei - lack perineuronal nets (Brückner et al., 1994; Hobohm et al., 1998). Labelling for NP-NF was specifically found in SIF motoneurons, and was not detected in any other cell type in the ocular motor nuclei. NP-NF labelling was reported as a reliable marker for motoneurons, but that it is not restricted to this cell type (Tsang et al., 2000).
These results demonstrated that MIF motoneurons differ in their histochemical properties from those of SIF motoneurons and are different in functions and physiology.

2.4.1 Different premotor inputs to MIF- and SIF motoneurons

Experiments applying different transsynaptic tracers in monkeys revealed that SIF- and MIF motoneurons receive different inputs serving different functions. SIF motoneurons are targeted by premotor afferents involved in generation of eye movements, e.g. saccadic burst neurons, secondary vestibulo-ocular neurons, whereas the peripheral MIF motoneurons are targeted only by afferents from premotor sources involved in gaze holding, e.g. the prepositus hypglossus nucleus (Wasicky et al., 2004; Büttner-Ennever, 2006; Ugolini et al., 2006).
It is well known, that in monkey motoneurons providing horizontal and vertical eye movements are controlled by inhibitory inputs mediated by different transmitters. Gamma-aminobutyric acid (GABA) is the major inhibitory neurotransmitter utilized by premotor neurons involved in vertical eye movements, glycine is used by premotor neurons associated with horizontal eye movements (Spencer et al., 1989; Spencer and Baker, 1992). There are specific disorders for the vertical eye movement system that affect only one direction, e.g. isolated upgaze or downgaze palsy or upbeat or downbeat nystagmus, which indicate that up- and downgaze pathways are organized in a different way (Leigh and Zee, 2006). There may be other characteristics specific to the vertical gaze system. The calcium-binding protein calretinin (CR) has been identified in several brainstem regions known to contain premotor neurons involved in vertical eye movements (Horn et al., 2003; Baizer and Baker, 2006).
The abducens internuclear neurons (INT) and the ascending tract of Deiters (ATD) pathways are the principle excitatory inputs to MR motoneurons, which carry eye

position and eye velocity signals (Fuchs et al., 1988) or head velocity signals (Reisine and Highstein, 1979), respectively. The abducens INTs terminate predominantly on the contralateral MR motoneurons and utilize aspartate and glutamate as excitatory neurotransmitter. ATD neurons are located in the ventral portion of the lateral vestibular nucleus and their axons project ipsilaterally to MR motoneurons and utilize glutamate as neurotransmitter (Spencer and Wang, 1996; Nguyen and Spencer, 1999). Other transmitter-related inputs to motoneurons of extraocular muscles involve orexin-A positive afferents that specifically target LP motoneurons in CCN, the motoneurons of multiply innervated non-twitch muscle fibers in the C- and S-group of nIII and the preganglionic neurons of the ciliary ganglion (Schreyer et al., 2009). Orexin-A is synthesized by neurons of the hypothalamus and helps to maintain wakefulness through excitatory projections to nuclei involved in arousal (Sakurai, 2007). There may be other characteristics specific to the vertical gaze system. Apart from the description of the orexin input and a preliminary report on GABA-related markers associated with MIF motoneurons in the C-group (Ying et al., 2008). There is no systematic study on transmitter-related markers associated with either SIF- or MIF motoneurons.

The present work addresses questions on the organization of premotor inputs to different functional cell groups of the oculomotor nucleus complex and its vicinity. Thereby, the histochemistry of inputs to different motoneuron groups was studied with emphasis on those participating in vergence. This involved – after the delineation of preganglionic neurons of the ciliary ganglion in the supraoculomotor area – the inputs to peripheral motoneurons in the C- and S-group of the oculomotor nucleus. Another focus was the investigation of differential inputs to motoneurons involved in upgaze versus those involved in downgaze.

2.5 Aim of the study

1. Traditionally the Edinger-Westphal nucleus (EW) is considered to be the location of the parasympathetic cholinergic preganglionic neurons mediating pupillary constriction and lens accommodation. In all vertebrates the EW forms a cytoarchitecturally defined nucleus dorsomedial to the nIII. Tracing studies revealed a considerable variation in the location of the preganglionic neurons across species in relation to the EW. The neuropeptide urocortin (UCN) has been associated with the EW in several species including man. In a comparative study in rat, ferret, monkey and human, the location of cholinergic neurons within and around the nIII, which includes motoneurons of the extraocular muscles and the preganglionic neurons of the ciliary ganglion, was compared to the location of UCN-positive neurons and their location related to the EW.
   The results are described and discussed in paper 1, pp 32-37.

2. There are specific disorders for the vertical eye movement system, e.g. isolated upgaze or downgaze palsies, and selective upbeat or downbeat nystagmus, which indicates that up- and downgaze pathways have separate organizations. In monkey, it has been shown that the motoneurons providing horizontal and vertical eye movements are controlled by inhibitory inputs mediated by different transmitters. There may be other characteristics specific to the vertical gaze system. The calcium-binding protein calretinin (CR) has been identified in several brainstem regions known to contain premotor neurons involved in vertical eye movements. To further explore this point, we investigated the motonuclei of extraocular muscles for the presence of CR-positive terminal profiles, with specific emphasis on determining their relationship to the motoneuron populations activated for upgaze, those activated in downgaze and those used in lateral gaze.
   The results are described and discussed in paper 2, pp 38-50.

3. The oculomotor nucleus (nIII) contains the motoneurons of singly innervated (SIF) twitch- and multiply innervated (MIF) non-twitch muscles fibers of medial rectus (MR), inferior rectus (IR), inferior oblique (IO) and superior rectus (SR)

muscle – the trochlear nucleus (nIV) those of the superior oblique muscle. As described earlier the gamma-aminobutyric acid (GABA) is the major inhibitory neurotransmitter utilized by premotor neurons involved in vertical eye movements, glycine is used by premotor neurons related to horizontal eye movements. Here we studied the histochemical profile and transmitter inputs to the different motoneuron subgroups including MIF- and SIF motoneurons in nIII and nIV of monkey. Prelabelled motoneurons were immunostained for different transmitters or transmitter-related proteins: Gamma-aminobutyric acid (GABA), glutamate decarboxylase, glycine transporter 2, GABA-receptors, vesicular glutamate transporter 1 and 2. The different histochemical profile of the subgroups of nIII and nIV provides a basis for anatomical identification and the interpretation of physiological data.

The results are described and discussed in paper 3, pp 51-69.

4. Motoneuron groups of individual eye muscles in human were identified. This was based on a comparison with the localization of motoneurons derived from tract-tracing experiments in monkey and on the cytoarchitecture and differential histochemical inputs to motoneuron subgroups revealed by immunohistochemical staining for different markers: non-phosphorylated neurofilaments, glutamate decarboxylase, calretinin and glycine receptor. Seven subgroups in the oculomotor nucleus of human have been identified and present a new map of the human oculomotor subgroups.

   The results are described and discussed in paper 4, pp 70-86.

3 Results

3.1 Paper 1, pp 32-37:

*The Edinger-Westphal nucleus represents different functional cell groups in different species***.**

3.2 Paper 2, pp 38-50:

Calretinin inputs are confined to motoneurons for upward eye movements in Monkey.

3.3 Paper 3, pp 51-69:

Transmitter input to different motoneuron subgroups in the oculomotor and trochlear nucleus in monkey.

3.4 Paper 4, pp 70-86:

Delineation of motoneuron subgroups supplying individual eye muscles in the human oculomotor nucleus.

BASIC AND CLINICAL ASPECTS OF VERTIGO AND DIZZINESS

The Edinger–Westphal Nucleus Represents Different Functional Cell Groups in Different Species

Anja K.E. Horn, Christina Schulze, and Susanne Radtke-Schuller

Institute of Anatomy, Ludwig-Maximilian-University of Munich, Munich, Germany

In all vertebrates, including humans, the Edinger–Westphal nucleus (EW) forms a circumscribed cell group dorsomedial to the oculomotor nucleus (nIII). Traditionally the EW is considered the location of parasympathetic preganglionic neurons of the ciliary ganglion, mediating pupillary constriction and accommodation. In a comparative study in rat, ferret, monkey, and human, the location of cholinergic neurons within and around the nIII, which includes motoneurons of the extra-ocular muscles and the preganglionic neurons of the ciliary ganglion, was compared to the location of urocortin-positive neurons. Irrespective of the species, the cholinergic and urocortin-positive neurons form largely separated cell populations adjacent to each other. Only in monkey, cholinergic putative preganglionic neurons were found within the cytoarchitecturally defined EW, whereas in rat, ferret, and human the EW is almost exclusively composed of urocortin-positive neurons. In humans, the presumed preganglionic neurons are located as an inconspicuous group of choline acetyltransferase-positive neurons dorsal to the urocortin-positive EW.

Key words: **parasympathetic; ciliary ganglion; pupil; lens; oculomotor nucleus; urocortin; choline acetyltransferase; rat; ferret; monkey; human**

Introduction

Traditionally the Edinger–Westphal nucleus (EW) is considered the location of the parasympathetic cholinergic preganglionic neurons of the ciliary ganglion mediating pupillary constriction and lens accommodation.[1,2] In all vertebrates the EW forms a cytoarchitecturally distinct nucleus of mostly small basophil neurons dorsomedial to the oculomotor nucleus (nIII). However, tract-tracing methods revealed a considerable variation in the location of the parasympathetic preganglionic neurons of the pupil and accommodation reflex across species with respect to the location in the cytoarchitecturally defined EW.[3] Recently, an additional cell group containing the neuropeptide urocortin 1 has been found associated with the EW in several species including man.[4–7] Urocortin (UCN) is an endogenous ligand for the corticotrophin-releasing factor receptors CRF-1 and CRF-2, and it is involved in the regulation of many behaviors, including anxiety, food intake, alcohol consumption, and stress.[8] In a comparative approach, we identified the cholinergic and urocortin-expressing neuron populations in nIII and the overlying peri-oculomotor region (pIII) in rat, ferret, monkey, and human to elucidate their relationship to the cytoarchitecturally defined EW.

Materials and Methods

All animal and human tissues were obtained in accordance with state regulations and with

Address for correspondence: Anja K.E. Horn, Institute of Anatomy, Ludwig-Maximilian-University of Munich, D-80336 Munich Germany. Voice: +49 89 5160 4880; fax: +49 89 5160 4802. Anja.Bochtler@med.uni-muenchen.de

Basic and Clinical Aspects of Vertigo and Dizziness: Ann. N.Y. Acad. Sci. 1164: 45–50 (2009).
doi: 10.1111/j.1749-6632.2009.03856.x

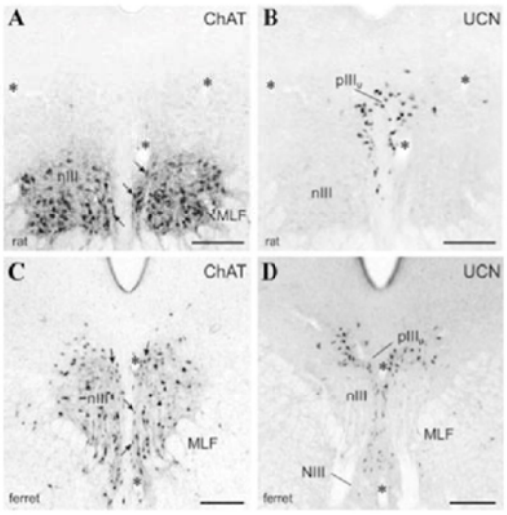

Figure 1. Transverse sections through the oculomotor (nIII) of rat (**A, B**) and ferret (**C, D**) stained for choline acetyltransferase (ChAT) (**A, C**) or urocortin (UCN) (**B, D**). Note that the UCN-positive neurons (pIII$_U$) in these species are located within the EW as defined by Nissl-staining (compare to Fig. 4A,B). For better correlation the corresponding blood vessels are labelled by asterisks. The arrows indicate small ChAT-positive neurons that may represent preganglionic neurons or motoneurons of multiply innervated muscle fibers. MLF, medial longitudinal fascicle; nIII, oculomotor nerve. Scale bar = 250 μm.

approval of the appropriate state and university committees. Frozen or paraffin-embedded midbrain sections of rat, ferret, monkey, and human that had been fixed with 4% paraformaldehyde in 0.1M phosphate buffer were immunostained for choline acetyltransferase (ChAT) and urocortin (UCN). For an overview of the cytoarchitecture, a series of sections was stained with 0.5% cresyl violet. In addition combined immunofluorescence staining was applied on rat, ferret, and monkey tissue to detect ChAT and UCN simultaneously on selected sections. A detailed description of antibody sources and staining procedures is given in a previous paper.[9]

Results

In all species studied here the ChAT- and UCN-immunoreactive neurons in the oculomotor nucleus and the peri-oculomotor region formed independent cell populations in close proximity to each other (Figs. 1, 2, 3). In the ferret a considerable portion of ChAT-positive neurons was also found in the territory of the UCN-positive populations (pIII$_U$) (Figs. 1C, D, 3B). The analysis of double-immunostained sections confirmed that both populations are separate also on a cellular level. Only in rat and ferret a few UCN-positive neurons showed additional faint ChAT-immunofluorescence, which has also been noticed in cat[6] (Fig. 3A, B, open circles). With the exception of monkey, in rat, ferret, and man, the cytoarchitecturally defined EW was occupied by UCN-positive neurons (pIII$_U$), which extended rostrally into the area of the anteromedian nucleus as well[6,9] (Figs. 1B,D, 2B,D, 3A–D). In humans the distribution of UCN-positive neurons coincides largely with the territory of the EW as defined by Olszewski and Baxter[10] in Nissl-stained sections (Fig. 2D, 4D). At caudal levels the UCN population (pIII$_U$) appears as two separate groups, which merge at more rostral levels, but they are still apparent as a medial and a lateral part (Fig. 2D, arrows). A few small, moderately ChAT-positive neurons were present in the lateral portion of the UCN-positive neurons (Fig. 2C arrows; 3D). Co-expression of UCN and ChAT could not be assessed in the human material for technical reasons. In monkey the UCN-positive neurons are arranged as a widespread cytoarchitecturally inconspicuous group lateral to the cytoarchitecturally defined EW (Fig. 2B, 3C, 4C).

Two main populations of ChAT-immunoreactive neurons, based on their size, location, and morphology, were identified in nIII and the peri-oculomotor region (pIII) in rat and ferret: medium-sized multipolar neurons within nIII are likely to represent motoneurons of singly-innervated muscle fibers (SIF), whereas the smaller ChAT-positive neurons in the periphery of nIII may include the motoneurons of multiply innervated muscle fibers (MIF) and preganglionic

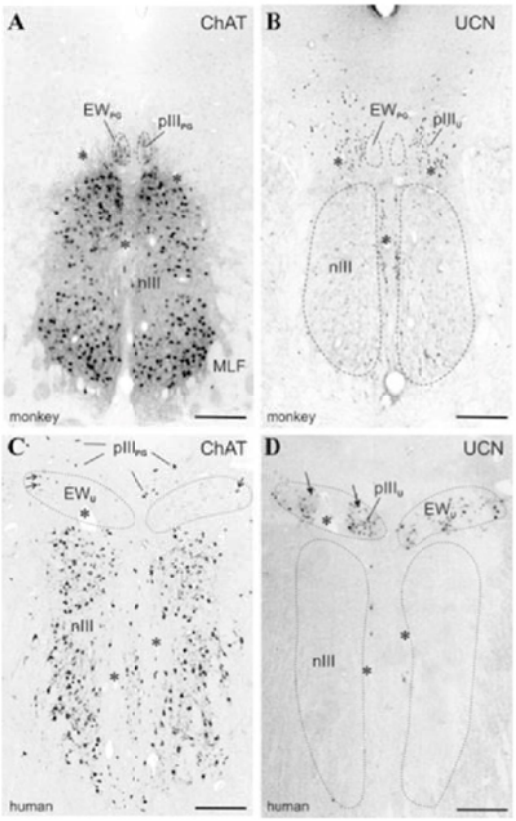

Figure 2. Transverse sections through the oculomotor (nIII) and Edinger-Westphal nucleus of monkey (**A, B**) and human (**C, D**) stained for choline acetyltransferase (ChAT) (**A, C**) or urocortin (UCN) (**B, D**). Note that in monkey the ChAT-positive neurons are located within the EW, therefore termed EW_{PG}, whereas in human the EW consists of UCN-positive neurons ($pIII_U$)—apparent as two groups (**D**, arrows)—therefore termed EW_U. Note that few ChAT-positive neurons are scattered in the lateral $pIII_U$ in EW_U (**C**, arrows). The ChAT-neurons dorsal to EW_U are considered as the preganglionic neurons ($pIII_{PG}$) of the ciliary ganglion in human (**C**). For better correlation the corresponding blood vessels are labelled by asterisks. MLF, medial longitudinal fascicle. Scale bar = 500 μm.

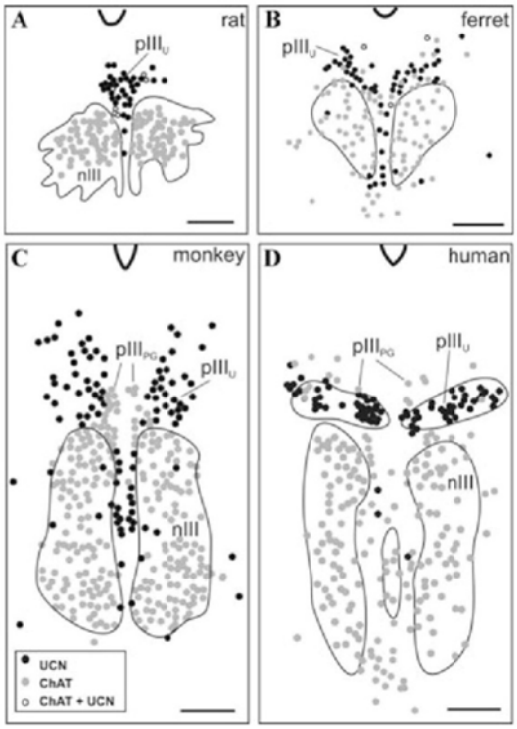

Figure 3. Plots of transverse sections through the oculomotor (nIII) and Edinger-Westphal nucleus of rat (**A**), ferret (**B**), monkey (**C**), and human (**D**). They are generated from sections stained for urocortin (UCN, black dots) and choline acetyltransferase (ChAT, gray dots) and demonstrate the spatial relationship of cholinergic presumed preganglionic neurons ($pIII_{PG}$) and the UCN-positive neurons ($pIII_U$) in the peri-oculomotor region. Whereas the ChAT- and UCN-positive cell populations seem rather separated in monkey (**C**), and human (**D**), few UCN-positive neurons expressing faint ChAT-immunofluorescence were noticed in rat and ferret (**A**, **B**, open circles). Scale bars = 250 μm (**A**, **B**); 0.5 mm (**C**, **D**).

neurons (PG) of the ciliary ganglion (Fig. 1A,C; arrows). In rat and monkey both groups can be distinguished by their different histochemical properties.[9,11,12] The presence of ChAT-positive neurons is a main feature of the cytoarchitecturally defined EW (termed EW_{PG}, see Discussion) in monkey (Fig. 2A; 3C). They represent the preganglionic neurons of the ciliary ganglion in this species[6,9,13] (Fig. 4C). Unlike in rat and monkey, the ferret showed a rather widespread distribution of ChAT-positive neurons in the peri-oculomotor region (Fig. 1C; 3B), where the location of MIF motoneurons and preganglionic neurons has still to be determined.

In humans a consistent group of ChAT-positive neurons was found dorsally to the UCN-positive neurons ($pIII_U$) in EW aside

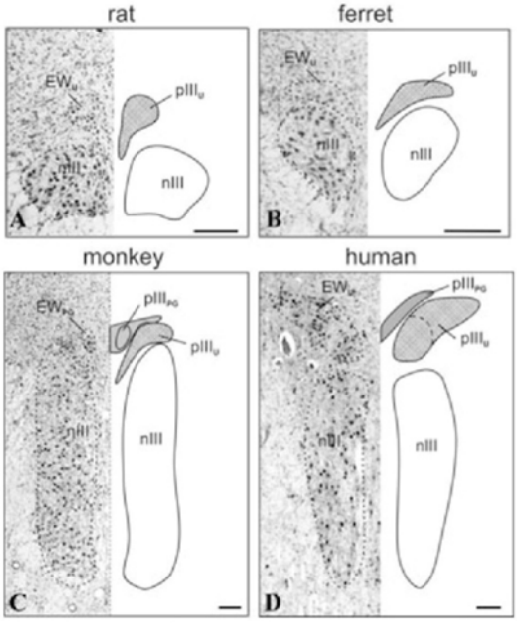

Figure 4. Schematic drawing of transverse sections through the oculomotor (nIII) and Edinger-Westphal nucleus (EW_U; EW_{PG}) in rat (**A**), ferret (**B**), monkey (**C**), and human (**D**) showing the cytoarchitecturally defined nuclei on the left by a Nissl-staining and the functional cell populations, the preganglionic neurons of the ciliary ganglion ($pIII_{PG}$) and the urocortin-positive neurons ($pIII_U$) on the right in each panel. The exact location of $pIII_{PG}$ in rat and ferret has not been determined yet. Scale bar = 250 μm.

from the ChAT-positive SIF motoneurons within the nIII and smaller presumed MIF motoneurons in the immediate vicinity of nIII.[9] These ChAT-positive neurons are scattered over the whole width of the underlying EW (here EW_U, see Discussion) and cannot be assigned to a cytoarchitectural entity in Nissl-stained sections (Fig. 2C, 3D, 4D). They were considered the preganglionic neurons of the ciliary ganglion, based on their similar morphology and histochemical properties with those in monkey.[9]

Discussion

This work extends our observations on man and monkey to include ferret and rat. In accordance with previous studies, we found that the UCN- and ChAT-positive cells form two largely separated neuronal groups, which did not correspond to the cytoarchitecturally defined EW in the same way across species.[6,9,14,15] In monkey and bird, the cytoarchitecturally defined EW consists of ChAT-positive neurons, which represent the preganglionic neurons of the ciliary ganglion,[6,9,13,16–19] whereas in mouse, rat, ferret, cat, and human the EW consists of the UCN-positive neuron population.[4,6,7,9,20,21] Because of these variations across species, a new nomenclature had been developed, which specifies functional cell groups of the peri-oculomotor region (pIII). That is, preganglionic neurons ($pIII_{PG}$) and UCN-positive neurons ($pIII_U$) can be defined as independent groups of their allocation to a distinct cytoarchitectural nucleus.[6,9,18] On the other hand, since the term "EW" is well established and used in most atlases, it is kept for descriptions based on the cytoarchitectural boundaries as defined in Nissl-staining, but is supplemented by the subscript suffix "PG" for preganglionic and "U" for urocortin as indicator for the main population that it contains. Accordingly, the EW in rat, ferret, and human is assigned as EW_U (Figs. 2C,D, 4A,B,D) and in monkey as EW_{PG} (Fig. 2A,B, 4C). The knowledge of the exact location of functional cell groups is important for the study of clinicopathological cases. Attempts have been made to correlate the striking degeneration of the EW_U in Alzheimer disease with deficits in the pupillary response. Since in light of our results the EW_U does not contain the preganglionic neurons, further studies should assess the overlying cholinergic preganglionic neuron population.[22] On the other hand the degeneration of the EW_U in Alzheimer patients may correlate with symptoms related to UCN function (see below).[23,24]

One common feature across all species is the closeness of the UCN-positive neurons ($pIII_U$) and the preganglionic neurons of the ciliary ganglion ($pIII_{PG}$). Major projection targets of UCN-positive neurons are the lateral septum,

the dorsal raphe nucleus, and sympathetic preganglionic neurons in the spinal cord by which various biological functions, such as stress responses, alcohol consumption, or anxiety may be conveyed.[25–27] Although not shown yet, an interaction of UCN neurons and preganglionic neurons—either directly or by common inputs—appears likely and may be indicated by changes in pupil size, accommodation, and fixation ability during stress or alcohol consumption.[24,28]

Acknowledgments

Grant sponsor: Deutsche Forschungsgemeinschaft, grant number: HO 1639/4-2/4-3; C.S. was supported by a graduate student fellowship (Bayerisches Elite-Förderungsgesetz). We thank Prof. U. Büttner (Department of Neurology, LMU Munich), Dr. S. Yakushin (Mount Sinai Hospital, New York), and Prof. M. Mustari (Emory University, Atlanta) for their continuous support and their generous supply of primate brain tissue. We are thankful to A. Messoudi and G. Ziegleder for their excellent technical support.

Conflicts of Interest

The authors declare no conflicts of interest.

References

1. Edinger, L. 1885. Über den Verlauf der centralen Hirnnervenbahnen mit Demonstrationen von Präparaten. *Arch. Psychiat. Nervenkr.* **16:** 858–859.
2. Westphal, C. 1887. Über einen Fall von chronischer progressiver Lähmung der Augenmuskeln (Ophtalmoplegia externa) nebst Beschreibung von Ganglienzellengruppen im Bereiche des Oculomotoriuskerns. *Arch. Psychiat. Nervenheilk.* **98:** 846–871.
3. Büttner-Ennever, J. A. 2006. The extraocular motor nuclei: organization and functional neuroanatomy. *Prog. Brain Res.* **151:** 95–125.
4. Vaughan, J., C. Donaldson, J.C. Bittencourt, *et al*. 1995. Urocortin, a mammalian neuropeptide related to fish urotensin I and to corticotropin-releasing factor. *Nature* **378:** 287–292.
5. Yamamoto, H., T. Maeda, M. Fujimura & M. Fujimiya. 1998. Urocortin-like immunoreactivity in the substantia nigra, ventral tegmental area and Edinger-Westphal nucleus of rat. *Neurosci. Lett.* **243:** 21–24.
6. May, P.J., A.J. Reiner & A.E. Ryabinin. 2008. Comparison of the distributions of Urocortin-containing and cholinergic neurons in the perioculomotor midbrain of the cat and Macaque. *J. Comp. Neurol.* **507:** 1300–1316.
7. Ryabinin, A.E., N.O. Tsivkovskaia & S.A. Ryabinin. 2005. Urocortin 1-containing neurons in the human Edinger-Westphal nucleus. *Neurosci.* **134:** 1317–1323.
8. Pan, W. & A.J. Kastin. 2008. Urocortin and the brain. *Prog. Neurobiol.* **84:** 148–156.
9. Horn, A., A. Eberhorn, W. Härtig, *et al*. 2008. Perioculomotor cell groups in monkey and man defined by their histochemical and functional properties: a reappraisal of the Edinger-Westphal Nucleus. *J. Comp. Neurol.* **507:** 1317–1335.
10. Olszewski, J. & D. Baxter. 1982. *Cytoarchitecture of the human brain stem*. S. Karger. Basel, München, Paris, London, New York, Sydney.
11. Eberhorn, A.C., J.A. Büttner-Ennever & A.K.E. Horn. 2006. Identification of motoneurons innervating multiply- or singly-innervated extraocular muscle fibres in the rat. *Neurosci.* **137:** 891–903.
12. Eberhorn, A.C., P. Ardelenanu, J.A. Büttner-Ennever & A.K.E. Horn. 2005. Histochemical differences between motoneurons supplying multiply and singly innervated extraocular muscle fibers. *J. Comp. Neurol.* **491:** 352–366.
13. Akert, K., M.A. Glicksman, W. Lang, *et al*. 1980. The Edinger-Westphal nucleus in the monkey. A retrograde tracer study. *Brain Res.* **184:** 491–498.
14. Vasconcelos, L.A.P., C. Donaldson, L.V. Sita, *et al*. 2003. Urocortin in the central nervous system of a primate (*Cebus apella*): sequencing, immunohistochemical, and hybridization histochemical characterization. *J. Comp. Neurol.* **463:** 157–175.
15. Cunha, R.P., A. Reiner & C.A.B. Toledo. 2007. Involvement of urocortinergic neurons below the midbrain gray in the physiological response to restraint stress in pigeons. *Brain Res.* **1147:** 175–183.
16. Sekiya, H., K. Kawamura & S. Ishikawa. 1984. Projection from the Edinger-Westphal complex of monkeys as studied by means of retrograde axonal transport of horseradish peroxidase. *Arch. Ital. Biol.* **122:** 311–319.
17. Burde, R.M. & A.D. Loewy. 1980. Central origin of oculomotor parasympathetic neurons in the monkey. *Brain Res.* **198:** 434–439.
18. May, P. J., W. Sun & J.T. Erichsen. 2008. Defining the pupillary component of the perioculomotor preganglionic population within a unitary primate

Edinger-Westphal nucleus. *Prog. Brain Res.* **171:** 97–106.
19. Gamlin, P.D.R. & A. Reiner. 1991. The Edinger-Westphal nucleus: sources of input influencing accommodation, pupilloconstriction, and choroidal blood flow. *J. Comp. Neurol.* **306:** 425–438.
20. Kozicz, T., H. Yanaihara & A. Arimura. 1998. Distribution of urocortin-like immunoreactivity in the central nervous system of the rat. *J. Comp. Neurol.* **391:** 1–10.
21. Weitemier, A.Z., N.O. Tsivkovskaia & A.E. Ryabinin. 2005. Urocortin 1 distribution in mouse brain is strain-dependent. *Neurosci.* **132:** 729–740.
22. Scinto, L.F.M., M. Frosch, C.K. Wu, *et al*. 2001. Selective cell loss in Edinger-Westphal in asymptomatic elders and Alzheimer's patients. *Neurobiol. Aging* **22:** 729–736.
23. Magri, F., L. Cravello, L. Barili, *et al*. 2006. The stress system in the human brain in depression and neurodegeneration. *Aging Clin. Exp. Res.* **18:** 167–170.
24. Swaab, D.F., A.M. Bao & P.J. Luccasson. 2005. The stress system in the human brain in depression and neurodegeneration. *Ageing Res. Rev.* **4:** 141–194.
25. Ryabinin, A.E. & A.Z. Weitemier. 2006. The urocortin 1 neurocircuit: Ethanol-sensitivity and potential involvement in alcohol consumption. *Brain Res. Rev.* **52:** 368–380.
26. Bachtell, R.K., A.Z. Weitemier, A. Galvan-Rosas, *et al*. 2003. The Edinger-Westphal-lateral septum urocortin pathway and its relation to alcohol-induced hypothermia. *J. Neurosci.* **23:** 2477–2487.
27. Kozicz, T. 2007. On the role of urocortin 1 in the non-preganglionic Edinger-Westphal nucleus in stress adaptation. *Gen. Comp. Endocrinol.* **153:** 235–240.
28. Campbell, H., M.J. Doughty, G. Heron & R.G. Ackerley. 2001. Influence of chronic alcohol abuse and ensuing forced abstinence on static subjective accommodation function in humans. *Ophthal. Physiol. Opt.* **21:** 197–205.

RESEARCH ARTICLE

Calretinin Inputs Are Confined to Motoneurons for Upward Eye Movements in Monkey

Christina Zeeh,[1] Bernhard J. Hess,[2] and Anja K.E. Horn[1,3]*

[1]German Center for Vertigo and Balance Disorders, University of Munich, 81377 Munich, Germany
[2]Vestibulo-Oculomotor Laboratory Zürich, Department of Neurology, Zürich University Hospital, 8091 Zürich, Switzerland
[3]Institute of Anatomy and Cell Biology, Department I, Ludwig-Maximilians University Munich, 80336 Munich, Germany

ABSTRACT

Motoneurons of extraocular muscles are controlled by different premotor pathways, whose selective damage may cause directionally selective eye movement disorders. The fact that clinical disorders can affect only one direction, e.g., isolated up-/downgaze palsy or up-/downbeat nystagmus, indicates that up- and downgaze pathways are organized separately. Recent work in monkey revealed that a subpopulation of premotor neurons of the vertical eye movement system contains the calcium-binding protein calretinin (CR). With combined tract-tracing and immunofluorescence, the motoneurons of vertically pulling eye muscles in monkey were investigated for the presence of CR-positive afferent terminals. In the oculomotor nucleus, CR was specifically found in punctate profiles contacting superior rectus and inferior oblique motoneurons, as well as levator palpebrae motoneurons, all of which participate in upward eye movements. Double-immunofluorescence labeling revealed that CR-positive terminals lacked the γ-aminobutyric acid (GABA)-synthesizing enzyme glutamate decarboxylase, which is present in inhibitory afferents to all motoneurons mediating vertical eye movements. Therefore, CR-containing afferents are considered to be excitatory. In conclusion, a strong CR input is confined to motoneurons mediating upgaze, which derive from premotor pathways mediating saccades and smooth pursuit, but not from secondary vestibulo-ocular neurons in the magnocellular part of the medial vestibular nucleus. The functional significance of CR in these connections is unclear, but it may serve as a useful marker to locate upgaze pathways in the human brain. J. Comp. Neurol. 521:3154–3166, 2013.

INDEXING TERMS: upgaze; levator palpebrae; inferior oblique; superior oblique

The vertebrate eye is rotated by six extraocular muscles. Horizontal eye movements are mediated by the medial (MR) and lateral rectus (LR) muscles, upward movements by the superior rectus (SR) and inferior oblique (IO) muscles, and downward movements by the inferior rectus (IR) and superior oblique (SO) muscles (for review, see Leigh and Zee, 2006). The motoneurons of individual eye muscles are located within the abducens (nVI), trochlear (nIV), and oculomotor nuclei (nIII) in the tegmentum of the brainstem, and have been well described in many species (Evinger, 1988; Büttner-Ennever, 2006). In nonhuman primates, the topography of the motoneurons within the nIII has been well studied with tract-tracing methods (Augustine et al., 1981; Büttner-Ennever and Akert, 1981; Spencer and Porter, 1981; Clarke et al., 1987; Evinger, 1988; McClung et al., 2001). A common feature is the crossed innervation of the SR, whose motoneurons are located in the middle part of nIII, close to the midline. In addition, the motoneurons of the levator palpebrae muscle (LP) are located in a separate central caudal nucleus (CCN), and they are active during combined upward eye and lid movements (Porter et al., 1989; Fuchs et al., 1992).

Because motoneurons of extraocular muscles are controlled by different premotor pathways, they may be

Additional Supporting Information may be found in the online version of this article.

Grant sponsor: Deutsche Forschungsgemeinschaft (DFG); Grant number: HO 1639/4-3 (to A.K.E.H.); Grant sponsor: Graduiertenförderung nach dem BayEFG (to C.Z.); Grant sponsor: the Swiss National Science Foundation; Grant number: 31-47287.96; Grant sponsor: the Betty and David Koetser Foundation for Brain Research (to B.J.H.).

*Correspondence to: Anja Horn, Ph. D., Institute of Anatomy and Cell Biology, Dept. I, Ludwig-Maximilians Unversity Munich, Pettenkoferstr. 11, D-80336 Munich, Germany. E-mail: Anja.Bochtler@med.uni-muenchen.de

Received September 28, 2012; Revised March 13, 2013;
Accepted for publication March 29, 2013.
DOI 10.1002/cne.23337
Published online May 21, 2013 in Wiley Online Library (wileyonlinelibrary.com)

affected selectively in certain eye movement disorders. There are specific disorders for the vertical eye movement system, e.g., isolated upgaze or downgaze palsies, and selective upbeat or downbeat nystagmus, which indicates that up- and downgaze pathways have separate organizations (Leigh and Zee, 2006). In monkey, it has been shown that the motoneurons providing horizontal and vertical eye movements are controlled by inhibitory inputs mediated by different transmitters.

Whereas γ-aminobutyric acid (GABA) is the major inhibitory neurotransmitter utilized by premotor neurons involved in vertical eye movements, glycine is used by premotor neurons related to horizontal eye movements (Spencer et al., 1989; Spencer and Baker, 1992). The abducens internuclear neurons and the ascending tract of Deiters (ATD) pathways are the principle excitatory inputs to MR motoneurons, which carry eye position and eye velocity signals (Fuchs et al., 1988) or head velocity signals (Reisine and Highstein, 1979), respectively. The abducens internuclear neurons terminate predominantly on the contralateral MR motoneurons and utilize aspartate and glutamate as excitatory neurotransmitter. ATD neurons are located in the ventral portion of the lateral vestibular nucleus, and their axons project ipsilaterally to MR motoneurons and utilize glutamate as neurotransmitter (Spencer and Wang, 1996; Nguyen and Spencer, 1999).

Other transmitter-related inputs to motoneurons of extraocular muscles involve orexin-A-positive afferents that specifically target LP motoneurons in CCN, the motoneurons of multiply innervated nontwitch muscle fibers in the C- and S-group of nIII, and the preganglionic neurons of the ciliary ganglion (Schreyer et al., 2009). Orexin-A is synthesized by neurons of the hypothalamus and helps to maintain wakefulness through excitatory projections to nuclei involved in arousal (Sakurai, 2007). There may be other characteristics specific to the vertical gaze system. The calcium-binding protein calretinin (CR) has been identified in several brainstem regions known to contain premotor neurons involved in vertical eye movements (Horn et al., 2003; Baizer and Baker, 2006). To further explore this point, we investigated the motonuclei of extraocular muscles for the presence of CR-positive terminal profiles, with specific emphasis on determining their relationship to the motoneuron populations activated for upgaze (SR, IO, and LP motoneurons), those activated in downgaze (IR and SO motoneurons), and those used in lateral gaze (MR and LR motoneurons).

MATERIALS AND METHODS

All procedures and surgical interventions were undertaken at the Department of Neurology at the University Hospital in Zürich. They accorded with the National Institutes of Health Guide for the care and the use of laboratory animals and were approved by the Veterinary Office of the Canton of Zürich.

Eye muscle injections

To identify the motoneurons of the eye muscles involved in upgaze, four macaque monkeys received a tracer injection of unconjugated wheat germ agglutinin (WGA; 5%; EY Lab, San Mateo, CA) into the SR and IO of one eye. For tracer injection, the animals were initially anesthetized with ketamine (Ketalar 1–2 mg/kg), which was followed by isoflurane inhalation. Under sterile conditions, the SR or IO of one eye was exposed by retracting the eyelid, and making a conjunctival incision. Tracer volumes of 5–20 μl were injected through a Hamilton syringe into the belly of the respective muscle. After a survival time of 3 days, the animals were killed with an overdose of sodium pentobarbital (80 mg/kg body weight; Merial, Halbergmoos, Germany) and transcardially perfused with 0.9% saline followed by 4% paraformaldehyde in 0.1 M phosphate buffer (pH 7.4). After removal from the skull, the brains were equilibrated in increasing concentrations of sucrose, 10–30%, in 0.1 M phosphate buffer for frozen sectioning. Sections from additional cases of 4% paraformaldehyde-fixed brains from previous studies were used for immunocytochemical staining. The brainstems were cut at 40 μm in the transverse plane by using a cryostat (Microm HM 560; Walldorf, Germany).

Immmunocytochemical labeling

The visualization of CR-containing nerval structures within the monkey motor nuclei of extraocular muscles was performed with immunoperoxidase methods on free-floating sections. Combined immunofluorescence for the injected tracer (WGA) and CR served to localize CR-positive neuronal profiles in relation to labeled motoneurons of extraocular muscles involved in upgaze. To determine whether CR-positive profiles represent inhibitory GABAergic nerve endings, selected free-floating sections were immunostained for the simultaneous detection of CR and glutamate decarboxylase (GAD), the synthesizing enzyme of GABA, by using immunofluorescence. For quantitative analysis of CR-positive terminals associated with eye muscle motoneurons, combined immunoperoxidase labeling was used to simultaneously detect choline acetyltransferase (ChAT) and CR in 10 μm paraffin sections of one additional case.

Antibody details

Wheat germ agglutinin

The tracer WGA (EY Lab) was detected with a polyclonal goat antibody (AS-2024; Lot No. V0128; Vector, Burlingame, CA).

TABLE 1.
Primary antibodies used in this study including their sources and dilutions.

Antibody	Host	Antigen	Manufacturer	Cat.No.	Dilution
ChAT	Goat	Cholinacetyltransferase human placental enzyme	Millipore, Billerica, MA	AB144P	1:100
CR	Rabbit	Calretinin	Swant, Bellinzona, Switzerland	7699/3H	1:2,500 1:1,000 (fluorescence)
$GAD_{65/67}$	Rabbit	Glutamate decarboxylase	Millipore	AB1511	1:500 (fluorescence)
GAD	Mouse	Glutamate decarboxylase	Biotrend, Cologne, Germany	GC3108	1:1,000 (fluorescence)
WGA	Goat	Wheat germ agglutinin	Axxora,Vector, Burlingame, CA	AS-2024	1:1,000 1:250 (fluorescence)

Choline acetyltransferase

Cholinergic motoneurons were detected with a polyclonal antibody against ChAT raised in goat (AB144P, Lot LV1583390; Millipore, Billerica, MA). The antibody is directed against the whole enzyme isolated from human placenta, which is identical to the brain enzyme (Bruce et al., 1985). In immunoblots, these antibodies recognize a 68–70-kDa protein. The appearance and distribution of ChAT-positive neurons with these antibodies in the present study are identical to data from previous reports (Ichikawa and Shimizu, 1998; Eberhorn et al., 2005; Horn et al., 2008).

Calretinin

A rabbit polyclonal antibody (7699/3H, Lot 18299; Swant, Bellinzona, Switzerland) against CR was used to detect CR-containing neuronal profiles. CR is a calcium-binding protein of the EF-hand family related to calbindin D-28k and calmodulin, with a widespread distribution throughout the brain (for review, see Andressen et al., 1993). The antiserum is produced by the immunization of rabbits with recombinant human CR containing a 6-his (hexa histidine) tag at the N-terminal. In western blots of whole brain tissue from different species, the antibody recognizes a single band of 29–30 kDa (Schwaller et al., 1999). In CR knockout mice, the antibody shows no CR immunoreactivity (manufacturer's data sheet).

Glutamic acid decarboxylase

GABAergic terminals were detected with a mouse monoclonal antibody against the GABA-synthesizing enzyme GAD ($GAD_{65/67}$, GC3108, batch number Z05507, clone 1111; Biotrend, Cologne, Germany) or the rabbit polyclonal antibody against GAD 65 and 67 (AB1511, Lot NG17374444; Millipore).

Two molecular forms of GAD_{65} and GAD_{67} are known from different species. The antibody GC 3108 recognizes a linear epitope at the C-terminus of rat GAD, common to both isoforms. Whereas GAD_{67} is a cytoplasmic protein consisting of 594 amino acid residues, GAD_{65} is an amphiphilic and membrane-anchored protein consisting of 585 amino acid residues. There is 65% amino acid sequence homology between the two isoforms (Karlsen et al., 1991; Li et al., 1995, Bu et al., 1992). The hybridoma secreting the antibody to $GAD_{65/67}$ was generated by fusion of splenocytes from a mouse immunized with fragments of recombinant human GAD_{65} fused to glutathione-S-transferase (Ziegler et al., 1996).

An overview of the antibodies used, with the suppliers and dilutions used in the present study, is given in Table 1.

Controls

Controls for each reaction were carried out by the omission of primary antibodies, which in each case led to unstained sections.

Deparaffination procedure

Paraffin-embedded sections were dewaxed in three changes of xylene for 5, 15, and 30 minutes, respectively. Sections were rehydrated in decreasing concentration of alcohol (100%, 96%, 90%, and 70%) and then rinsed in distilled water for 10 minutes. For antigen demasking, the sections were reacted in a solution containing sodium citrate buffer (2.94 g dissolved in 1,000 ml distilled water, pH adjusted to 8.5–9 with 0.1 M sodium hydroxide) at +80°C for 15 minutes in a water-bath. Sections were allowed to cool to room temperature for 15 minutes in citrate buffer, rinsed briefly in distilled water, and transferred to Tris buffer (TBS; pH 7.6) (Jiao et al., 1999).

Visualization of the tracer

To localize the tracer, brainstem sections were immunocytochemically treated with an antibody against WGA (1:1,000), as described previously (Eberhorn et al., 2005). The antigenic sites were visualized with a reaction in 0.025% diaminobenzidine (DAB) and 0.015% H_2O_2 in 0.1 M TBS (pH 7.6) for 10 minutes.

Single immunoperoxidase labeling for CR

All sections were washed in 0.1 M TBS (pH 7.4) before and after pretreatment with 1% H_2O_2, in 0.1 M

TBS for 30 minutes to suppress endogenous peroxidase activity. For detection of CR immunoreactivity, the sections were blocked with 5% normal horse serum in 0.1 M TBS, pH 7.4, containing 0.3% Triton X-100 (Sigma, St. Louis, MO) for 1 hour, and subsequently processed with rabbit anti-CR (1:2,500, Swant, 7699/3H) in TBS with 5% normal horse serum and 0.3% Triton X-100 (Sigma) for 48 hours at 4°C. After several buffer washes in 0.1 M TBS, the sections were incubated in horse anti-rabbit (1:200; Vector) in 0.1 M TBS (pH 7.4) containing 2% bovine serum albumin for 1 hour at room temperature. Following three buffer washes, all sections were incubated in ExtrAvidin-peroxidase (avidin-conjugated horseradish peroxidase, 1:1,000; Sigma) for 1 hour at room temperature. After two rinses in 0.1 M TBS, pH 7.4, and one rinse in 0.05 M Tris buffer, pH 7.6, the antigenic sites were visualized by a reaction in 0.025% DAB and 0.015% H_2O_2 in 0.05 M TBS (pH 7.6) for 10 minutes, which yielded a brown reaction product. After washing, the sections were mounted, air-dried, dehydrated in alcohol, and coverslipped with DPX (Sigma).

Combined immunofluorescence labeling for WGA and CR

In selected cryostat sections, combined immunofluorescence labeling was used to simultaneously detect the tracer WGA and CR. Free-floating sections were pretreated with 5% normal donkey serum in 0.3% Triton X-100 in 0.1 M TBS (pH 7.4) for 1 hour at room temperature. Then sections were incubated in a cocktail containing rabbit anti-CR (1:1,000, Swant 7699/4) and goat anti-WGA (1:250, AS-2024; Axxora, San Diego, CA) in 5% normal donkey serum with 0.3% Triton X-100 in 0.1 M TBS, for 48 hours at 4°C. After three washes in 0.1 M TBS, sections were treated with a cocktail containing Cy^3-tagged donkey anti-rabbit (1:200, Dianova, Jackson ImmunoResearch, West Grove, PA) and Alexa 488–tagged donkey anti-goat (1:200; Molecular Probes, Eugene, OR) in 0.1 M TBS for 2 hours at room temperature. After several buffer rinses, free-floating cryosections were mounted on glass slides and dried at room temperature. Sections were coverslipped with Gel Mount permanent aqueous mounting medium (Biomeda, Foster City, CA) and stored in the dark at 4°C.

Combined immunoperoxidase staining for ChAT and CR

For quantitative analysis of CR-positive terminals, combined immunoperoxidase labeling was used to simultaneously detect ChAT and CR in 10 μm paraffin sections. After the sections were dewaxed, CR was detected by using the single immunostaining protocol (see above), but with a final reaction with 0.025% DAB, 0.2% ammonium nickel sulfate (Riedel-de Haën, Seelze, Germany) and 0.015% H_2O_2 in 0.05 M TBS (pH 7.6) for 10 minutes to yield a black reaction product. After thorough washing and blocking of residual peroxidase activity in 1% H_2O_2 in 0.1 M TBS for 30 minutes, the sections were blocked with 5% normal horse serum in 0.1 M TBS, pH 7.4, containing 0.3% Triton X-100 (Sigma) for 1 hour, and then incubated with goat anti-ChAT (1:100, Millipore AB144P) in 0.1 M TBS, pH 7.4, containing 0.3% Triton X-100 (Sigma) for 48 hours at room temperature. After washing in 0.1 M TBS, the sections were incubated in biotinylated horse anti-goat IgG (1:200; Vector) in TBS containing 2% bovine serum albumin for 1 hour at room temperature. The antigen binding site was detected by incubating sections in ExtrAvidin-peroxidase (1:1,000; Sigma) for 1 hour and a subsequent reaction with 0.025% DAB and 0.015% H_2O_2 in 0.05 M TBS (pH 7.6) for 10 minutes to yield a brown staining. After washing, the sections were mounted, air-dried, dehydrated in alcohol, and coverslipped with DPX (Sigma).

Combined immunfluorescence labeling for CR and GAD

To determine whether CR-positive profiles represent inhibitory GABAergic nerve endings, selected cryosections were immunostained for the simultaneous detection of CR and GAD. Sections were pretreated with 5% normal donkey serum in 0.3% Triton X-100 in 0.1 M TBS (pH 7.4) for 1 hour at room temperature. Then sections were incubated in a cocktail containing either rabbit anti-CR (1:2,500, Swant 7699/3H) and mouse anti-GAD (1:1,000, GC3108; Biotrend, Miramar Beach, FL) or mouse anti-CR (1:1,000, Swant, 6B3) and rabbit anti-$GAD_{65/67}$ (1:500; Millipore AB1511) in 5% normal donkey serum with 0.3% Triton X-100 in 0.1 M TBS (pH 7.4) for 48 hours at 4°C. After three washes in TBS, sections were treated with a cocktail containing Cy^3-tagged donkey anti-mouse (1:200, Dianova, Jackson ImmunoResearch) and Alexa 488–tagged donkey anti-rabbit (1:200; Molecular Probes) in 0.1 M TBS (pH 7.4) and 2% bovine serum albumin for 1 hour at room temperature. After several buffer rinses, free-floating cryosections were mounted on glass slides and dried at room temperature. Sections were coverslipped with Gel Mount permanent aqueous mounting medium (Biomeda) and stored in the dark at 4°C.

Analysis of stained sections

The slides were examined either with a Leica microscope DMRB (Bensheim, Germany) or with a Zeiss

Axioplan microscope (Carl Zeiss MicroImaging, Jena, Germany) equipped with appropriate filters for red fluorescent Cy^3 (Leica: N2.1; excitation filter BP 515–560 nm, dichromatic mirror: 580 nm, suppression filter LP 590 nm; Zeiss: excitation filter BP 546 nm, dichromatic beam splitter FT 580 nm, barrier filter LP 590 nm) and green fluorescent Alexa 488 (Leica: I3; excitation filter BP 450–490 nm, dichromatic mirror: 510 nm, suppression filter LP 515 nm; Zeiss: excitation filter BP 475 nm; dichromatic beam splitter FT 500 nm, barrier filter LP 530 nm).

Photographs were taken with a digital camera (Pixera Pro 600 ES, Klughammer, Markt Indersdorf, Germany), captured on a computer with Pixera Viewfinder software (Klughammer), and processed in Photoshop 7.0 (Adobe Systems, Mountain View, CA). Selected double-labeled immunofluorescence sections were imaged with a Leica TCS SP2 laser-scanning confocal fluorescence microscope (Leica, Heidelberg, Germany). Images were taken with a 63× oil objective at a resolution of approximately 310 nm per pixel. Dual-channel imaging of Alexa 488 and Cy^3 fluorescence was sequentially recorded at 488 nm excitation/525–550 nm emission and 564 nm excitation/555–620 nm emission. Z-series were collected every 0.31 μm through the section. Image stacks were processed by using ImageJ (public domain, Java-based image processing program developed at the National Institutes of Health). The sharpness, contrast, and brightness were adjusted to reflect the appearance of the labeling seen through the microscope. The pictures were arranged and labeled with CorelDraw (version 11.0; Corel, Ottawa, Canada). Purely red–green images were converted to magenta–green in Photoshop and are provided as supplementary material.

Quantification of CR inputs

The CR input to all motoneuronal groups in nIII, nIV, and nVI was quantified by counting immunoreactive punctae along the measured length of the contour of a motoneuron with Image J at a focus plane. The values were transfered onto a spreadsheet table (Microsoft Excel, 2010). The analysis of each chosen group was performed on sections from two different cases. The immunoreactive punctae along the outlines of at least 35 cells in each motoneuron subgroup were counted. Simultaneous ChAT immunolabeling was used to identify the motoneurons in the nuclei. Immunoreactive punctae were counted when the soma and the CR-positive terminal were in the same focal plane and no space was seen between them. The ratio of the number of punctae per μm of cell outline was calculated with Excel software (Microsoft 2010). From there the mean terminal density of inputs and the standard error of the mean were calculated for all motoneuronal subgroups, including those of the LP. Data were analyzed with the PRISM 5 software (GraphPad Prism 5, San Diego, CA). Statistical analysis was performed by using a two-way analysis of variance (ANOVA).

RESULTS

Retrograde labeling of motoneurons for upgaze

To delineate the area within nIII occupied by motoneurons for upgaze, tracer injections were placed into the SR or IO. Tracer injection into the SR led to a selective labeling of motoneurons in the middle portion in the caudal half of the contralateral oculomotor nucleus (nIII). A similar area at the same level in nIII is occupied by the IO motoneurons in the ipsilateral IO. A case in which all upgaze muscles were retrogradely labeled illustrates that IO and SR subgroups of opposite eyes are pretty much intermingled in nIII, although the SR motoneurons are concentrated more medially, and the IO motoneurons more laterally (Fig. 1A). Within the nucleus, labeled dendrites were not observed leaving the IO/SR subdivision to enter the MR/IR subdivision. However, incomplete filling of their dendrites precludes absolute claims in this regard. After tracer injections into the SR, additional labeling was present in the CCN, most likely due to spread of the tracer to the adjacent LP muscle (Porter et al., 1989).

CR within the motonuclei of extraocular muscles

Only few scattered CR-positive neurons were present within the nVI and the rostral nIII, but a cluster of CR-positive cells was seen in the supraoculomotor area (SOA; Figs. 1C, arrows, 2A). These neurons were located within the centrally projecting Edinger–Westphal nucleus (EWcp), which contains non-preganglionic, urocortin-1–positive cells (May et al., 2008; Horn et al., 2008; Kozicz et al., 2011).

Within the motonuclei of extraocular muscles, a large supply of CR-immunoreactive punctae profiles was found. However, these terminals were not evenly distributed. A strong supply of CR-positive punctae profiles was selectively confined to the middle portion of the caudal half of nIII, which corresponds to the IO and SR subgroups (Fig. 1C). Some CR- positive axons were present within nVI and nIV. They mainly traversed these nuclei with only a few fibers terminating (Figs. 1B,D, 3D,F). In addition, strong CR labeling high-lighted the CCN dorsal to the rostral nIV and caudal nIII (Fig. 1B).

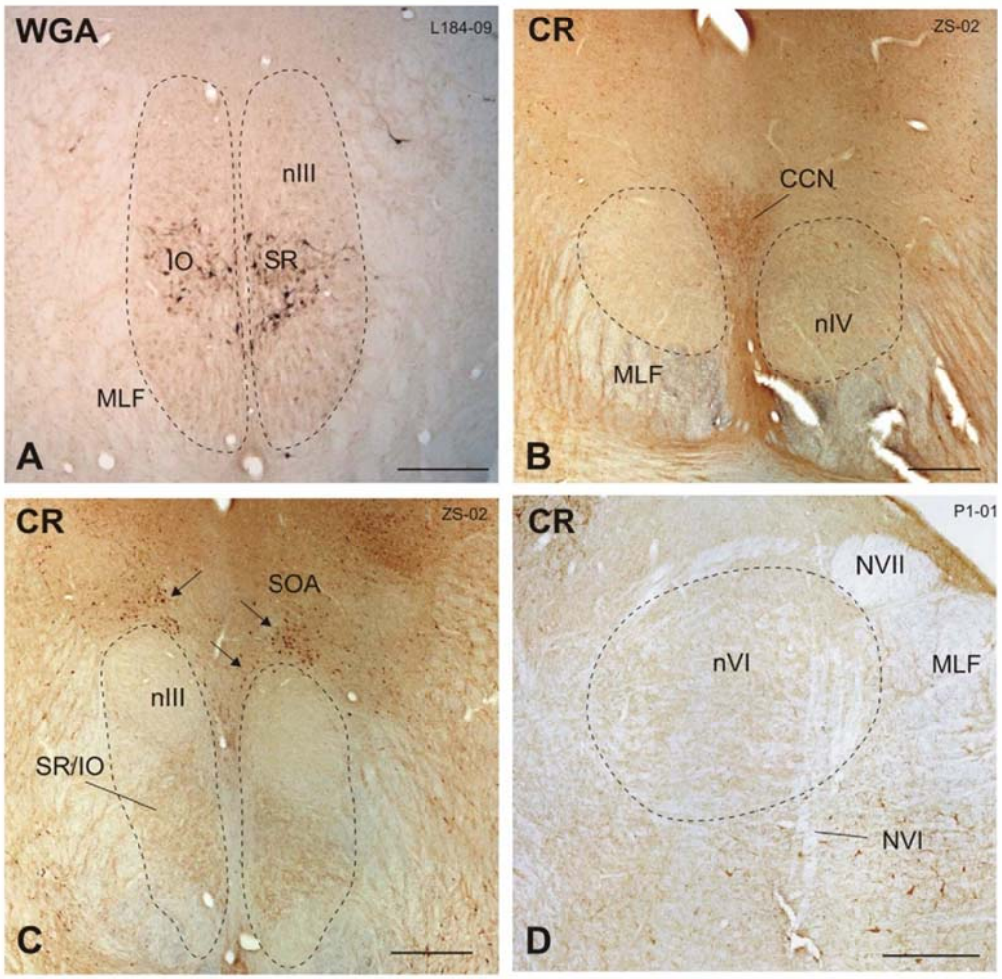

Figure 1. (**A–D**) Frontal sections through the oculomotor (nIII) (A,C), trochlear (nIV) (B), and abducens nucleus (nVI) (D) in monkey. Injections into the inferior oblique (IO) and superior rectus (SR) muscles of the left eye resulted in tracer-labeled neurons in the midportion of nIII. They occupy similar territories, but on different sides: the IO ipsilateral, the SR contralateral (A). Immunostained profiles for calretinin (CR) are confined to the central caudal nucleus (CCN), which contains levator palpebrae motoneurons (B) and the midportion of nIII in the region containing SR and IO motoneurons (C, compare to A), all involved in upgaze. Note the CR-positive neurons in the supraoculomotor area (SOA) (C, arrows). Only a few CR-positive profiles were found in nIV (B) and nVI (D). Scale bar = 500 μm in A–D. MLF, medial longitudinal fascicle; NVII, facial nerve; NVI, abducens nerve.

The ventral and dorsal part of nIII, which contained MR and and IR motoneurons, showed almost no CR-positive punctae (Figs. 1C, 3A,E). Close inspection of sections simultaneously stained for the tracer revealed numerous CR-positive punctate profiles (red) in close association with the dendrites and somata of tracer-labeled motoneurons (in green; Fig. 2B,C) and confirmed that CR-positive profiles were primarily confined to SR, IO, and LP motoneuronal groups (Fig. 2A).

CR and GAD

Close inspection of nIII in double-immunofluorescence preparations for GAD and CR revealed that profiles only contained either CR (green) or the GABA-synthesizing enzyme GAD (red), not both. These observations indicate that CR and GABA inputs represent largely independent afferent systems, with no colocalization, which would have been indicated by a yellow color (Fig. 2D).

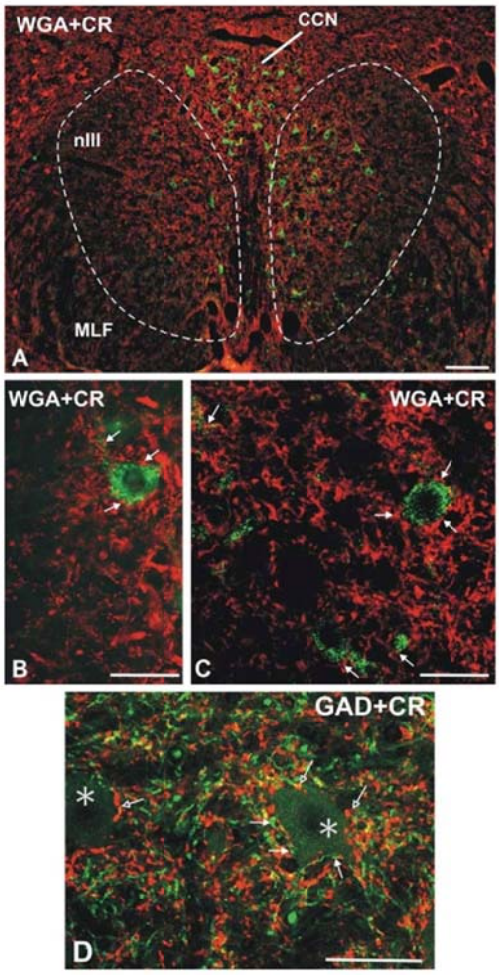

Figure 2. Fluorescence photomicrographs of frontal sections through the oculomotor nucleus (nIII) of a monkey showing the location of tracer-labeled neurons (green) and calretinin (CR)-positive profiles (red). (**A**) The overview demonstrates the location of inferior oblique (IO) in the left nIII, superior rectus (SR) in the right nIII, and levator palpebrae motoneurons (LP) in the central caudal nucleus (CCN). Note that red CR-positive punctate labeling is mainly confined to the IO, SR, and LP subgroups. (**B,C**) Detailed views of fluorescence (B) and confocal scanning analysis (C) demonstrating that numerous CR-positive punctate profiles are in close contact with the dendrites and somata of wheat germ agglutinin (WGA)-labeled motoneurons (white arrows). (**D**) Confocal scanning view shows combined immunofluorescence for glutamate decarboxylase (GAD) in red (white solid arrows) and CR in green (white open arrows). Note that both labeled populations represent largely independent systems, with no colocalization. A magenta-green version of this figure is provided as Supporting Information Figure 1. MLF, medial longitudinal fascicle. Scale bar = 200 μm in A; 50 μm in B–D.

Quantitative analysis of the CR input to the motoneurons of nIII, nIV, and nVI

For further clarification, the CR input to all motoneuronal groups in nIII, nIV, and nVI was quantified by counting immunoreactive punctae along the outlines of the perimeter of somata and proximal dendrites (Figs. 3, 4). The entire populations of every subgroup were quantified, cells without and with associated terminals. As is apparent from visual inspection of the immunocytochemical staining, the strongest CR input was found at motoneurons involved in upgaze, e.g., SR, IO, and LP (Figs. 3B,C, 4). All upgaze motoneurons received a dense supply from CR-positive punctae, which appeared along their cell perimeters at an average density of 0.1 punctae/μm (standard error of the mean [SEM] 0.008) for the LP and 0.08 punctae/μm for the SR/IO (SEM 0.012). In contrast, only a few motoneurons in nVI and nIV were associated with any CR-positive profiles, resulting in an average density of 0.01 punctae/μm for LR motoneurons (SEM 0.002) and 0.018 punctae/μm for the SO motoneurons (SEM 0.004) (Figs. 3D,F, 4). A slightly larger population of IR and MR motoneurons was in close association with a few CR-positive punctae, at an average density of 0.01 punctae/μm (SEM 0.003) for the MR and 0.019 punctae/μm (SEM 0.005) for the IR (Figs. 3A,E, 4). Thus the density of CR-positive punctae around motoneurons for upgaze was significantly stronger compared to those few of downgaze or horizontal gaze ($P < 0.001$; Fig. 4). Even those downgaze and horizontal gaze motoneurons receiving some CR input were contacted by significantly fewer CR-positive punctae, when separately analyzed and compared with the CR input of upgaze motoneurons (Bonferroni's multiple comparison test; $P < 0.001$; data not shown).

DISCUSSION

With combined retrograde-tracer labeling and immunostaining for the calcium-binding protein CR, immunostained terminals were identified, which were rather specifically associated with motoneurons that are active during upgaze (Becker and Fuchs, 1988; Fuchs et al., 1992; Leigh and Zee, 2006). Although not proved by electron microscopic analysis, a direct synaptic relationship between CR-positive terminals and upgaze motoneurons was previously suggested by a study of CR-positive afferents terminating in nIII (Ahlfeld et al., 2011). Upgaze motoneurons include those supplying the SR and IO, as well as the LP motoneurons in CCN, which elevate the upper eyelid (Porter et al., 1989). Several studies have shown that the upper lid closely follows the movement of the globe (Becker and Fuchs, 1988; Evinger et al., 1991). This lid-eye coupling is

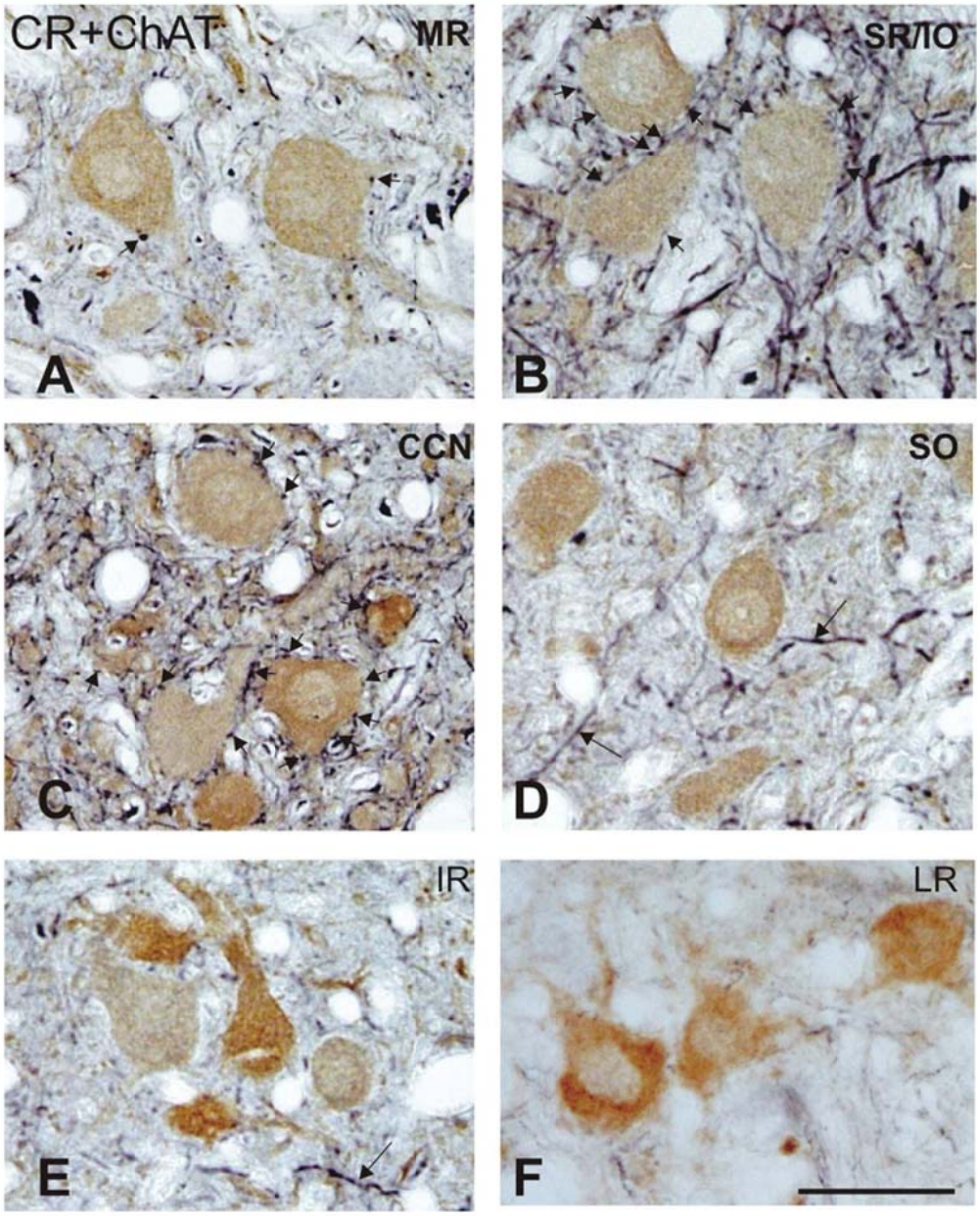

Figure 3. (**A–F**) Frontal sections through the oculomotor nucleus (nIII) (A,B,C,E), the trochlear nucleus (nIV) (D), and the abducens nucleus (nVI) (F) in monkey. Combined immunoperoxidase labeling was used to simultaneously detect choline acetyltransferase (ChAT) in brown and calretinin (CR) in black. Note that motoneuronal subgoups involved in upgaze are covered by numerous calretinin-containing afferents (black) (B,C) whereas only a few motoneurons not involved in upgaze are in contacted by CR (A,D,E,F). Scale bar = 50 μm in F (applies to A–F). CCN, central caudal nucleus; IO, inferior oblique; LR, lateral rectus; SO, superior oblique; and SR, superior rectus motoneurons.

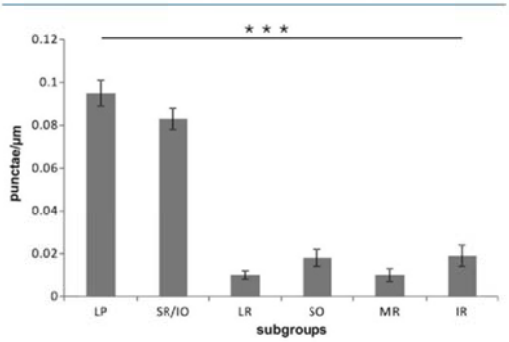

Figure 4. Histogram demonstrating quantitative analysis of the calretinin (CR) input to motoneurons of the oculomotor nucleus (nIII), the trochlear nucleus (nIV), and the abducens nucleus (nVI). The CR input to all motoneuronal groups was quantified by counting immunoreactive punctae along the measured length of the contour of a motoneuron. The mean terminal density of inputs and the standard error of the mean were calculated for all motoneuronal subgroups. The strongest input is seen to the motoneurons of superior rectus (SR), inferior oblique (IO), and levator palpebrae (LP) motoneurons. The number of counted CR-positive punctae associated with upgaze motoneurons is significantly higher compared to those around "non-upgaze" motoneurons (***, $P < 0.001$). IR, inferior rectus; LR, lateral rectus; MR, medial rectus; and SO, superior oblique motoneurons.

mediated by the concomitant activation of the LP, SR, and IO muscles during upward eye movements (Fuchs et al., 1992)—presumably via projections from the M-group (Horn et al., 2000), whereas downward eye movements are caused by the activation of the IR and SO, which is accompanied by the relaxation of the LP (Fuchs et al., 1992).

This observation does not apply for all species. In cat, a rich supply of CR-positive terminals is present within the MR subdivision of nIII. This fits well with the finding that a high percentage (80%) of noncholinergic internuclear neurons within the cat nVI express CR immunoreactivity (De la Cruz et al., 1998), in light of the fact that internuclear neurons activate the MR. Accordingly, the lack of CR-positive terminals in MR subdivisions in monkey goes along with the relative lack of CR-positive neurons in nVI in this species (McCrea and Horn, 2006).

Do CR-containing afferents provide an excitatory or inhibitory input?

Previous work in monkey has shown that the motoneurons of extraocular muscles subserving vertical eye movements receive a strong supply of GABAergic afferents, whereas the nVI and the MR subgroups of nIII receive far fewer GABAergic afferents, and instead receive a strong selective input from glycinergic terminals (Spencer and Baker, 1992; Spencer et al., 1992). Both findings are supported by pharmacological studies (Precht et al., 1973; Spencer et al., 1989). The present study demonstrates that GAD-positive and CR-positive punctae formed independent populations, which did not overlap, indicating that CR-positive afferents are not GABAergic. Because glycine, the other known classical inhibitory neurotransmitter, is not present in terminals contacting the vertical gaze motoneurons of monkey (Spencer and Baker, 1992), the CR-positive profiles contacting motoneurons in nIII in the present study are considered to be excitatory afferents. Electron microscopic analysis is required to prove this point.

Possible sources of CR-positive afferents to upgaze motoneurons

By using combined immunochemistry and tract-tracing methods following an injection of retrograde tracer into the nIII in monkey, the mesencephalic rostral interstitial nucleus of the medial longitudinal fascicle (RIMLF), the interstitial nucleus of Cajal (INC), and the vestibular nuclei, including the Y-group, have been identified as sources of CR afferents to nIII motoneurons (Ahlfeld et al., 2011). The RIMLF is known as the location of premotor saccadic burst neurons for vertical saccades (Büttner-Ennever et al., 1982). Recording and anatomical studies revealed that burst neurons for upward and downward saccades are intermingled within the RIMLF (Büttner-Ennever and Büttner, 1978; Horn and Büttner-Ennever, 1998). All the retrogradely labeled premotor neurons in the RIMLF were found to express the calcium-binding protein parvalbumin, with 40% of them additionally expressing CR (Horn et al., 2003). Because mainly upgaze motoneurons in nIII receive a CR-positive input, it is reasonable to assume that the CR-positive premotor neurons in the RIMLF are up-burst neurons (Ahlfeld et al., 2011).

In monkey the M-group represents another premotor upgaze center targeting motoneurons of SR, IO, and LP (Horn et al., 2000). It is most likely involved in eye–lid coordination. To what extent the M-group contributes CR inputs to upgaze motoneurons remains to be studied. In correspondence to the burst neurons in RIMLF, the CR-positive population in the INC may provide excitatory premotor burst and burst-tonic inputs for upgaze for concomitant activation of the LP motoneurons when SR and IO motoneurons are activated by the RIMLF (Helmchen et al., 1996; Chen and May, 2007; Ahlfeld et al., 2011). The medium-sized secondary vestibulo-ocular neurons in the magnocellular part of the medial and superior vestibular nuclei did not provide a CR input to upgaze

motoneurons (Ahlfeld et al., 2011; Goldberg et al., 2012), but a CR-positive projection arises from small vestibular neurons, which may represent the origin of parallel vestibulo-ocular pathways, which are not directly activated from vertical canal afferents, and numerous medium-sized premotor neurons within the dorsal Y-group, which corresponds to the infracerebellar nucleus (Gacek 1978; Goldberg et al., 2012).

The Y-group is disynaptically activated from vestibular afferents (Highstein and Reisine, 1979; Blazquez et al., 2000), and it is targeted by direct inhibitory afferents from Purkinje cells in the flocculus, most of them coding for downward eye movements (Partsalis et al., 1995; Krauzlis and Lisberger, 1996). Accordingly, the floccular target neurons in the Y-group encode upward eye movements, and electrical activation of the Y-group results in excitatory postsynaptic potentials (EPSPs) in IO and SR subgroups in nIII and slow upward eye movements (Chubb and Fuchs, 1982; Sato and Kawasaki, 1987). In cat, the efferent fibers from the Y-group travelling to the oculomotor nuclei were shown to project mainly through the crossing ventral tegmental tracts (CVTT) (Sato and Kawasaki, 1987; Uchino et al., 1994), and this is suggested for monkey and human as well (Sato and Kawasaki, 1991; Pierrot-Deseilligny and Tilikete, 2008; Zwergal et al., 2009). Together with vestibular nuclei neurons that are targeted by floccular projections, the Y-group participates in the generation of upward smooth-pursuit eye movements (Chubb and Fuchs, 1982). Furthermore, the Y-group is considered as the source of a head-velocity–related oculomotor signal, which is necessary to maintain eye position during head rotation, as seen for the suppression of the vertical vestibulo-ocular reflex (Chubb and Fuchs, 1982). The present and previous results suggest that the projection fibers mediating these functions contain CR (Ahlfeld et al., 2011).

Asymmetrical organization of premotor pathways for vertical eye movements

Although a similar activation pattern of coacting muscle pairs is required for eye movements in both vertical directions, previous studies have indicated that an asymmetry for both directions exists under several aspects. For the saccadic system, a different course of premotor pathways for up- and downgaze is indicated by tract-tracing, experimental lesions, and clinical studies: premotor fibers from the RIMLF targeting upgaze motoneurons travel through the posterior commissure (PC) and activate the contralateral motoneurons of upward moving eye muscles on both sides (Moschovakis et al., 1991a), whereas downgaze motoneurons are controlled only from premotor neurons of the ipsilateral RIMLF (Moschovakis et al., 1991b; Pierrot-Deseilligny, 2011). Accordingly, PC lesions result in an upgaze palsy (Büttner-Ennever et al., 1982; Pierrot-Deseilligny et al., 1982; Partsalis et al., 1994). For the vestibulo-ocular reflex, several excitatory pathways inside and outside the medial longitudinal fascicle (MLF) exist for upward eye movements, but only one pathway via the MLF is known for downward movements (Pierrot-Deseilligny and Tilikete, 2008; Goldberg et al., 2012). Accordingly, small lesions involving different parts of the brainstem or cerebellum can lead to either upbeat or downbeat nystagmus (Büttner et al., 1995; Pierrot-Deseilligny and Milea, 2005; Pierrot-Deseilligny and Tilikete, 2008). Contrary views exist about the influence of gravity, which may also contribute to the asymmetry of vertical eye movements, facilitating downward eye movements and restraining upward eye movements (Pierrot-Deseilligny et al., 2007), which therefore may require supplementary support to rebalance the asymmetry (Pierrot-Deseilligny and Tilikete, 2008). Several clinical studies indicate that upward eye movements are more readily impaired with aging compared to downward eye movements (Chamberlain, 1970; Clark and Isenberg, 2001; Oguro et al., 2004). Whether this is caused by biomechanical changes in the orbit (Clark and Demer, 2002) or degenerative changes with aging remains to be clarified (Henson et al., 2003; Schneider et al., 2011).

Functional significance of calretinin

It is unclear why CR is present in specific premotor pathways of the oculomotor system, such as the upgaze pathway. Whereas the calcium-binding protein parvalbumin is present in many fast-firing or highly active neurons of the oculomotor system, such as the saccadic burst neurons in the RIMLF and interstitial nucleus of Cajal, or the omnipause neurons in the nucleus raphe interpositus (Horn, 2006), no obvious association of CR with specific properties is known. So far, CR has been found in many different types of neurons, for example, in vestibular primary afferents (Desmadryl and Dechesne, 1992), cerebellar granule cells (Bastianelli, 2003), neurons in the auditory nuclei (Clarkson et al., 2010), and interneurons in the hippocampus (Seress et al., 1993). The suggested functions of CR involve a protective role (D'Orlando et al., 2002) or a function in synaptic plasticity (Gurden et al., 1998). Consistent evidence has been found for a central role in regulation of neuronal excitability (Gall et al., 2005; Camp and Wijesinghe, 2009). Accordingly, the specific presence of CR in premotor up-burst neurons of the INC and RIMLF, in addition to parvalbumin, may reflect different calcium control mechanisms for upgaze neurons compared to downgaze neurons (Horn et al., 2003). This may

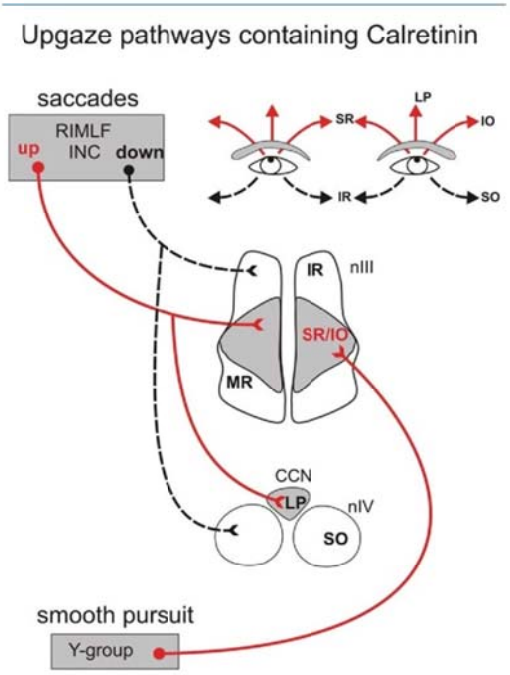

Figure 5. Summary diagram demonstrating the premotor pathways for upward eye movements (red), which are associated with calretinin. RIMLF, rostral interstitial nucleus of the medial longitudinal fascicle; INC, interstitial nucleus of Cajal; CCN, central caudal nucleus; nIII, oculomotor nucleus; nIV, trochlear nucleus; LP, levator palpebrae; SO, superior oblique; MR, medial rectus; IR, inferior rectus and SR, superior rectus motoneurons

correlate with a different vulnerability of the upgaze system in aging (Oguro et al., 2004). A hyperdevelopment of the upgaze system may not only be represented by more numerous parallel pathways compared to the downgaze system, but also by additional calcium-binding proteins, which control the excitability of motoneurons. The increasing impairment of upward eye movements with aging may also be caused by a decline in CR, as has been observed for the auditory system (Ouda et al., 2012).

In conclusion, this is the first description of a difference in the histochemical properties of premotor pathways mediating upgaze versus downgaze in the primate (Fig. 5). Preliminary observations in human brainstem tissue immunostained for CR revealed similar results (Horn et al., 2009). Although the functional relevance is not yet clear and CR is not present in all upgaze pathways, further investigation of these differences may open up experimental or therapeutic strategies to manipulate specific upgaze pathways selectively. In addition, the finding that CR is associated with upgaze pathways may be useful for correlative clinical–anatomical postmortem studies in human to analyze premotor saccadic up-burst neurons in the RIMLF in cases with vertical gaze paresis or the premotor upgaze pathways for lesions in cases with downbeat nystagmus (Leigh and Zee, 2006).

ACKNOWLEDGMENTS

The authors thank Ahmed Messoudi and Carla Bettoni for excellent technical assistance, as well as Michael Faust and Karoline Lienbacher for their help in imaging with the confocal laser scanning microscope in the Department of Biology.

CONFLICT OF INTEREST STATEMENT

The authors declare that they have no conflict of interest.

ROLE OF AUTHORS

All authors had full access to all the data in the study and take responsibility for the integrity of the data and the accuracy of the data analysis. Study concept and design: CZ, BH, and AKEH. Acquisition of data: CZ, BH, and AKEH. Analysis and interpretation of data: CZ and AKEH. Drafting of the manuscript: CZ. Critical revision of the manuscript for important intellectual content: BH. and AKEH. Obtained funding: CZ, BH, and AKEH. Technical and material support: BH. Study supervision: AKEH.

LITERATURE CITED

Ahlfeld J, Mustari M, Horn AKE. 2011. Sources of calretinin inputs to motoneurons of extraocular muscles involved in upgaze. Ann N Y Acad Sci 1233:91–99.

Andressen C, Blümcke I, Celio MR. 1993. Calcium-binding proteins–selective markers of nerve cells. Cell Tissue Res 271:181–208.

Augustine JR, Deschamps EG, Ferguson JGJ. 1981. Functional organization of the oculomotor nucleus in the baboon. Am J Anat 161:393–403.

Baizer JS, Baker JF. 2006. Immunoreactivity for calretinin and calbindin in the vestibular nuclear complex of the monkey. Exp Brain Res 172:103–113.

Bastianelli E. 2003. Distribution of calcium-binding proteins in the cerebellum. Cerebellum 2:242–262.

Becker W, Fuchs AF. 1988. Lid-eye coordination during vertical gaze changes in man and monkey. J Neurophysiol 60:1227–1252.

Blazquez P, Partsalis A, Gerrits NM, Highstein SM. 2000. Input of anterior and posterior semicircular canal interneurons encoding head-velocity to the dorsal Y group of the vestibular nuclei. J Neurophysiol 83:2891–2904.

Bruce G, Wainer BH, Hersh LB. 1985. Immunoaffinity purification of human choline acetyltransferase: comparison of the brain and placental enzymes. J Neurochem 45:611–620.

Bu D-F, Erlander MG, Hitz BC, Tillakaratne NJK, Kaufman DL, Wagner-McPherson CB, Evans GA, Tobin AJ. 1992. Two

human glutamate decarboxylases, 65-kDa GAD and 67-kDa GAD, are each encoded by a single gene. Proc Natl Acad Sci U S A 89:2115–2119.

Büttner-Ennever JA. 2006. The extraocular motor nuclei: organization and functional neuroanatomy. Prog Brain Res 151:95–125.

Büttner-Ennever JA, Akert K. 1981. Medial rectus subgroups of the oculomotor nucleus and their abducens internuclear input in the monkey. J Comp Neurol 197:17–27.

Büttner-Ennever JA, Büttner U. 1978. A cell group associated with vertical eye movements in the rostral mesencephalic reticular formation of the monkey. Brain Res 151:31–47.

Büttner-Ennever JA, Büttner U, Cohen B, Baumgartner G. 1982. Vertical gaze paralysis and the rostral interstitial nucleus of the medial longitudinal fasciculus. Brain 105:125–149.

Büttner U, Helmchen C, Büttner-Ennever JA. 1995. The localizing value of nystagmus in brainstem disorders. Neuro-Ophthalmology 15:283–290.

Camp AJ, Wijesinghe R. 2009. Calretinin: modulator of neuronal excitability. Int J Biochem Cell Biol 41:2118–2121.

Chamberlain W. 1970. Restriction in upward gaze with advancing age. Trans Am Ophthalmol Soc 68:234–244.

Chen B, May PJ. 2007. Premotor circuits controlling eyelid movements in conjunction with vertical saccades in the cat: II. Interstitial nucleus of Cajal. J Comp Neurol 500:676–692.

Chubb MC, Fuchs AF. 1982. Contribution of y group of vestibular nuclei and dentate nucleus of cerebellum to generation of vertical smooth eye movements. J Neurophysiol 48:75–99.

Clark RA, Demer JL. 2002. Effect of aging on human rectus extraocular muscle paths demonstrated by magnetic resonance imaging. Am J Ophthalmol 134:872–878.

Clark RA, Isenberg SJ. 2001. The range of ocular movements decreases with aging. J AAPOS 5:26–30.

Clarke RJ, Alessio ML, Pessoa VF. 1987. Distribution of motoneurones innervating extraocular muscles in the brain of the marmoset (*Callithrix jacchus*). Acta Anat 130:191–196.

Clarkson C, Juíz JM, Merchán MÁ. 2010. Long-term regulation in calretinin staining in the rat inferior colliculus after unilateral auditory cortical ablation. J Comp Neurol 518:4261–4276.

De la Cruz RR, Pastor AM, Martinez-Guijarro FJ, Lopez-Garcia C, Delgado-García JM. 1998. Localization of parvalbumin, calretinin, and calbindin D-28K in identified extraocular motoneurons and internuclear neurons of the cat. J Comp Neurol 390:377–391.

D'Orlando C, Celio MR, Schwaller B. 2002. Calretinin and calbindin D-28k, but not parvalbumin protect against glutamate-induced delayed excitotoxicity in transfected N18-RE 105 neuroblastoma-retina hybrid cells. Brain Res 945:181–90.

Desmadryl G, Dechesne CJ. 1992. Calretinin immunoreactivity in chinchilla and guinea pig vestibular end organs characterizes the calyx unit subpopulation. Exp Brain Res 89:105–108.

Eberhorn AC, Ardeleanu P, Büttner-Ennever JA, Horn AKE. 2005. Histochemical differences between motoneurons supplying multiply and singly innervated extraocular muscle fibers. J Comp Neurol 491:352–366.

Evinger C. 1988. Extraocular motor nuclei: location, morphology and afferents. In: Büttner-Ennever JA, editor. Review of occulomotor research. New York: Elsevier. p 81–117.

Evinger C, Manning KA, Sibony PA 1991. Eyelid movements. Mechanisms and normal data. Invest Ophthalmol Vis Sci 32:387–400.

Fuchs AF, Scudder CA., Kaneko CR. 1988. Discharge patterns and recruitment order of identified motoneurons and internuclear neurons in the monkey abducens nucleus. J Neurophysiol 60:1874–1895.

Fuchs AF, Becker W, Ling L, Langer TP, Kaneko CR. 1992. Discharge patterns of levator palpebrae superioris motoneurons during vertical lid and eye movements in the monkey. J Neurophysiol 68:233–243.

Gacek RR. 1978. Location of commissural neurons in the vestibular nuclei of the cat. Exp Neurol 59:479–491.

Gall D, Roussel C, Nieus T, Cheron G, Servais L, D'Angelo E, Schiffmann SN. 2005. Role of calcium binding proteins in the control of cerebellar granule cell neuronal excitability: experimental and modeling studies. Prog Brain Res 148:321–328.

Goldberg JM, Wilson VJ, Cullen KE, Angelaki DE, Broussard DM, Büttner-Ennever JA, Fukushima K, Minor LB. 2012. The vestibular system. A sixth sense. New York: Oxford University Press.

Gurden H, Schiffmann SN, Lemaire M, Bohme GA, Parmentier M, Schurmans S. 1998. Calretinin expression as a critical component in the control of dentate gyrus long-term. potentiation induction in mice. Eur J Neurosci 10:3029–3033.

Helmchen C, Rambold H, Büttner, U. 1996, Saccade-related burst neurons with torsional and vertical on-directions in the interstitial nucleus of Cajal of the alert monkey. Exp Brain Res 112:63–78.

Henson C, Staunton H, Brett FM. 2003. Does ageing have an effect on midbrain premotor nuclei for vertical eye movement? Mov Disord 18:688–694.

Highstein SM, Reisine H. 1979. Synaptic and functional organization of vestibulo-ocular reflex pathways. Prog Brain Res 50:431–442.

Horn AKE. 2006. The reticular formation. Prog Brain Res 151:127–155.

Horn AKE, Büttner-Ennever JA. 1998. Premotor neurons for vertical eye-movements in the rostral mesencephalon of monkey and man: the histological identification by parvalbumin immunostaining. J Comp Neurol 392:413–427.

Horn AKE, Büttner-Ennever JA, Gayde M, Messoudi A. 2000 Neuroanatomical identification of mesencephalic premotor neurons coordinating eyelid with upgaze in the monkey and man. J Comp Neurol 420:19–34.

Horn AKE, Brückner G, Härtig W, Messoudi A. 2003. Saccadic omnipause and burst neurons in monkey and human are ensheathed by perineuronal nets but differ in their expression of calcium-binding proteins. J Comp Neurol 455:341–352.

Horn AKE, Eberhorn A, Härtig W, Ardeleanu P, Messoudi A, Büttner-Ennever JA. 2008. Perioculomotor cell groups in monkey and man defined by their histochemical and functional properties: reppraisal of the Edinger-Westphal nucleus. J Comp Neurol 507:1317–1335.

Horn AKE, Che Ngwa E, Büttner-Ennever JA. 2009. Histochemistry and location of motoneuron subgroups in the oculomotor nucleus of human. Soc Neurosci Abstr 35:356.10.

Ichikawa T, Shimizu T. 1998. Organization of choline acetyltransferase-containing structures in the cranial nerve motor nuclei and spinal cord of the monkey. Brain Res 779:96–103.

Jiao Y, Sun Z, Lee T, Fusco FR, Kimble TD, Meade CA, Cuthbertson S, Reiner A. 1999. A simple and sensitive antigen retrieval method for free-floating and slide-mounted tissue sections. J Neurosci Methods 93:149–162.

Karlsen AE, Hagopian WA, Grubin CE, Dube S, Disteche CM, Adler DA, Bärmeier H, Mathewes S, Grant FJ, Foster D and Lernmark A. 1991. Cloning and primary structure of a human islet isoform of glutamic acid decarboxylse from chromosome 10. Proc Natl Acad Sci U S A 88:8337–8341.

Kozicz T, Bittencourt JC, May PJ, Reiner A, Gamlin PDR, Palkovits M, Horn AKE, Toledo CAB, Ryabinin AE. 2011. The Edinger-Westphal nucleus: a historical, structural, and functional perspective on a dichotomous terminology. J Comp Neurol 519:1413–1434.

Krauzlis RJ, Lisberger SG.1996. Directional organization of eye movement and visual signals in the floccular lobe of the monkey cerebellum. Exp Brain Res 109:289–302.

Leigh RJ, Zee DS (eds.). 2006. The neurology of eye movements. New York: Oxford University Press.

Li L, Jiang J, Hagopian WA, Karlsen AE, Skelly M, Baskin DG, Lernmark A. 1995. Differential detection of rat islet and brain glutamic acid decarboxylase (GAD) isoforms with sequence-specific peptide antibodies. J Histochem Cytochem 43:53–59.

May PJ, Reiner AJ, Ryabinin AE. 2008. Comparison of the distributions of urocortin-.containing and cholinergic neurons in the perioculomotor midbrain of the cat and Macaque. J Comp Neurol 507:1300–1316.

McClung JR, Shall MS, Goldberg J. 2001. Motoneurons of the lateral and medial rectus extrocular muscles in squirrel monkey and cat. Cell Tissue Org 168:220–227.

McCrea RA, Horn AKE. 2006. Nucleus prepositus. Prog Brain Res 151:205–230.

Moschovakis AK, Scudder CA, Highstein SM. 1991a. The structure of the primate oculomotor burst generator. I. Medium-lead burst neurons with upward on-directions. J Neurophysiol 65:203–217.

Moschovakis AK, Scudder CA, Highstein SM, Warren JD. 1991b. The structure of the primate oculomotor burst generator. II. Medium-lead burst neurons with downward on-directions. J Neurophysiol 65:218–229.

Nguyen LT, Spencer RF. 1999. Abducens internuclear and ascending tract of Deiters. Inputs to medial rectus motoneurons in the cat oculomotor nucleus: neurotransmitters. J Comp Neurol 411:73–86.

Oguro H, Okada K, Suyama N, Yamashita K, Yamaguchi S, Kobayashi S. 2004. Decline of vertical gaze and convergence with aging. Gerontology 50:177–181.

Ouda L, Burianova J, Syka J. 2012. Age-related changes in calbindin and calretinin immunoreactivity in the central auditory system of the rat. Exp Gerontol 47:497–506.

Partsalis AM, Highstein SM, Moschovakis AK. 1994. Lesions of the posterior commissure disable the vertical neural integrator of the primate oculomotor system. J Neurophysiol 71:2582–2585.

Partsalis AM, Zhang Y, Highstein SM. 1995. Dorsal Y group in the squirrel monkey. II. Contribution of the cerebellar flocculus to neuronal responses in normal and adapted animals. J Neurophysiol 73:632–650.

Pierrot-Deseilligny C. 2011. Nuclear, internuclear, and supranuclear ocular motor disorders. In: Kennard C, Leigh RJ, editors. Handbook of clinical neurology. New York: Elsevier. p 319–331.

Pierrot-Deseilligny C, Milea D. 2005. Vertical nystagmus: clinical facts and hypotheses. Brain 128:1237–1246.

Pierrot-Deseilligny C, Tilikete C. 2008. New insights into the upward vestibulo-oculomotor pathways in the human brainstem. Prog Brain Res 171:509–518.

Pierrot-Deseilligny C, Chain F, Gray F, Serdaru M, Escourolle R, Lhermitte F. 1982. Parinaud's syndrome: electro-oculographic and anatomical analyses of six vascular cases with gaze organization in the premotor structures. Brain 105:667–696.

Pierrot-Deseilligny C, Richeh W, Bolgert F. 2007. Upbeat nystagmus due to a caudal medullary lesion and influenced by gravity. J Neurol 254:120–121.

Porter JD, Burns LA, May PJ. 1989. Morphological substrate for eyelid movements: innervation and structure of primate levator palpebrae superioris and orbicularis oculi muscles. J Comp Neurol 287:64–81.

Precht W, Baker R, Okada Y. 1973. Evidence for GABA as the synaptic transmitter of the inhibitory vestibulo-ocular pathway. Exp Brain Res 18:415–428.

Reisine H, Highstein SM.1979. The ascending tract of Deiters' conveys a head velocity signal to medial rectus motoneurons. Brain Res 170:172–176.

Sakurai T. 2007. The neural circuit of orexin (hypocretin): maintaining sleep and wakefulness. Nat Rev Neurosci 8:171–181.

Sato Y, Kawasaki T. 1987. Target neurons of floccular caudal zone inhibition in Y-group nucleus of vestibular nuclear complex. J Neurophysiol 57:460–480.

Sato Y, Kawasaki T. 1991. Identification of the Purkinje cell/climbing fiber zone and its target neurons responsible for eye-movement control by the cerebelar flocculus. Brain Res Rev 16:39–64.

Schneider R, Chen AL, King SA, Riley DE, Gunzler SA, Devereaux MW, Leigh RJ. 2011. Influence of orbital eye position on vertical saccades in progressive supranuclear palsy. Ann N Y Acad Sci 1233:64–70.

Schreyer S, Büttner-Ennever JA, Tang X, Mustari MJ, Horn AKE. 2009. Orexin-A inputs onto visuomotor cell groups in the monkey brain. Neuroscience 164:629–640.

Schwaller B, Brückner G, Celio MR, Härtig W. 1999. A polyclonal goat antiserum against the calcium-binding protein calretinin is a versatile tool for various immunocytochemical techniques. J Neurosci Methods 92:137–144.

Seress L, Nitsch R, Leranth C. 1993. Calretinin immunoreactivity in the monkey hippocampal formation–I. Light and electron microscopic characteristics and co-localization with other calcium-binding proteins. Neuroscience 55:775–796.

Spencer RF, Baker R. 1992. GABA and glycine as inhibitory neurotransmitters in the vestibulo-ocular reflex. Ann N Y Acad Sci 656:602–611.

Spencer RF, Porter JD. 1981. Innervation and structure of extraocular muscles in the monkey in comparison to those of the cat. J Comp Neurol 198:649–665.

Spencer RF, Wang S-F. 1996. Immunhistochemical localization of neurotransmitters utilized by neurons in the rostral interstitial nucleus of the medial longitudinal fasciculus (riMLF) that project to the oculomotor and trochlear nucleus in cat. J Comp Neurol 366:134–148.

Spencer RF, Wenthold RJ, Baker R. 1989. Evidence for glycine as an inhibitory neurotransmitter of vestibular, reticular, and prepositus hypoglossi neurons that project to the cat abducens nucleus. J Neurosci 9:2718–2736.

Spencer RF, Wang S-F, Baker R. 1992. The pathways and functions of GABA in the oculomotor system. Prog Brain Res 90:307–331.

Uchino Y, Sasaki M, Isu N, Hirai N, Imagawa M, Endo K, Graf WM. 1994. Second-order vestibular neuron morphology of the extra-MLF anterior canal pathway in the cat. Exp Brain Res 97:387–396.

Ziegler B, Augstein A, Schröder D, Mauch L, Hahmann J, Schlosser M, Ziegler M. 1996. Glutamate decarboxylase (GAD) is not detectable on the surface of rat islet cells examined by cytofluorometry and complement-dependent antibody-mediated cytotoxicity of monoclonal GAD antibodies. Horm Metab Res 28:11–15.

Zwergal A, Strupp M, Brandt T, Büttner-Ennever J. 2009. Parallel ascending vestibular pathways: anatomical localization and functional specialization. Ann N Y Acad Sci 1164:51–59.

frontiers in Neuroanatomy

ORIGINAL RESEARCH
published: 24 July 2015
doi: 10.3389/fnana.2015.00095

Transmitter inputs to different motoneuron subgroups in the oculomotor and trochlear nucleus in monkey

*Christina Zeeh[1], Michael J. Mustari[2], Bernhard J. M. Hess[3] and Anja K. E. Horn[1]**

[1] Institute of Anatomy and Cell Biology, Department I, Ludwig-Maximilians University, Munich, Germany, [2] Washington National Primate Research Center and Department of Ophthalmology, University of Washington, Seattle, WA, USA, [3] Vestibulo-Oculomotor Laboratory Zürich, Department of Neurology, University Hospital, Zürich, Switzerland

In all vertebrates the eyes are moved by six pairs of extraocular muscles enabling horizontal, vertical and rotatory movements. Recent work showed that each extraocular muscle is controlled by two motoneuronal groups: (1) Motoneurons of singly-innervated muscle fibers (SIF) that lie within the boundaries of motonuclei mediating a fast muscle contraction; and (2) motoneurons of multiply-innervated muscle fibers (MIF) in the periphery of motonuclei mediating a tonic muscle contraction. Currently only limited data about the transmitter inputs to the SIF and MIF motoneurons are available. Here we performed a quantitative study on the transmitter inputs to SIF and MIF motoneurons of individual muscles in the oculomotor and trochlear nucleus in monkey. Pre-labeled motoneurons were immunostained for GABA, glutamate decarboxylase, GABA-A receptor, glycine transporter 2, glycine receptor 1, and vesicular glutamate transporters 1 and 2. The main findings were: (1) the inhibitory control of SIF motoneurons for horizontal and vertical eye movements differs. Unlike in previous primate studies a considerable GABAergic input was found to all SIF motoneuronal groups, whereas a glycinergic input was confined to motoneurons of the medial rectus (MR) muscle mediating horizontal eye movements and to those of the levator palpebrae (LP) muscle elevating the upper eyelid. Whereas SIF and MIF motoneurons of individual eye muscles do not differ numerically in their GABAergic, glycinergic and vGlut2 input, vGlut1 containing terminals densely covered the supraoculomotor area (SOA) targeting MR MIF motoneurons. It is reasonable to assume that the vGlut1 input affects the near response system in the SOA, which houses the preganglionic neurons mediating pupillary constriction and accommodation and the MR MIF motoneurones involved in vergence.

Keywords: Glycine, GABA, vGlut, C-group, extraocular muscles

Abbreviations: AD, averaged density; AMPA receptors, α-amino-3-hydroxy-5-methyl-4-isoxazolepropionic acid receptor; ATD, ascending tract of Deiters; CCN, central caudal nucleus; ChAT, choline acetyltransferase; CMRF, central mesencephalic reticular formation; CR, calretinin; CTB, Cholera toxin subunit B; EWpg, preganglionic Edinger-Westphal nucleus; GABA, gamma-aminobutyric acid; GABA-A, GABA-A receptor; GAD, glutamate decarboxylase; GlyR, glycine receptor; GlyT, glycine transporter; INC, interstitial nucleus of Cajal; INT, internuclear neurons; IO, inferior oblique muscle; IPSP, inhibitory postsynaptic potential; IR, inferior rectus muscle; LP, levator palpebrae muscle; LR, lateral rectus muscle; LVN, lateral vestibular nucleus; MIF, multiply-innervated muscles fibers; MLF, medial longitudinal fasciculus; MR, medial rectus muscle; MVN, medial vestibular nucleus; MVNm, MVN magnocellular part; MVNp, MVN parvocellular part; nIII, oculomotor nucleus; nIV, trochlear nucleus; NMDA, N-methyl-D-aspartate; nVI, abducens nucleus; PPH, prepositus nucleus; RIMLF, rostral interstitial nucleus of the medial longitudinal fasciculus; SIF, singly-innervated muscles fibers; SO, superior oblique muscle; SOA, supraoculomotor area; SR, superior rectus muscle; SVN, superior vestibular nucleus; SVNm, SVN magnocellular part; TBS, Tris buffered saline; vGlut, vesicular glutamate transporter; VOR, vestibulo-ocular reflex; WGA-HRP, wheat germ agglutinin conjugated to horseradish peroxidase.

OPEN ACCESS

Edited by:
Ricardo Insausti, University of Castilla-La Mancha, Spain

Reviewed by:
José M. Delgado-García, University Pablo de Olavide, de Seville, Spain
Zoltan Rusznak, Neuroscience Research Australia, Australia

***Correspondence:**
Anja K. E. Horn, Institute of Anatomy and Cell Biology, Department I, Ludwig-Maximilians University, Pettenkoferstraße 11, D-80336 Munich, Germany
anja.bochtler@med.uni-muenchen.de

Received: 07 May 2015
Accepted: 06 July 2015
Published: 24 July 2015

Citation:
Zeeh C, Mustari MJ, Hess BJM and Horn AKE (2015) Transmitter inputs to different motoneuron subgroups in the oculomotor and trochlear nucleus in monkey. Front. Neuroanat. 9:95. doi: 10.3389/fnana.2015.00095

Introduction

The vertebrate eye is rotated by six extraocular muscles: four recti (superior, inferior, medial and lateral recti muscles) and two oblique muscles (superior and inferior oblique). The muscles are innervated by motoneurons lying in the tegmentum of the brainstem. Motoneurons of the oculomotor nucleus (nIII) innervate the ipsilateral medial rectus (MR), inferior rectus (IR), inferior oblique (IO) and contralateral superior rectus (SR) muscles. Motoneurons of the trochlear nucleus (nIV) control the contralateral superior oblique muscle (SO), and motoneurons of the abducens nucleus (nVI) activate the ipsilateral lateral rectus (LR) muscle (Büttner-Ennever, 2006). The levator palpebrae (LP) motoneurons lie in a separate cluster at the midline in caudal nIII termed the central caudal nucleus (CCN; Porter et al., 1989).

Each eye muscle has a highly complex morphology and consists of at least six different muscle fiber types, which can be divided into two main categories. Firstly, there are slowly contracting (non-twitch) muscle fibers innervated by multiple "en grappe" endplates that are distributed along the whole muscle fiber (multiply-innervated fibers, MIF). Secondly, there are fast contracting (twitch) muscle fibers innervated by one single "en plaque" ending in the middle third of the muscle fiber (singly-innervated fibers, SIF; Chiarandini and Stefani, 1979; Lynch et al., 1994; for review: Spencer and Porter, 2006). Tract-tracing experiments in monkey and rat revealed that the MIF and SIF motoneurons of all eye muscles form anatomically separated populations. SIF motoneurons lie within the boundaries of the classical motonuclei (nIII, nIV, nVI), whereas the MIF motoneurons appear in subgroups in the periphery of the motonuclei (Büttner-Ennever et al., 2001; Eberhorn et al., 2005). Thereby, in monkey the MIF motoneurons of the MR and IR are situated together in the C-group at the dorsomedial border of nIII. Those of IO and SR are located midline within the S-group sandwiched between the two oculomotor nuclei. The MIF motoneurons of the SO form a dorsal cap of nIV, and those of the LR are arranged as a shell around the medial and ventral aspect of nVI (Büttner-Ennever et al., 2001). Recent studies in monkey revealed that neurons within these peripheral cell groups also give rise to the palisade endings located at the myotendinous junctions of MIFs (Lienbacher et al., 2011; Zimmermann et al., 2011).

Experiments injecting retrograde transsynaptic tracers into monkey eye muscles revealed that SIF and MIF motoneurons receive inputs from different premotor neurons subserving different functions. Whereas SIF motoneurons are targeted by premotor afferents involved in the generation of eye movements, e.g., saccadic burst neurons, secondary vestibulo-ocular neurons, the peripheral MIF motoneurons are targeted mainly by afferents from premotor sources involved in gaze holding (Wasicky et al., 2004; Ugolini et al., 2006).

Significant progress has been made in the histochemical characterization of premotor inputs to motoneurons of individual extraocular eye muscles (for review: McElligott and Spencer, 2000; Horn, 2006; Sekirnjak and du Lac, 2006). These inputs differ in several points, one of them being the selective association of the calcium-binding protein calretinin (CR) with nerve endings targeting motoneurons involved in upgaze (Zeeh et al., 2013). Monkey studies with different methodical approaches suggest that GABA is the major inhibitory neurotransmitter of premotor neurons involved in vertical eye movements, whereas glycine acts as inhibitory transmitter of premotor neurons mediating horizontal eye movements (Spencer et al., 1989, 1992; Spencer and Baker, 1992). So far, few attempts have been made to study differing transmitter-related inputs to MIF vs. SIF motoneurons (Ying et al., 2008). In the present study we investigated the presence of glycinergic, GABAergic and glutamatergic inputs to SIF and MIF motoneurons of nIII and nIV in monkey. Preliminary results have been reported in abstract form (Schulze et al., 2009).

Materials and Methods

The tracer injections were undertaken either at the Department of Neurology at the University Hospital in Zürich (case 2) or at the National Primate Research Center at the University of Washington in Seattle (case 1). All experimental procedures conformed to the state and university regulations for laboratory animal care, including the Guide Principles of Laboratory Animal Care (NIH 8th edition, revised 2011) and they were approved by animal care officers and the institutional Animal Care and Use Committees. The surgical procedures for tracer-injections into the extraocular muscle were described in detail in a previous report (Büttner-Ennever et al., 2001). All experimental cases are listed in **Table 1**.

To identify the MR MIF motoneurons prior to glutamate decarboxylase (GAD) or vesicular glutamate transporters (vGlut) immunostaining, two macaque monkeys (case 1, case 2) received a tracer injection of cholera toxin subunit B (CTB) into the MR of the left eye. Each monkey was therefore sedated with Ketamine (Ketalar 1–2 mg/kg) and kept in a surgical plane of anesthesia using Isoflurane inhalation. Under sterile conditions, the MR of the left eye was exposed by retracting the eye lid and by making a conjunctival incision. Volumes of 5 µl (case 1) and 3 µl (case 2) of CTB (1% in aqua bidest) were injected into the myotendinous junctions of the left MR. For post-operative treatment the monkeys received antibiotics and analgesics.

After a survival time of 4 days, the monkeys were euthanized with an overdose of sodium-pentobarbital (80 mg/kg body weight, Merial, Halbergmoos, Germany). Then, the animals were transcardially perfused with 0.9% saline followed by either 4% paraformaldehyde in 0.1 M phosphate buffer or a mixture of 1% paraformaldehyde and 2.5% glutaraldehyde (for GABA staining) in 0.1 M phosphate buffer. Paraformaldehyde fixed brain tissue of five additional monkeys (case 3, case 4, case 5, case 6, case 9) and glutaraldehyde fixed brain tissue of two monkeys (case 7, case 8), all from other projects without eye muscle injections, were used for immunohistochemical staining of transmitter-related proteins only. The brains were removed from the skull and immersed in 10% sucrose in 0.1 M phosphate buffer and transferred to 30% sucrose for frozen sectioning. Alternatively,

one 4% paraformaldehyde-fixed brain was embedded in paraffin.

Frozen sections of the brainstems were cut at 40 μm in the transverse stereotaxic plane using a cryostat (MICROM HM 560) and collected free-floating in cold 0.1 M phosphate buffer (pH 7.4). The paraffin block was cut at 10 μm using a sliding microtome (Leica, SM 2000 R) and mounted on superfrost slides (Thermo Scientific, Menzel-Gläser Superfrost Plus). A case from a previous study was used to demonstrate the location of MR SIF and MIF motoneurons (case 10) in **Figure 1** (Büttner-Ennever et al., 2001).

Immmunocytochemical Labeling

Immunohistochemistry was performed on cryo-sections (free-floating) or on paraffin-sections (on slide) applying the antibodies directed against the following antigens: GABA (mAB93), glycine transporter 2 (GlyT2), glycine receptor 1 (GlyR1). On selected sections the motoneurons were identified with the cholinergic marker anti-choline acetyltransferase (ChAT) and combined with immunostaining for either: (1) GABA-A receptor (GABA-A); (2) glutamate decarboxylase (GAD); (3) vesicular glutamate transporter 1 (vGlut1); or (4) vesicular glutamate transporter 2 (vGlut2).

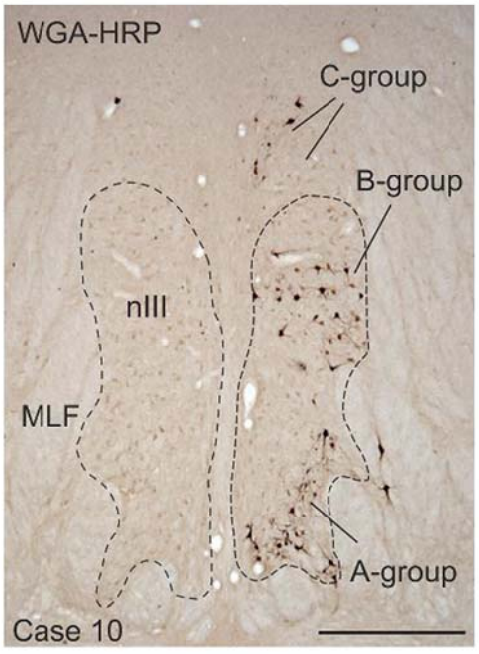

FIGURE 1 | Coronal section through the oculomotor nucleus (nIII) of a monkey, who had received an injection with wheat germ agglutinin-horseradish peroxidase (WGA-HRP) into the medial rectus (MR) muscle of the right eye. Retrogradely labeled neurons are found at three locations: ventral in the A-group, dorsolateral in the B-group and in the periphery dorsomedial to nIII in the C-group.Within the C-group motoneurons of multiply-innervated muscle fibers (MIF) in the MR are located in the medial part. Scale bar = 500 μm.

An overview of all antibodies with dilutions is given in **Table 2**.

Antisera

Cholera Toxin Subunit B (CTB)

The polyclonal goat anti-choleragenoid antibody (703, LOT 10327A4A, List Laboratories Inc., Campbell, CA, USA) was used to detect the tracer CTB (103B, List) provided by the same manufacturer. This tracing and detection method has been successfully applied in numerous previous studies (e.g., Büttner-Ennever et al., 2001).

GABA93 MAb

A monoclonal antibody against GABA (GABA93 MAb) was used for the detection of GABA. The specificity of GABA 93 MAb has been published previously (Holstein et al., 2004).

GABA-A Receptor (GABA-A)

For the detection of GABA-A receptors, we used a monoclonal antibody directed against the beta-chain of the GABA-A receptor (MAB341; formerly Roche 1381458, LOT 0612047758, Clone BD17, Chemicon now part of Milipore, Billerica, MA, USA; Bedford et al., 2001). This antibody is purified from GABA benzodiazepine receptor from bovine cortex.

Glutamate Decarboxylase (GAD)

Alternatively, GABAergic terminals were detected with a mouse monoclonal antibody against the GABA-synthetizing enzyme GAD ($GAD_{65/67}$ GC3108, batch number Z05507, clone 1111, Biotrend, Cologne, Germany) or the rabbit polyclonal antibody against glutamate decarboxylase 65&67 (AB1511, LOT NG17374444, Millipore, Billerica, MA, USA). This antibody is derived from a synthetic peptide from the carboxy-terminus as predicted from the cloned rat GlyT2.

Glycine Receptor (GlyR)

A mouse monoclonal antibody against the glycine-receptor was used to detect its localization (146 111, clone mAb2b (GlyR2b), Synaptic Systems, Goettingen, Germany). This antibody mAb2b specifically binds to the N-terminus of the alpha-1-subunit of the glycine receptor (Lorenzo et al., 2006).

Vesicular Glutamate Transporters (vGluts)

Two different types of vGluts were detected in the study: vGlut1 and vGlut2.

For vGlut1 rabbit polyclonal antibodies were used (1350303, Synaptic Systems, Goettingen, Germany) that were generated against fusion proteins containing glutathione-S-transferase and carboxy-terminal and vGlut1 specific peptides (Bellocchio et al., 1998; Takamori et al., 2000). For the immunolabeling of vGlut2, a rabbit polyclonal antibody was used (8135402, Synaptic Systems, Goettingen, Germany). This antibody was developed against fusion proteins containing glutathione-S-transferase and fragments from the carboxy-terminus of rat vGlut2 (Fremeau et al., 2001; Takamori et al., 2001).

Choline Acetyltransferase (ChAT)

Cholinergic motoneurons were detected with a polyclonal antibody against ChAT raised in goat (AB144P, LOT LV1583390, Millipore, Billerica, MA, USA). The antibody is directed against the whole enzyme isolated from human placenta, which is identical to the brain enzyme (Bruce et al., 1985).

Controls

Controls for each primary antibody were carried out by the omission of primary antibodies, which in each case led to unstained sections.

Deparaffination Procedure

Paraffin embedded sections were dewaxed in three changes of xylene for 5, 15 and 30 min, respectively. Sections were rehydrated in decreasing concentration of alcohol and then rinsed in distilled water for 10 min. For antigen demasking the sections were reacted in 0.01M sodium citrate buffer (pH 8.5–9) at +80°C in a waterbath for 15 min. Then, sections in citrate buffer were allowed to cool down to room temperature for 15 min, rinsed shortly in distilled water and transferred to Tris buffered saline (TBS; pH 7.6) for subsequent immunostaining (Jiao et al., 1999).

Visualization of the Tracer

To localize the tracer, brainstem sections were immunohistochemically stained with a polyclonal goat antibody against CTB (1:20,000; List Biological laboratories, 703) as described previously (Eberhorn et al., 2006). The antigenic sites were visualized with a reaction in 0.025% diaminobenzidine and 0.015% H_2O_2 in 0.1 M TBS (pH 7.6) for 10 min.

Combined Immunoperoxidase Labeling for Tracer and Different Markers

In selected frozen sections combined immunoperoxidase labeling was used to simultaneously detect the tracer CTB and either GAD or vGlut1. All sections were washed in 0.1 M TBS (pH 7.4) and treated with 1% H_2O_2 in 0.1 M TBS for 30 min to suppress endogenous peroxidase activity. The sections were blocked with 5% normal horse serum in 0.1 M TBS, pH 7.4, containing 0.3% Triton X-100 (Sigma, St. Louis, MO, USA) for 1 h, and subsequently processed with either rabbit anti-vGlut1 (1:3000, Synaptic Systems, 135003) or mouse anti-GAD (1:4000, Biotrend GC 3108) in TBS with 5% normal horse serum and 0.3% Triton X-100 for 48 h at room temperature. After several buffer washes in 0.1 M TBS, the sections were incubated in biotinylated horse anti-rabbit (for vGlut1 1:200; Vector laboratories, Burlingame, CA, USA) or biotinylated horse anti-mouse (for GAD 1:200; Vector laboratories, Burlingame, CA, USA) in 0.1 M TBS (pH 7.4) containing 2% bovine serum albumin for 1 h at room temperature. Following three buffer washes, all sections were incubated in ExtrAvidin-peroxidase (avidin conjugated horseradish peroxidase, 1:1000; Sigma, St. Louis, MO, USA) for 1 h at room temperature. After two rinses in 0.1 M TBS, pH 7.4, and one rinse in 0.05 M TBS, pH 7.6, the antigenic sites were visualized by a reaction in 0.025% DAB, 0.2% ammonium nickel sulfate (Riedl-De Haën; Germany) and 0.015% H_2O_2 in 0.05 M TBS (pH 7.6) for 10 min, which yielded a black reaction-product. For the detection of CTB the sections were immunocytochemically treated with anti-CTB (1:20,000, List Biological Laboratories, 703) and visualized with a reaction in 0.025% diaminobenzidine and 0.015% H_2O_2 in 0.1 M TBS (pH 7.6) for 10 min which yielded a brown-reaction product as described above. After washing, the sections were mounted, air-dried, dehydrated in alcohol and cover-slipped with DPX (Sigma, St. Louis, MO, USA).

Combined Immunofluorescence Labeling for Tracer and Different Markers

Selected frozen sections were immunostained for the simultaneous detection of CTB and GAD or vGlut1. After a pretreatment with 5% normal donkey serum in 0.3% Triton X-100 (Sigma, St. Louis, MO, USA) in 0.1 M TBS (pH 7.4) at room temperature for 1 h sections were incubated in a cocktail containing goat anti-CTB (1:5000, List Biological Laboratories, 703) and either rabbit anti-$GAD_{65/67}$ (1:500, Millipore, AB1511) or rabbit anti-vGlut1 (1:1000, Synaptic Systems, 135303) in 5% normal donkey serum with 0.3% Triton X-100 in 0.1 M TBS (pH 7.4) at 4°C for 48 h. After three washes in TBS, sections were treated with a cocktail containing Cy^3-tagged donkey anti-rabbit (1:200, Dianova, Jackson Immuno Research, Baltimore, MA, USA) and Alexa-488 tagged donkey anti-goat (1:200; Molecular Probes, OR, USA) in 0.1 M TBS (pH 7.4) and 2% bovine serum albumin for 2 h at room temperature. After several buffer rinses free-floating frozen sections were mounted on glass slides and dried at room temperature. Sections were cover-slipped with GEL/MOUNT permanent aqueous mounting medium (Biomeda, CA, USA) and stored in the dark at 4°C.

Single Immunoperoxidase Labeling for Transmitter and Transmitter Related Proteins

Frozen or paraffin sections were immunocytochemically treated with antibodies against one of the following antigens: GABA (93MAb), glycine transporter 2 (GlyT2), glycine receptor (GlyR) or vesicular glutamate transporter 2 (vGlut2). All sections were washed in 0.1 M TBS (pH 7.4) and then pretreated with 1% H_2O_2 in 0.1 M TBS for 30 min and thoroughly washed. The sections were then blocked with either 5% normal horse serum (for GABA or GlyR) or 5% normal rabbit serum (for GlyT2) or 5% normal goat serum (for vGlut2) in 0.1 M TBS, pH 7.4 containing 0.3% Triton X-100 (Sigma, St. Louis, MO, USA) for 1 h. This was followed by an incubation in either mouse anti-GABA (1:3000, Holstein), mouse anti-GlyR1 (1:1000, Synaptic Systems 146 111) in TBS with 5% normal horse serum and 0.3% Triton X-100 or sheep anti-GlyT2 (1:5000, Millipore AB1771) in TBS with 5% normal rabbit serum and 0.3% Triton X-100 or rabbit anti-vGlut2 (1:500, Synaptic Systems 135402) in TBS with 5% normal goat serum and 0.3% Triton X-100 at room temperature for 48 h. After several buffer washes in 0.1 M TBS the sections were incubated in either biotinylated horse anti-mouse IgG (1:200; Vector laboratories, Burlingame, CA, USA; for GABA or GlyR) or biotinylated rabbit anti-sheep (1:200; Vector laboratories, Burlingame, CA, USA; for GlyT2) or biotinylated goat anti-rabbit (1:200; Vector laboratories, Burlingame, CA,

USA; for vGlut2) in TBS containing 2% bovine serum albumin at room temperature for 1 h. Antigenic sites were detected after incubation in ExtrAvidin-peroxidase (avidin conjugated horseradish peroxidase, 1:1000; Sigma, St. Louis, MO, USA) and subsequent reaction in 0.025% diaminobenzidine and 0.015% H_2O_2 in 0.05 M TBS (pH 7.6) for 10 min to yield a brown reaction product (see above). For vGlut2 the antigenic sites were visualized with a reaction in 0.025% diaminobenzidine, 0.2% ammonium nickel sulfate (Riedl-De Haën; Germany) and 0.015% H_2O_2 in 0.05 M Tris-buffer (pH 7.6) for 10 minto yield a black reaction-product. After washing, the sections were mounted, air-dried, dehydrated in alcohol and cover-slipped with DPX (Sigma, St. Louis, MO, USA).

Combined Immunoperoxidase Labeling for ChAT and Different Markers

In selected frozen and paraffin sections, combined immunoperoxidase labeling served to simultaneously detect ChAT and either GABA-A, GAD, vGlut1 or vGlut2.

Therefore the sections were washed in 0.1 M TBS (pH 7.4) and then pretreated with 1% H_2O_2 in 0.1 M TBS for 30 min. After washing, the sections were blocked with 5% normal horse serum in 0.1 M TBS, pH 7.4, containing 0.3% Triton X-100 (Sigma, St. Louis, MO, USA) for 1 h and subsequently processed with mouse antibodies against either GABA-A receptor (1:1000, Chemicon, now Millipore, MAB341) or GAD (1:4000, Biotrend, Cologne, Germany GC3108) or with rabbit antibodies against either vGlut1 (1:3000, Synaptic Systems, 135303) or vGlut2 (1:500, Synaptic Systems, 135402) in TBS with 5% normal horse serum and 0.3% Triton X-100 at room temperature for 48 h. After several buffer washes in 0.1 M TBS, the sections were incubated in biotinylated horse anti-mouse IgG (1:200; Vector laboratories, Burlingame, CA, USA; for GABA-A receptor and GAD) or biotinylated horse anti-rabbit IgG (1: 200; Vector laboratories, Burlingame, CA, USA; for vGlut1 and vGlut2) in TBS containing 2% bovine serum albumin for 1 h at room temperature. After several buffer washes and an 1 h incubation in ExtrAvidin-peroxidase (avidin conjugated horseradish peroxidase, 1:1000; Sigma, St. Louis, MO, USA) at room temperature antigenic sites were detected with 0.025% diaminobenzidine, 0.2% ammonium nickel sulfate (Riedl-De Haën; Germany) and 0.015% H_2O_2 in 0.05 M TBS (pH 7.6) for 10 min to yield a black reaction-product.

For the subsequent detection of ChAT, sections were thoroughly washed and incubated in 1% H_2O_2 in 0.1 M TBS for 30 min to block residual peroxidase activity. Then, the sections were incubated in 5% normal horse serum in 0.1 M TBS, pH 7.4, containing 0.3% Triton X-100 (Sigma, St. Louis, MO, USA) for 1 h, and treated with goat anti-ChAT (1:100, Millipore AB144P) in 0.1 M TBS, pH 7.4, containing 0.3% Triton X-100 for 48 h at room temperature. After washing in 0.1 M TBS, the sections were incubated in biotinylated horse anti-goat IgG (1:200; Vector laboratories, Burlingame, CA, USA) in TBS containing 5% bovine serum albumin for 1 h at room temperature. The antigen binding sides were detected by incubating sections in ExtrAvidin-peroxidase (avidin conjugated horseradish peroxidase, 1:1000; Sigma, St. Louis, MO, USA) and a subsequent reaction with 0.025% diaminobenzidine and 0.015% H_2O_2 in 0.05 M TBS (pH 7.6) for 10 min to yield a brown staining. After washing, the sections were mounted, air-dried, dehydrated in alcohol and cover-slipped with DPX (Sigma, St. Louis, MO, USA).

Analysis of Stained Sections

The slides were examined and analyzed with a Leica microscope DMRB (Bensheim, Germany). Photographs were taken with a digital camera (Pixera Pro 600 ES; Klughammer, MarktIndersdorf, Germany) mounted on the microscope. The images were captured on a computer with Pixera Viewfinder software (Klughammer) and processed with Photoshop 7.0 (Adobe Systems, Mountain View, CA, USA). In each complete image the sharpness, contrast, and brightness were adjusted using the unsharp mask and levels adjustment tool of Photoshop until the appearance of the labeling seen through the microscope was achieved. The images were arranged and labeled with CorelDraw (version 11.0; Corel Corporation).

The dual immunofluorescence staining of selected sections was imaged with a Leica TCS SP5 laser-scanning confocal fluorescence microscope (Leica, Heidelberg, Germany). Images were taken with a 63× oil objective at a resolution of approximately 310 nm per pixel. Dual-channel imaging of Alexa 488 and Cy^3 fluorescence was sequentially recorded at 488 nm excitation/525–550 nm emission and 564 nm excitation/555–620 nm emission. Z-series were collected at 0.31 µm optical sections taken through the section. Image stacks were processed using ImageJ (public domain, Java-based image processing program developed at the National Institutes of Health).

Puncta Counts and Cell Perimeter Measurements

The GAD-, and GlyT2- input to ChAT-positive motoneurons of nIII and nIV was quantified by counting immunoreactive puncta along the measured length of the contour of a motoneuron with Image J as described previously (Che Ngwa et al., 2014). Only those GAD-positive/Gly-positive puncta were counted, that were in the same focal plane as the attached somata and no space was seen between them suggestive for direct synaptic inputs. The analysis of each chosen group was performed on 10 µm paraffin sections. Frozen sections from two additional cases were used as a visual control for these results. At least 22 cells in each motoneuron group were analyzed.

For the quantitative analysis of GAD inputs to MR MIF motoneurons within the C-group the respective motoneurons had been pre-labeled by a tracer injection into the MR (see "Tracer Injection Case" Section). In that case the immunocytochemical detection of the tracer was combined with immunolabeling for GAD. IR MIF motoneurons were identified on the basis of their location within the C-group. The MR MIF motoneurons lie more medially, whereas the IR-MIF motoneurons lie closer to the dorsomedial border of nIII (Tang et al., 2015).

The ratio of the number of puncta per µm of cell outline was calculated with Excel software (Microsoft 2010).

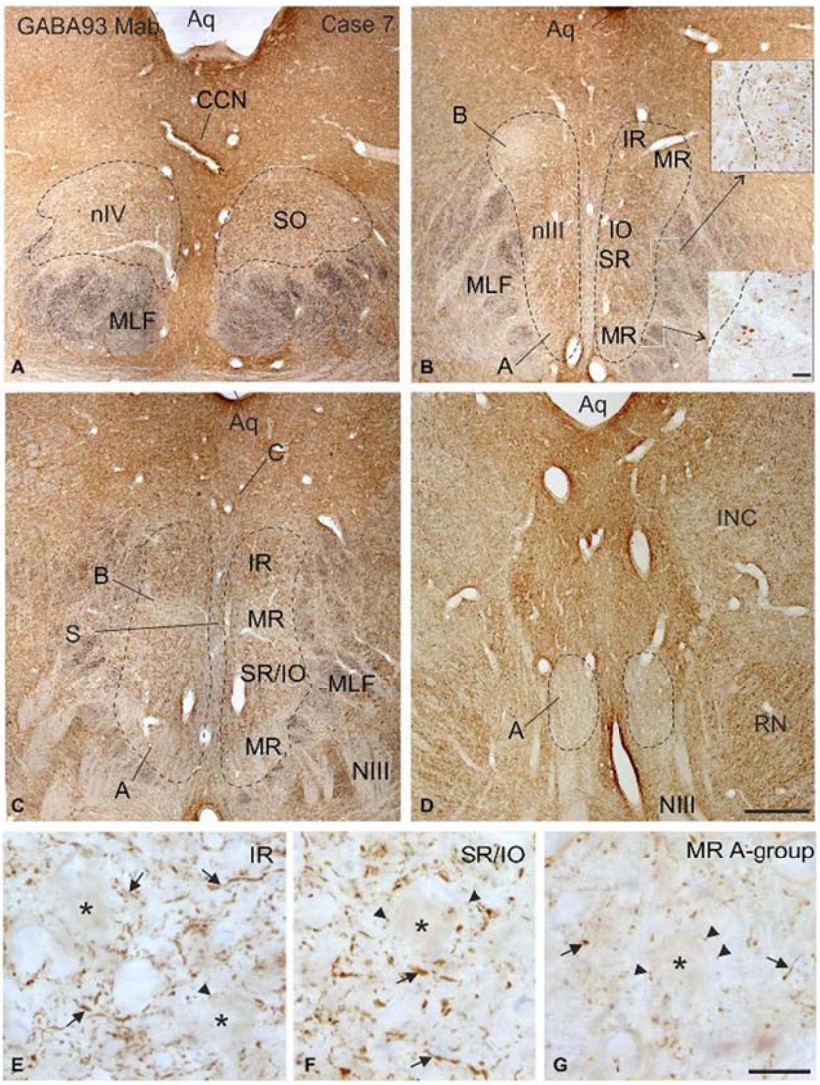

FIGURE 2 | Overview of coronal sections through the oculomotor (nIII) and trochlear nucleus (nIV) in monkey to demonstrate the immunostaining for gamma-aminobutyric acid (GABA). A dense labeling of GABA-positive terminals is found in nIV. **(A)** All subgroups in nIII express a similar strong GABA-immunoreactivity, except the MR A and B-group, where a weaker labeling is observed **(B–D)**. Note numerous GABAergic fibers are present in the medial longitional fascicle (MLF) next to the middle part of nIII containing motoneurons of vertically pulling eye muscles (**B**, upper inset), whereas much fewer GABA-positive fibers are found within the MLF portion adjacent to the MR A-group (**B**, lower inset). Detailed views of motoneuronal groups for vertical **(E,F)** and horizontal eye movements **(G)** reveal that most GABA immunoreactive profiles represent traversing fibers and cut axons (arrows) and only weakly stained puncta may form terminals (arrow heads) around motoneuronal somata (**E–G**, asterisks). Aq, aqueduct; CCN, central caudal nucleus, NIII, oculomotor nerve; INC, interstitial nucleus of Cajal; IO, inferior oblique muscle; RN, red nucleus; SR, superior rectus muscle; MlF, multiply innervated muscle fibers. Scale bar = 500 μm in **(D)** (applies to **A–D**); 30 μm in inset of **(B)**; scale bar = 30 μm in **(G)** (applies to **E–G**).

The average and mean terminal density of inputs, and the standard error of the mean, were calculated for all motoneuronal subgroups, including those of the LP. Data were analyzed with the PRISM 5 software (GraphPad Prism 5, San Diego, CA, USA). Statistical analysis was performed using a one-way analysis of variance (ANOVA) followed by a Bonferroni ś Multiple Comparison Test (*post hoc* test) to determine the differences between all subgroups (11 groups for the statistical analysis of GABAergic input, **Figure 5**; nine groups for the statistical analysis of glycinergic input **Figure 8**). The results were considered statistically significant at $p < 0.05$.

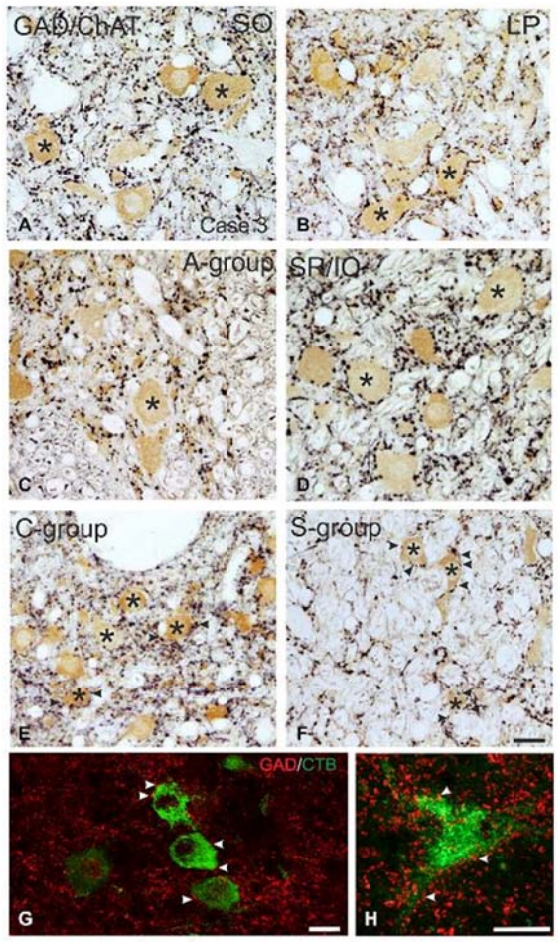

FIGURE 3 | Detailed view of coronal paraffin sections of the oculomotor (nIII) and trochlear nucleus (nIV) in the midbrain stained for glutamate decarboxylase (GAD) in black and choline acetyltransferase (ChAT) in brown (A–F). Numerous GAD-positive puncta outline most of the motoneuronal somata (asterisks) of the superior oblique (SO) **(A)** the levator palpebrae muscle (LP) **(B)** and the subgroup containing superior rectus (SR) and IO muscles. **(D)** In the MR subgroups fewer GAD-positive puncta are attached to the somata (**C**, asterisk), but are found in the neuropile contacting cut dendrites. A considerable number of GAD-positive puncta is found around MIF motoneurons in the C-group and S-group (**E,F**, asterisks indicate motoneurons; arrows). Detailed views of confocal images in **(G,H)** show tracer labeled MR MIF motoneurons (green) in the C-group that are in close association with GAD-positive (red) puncta suggestive for direct synaptic inputs (arrowheads). MIF, multiply innervated muscle fibers. Scale bar = 25 μm in **(F)** (applies to **A–F**); Scale bar = 25 μm in **(G)**; Scale bar = 25 μm in **(H)**.

Results

Tracer Injection Case

Medial Rectus Muscle

Injection into the MR resulted in selective labeling of three motoneuron subgroups as described earlier and shown in **Figure 1** (Büttner-Ennever et al., 2001). The A-group lies in the ventral and ventrolateral part of nIII and extends throughout the whole nIII except the most caudal part. The B-group forms a circular cell group located dorsolaterally in the caudal half of nIII. The peripheral C-group dorsomedial to the nuclear boundaries of nIII consists of MIF motoneurons and extends throughout the whole rostrocaudal length of the nIII (**Figure 1**).

GABAergic Input

SIF Motoneurons

Immunolabeling for different GABAergic markers resulted in a strong GABA- and GAD-expression within the motoneuronal subgroups of SR, IO and IR in nIII (**Figures 2B,C, 3D**). Similarily, the SO motoneurons in nIV and the LP motoneurons in CCN expressed strong immunoreactivity for GABA and GAD (**Figures 2A, 3A,B**). Visual inspection of all sections revealed a weaker GABA immunoreactivity in the MR subgroups, e.g., the ventral A-group and dorsolateral B-group, which are considered to be the SIF MR motoneurons (**Figures 2B,C,D**; Büttner-Ennever et al., 2001; Eberhorn et al., 2005). The weaker immunolabeling in MR subgroups was not so evident in sections immunostained for GAD (**Figure 3C**). The detailed views in **Figure 2** demonstrate a strong GABA-expression in axons travelling within the medial longitudinal fascicle (MLF; **Figures 2A–C**, insets in **Figure 2B**) and within the motoneuronal subgroups of eye muscles mediating vertical (**Figures 2E,F**, arrows) and horizontal gaze (**Figure 2G**, arrows). The rather weak GABA-immunoreactivity in presumed nerve endings around motoneurons (**Figures 2E–G**, asterisks) may be one reason for the differences seen in the GAD and GABA-staining pattern (**Figures 2E–G**, arrowheads). Since GAD immunoreactivity was strongly expressed in nerve endings (Ottersen and Storm-Mathisen, 1984), thin paraffin sections stained for GAD were used for the quantitative analysis of GABAergic input to motoneurons (**Figure 3**). The counting revealed a similarly dense GAD-positive puncta supply around the somata of presumed SIF motoneurons for SR/IO, IR, SO and LP in CCN with an averaged density (AD) of 0.08 puncta/μm (**Table 3**; **Figures 3A,B,D, 5**). SIF motoneurons of MR were contacted by fewer GAD-positive puncta, with an AD of 0.05 puncta/μm for the A-group and 0.06 puncta/μm for the B-group (**Table 3**; **Figures 3C, 5**). Immunostaining for the GABA-A receptor reflected that of GAD and GABA (**Figure 4**) with a weaker expression within the MR subgroups (**Figure 4**, compare C, F to G).

MIF Motoneurons

The close inspection of presumed non-twitch MIF motoneurons revealed the following picture. A high density of GAD-immunoreactive puncta and a strong immunostaining for GABA-A receptor was present in the C-group containing MR and IR MIF motoneurons (**Figures 3E, 4D**). This observation was clarified by the analysis of tracer-labeled MR MIF motoneurons for GAD-immunoreactivity. Numerous GAD-positive profiles were in close proximity to tracer-labeled MIF motoneurons suggesting synaptic contacts (**Figures 3G,H**, arrowheads). Similarily, numerous GAD-positive puncta were found around cholinergic neurons in the S-group, which represent MIF

TABLE 1 | An overview of injection, fixation and immunohistochemistry details for each case.

Case	Injection	Fixation	Sections	Immunhistochemistry
1	3 µl CTB, MR	4% paraformaldehyde	Frozen	CTB, CTB + GAD, CTB + vGlut1
2	5 µl CTB, MR	4% paraformaldehyde	Frozen	CTB, CTB + GAD
3		4% paraformaldehyde	Paraffin	GAD, vGlut1 or vGlut2 + ChAT
4		4% paraformaldehyde	Frozen	GABA-A +ChAT, GlyT2
5		4% paraformaldehyde	Frozen	GlyR
6		4% paraformaldehyde	Frozen	GlyT2
7		1% paraformaldehyde 2, 5% glutaraldehyde	Frozen	GABA
8		4% paraformaldehyde 0, 3% glutaraldehyde	Frozen	GABA
9		4% paraformaldehyde	Frozen	vGlut2
10	WGA-HRP	4% paraformaldehyde	Frozen	

CTB, cholera toxin subunit B; GAD, glutamate decarboxylase; vGlut, vesicular glutamate transporter; ChAT, choline acetyltransferase; GABA, gamma-aminobutyric acid, GABA-A, GABA receptor; GlyT, glycine transporter; GlyR, glycine receptor; MR, medial rectus muscle; WGA-HRP, wheat germ agglutinin conjugated to horseradish peroxidase.

motoneurons of SR and IO (**Figure 3F** arrows), and in the dorsal cap of nIV containing MIF motoneurons of SO (not shown).

The quantitative analysis for the MIF motoneurons resembled the visual impression and revealed a strong supply of GAD-positive puncta for the S-group, the C-group (both 0.09 puncta/µm) and for the SO MIF motoneurons (0.08 puncta/µm; **Figure 5**). The analysis of the GAD input to tracer-labeled MR motoneurons in the C-group revealed an AD of 0.07 puncta/µm for the MR MIF motoneurons and 0.1 puncta/µm for IR MIF motoneurons.

To determine the differences between the different motoneuronal groups within nIII and nIV, 11 subgroups were compared to each other (see **Figure 5**). According to ANOVA and the subsequent Bonferroniś Multiple Comparison Test a significant difference was determined between following subgroups (**Figure 5**): IR MIF motoneurons received a significantly higher GAD-positive supply compared to motoneurons of the A- and B-group. Motoneurons of the C- and S-group were contacted by significantly more GAD-positive puncta compared to MR SIF motoneurons of the A-group. For more details see **Figure 5**.

Immunohistochemical Localization of Glycine

Glycine Transporter 2 (GlyT2) and Glycine-Receptor 1 (GlyR1)

SIF Motoneurons

The strongest expression of glycine markers was found within the CCN. No differences in location and intensity in immunostaining were noted between GlyT2 and GlyR1 within the CCN, where the somata and proximal dendrites of LP motoneurons were completely outlined by immunoreactive puncta (**Figures 6A,D**, **7A,B**). This was confirmed by the quantitative analysis of GlyT2 input revealing an AD of 0.15 puncta/µm (**Figure 8**). A strong GlyT2 expression was also found in the MR A- and B-group (**Figures 6B,C,F,H**). In the subgroups containing motoneurons of the vertical pulling eye muscles only few GlyT2-positive traversing fibers and

TABLE 2 | An overview of the primary antibodies and dilutions used for immunolabeling.

Antibody	Host	Antigen	Manufacturer	Cat. No.	Dilution
GABA-A	Mouse	GABA-A receptor, beta-chain	Chemicon, now Millipore, Billerica, USA	MAB341	1:1000
GABA93 MAb	Mouse	GABA-glutaraldehyde-BSA conjugate	Holstein et al. (2004)	Holstein G, Mt. Sinai, Hospital, New York	1:3000
GAD	Mouse	Glutamate decarboxylase	Biotrend, Cologne, Germany	GC3108	1:4000
$GAD_{65/67}$	Rabbit	Glutamate decarboxylase	Millipore; Billerica, USA	AB1511	1:500 (fluorescence)
GlyT2	Sheep	Glycine transporter 2 (neuronal)	Millipore; Billerica, USA	AB1771	1:5000
GlyR	Mouse	Glycine receptor alpha-1-subunit	Synaptic systems, Goettingen, Germany	146 111	1:1000
ChAT	Goat	Choline acetyltransferase human placental enzyme	Millipore, Billerica, USA	AB144P	1:100
CTB	Goat	Choleragenoid	List Biological Laboratories, Campbell, California	703	1:20,000 1:5000 (fluorescence)
vGlut1	Rabbit	Vesicular glutamate transporter 1	Synaptic systems, Goettingen, Germany	135303	1:3000 1:1000 (fluorescence)
vGlut2	Rabbit	Vesicular glutamate transporter 2	Synaptic systems, Goettingen, Germany	135402	1:500

TABLE 3 | Quantification of GABAergic and glycinergic input to nIV and nIII subgroups.

GAD			Glycine		
Subgroups	**Puncta/μm**	**SEM**	**Subgroups**	**Puncta/μm**	**SEM**
SIF SR/IO	0.08	0.008	SIF SR/IO	0.02	0.006
SIF IR	0.08	0.007	SIF IR	0.01	0.004
SIF SO	0.08	0.008	SIF SO	0.01	0.004
LP	0.08	0.005	LP	0.15	0.015
SIF MR A	0.05	0.006	SIF MR A	0.06	0.006
SIF MR B	0.06	0.006	SIF MR B	0.07	0.006
MIF SR/IO	0.09	0.007	MIF SR/IO	0.02	0.008
MIF MR	0.07	0.005	MIF MR/IR	0.08	0.01
MIF IR	0.01	0.005			
MIF SO	0.08	0.005	MIF SO	0.02	0.01

SEM, standard error of the mean.

GlyT2-positive puncta attached to motoneuronal somata were detected (**Figures 6E,G**, arrows). The GlyR1-staining pattern resembled this observation (**Figures 7C,F**), but revealed only a weak immunoreactivity in the MR A- and B-group as well (**Figures 7C,E**, arrows). The systematic quantitative analysis confirmed a dense supply of GlyT2-positive putative terminals of SIF MR motoneurons in the A-group with an AD of 0.06 puncta/μm, and 0.07 puncta/μm for the B-group (**Table 3**). In contrast, only a low number of GlyT2-positive puncta was found attached to IR (0.01 puncta/μm), SR/IO (0.02 puncta/μm) and SO SIF motoneurons (0.01 puncta/μm; **Figures 6A,C,G, 8**).

MIF Motoneurons

The results for the C-group MIF motoneurons were similar to those of the MR SIF motoneurons within nIII. A considerable supply of glycinergic puncta was noted to the MIF motoneurons of the MR and IR in the C-group (0.08 puncta/μm; **Table 3**; **Figures 6C,H**, arrows) also seen in immunostaining for GlyR1 (**Figures 7C,D**, arrows). Putative MIF motoneurons of the S-group were located between traversing GlyT2-positive fibers (**Figure 6I**, arrowheads), but only few puncta profiles (0.02 puncta/μm) were in contact with the cell bodies (**Table 3**; **Figure 6I**, arrows). The same observation was made for putative SO MIF motoneurons in the dorsal cap of nIV (0.02 puncta/μm; **Table 3**; **Figure 6E**, arrow). To determine the differences between the different motoneuronal groups within nIII and nIV, nine subgroups were compared to each other (see **Figure 8**). According to ANOVA and the subsequent Bonferroni ś Multiple Comparison Test a significant difference was found between following subgroups (**Figure 8**): LP motoneurons in the CCN were contacted by significantly more GlyT2-positive puncta compared to MR SIF motoneurons of the A- and B-group, motoneurons of SR/IO and IR and compared to MIF motoneurons of the S-, C-group and of SO. The A- and B-group were associated with significantly more GlyT2-positive profiles compared to motoneurons of SR/IO, IR, and SO (**Figures 6B,C,E,F,G**). Motoneurons of the A- and B-group receive more GlyT2 inputs compared to MIF motoneurons of the S-group and of SO (**Figures 6F,I**). In addition, the density of the GlyT2 -positive puncta profiles to the C-group was significantly higher compared to the input to MIF motoneurons of the S-group and those of SO. The GlyT2 input to the C-group was also denser compared to that of SIF motoneurons of SR/IO, IR and SO. Thus the

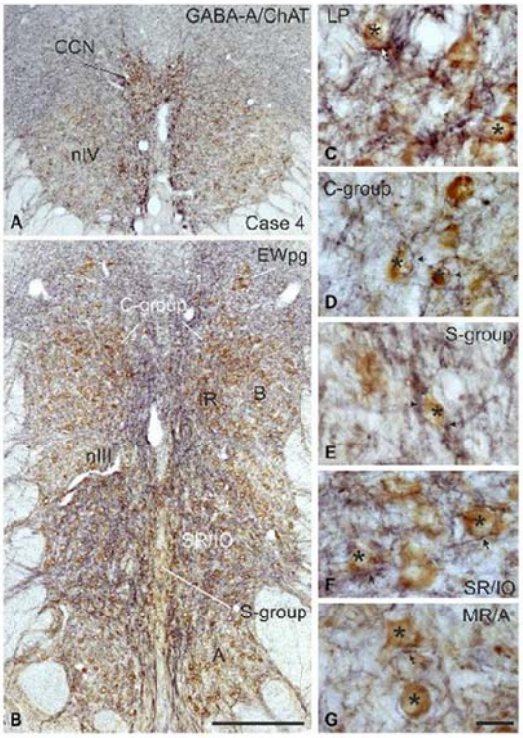

FIGURE 4 | Coronal sections of the oculomotor (nIII) and trochlear nucleus (nIV) of monkey stained for GABA-A receptor (GABA-A) in black and choline acetyltransferase (ChAT) in brown. The overview in **(A,B)** shows a strong GABA-A immunoreactivity associated with the motoneurons of the levator palpebrae muscle (LP) in the CCN, with those of the superior oblique in nIV **(A)** and SR and IO motoneurons. **(B)** The detailed views demonstrate the strong GABA-A expression (arrows) around motoneurons (asterisks) of the LP and SR/IO **(C,F)** and MIF-subgroups C and S **(D,E)** compared to MR SIF motoneurons of the A-group **(G)** GABA, gamma-aminobutyric acid; MIF, multiply innervated muscle fibers; SIF, singly innervated muscle fibers. Scale bar = 400 μm in **(B)** (applies to **A,B**); 30 μm in **(G)** (applies to **C–G**).

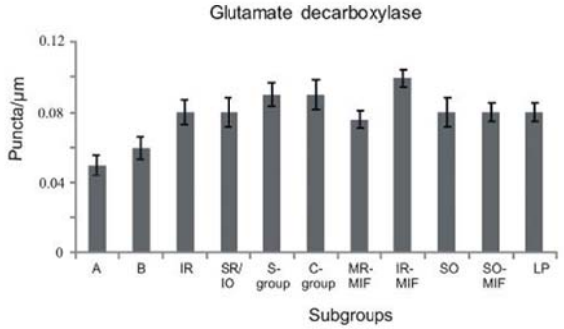

Subgroups with significant differences

ANOVA, Bonferroni's Multiple Comparison Test	
subgroups	summary
A vs C-group	*(p < 0.05)
A vs S-group	*(p < 0.05)
A vs IR-MIF	***(p < 0.001)
B vs IR-MIF	*(p < 0.05)

FIGURE 5 | Histogram demonstrating the quantitative analysis of glutamate decarboxylase (GAD) input to motoneurons of oculomotor (nIII) and trochlear nucleus (nIV). The mean terminal density of stained puncta and the standard error of the mean were calculated for all motoneural subgroups. Note a similar strong input to almost all motoneuronal subgroups in nIII and nIV. Only the motoneurons of MR (A- and B-group) receive a weaker supply by GAD-positive terminals. The table shows the results of the ANOVA and following Bonferroni's Multiple Comparison Test.

density of GlyT2-positive puncta around SIF motoneurons for horizontal eye movements was significantly higher compared to those for vertical eye movements. For more details see **Figure 8**.

Immunohistochemical Localization of vGlut

Immunolabeling for vGlut revealed that the nIII and nIV were completely devoid of vGlut1-positive terminals and neurons, except for a weak puncta labeling along the midline between both nIII (**Figures 9A–C**). A dense cluster of vGlut1-positive terminals was seen dorsolateral to nIII (**Figure 9C**). The supraoculomotor area (SOA) above nIII and the perioculomotor region around nIII contain fewer vGlut1 positive puncta (**Figure 9B**). At close inspection it was obvious that a considerable number of vGlut1-positive puncta was attached to putative MR MIF motoneurons in the medial C-group, but not IR MIF motoneurons (**Figures 9C,F**, arrows; Tang et al., 2015). Unlike for vGlut1, an even dense supply of vGlut2-positive puncta was found within nIII covering the somata of all motoneuronal subgroups (**Figure 10A**). Detailed views revealed a similar dense supply of vGlut2-positive puncta to MIF and SIF motoneurons as shown here for the C-group and SR/IO subgroup (**Figures 10B,C**).

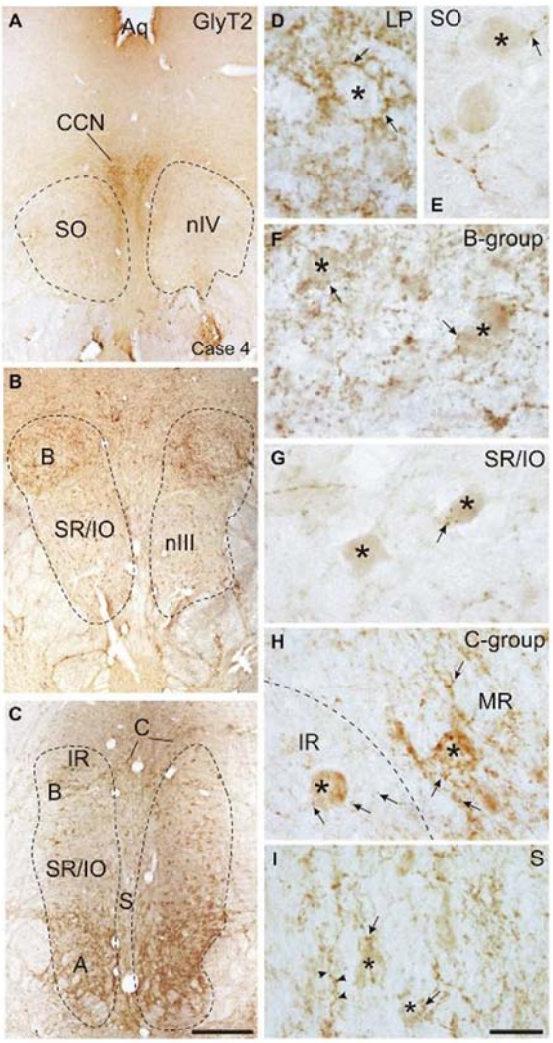

FIGURE 6 | Overviews of coronal sections through the monkey trochlear (nIV) and oculomotor nucleus (nIII) immunostained for glycine transporter 2 (GlyT2). A dense glycinergic input is found to levator palpebrae motoneurons (LP) in the CCN **(A,D)** and to **(A)** and **(B)** groups of the MR muscle **(B,C,F)** compared to a few GlyT2-positive fibers and puncta (arrow) scattered within nIV **(A,E)** and the superior rectus/inferior oblique (SR/IO) motoneuronal group **(B,C,G)**. **(H)** Shows a detailed view of the C-group (left side) with a MIF MR motoneuron (asterisk) covered with numerous GlyT2-positive puncta (arrows) next to a MIF inferior rectus (IR) motoneuron (asterisk) associated with only few GlyT2-positive puncta (arrows). Similarly, neurons in the S-group (asterisks) are associated with GlyT2-positive puncta and fibers (**I**, arrow). Aq, aquaeduct; IR, inferior rectus; SO, superior oblique. Scale bar = 500 µm in **(C)** (applies to **A–C**); Scale bar = 30 µm in **(I)** (applies to **D–I**).

Discussion

The present work in part confirms previous studies on the differing inhibitory input to motoneurons subserving horizontal and vertical eye movements, respectively. It extends these findings by a quantitative analysis of the differing transmitter inputs to MIF vs. SIF motoneurons in monkey. Additionally, we showed for the first time that vGlut1-positive terminals are only associated with MIF neurons. Although direct synaptic

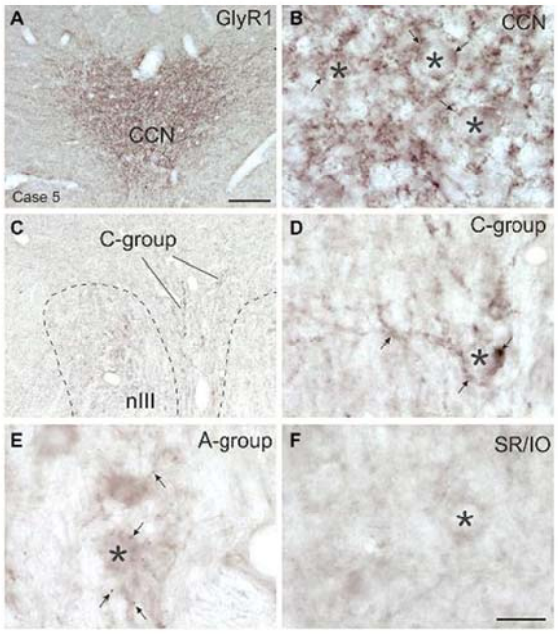

FIGURE 7 | Overviews and detailed views of immunoperoxidase labeling for glycine receptor 1 (GlyR1) in coronal sections of the oculomotor nucleus (nIII) in monkey. The strongest GlyR1 expression is present in the CCN as puncta profiles (**A,B**, stars and arrows). Unlike the motoneurons of the superior rectus and inferior oblique subgroup (SR/IO; **F**, asterisk) the MR SIF motoneurons (**E**, asterisks) show few GlyR1-positive puncta (**E**, arrows). The MIF motoneurons in the C-group (**C**, lines; **D**, asterisk) are associated with numerous GlyR1-positive puncta (**D**, arrows). MIF, multiply innervated muscle fibers; SIF, singly innervated muscle fibers. Scale bar = 200 μm in **(A)** (applies to **A**,**C**); Scale bar = 30 μm in **(F)** (applies to **B**,**D–F**).

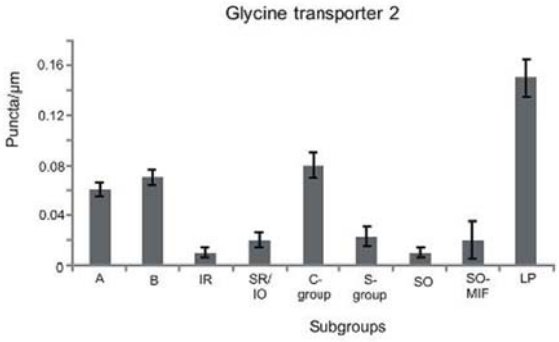

Subgroups with significant differences

ANOVA, Bonferroni's Multiple Comparison Test			
subgroups	summary	subgroups	summary
A vs SR/IO	***(p < 0.001)	SR/IO vs C-group	***(p < 0.001)
A vs IR	***(p < 0.001)	SR/IO vs LP	***(p < 0.001)
A vs S-group	*(p < 0.05)	IR vs C-group	***(p < 0.001)
A vs SO	***(p < 0.001)	IR vs LP	***(p < 0.001)
A vs SO-MIF	*(p < 0.05)	S-group vs C-group	***(p < 0.001)
A vs LP	***(p < 0.001)	S-group vs LP	***(p < 0.001)
B vs SR/IO	***(p < 0.001)	C-group vs SO	***(p < 0.001)
B vs IR	***(p < 0.001)	C-group vs SO-MIF	***(p < 0.001)
B vs S-group	*(p < 0.05)	C-group vs LP	***(p< 0.001)
B vs SO	***(p < 0.001)	SO vs LP	***(p < 0.001)
B vs SO-MIF	*(p < 0.05)	SO-MIF vs LP	***(p < 0.001)
B vs LP	***(p < 0.001)		

FIGURE 8 | Histogram demonstrating the quantitative analysis of the glycine transporter 2 (GlyT2) input to motoneurons in the trochlear (nIV), oculomotor (nIII) and CCN. The glycinergic input to all motoneural groups was quantified by counting immunoreactive puncta along the measured length of the contour of a motoneuron. The mean terminal density of inputs and the standard error of the mean were calculated for all motoneural subgroups. The strongest supply by GlyT2-positive puncta is seen to levator palpebrae motoneurons (LP), and fewer puncta are found around MR motoneurons of the A-, B- and C-group. The density of GlyT2-positive puncta around motoneurons for horizontal eye movements (MR) was significant stronger compared to those for vertical eye movements. The added table shows the results of the ANOVA and following Bonferroniś Multiple Comparison Test.

contacts were not proven by EM studies in the present work, the close proximity between motoneurons and nerve endings suggest synaptic inputs. The results are discussed against the background of the current knowledge on premotor sources targeting MIF and/or SIF motoneurons and their transmitters.

GABAergic Input to nIII and nIV

With the application of GABA and GAD antibodies our results confirm previous studies in monkey demonstrating that GABAergic neuronal profiles are predominantly associated with motoneurons subserving vertical eye movements (**Figures 2–5**; Spencer et al., 1992). Furthermore, the preferential presence of GABA-A around motoneurons of vertically pulling eye muscles is in line with the observation that postsynaptic inhibitory postsynaptic potentials (IPSPs) evoked by electrical stimulation of the labyrinth in rabbit are blocked by the GABA-A antagonist picrotoxin (Ito et al., 1970).

The strong GABAergic input to CCN may arise from the principal trigeminal nucleus, whose electrical stimulation in cat evoked IPSPs in LP motoneurons (May et al., 2012) possibly interrupting the tonic activity of LP to enable the orbicularis oculi muscle to contract during blinks (Evinger and Manning, 1993).

The reports of a GABAergic input to MR motoneurons are most controversial for different species, but may depend on differences in the methods and applied antibodies. In accordance with the present results a moderate supply of GABAergic terminals was noted in the MR subdivisions in monkey and cat using immunohistochemistry in frozen sections (Spencer et al., 1989; Spencer and Baker, 1992). However, studies applying postembedding GABA staining in semithin sections did not detect a significant difference of GABAergic input to tracer-labeled MR motoneurons compared to the other subdivisions in nIII, in cat and rabbit (de la Cruz et al., 1992; Wentzel et al., 1996), similar to the quantification of GAD-positive inputs in thin paraffin sections in the present study. In human, the number of GAD-positive profiles within the putative MR subgroups even exceeds that of motoneuron groups involved in vertical gaze. This may indicate an evolvement of inputs related to vergence, which is particularly prominent in human (see below; Che Ngwa et al., 2014). The

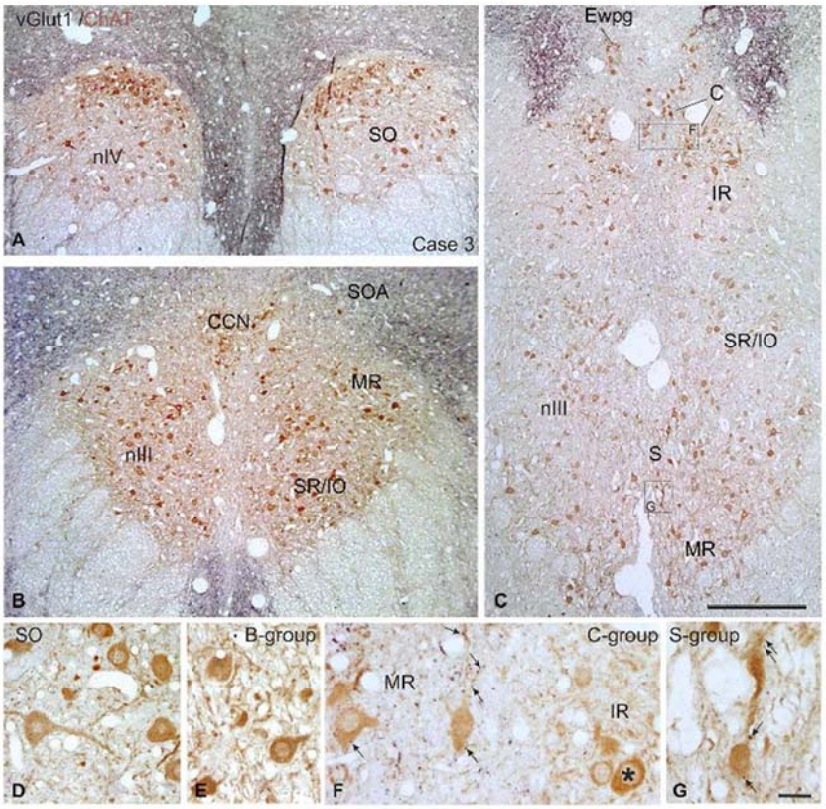

FIGURE 9 | Overviews of coronal paraffin sections through the monkey trochlear (nIV) and oculomotor nucleus (nIII) immunostained for the simultaneous detection of vesicular glutamate transporter1 (vGlut1) in black and choline acetyltransferase (ChAT) in brown (A–C). Note that SIF motoneuron subgroups in nIV **(A,D)** and nIII **(B,C,E)** are devoid of vGlut1-positive neuronal structures. Detailed views confirm the complete lack of vGlut1-positive puncta in nIV **(D)** and nIII with the B-group as examples **(E)**. Note that numerous vGlut1-positive puncta are attached only to MIF motoneurons in the C-group—and there confined to the MR motoneurons (**F**, arrows), but not present at IR motoneurons (**F**, asterisk). MIF motoneurons in the S-group are associated with few vGlut1-positive puncta (**G**, arrows). EWpg; preganglionic Edinger-Westphal nucleus; MIF, multiply innervated muscle fibers; SIF, singly innervated muscle fibers. Scale bar = 500 μm in **(C)** (applies to **A–C**), Scale bar = 30 μm in **(G)** (applies to **D–G**).

finding of a considerable GABAergic input to the C- and S-groups confirms previous observations in monkey (Ying et al., 2008).

Glycinergic Input to nIII

The considerable supply of GlyT2-positive nerve endings to MR subdivisions A and B resembled the labeling pattern of glycine-positive afferents in nIII of previous reports in monkey (**Figures 6–8**; Spencer and Baker, 1992; Poyatos et al., 1997). The similar distribution pattern of GlyT2-positive nerve endings in human nIII served there to identify the homolog MR subgroups (Che Ngwa et al., 2014). In cat, glycinergic terminals were found in all motoneuron subgroups except the MR subdivisions (Spencer and Baker, 1992). In rabbit, a glycinergic input was noted to all subdivisions in the nIII including the MR region (Wentzel et al., 1996), but may colocalize with GABA (Wentzel et al., 1993). Based on current knowledge about MIF motoneuron organization the glycinergic terminals around the midline are now considered to target the IO and SR MIF motoneurons within the S-group (Büttner-Ennever et al., 2001; Wasicky et al., 2004), rather than the SR/IO SIF motoneurons (Spencer and Baker, 1992; Spencer et al., 1992).The previously described association of GlyT2 with LP motoneurons in the CCN was confirmed and is in line with a strong expression of glycine receptor 1 seen here. The saccadic omnipause neurons were shown as one possible glycinergic source to CCN (Horn and Büttner-Ennever, 2008).

Functionally, glycine is similar to GABA as it increases chloride conductance and evokes, therefore, IPSPs. Consequently, the likelihood that the postsynaptic cell reaches the threshold for firing an action potential reduces. The colocalization of glycine and GABA in afferent inputs to MR motoneurons may indicate a co-release of both transmitters (Wentzel et al., 1993). As shown for abducens motoneurons it

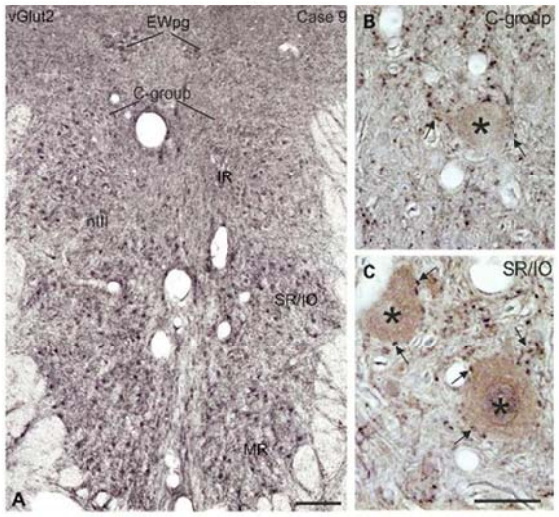

FIGURE 10 | Coronal section of the oculomotor nucleus (nIII) in monkey showing the expression of vesicular glutamate transporter 2 (vGlut2). (A) No differences were noted in the vGlut2 puncta labeling in different motoneuronal subgroups. The detailed views in **(B,C)** demonstrate the similar dense input of vGlut2-positive puncta (black) around cholinergic motoneurons (brown, asterisks) in the C-group and around motoneurons of the vertically pulling superior rectus/ inferior oblique (SR/IO) muscles (**B,C**, arrows). EWpg, preganglionic Edinger-Westphal nucleus. Scale bar = 250 μm in (**A**, 30 μm in **(C)** (applies to **B,C**).

is possible that GABA-A and glycine receptors are distributed differently at somatal or dendritic membranes (Lorenzo et al., 2007), which may play a role in tuning the IPSPs (Russier et al., 2002).

Glycine can also serve as co-agonist with glutamate at postsynaptic N-methyl-D-aspartate (NMDA) receptors (Johnson and Ascher, 1987). It is an open question as to whether the glycinergic input to the MR subdivisions in nIII, which showed a weak GlyR expression, serve as an inhibitory transmitter, or as a co-agonist of excitatory glutamatergic afferents, e.g., from internuclear neurons (INT) in nVI or ventral lateral vestibular nucleus (LVN; see below; Nguyen and Spencer, 1999).

Glutamatergic Input to nIII and nIV

This is the first description of the expression pattern of vGlut associated with eye muscle motoneurons. VGluts selectively package glutamate into synaptic vesicles and mediate glutamate transport and therefore are used as markers for glutamatergic neuronal profiles (Takamori et al., 2000; Fremeau et al., 2001, 2004; Zhou et al., 2007; for review: El Mestikawy et al., 2011). Whereas SIF and MIF motoneurons in nIII and nIV receive a dense vGlut2-positive supply, a specific vGlut1-positive input was found only to MIF motoneurons, mainly those of MR (**Figure 9F**).

Transient responses of glutamate transmission are mediated through ionotropic NMDA and non-NMDA (AMPA and kainate) receptors, whereas more persistent responses are mediated by metabotropic G-protein coupled receptors (Dingledine et al., 1999). Thereby AMPA receptors convey the fast component of postsynaptic responses, whereas NMDA receptors mediate long lasting slower postsynaptic responses. Both, NMDA-receptors and AMPA receptors (GluR4 subunit), are only expressed in SIF, but not in MIF motoneurons in monkey (Ying et al., 2008). This may indicate that SIF motoneurons participate in the fast and slow components of the postsynaptic response to glutamate. This is in line with *in vitro* studies on rat oculomotor neurons showing that smaller motoneurons with low-recruitment threshold currents have higher input resistances and exhibit tonic firing—as assumed for MIF motoneurons and whose firing pattern remains essentially unmodified by glutamate application (Torres-Torrelo et al., 2012). The phasic-tonic firing of larger motoneurons—such as SIF motoneurons—with lower input resistances and with high recruitment threshold currents, is strengthened by glutamate and could provide strong muscle contractions for (saccadic) eye movements (Torres-Torrelo et al., 2012).

Premotor Sources and their Association with Transmitters

Secondary vestibulo-ocular neurons (only SIF)

A well-established input to nIII and nIV arises from the vestibular nuclei subserving the vertical angular vestibulo-ocular reflex (VOR; for review: Büttner-Ennever and Gerrits, 2004; Straka and Dieringer, 2004; Highstein and Holstein, 2006; Goldberg et al., 2012). Primary afferents from the anterior and posterior canals activate secondary vestibular neurons in the magnocellular parts of the medial vestibular nucleus (MVNm) and superior vestibular nucleus (SVNm), which in turn send contralateral excitatory and ipsilateral inhibitory projections to the respective motoneurons of agonists and antagonists in nIII and nIV (Graf and Ezure, 1986; Iwamoto et al., 1990; Graf et al., 1997; Goldberg et al., 2012).

Extracellular tracer injections into SVNm or MVNm and single cell reconstructions of identified up and down position-vestibular-pause neurons indicated that secondary vestibular neurons target only SIF motoneurons, but not MIF motoneurons in the S- or C-group (McCrea et al., 1987; Wasicky et al., 2004). This is in line with the lack of transneuronally labeled secondary vestibular neurons in SVNm or MVNm after the injection of rabies virus into the myotendinous junction of eye muscles, from where only MIF (not SIF) motoneurons were retrogradely filled (Ugolini et al., 2006).

Glutamate and aspartate

Glutamate and/or aspartate are widely accepted as the major excitatory neurotransmitter of the secondary vestibular neurons (Demêmes and Raymond, 1982; for review: McElligott and Spencer, 2000) and may reflect at least one portion of the vGlut2-positive input to nIII and nIV. This is in line with the presence of numerous neurons expressing vGlut2 mRNA, but only few expressing weak vGlut1 mRNA signals in rat vestibular nuclei (Hisano et al., 2002; Zhang et al., 2011). The excitatory glutamatergic second-order vestibular inputs onto abducens neurons act through AMPA receptors (Straka and Dieringer, 1993). This pattern may apply to SIF motoneurons

in nIII and nIV, as indicated by their high expression of AMPA receptors (GluR1, 2, 3 and 4) in human and monkey (Williams et al., 1996; Ying et al., 2008). Both, glutamate and NMDA, produce a depolarization of NMDA receptors primarily located at dendrites, but are not associated with the excitatory second-order vestibular input to oculomotor motoneurons (Durand and Gueritaud, 1990).

Another source of glutamatergic input to nIII is conveyed by the ascending tract of Deiters (ATD; Nguyen and Spencer, 1999; Büttner-Ennever and Gerrits, 2004; Holstein, 2012). It originates from secondary vestibular neurons in the ventral MVN and the ventral LVN that receive excitatory inputs from the ipsilateral labyrinth, and target MR A and B subgroups in the ipsilateral nIII (not C-group; McCrea et al., 1987). The ATD carries head velocity signals, which are modulated by utricular inputs and the viewing distance of visual targets to generate disconjugate vergence eye movements (Reisine et al., 1981; Chen-Huang and McCrea, 1998; Angelaki, 2004). Postembedding immunostaining indicated that ATD afferents may use glutamate as a transmitter, whereas the additional aspartate-labeling was attributed to the metabolic pool (Nguyen and Spencer, 1999). This glutamate/aspartate projection targets primarily somata and proximal dendrites of MR motoneurons via synapses with asymmetric densities and spheroidal vesicles, the classical features of excitatory synapses (Nguyen and Spencer, 1999). These projections may well be included in vGlut2-positive afferents of the present study.

GABA

Electrophysiological and pharmacological studies have identified GABA as a major inhibitory transmitter of vertical secondary vestibulo-ocular neurons in different species (for review: McElligott and Spencer, 2000; Straka and Dieringer, 2004; Sekirnjak and du Lac, 2006). These inhibitory projections arise in the SVN and MVN, and target the ipsilateral SO and IR, or SR and IO motoneurons (Holstein, 2012), predominantly at their somata and proximal dendrites (Spencer and Baker, 1992; Wentzel et al., 1995). A fraction of the GABAergic fibers in the MLF seen in the present study may represent the inhibitory connections of the vertical VOR (see also Spencer et al., 1989; for review: Goldberg et al., 2012).

Non-secondary vestibulo-ocular connections (SIF and MIF)

Additional projections to nIII and nIV arise from non-secondary vestibular neurons, which are not directly activated by primary afferents from the semicircular canals (Goldberg et al., 2012). They include the dorsal y-group, which receives disynaptic inputs from vertical canal afferents (Blazquez et al., 2000), and projects to SIF *and* MIF motoneurons of SR and IO in the contralateral nIII and to IR and SO motoneurons on the ipsilateral side (Carpenter and Cowie, 1985; Wasicky et al., 2004). Electrical stimulation studies suggest that the y-group may be part of cerebellar pathways for vertical smooth-pursuit eye movements (Chubb and Fuchs, 1982). At least a subpopulation of non-secondary vestibular neurons from the parvocellular MVN (MVNp) and the dorsal y-group, which target only motoneurons of upward moving eye muscles, contains calretinin (CR; Ahlfeld et al., 2011; Zeeh et al., 2013). These CR terminals were found to be excitatory (Zeeh et al., 2013) and may contribute to the vGlut-positive input to SIF and MIF neurons seen here (**Figures 9**, **10**).

Abducens internuclear neurons (only SIF)

Another excitatory input to MR neurons arises from abducens INT, which carry a head-velocity and head position signal (burst, and burst-tonic) providing the neuroanatomical basis for conjugate horizontal eye movements (for review: Highstein and Holstein, 2006). In cat the tracer-labeled synaptic endings of abducens INTs within the contralateral MR subgroup were shown to express immunoreactivity for glutamate and aspartate (Nguyen and Spencer, 1999). The differing spatial location of glutamatergic afferents from INTs and the ATD indicates that the more proximal location of ATD synaptic input onto MR neurons may reduce the threshold for activation by the more distally located glutamatergic input from INTs during conjugate horizontal eye movements (Delgado-Garcia et al., 1986; Nguyen and Spencer, 1999). This may be used to reduce the synaptic delay from INT input to MR to ensure conjugacy of horizontal eye movements.

Since tracer injections into nVI result in afferent labeling of all MR subgroups including the MIF motoneurons in the C-group (Wasicky et al., 2004), a strong glutaminergic input via this pathway must be anticipated (Nguyen and Spencer, 1999). The more distal INT terminals on MR motoneurons are thought to act through NMDA and non-NMDA (AMPA) receptors at the same postsynaptic site (Brodin and Shupliakov, 1994). This arrangement is consistent with the known somato-dendritic distribution of NMDA and non-NMDA receptors on both, second-order vestibular (Cochran et al., 1987) and other extraocular motoneurons (Durand et al., 1987; Durand and Gueritaud, 1990; Durand, 1991; Straka and Dieringer, 1993).

RIMLF and INC (SIF, SIF and MIF)

Another monosynaptic input to SIF motoneurons of vertically pulling eye muscles originates from burst neurons in the rostral interstitial nucleus of the medial longitudinal fasciculus (RIMLF) and the interstitial nucleus of Cajal (INC) encoding vertical and torsional saccades (Moschovakis et al., 1991a,b; Horn and Büttner-Ennever, 1998; Kokkoroyannis et al., 1996; for review: Horn, 2006). Tracer-labeled afferents from RIMLF to nIII express glutamate and aspartate (Spencer and Wang, 1996). Both amino acids act on NMDA receptors, and in addition, glutamate acts on non-NMDA receptors and may mediate different components of the postsynaptic response, and could thereby contribute to vGlut2 inputs.

GABAergic premotor neurons in the dorsomedial part of the RIMLF in cat (Spencer and Wang, 1996) and in INC in monkey (Horn et al., 2003) may monosynaptically inhibit the motoneurons of anatogonistic eye muscles during up or

downward saccades as shown by intracellular recording studies in cat (Sugiuchi et al., 2013). Since lesions of INC result in vertical gaze-holding deficits with a head-tilt (Büttner et al., 2002) the INC is considered to function as velocity-to-position integrator of vertical eye movements (for review: Fukushima and Kaneko, 1995). This function may be provided by premotor burst-tonic and tonic neurons that receive a burst signal from RIMLF and project monosynaptically to motoneurons of vertical pulling eye muscles to transmit eye position signals (Dalezios et al., 1998; Horn and Büttner-Ennever, 1998; Sugiuchi et al., 2013). It is reasonable to assume that these premotor fibers target SIF *and* MIF motoneurons, as indicated from tract-tracing after small biocytin injections into INC in monkey (Kokkoroyannis et al., 1996). The differing projections from RIMLF and INC to SIF and MIF motoneurons conform to the concept that SIF motoneurons are driven only from burst neurons in RIMLF and INC to generate the eye movement, whereas the burst-tonic and tonic input from INC targets also MIF motoneurons for gaze holding. Taken together it can be reasoned that premotor excitatory burst and burst-tonic neurons in RIMLF and INC provide a glutamatergic input to the motoneurons of vertical eye movers, and thereby may form a portion of the vGlut2-positive input to nIII and nIV.

Prepositus nucleus

A strong projection from the prepositus nucleus (PPH) to the ipsilateral MR subgroup has been demonstrated (Baker et al., 1977; McCrea and Baker, 1985; Belknap and McCrea, 1988; for review: McCrea and Horn, 2006). Correlation of the neural activity of antidromically activated PPH neurons, with the resultant ipsilateral eye movements and contralateral head movements, suggest an inhibitory action of this projection (Delgado-García et al., 1989), although excitatory projections to nIV may also be present (Baker et al., 1977). Since no GABAergic projection from PPH to nIII has been found in monkey (Carpenter et al., 1992), the inhibition may be transmitted via glycine, as is the case for the abducens nucleus (Spencer et al., 1989). Whether the GlyT2-positive input to MR motoneurons in this study may represent inhibitory projections from the PPH remains to be studied (**Figures 6–8**).

Inputs to only MIF motoneurons: Premotor sources and association with transmitters

The most selective transmitter-related input was found from vGlut1-positive afferents to MR MIF motoneurons including their dendrites, which reach up into the supraoculomotor area (SOA) approaching the preganglionic neurons in the preganglionic Edinger-Westphal nucleus (EWpg) controlling pupillary constriction and lens accommodation for the near response (Tang et al., 2015; for review: McDougal and Gamlin, 2015). Thereby the SOA is a well-suited target for premotor inputs controlling the near response as suggested by the abundance of synaptic contacts at the distal dendrites of MR MIF motoneurons compared to only few synapses targeting their somata and proximal dendrites (Erichsen et al., 2014). One source may arise from "near response neurons" in the SOA that increase their activity during convergence and can be antidromically activated from MR subgroups (Judge and Cumming, 1986; Mays et al., 1986; Zhang et al., 1991, 1992).

In monkey, a selective premotor input only to MIF motoneurons was first described from the pretectum (Gamlin and Clarke, 1995; Büttner-Ennever et al., 1996; Wasicky et al., 2004). This includes the nucleus of the optic tract, which projects specifically to MIF motoneurons of nIII and nIV, and the olivary pretectal nucleus, which targets primarily pupil-related preganglionic neurons in the rostral EWpg via excitatory synapses (Gamlin and Clarke, 1995; Büttner-Ennever et al., 1996; Wasicky et al., 2004; Sun and May, 2014a,b). Another possible source is the central mesencephalic reticular formation (CMRF), which is associated with horizontal and vertical conjugate eye movements (Waitzman et al., 1996; Wang et al., 2013). Recent tracer studies in monkey demonstrated a strong projection from premotor neurons in the CMRF to the SOA including the C-group and the EWpg (Bohlen et al., 2015). This projection is bilateral and, if excitatory, may participate in the control of vergence and the near triad (Bohlen et al., 2015). Whether glutamatergic neurons in the SOA, in the pretectal nuclei or the CMRF give rise to the selective vGlut1 input to the somata or dendrites of MIF motoneurons, remains to be studied (Fujiyama et al., 2003).

Conclusion

In conclusion the exclusive vGlut1 input to MIF motoneurons and the higher density of GABA/glycinergic inputs to MR MIF motoneurons in the C-group compared to SIF motoneurons within nIII confirm the concept that SIF and MIF motoneurons receive different inputs from premotor areas involved in different functions: SIF motoneurons in generating eye movements, MIF motoneurons in gaze holding including vergence in the near response (Wasicky et al., 2004; Büttner-Ennever, 2006; Ugolini et al., 2006). MIF neuron groups were shown to contain also the cell bodies of palisade endings inserting at the myotendinous junction of extraocular muscles (Lienbacher et al., 2011; Zimmermann et al., 2011). But up to date it is not clear, whether they form a separate population of presumed sensory neurons or are part of motoneurons giving rise to the multiple innervation and palisade endings at non-twitch muscle fibers (Lienbacher and Horn, 2012).

Although all SIF motoneurons are involved in similar tasks exhibiting similar firing behavior during eye movments, the functional significance of differences in the chemical properties of premotor inputs—as seen for the specific expression of calretinin in excitatory premotor pathways for upgaze—is unclear (Zeeh et al., 2013). Transmitter inputs may not only convey a specific postsynaptic reponse, but may modulate the excitability of the motoneurons, for example by opening chloride channels conveyed by GABA and glycine (Lorenzo et al., 2007). Recent *in vivo* studies in rat demonstrated that the firing properties of motoneurons in nIII (tonic and phasic discharge) as function of recruitment threshold current and cell size can be modified by glutamatergic input (Torres-Torrelo et al., 2012). Based on their findings from *in vitro* studies of rat nIII motoneurons superfused with GABA, the authors

propose that motoneuron firing rates are essentially driven by transient neurotransmission of different transmitters. Thereby this transient mechanism could act as a modulation system refining the output of the motoneurons (Torres-Torrelo et al., 2014).

Funding

Supported by Deutsche Forschungsgemeinschaft DFG HO 1639/4–4, "Graduiertenförderung nach dem BayEFG", the Swiss National Science Foundation; Grant number: 31–47287.96; the Betty and David Koetser Foundation for Brain Research (to BH) and National Institutes of Health EY013308; ORIP-0D010425; Research to Prevent Blindness.

Acknowledgments

We thank Dr. Gay R. Holstein (Mount Sinai School of Medicine) for providing the GABA93 MAb antibody used in this study as well as Ahmed Messoudi for excellent technical assistance.

References

Ahlfeld, J., Mustari, M., and Horn, A. K. E. (2011). Sources of calretinin inputs to motoneurons of extraocular muscles involved in upgaze. *Ann. N. Y. Acad. Sci.* 1233, 91–99. doi: 10.1111/j.1749-6632.2011.06168.x

Angelaki, D. E. (2004). Eyes on target: What neurons must do for the vestibuloocular reflex during linear motion. *J. Neurophysiol.* 92, 20–35. doi: 10.1152/jn.00047.2004

Baker, R., Berthoz, A., and Delgado-García, J. (1977). Monosynaptic excitation of trochlear motoneurons following electrical stimulation of the prepositus hypoglossi nucleus. *Brain Res.* 121, 157–161. doi: 10.1016/0006-8993(77)90445-0

Bedford, F. K., Kittler, J. T., Muller, E., Thomas, P., Uren, J. M., Merlo, D., et al. (2001). GABA A receptor cell surface number and subunit stability are regulated by the ubiquitin-like protein Plic-1. *Nat. Neurosci.* 4, 908–916. doi: 10.1038/nn0901-908

Belknap, D. B., and McCrea, R. A. (1988). Anatomical connections of the prepositus and abducens nuclei in the squirrel monkey. *J. Comp. Neurol.* 268, 13–28. doi: 10.1002/cne.902680103

Bellocchio, E. E., Hu, H., Pohorille, A., Chan, J., Pickel, V. M., and Edwards, R. H. (1998). The localization of the brain-specific inorganic phosphate transporter suggests a specific presynaptic role in glutamatergic transmission. *J. Neurosci.* 18, 8648–8659.

Blazquez, P., Partsalis, A., Gerrits, N. M., and Highstein, S. M. (2000). Input of anterior and posterior semicircular canal interneurons encoding head-velocity to the dorsal Y group of the vestibular nuclei. *J. Neurophysiol.* 83, 2891–2904.

Bohlen, M. O., Warren, S., and May, P. J. (2015). A central mesencephalic reticular formation projection to the supraoculomotor area in macaque monkeys. *Brain Struct. Funct.* doi: 10.1007/s00429-015-1039-2 [Epub ahead of print].

Brodin, L., and Shupliakov, O. (1994). Functional diversity of central glutamate synapses--pre- and post-synaptic mechanisms. *Acta Physiol. Scand.* 150, 1–10. doi: 10.1111/j.1748-1716.1994.tb09653.x

Bruce, G., Wainer, B. H., and Hersh, L. B. (1985). Immunoaffinity purification of human choline acetyltransferase: comparison of the brain and placental enzymes. *J. Neurochem.* 45, 611–620. doi: 10.1111/j.1471-4159.1985.tb04030.x

Büttner, U., Brandt, T., and Helmchen, C. (2002). The direction of nystagmus is important for the diagnosis of central paroxysmal positioning nystgmus (cPPV). *Neuroophthal.* 21, 97–104. doi: 10.1076/noph.21.2.97.3919.

Büttner-Ennever, J. A., Cohen, B., Horn, A. K. E., and Reisine, H. (1996). Pretectal projections to the oculomotor complex of the monkey and their role in eye movements. *J. Comp. Neurol.* 366, 348–359. doi: 10.1002/(sici)1096-9861(19960304)366:2<348::aid-cne12>3.3.co;2-e

Büttner-Ennever, J. A., and Gerrits, N. M. (2004). "Vestibular System," in *The human nervous system*, eds Paxinos, G., and Mai, J. K. (Amsterdam: Elsevier Academic Press), 479–510.

Büttner-Ennever, J. A., Horn, A. K. E., Scherberger, H., and D'ascanio, P. (2001). Motoneurons of twitch and nontwitch extraocular muscle fibers in the abducens, trochlear and oculomotor nuclei of monkeys. *J. Comp. Neurol.* 438, 318–335. doi: 10.1002/cne.1318

Büttner-Ennever, J. A. (2006). The extraocular motor nuclei: organization and functional neuroanatomy. *Prog. Brain Res.* 151, 95–125. doi: 10.1016/s0079-6123(05)51004-5

Carpenter, M. B., and Cowie, R. J. (1985). Connections and oculomotor projections of the superior vestibular nucleus and cell group 'y'. *Brain Res.* 336, 265–287. doi: 10.1016/0006-8993(85)90653-5

Carpenter, M. B., Periera, A. B., and Guha, N. (1992). Immunocytochemistry of oculomotor afferents in the squirrel monkey (Saimiri Sciureus). *J. Himforsch.* 33, 151–167.

Che Ngwa, E., Zeeh, C., Messoudi, A., Büttner-Ennever, J. A., and Horn, A. K. E. (2014). Delineation of motoneuron subgroups supplying individual eye muscles in the human oculomotor nucleus. *Front. Neuroanat.* 8:2. doi: 10.3389/fnana.2014.00002

Chen-Huang, C., and McCrea, R. A. (1998). Viewing distance related sensory processing in the ascending tract of deiters vestibulo-ocular reflex pathway. *J. Vestib. Res.* 8, 175–184. doi: 10.1016/S0957-4271(97)00001-3

Chiarandini, D. J., and Stefani, E. (1979). Electrophysiological identification of two types of fibres in rat extraocular muscles. *J. Physiol.* 290, 453–465. doi: 10.1113/jphysiol.1979.sp012783

Chubb, M. C., and Fuchs, A. F. (1982). Contribution of y group of vestibular nuclei and dentate nucleus of cerebellum to generation of vertical smooth eye movements. *J. Neurophysiol.* 48, 75–99.

Cochran, S. L., Kasik, P., and Precht, W. (1987). Pharmacological aspects of excitatory synaptic transmission to second-order vestibular neurons in the frog. *Synapse* 1, 102–123. doi: 10.1002/syn.890010114

Dalezios, Y., Scudder, C. A., Highstein, S. M., and Moschovakis, A. K. (1998). Anatomy and physiology of the primate interstitial nucleus of Cajal. II. Discharge pattern of single efferent fibers. *J. Neurophysiol.* 80, 3100–3111.

de la Cruz, R. R., Pastor, A. M., Martinez-Guijarro, F. J., López-García, C., and Delgado-García, J. M. (1992). Role of GABA in the extraocular motor nuclei of the cat: a postembedding immunocytochemical study. *Neuroscience* 51, 911–929. doi: 10.1016/0306-4522(92)90529-b

Delgado-García, J. M., del Pozo, F., and Baker, R. (1986). Behavior of neurons in the abducens nucleus of the alert cat. II. Internuclear neurons. *Neuroscience* 17, 953–973. doi: 10.1016/0306-4522(86)90073-4

Delgado-García, J. M., Vidal, P. P., Gómez, C. M., and Berthoz, A. (1989). A neurophysiological study of prepositus hypoglossi neurons projecting to oculomotor and preoculomotor nuclei in the alert cat. *Neuroscience* 29, 291–307. doi: 10.1016/0306-4522(89)90058-4

Demêmes, D., and Raymond, J. L. (1982). Radioautographic identification of glutamic acid labeled nerve endings in the cat oculomotor nucleus. *Brain Res.* 231, 433–437. doi: 10.1016/0006-8993(82)90379-1

Dingledine, R., Borges, K., Bowie, D., and Traynelis, S. F. (1999). The glutamate receptor ion channels. *Pharmacol. Rev.* 51, 7–61.

Durand, J., Engberg, I., and Tyc-Dumont, S. (1987). L-glutamate and N-methyl-D-asparatate actions on membrane potential and conductance of cat abducens motoneurones. *Neurosci. Lett.* 79, 295–300. doi: 10.1016/0304-3940(87)90447-2

Durand, J., and Gueritaud, J. P. (1990). Excitatory amino acid actions on membrane potential and conductance of brainstem motoneurons, in *Amino-Acids, Chemistry, Biology and Medicine*, eds Lubec, G. and Rosenthal L. (Escom: Leiden), 255–262.

Durand, J. (1991). NMDA actions on rat abducens motoneurons. *Eur. J. Neurosci.* 3, 621–633. doi: 10.1111/j.1460-9568.1991.tb00848.x

Eberhorn, A. C., Ardenelau, P., Büttner-Ennever, J. A., and Horn, A. K. E. (2005). Histochemical differences between motoneurons supplying multiply and singly

innervated extraocular muscle fibers. *J. Comp. Neurol.* 491, 352–366. doi: 10.1002/cne.20715

Eberhorn, A. C., Büttner-Ennever, J. A., and Horn, A. K. E. (2006). Identification of motoneurons innervating multiply- or singly-innervated extraocular muscle fibres in the rat. *Neuroscience* 137, 891–903. doi: 10.1016/j.neuroscience.2005.10.038

El Mestikawy, S., Wallén-Mackenzie, Å., Fortin, G. M., Descarries, L., and Trudeau, L.-E. (2011). From glutamate co-release to vesicular synergy: vesicular glutamate transporters. *Nat. Rev. Neurosci.* 12, 204–216. doi: 10.1038/nrn2969

Erichsen, J. T., Wright, N. F., and May, P. J. (2014). Morphology and ultrastructure of medial rectus subgroup motoneurons in the macaque monkey. *J. Comp. Neurol.* 522, 626–641. doi: 10.1002/cne.23437

Evinger, C., and Manning, K. A. (1993). Pattern of extraocular muscle activation during reflex blinking. *Exp. Brain Res.* 92, 502–506. doi: 10.1007/bf00229039

Fremeau, R. T., Jr., Troyer, M. D., Pahner, I., Nygaard, G. O., Tran, C. H., Reimer, R. J., et al. (2001). The expression of vesicular glutamate transporters defines two classes of excitatory synapse. *Neuron* 31, 247–260. doi: 10.1016/s0896-6273(01)00344-0

Fremeau, R. T., Jr., Voglmaier, S., Seal, R. P., and Edward, R. H. (2004). VGluts define subsets of excitatory neurons and suggest a novel role for glutamate. *Trends Neurosci.* 27, 98–103. doi: 10.1016/j.tins.2003.11.005

Fujiyama, F., Hioki, H., Tomioka, R., Taki, K., Tamamaki, N., Nomura, S., et al. (2003). Changes of immunocytochemical localization of vesicular glutamate transporters in the rat visual system after the retinofugal denervation. *J. Comp. Neurol.* 465, 234–249. doi: 10.1002/cne.10848

Fukushima, K., and Kaneko, C. R. (1995). Vestibular integrators in the oculomotor system. *Neurosci. Res.* 22, 249–258. doi: 10.1016/0168-0102(95)00904-8

Gamlin, P. D., and Clarke, R. J. (1995). The pupillary light reflex pathway of the primate. *J. Am. Optom. Assoc.* 66, 415–418.

Graf, W., and Ezure, K. (1986). Morphology of vertical canal related second order vestibular neurons in the cat. *Exp. Brain Res.* 63, 35–48. doi: 10.1007/bf00235644

Graf, W., Spencer, R., Baker, H., and Baker, R. (1997). Excitatory and inhibitory vestibular pathways to the extraocular motor nuclei in goldfish. *J. Neurophysiol.* 77, 2765–2779.

Goldberg, J. M., Wilson, V., Cullen, K., Angelaki, D., Broussard, D. M., Büttner-Ennever, J. A., et al. (2012). *The Vestibular System: a Sixth Sense.* New York: Oxford University Press.

Highstein, S. M., and Holstein, G. R. (2006). The anatomy of the vestibular nuclei. *Prog. Brain Res.* 151, 157–203. doi: 10.1016/S0079-6123(05)51006-9

Hisano, S., Sawada, K., Kawano, M., Kanemoto, M., Xiong, G., Mogi, K., et al. (2002). Expression of inorganic phosphate/vesicular glutamate transporters (BNPI/VGLUT1 and DNPI/VGLUT2) in the cerebellum and precerebellar nuclei of the rat. *Mol. Brain Res.* 107, 23–31. doi: 10.1016/s0169-328x(02)00442-4

Holstein, G. R., Martinelli, G. P., Henderson, S. C., Friedrich, V. L. J. Jr., Rabbitt, R. D., and Highstein, S. M. (2004). Gamma-aminobutyric acid is present in a spatially discrete subpopulation of hair cells in the crista ampullaris of the toadfish, Opsanus tau. *J. Comp. Neurol.* 471, 1–10. doi: 10.1002/cne.11025

Holstein, G. R. (2012). "The vestibular system," in *The Human Nervous System*, eds Mai, J. K. and Paxinos, G. 3rd Edn. (Amsterdam, Boston: Elsevier), 1239–1269.

Horn, A. K. E., and Büttner-Ennever, J. A. (1998). Premotor neurons for vertical eye-movements in the rostral mesencephalon of monkey and man: the histological identification by parvalbumin immunostaining. *J. Comp. Neurol.* 392, 413–427. doi: 10.1002/(sici)1096-9861(19980323)392:4<413::aid-cne1>3.3.co;2-s

Horn, A. K. E., and Büttner-Ennever, J. A. (2008). Brainstem circuits controlling lid-eye coordination in monkey. *Prog. Brain Res.* 171, 87–95. doi: 10.1016/s0079-6123(08)00612-2

Horn, A. K. E., Helmchen, C., and Wahle, P. (2003). GABAergic neurons in the rostral mesencephalon of the Macaque monkey that control vertical eye movements. *Ann. N. Y. Acad. Sci.* 1004, 19–28. doi: 10.1196/annals.1303.003

Horn, A. K. E. (2006). The reticular formation. *Prog. Brain Res.* 151, 127–155. doi: 10.1016/S0079-6123(05)51005-7

Ito, M., Highstein, S. M., and Tsuchiya, T. (1970). The postsynaptic inhibition of rabbit oculomotor neurones by secondary vestibular impulses and its blockage by picrotoxin. *Brain Res.* 17, 520–523. doi: 10.1016/0006-8993(70)90260-x

Iwamoto, Y., Kitama, T., and Yoshida, K. (1990). Vertical eye movement-related secondary vestibular neurons ascending in medial longitudinal fasciculus in cat. II. Direct connections with extraocular motoneurons. *J. Neurophysiol.* 63, 918–935.

Judge, S. J., and Cumming, B. G. (1986). Neurons in the monkey midbrain with activity related to vergence eye movement and accommodation. *J. Neurophysiol.* 55, 915–930.

Jiao, Y., Sun, Z., Lee, T., Fusco, F. R., Kimble, T. D., and Meade, C. A. (1999). A simple and sensitive antigen retrieval method for free-floating and slide-mounted tissue sections. *J. Neurosci. Methods* 93, 149–162. doi: 10.1016/s0165-0270(99)00142-9

Johnson, J. W., and Ascher, P. (1987). Glycine potentiates the NMDA response in cultured mouse brain neurons. *Nature* 325, 529–531. doi: 10.1038/325529a0

Kokkoroyannis, T., Scudder, C. A., Balaban, C. D., Highstein, S. M., and Moschovakis, A. K. (1996). Anatomy and physiology of the primate interstitial nucleus of Cajal I. Efferent projections. *J. Neurophysiol.* 75, 725–739.

Lienbacher, K., and Horn, A. E. (2012). Palisade endings and proprioception in extraocular muscles: a comparison with skeletal muscles. *Biol. Cybern.* 106, 643–655. doi: 10.1007/s00422-012-0519-1

Lienbacher, K., Mustari, M., Ying, H. S., Büttner-Ennever, J. A., and Horn, A. K. E. (2011). Do palisade endings in extraocular muscles arise from neurons in the motor nuclei? *Invest. Ophthalmol. Vis. Sci.* 52, 2510–2519. doi: 10.1167/iovs.10-6008

Lorenzo, L. E., Barbe, A., Portalier, P., Fritschy, J. M., and Bras, H. (2006). Differential expression of GABAA and glycine receptors in ALS-resistant vs. ALS-vulnerable motoneurons: possible implications for selective vulnerability of motoneurons. *Eur. J. Neurosci.* 23, 3161–3170. doi: 10.1111/j.1460-9568.2006.04863.x

Lorenzo, L. E., Russier, M., Barbe, A., Fritschy, J. M., and Bras, H. (2007). Differential organization of γ-aminobutyric acid type A and glycine receptors in the somatic and dendritic compartments of rat abducens motoneurons. *J. Comp. Neurol.* 504, 112–126. doi: 10.1002/cne.21442

Lynch, G. S., Frueh, B. R., and Williams, D. A. (1994). Contractile properties of single skinned fibers from the extraocular muscles, the levator and superior rectus, of the rabbit. *J. Physiol.* 475, 337–346. doi: 10.1113/jphysiol.1994.sp020074

Mays, L. E., Porter, J. D., Gamlin, P. D., and Tello, C. A. (1986). Neural control of vergence eye movements: neurons encoding vergence velocity. *J. Neurophysiol.* 56, 1007–1021.

May, P. J., Vidal, P. P., Baker, H., and Baker, R. (2012). Physiological and anatomical evidence for an inhibitory trigemino-oculomotor pathway in the cat. *J. Comp. Neurol.* 520, 2218–2240. doi: 10.1002/cne.23039

McCrea, R. A., and Baker, R. (1985). Anatomical connections of the nucleus prepositus of the cat. *J. Comp. Neurol.* 237, 377–407. doi: 10.1002/cne.902370308

McCrea, R. A., and Horn, A. K. (2006). Nucleus prepositus. *Prog. Brain Res.* 151, 205–230. doi: 10.1016/s0079-6123(05)51007-0

McCrea, R. A., Strassman, E., May, E., and Highstein, S. M. (1987). Anatomical and physiological characteristics of vestibular neurons mediating the horizontal vestibulo-ocular reflex of the squirrel monkey. *J. Comp. Neurol.* 264, 547–570. doi: 10.1002/cne.902640408

McDougal, D. H., and Gamlin, P. D. (2015). Autonomic control of the eye. *Compr. Physiol.* 5, 439–473. doi: 10.1002/cphy.c140014

McElligott, J., and Spencer, R. (2000). "Neuropharmacological aspects of the vestibulo-ocular reflex," in *Neurochemistry of the vestibular system*, eds Beitz, A. J. and Anderson, J. H. (London: CRC Press. P), 199–222.

Moschovakis, A. K., Scudder, C. A., and Highstein, S. M. (1991a). The structure of the primate oculomotor burst generator. I. Medium-lead burst neurons with upward on-directions. *J. Neurophysiol.* 65, 203–217.

Moschovakis, A. K., Scudder, C. A., Highstein, S. M., and Warren, J. D. (1991b). The structure of the primate oculomotor burst generator. II. Medium-lead burst neurons with downward on-directions. *J. Neurophysiol.* 65, 218–229.

Nguyen, L. T., and Spencer, R. F. (1999). Abducens internuclear and ascending tract of Deiters inputs to medial rectus motoneurons in the cat oculomotor nucleus: Neurotransmitters. *J. Comp. Neurol.* 411, 73–86. doi: 10.1002/(sici)1096-9861(19990816)411:1<73::aid-cne6>3.0.co;2-7

Ottersen, O. P., and Storm-Mathisen, J. (1984). Glutamate- and GABA-containing neurons in the mouse and rat brain, as demonstrated with a new immunocytochemical technique. *J. Comp. Neurol.* 229, 374–392. doi: 10.1002/cne.902290308

Porter, J. D., Burns, L. A., and May, P. J. (1989). Morphological substrate for eyelid movements: innervation and structure of primate levator palpebrae superioris and orbicularis oculi muscles. *J. Comp. Neurol.* 287, 64–81. doi: 10.1002/cne.902870106

Poyatos, I., Ponce, J., Aragón, C., Giménez, C., and Zafra, F. (1997). The glycine transporter GlyT2 is a reliable marker for glycine-immunoreactive neurons. *Mol. Brain Res.* 49, 63–70. doi: 10.1016/s0169-328x(97)00124-1

Reisine, H., Strassman, A., and Highstein, S. M. (1981). Eye position and head velocity signals are conveyed to medial rectus motoneurons in the alert cat by the ascending tract of Deiters'. *Brain Res.* 211, 153–157. doi: 10.1016/0006-8993(81)90075-5

Russier, M., Kopysova, I. L., Ankri, N., Ferrand, N., and Debanne, D. (2002). GABA and glycine co-release optimizes functional inhibition in rat brainstem motoneurons *in vitro*. *J. Physiol.* 541, 123–137. doi: 10.1113/jphysiol.2001.016063

Schulze, C., Mustari, M. J., Holstein, G. R., and Horn, A. K. E. (2009). Transmitter inputs to different motoneuron subgroups in the oculomotor and trochlear nucleus in monkey. *Soc. Neurosci.* Abstr. 356.9.

Sekirnjak, C., and du Lac, S. (2006). Physiological and anatomical properties of mouse medial vestibular nucleus neurons projecting to the oculomotor nucleus. *J. Neurophysiol.* 95, 3012–3023. doi: 10.1152/jn.00796.2005

Spencer, R. F., and Baker, R. (1992). GABA and glycine as inhibitory neurotransmitters in the vestibulo-ocular reflex. *Ann. N. Y. Acad. Sci.* 656, 602–611. doi: 10.1111/j.1749-6632.1992.tb25239.x

Spencer, R. F., and Porter, J. D. (2006). Biological organization of the extraocular muscles. *Prog. Brain Res.* 151, 43–80. doi: 10.1016/s0079-6123(05)51002-1

Spencer, R. F., Wang, S. F., and Baker, R. (1992). The pathways and functions of GABA in the oculomotor system. *Prog. Brain Res.* 90, 307–331. doi: 10.1016/S0079-6123(08)63620-1

Spencer, R. F., and Wang, S. F. (1996). Immunohistochemical localization of neurotransmitters utilized by neurons in the rostral interstitial nucleus of the medial longitudinal fasciculus (riMLF) that project to the oculomotor and trochlear nuclei in the cat. *J. Comp. Neurol.* 366, 134–148. doi: 10.1002/(sici)1096-9861(19960226)366:1<134::aid-cne9>3.0.co;2-4

Spencer, R. F., Wenthold, R. J., and Baker, R. (1989). Evidence for glycine as an inhibitory neurotransmitter of vestibular, reticular and prepositus hypoglossi neurons that project to the cat abducens nucleus. *J. Neurosci.* 9, 2718–2736.

Straka, H., and Dieringer, N. (1993). Electrophysiological and pharmacological characterization of vestibular inputs to identified frog abducens motoneurons and internuclear neurons *in vitro*. *Eur. J. Neurosci.* 5, 251–260. doi: 10.1111/j.1460-9568.1993.tb00491.x

Straka, H., and Dieringer, N. (2004). Basic organization principles of the VOR: lessons from frogs. *Prog. Neurobiol.* 73, 259–309. doi: 10.1016/j.pneurobio.2004.05.003

Sugiuchi, Y., Takahashi, M., and Shinoda, Y. (2013). Input-output organization of inhibitory neurons in the interstitial nucleus of Cajal projecting to the contralateral trochlear and oculomotor nucleus. *J. Neurophysiol.* 110, 640–657. doi: 10.1152/jn.01045.2012

Sun, W., and May, P. J. (2014a). Central pupillary light reflex circuits in the cat: I. The olivary pretectal nucleus. *J. Comp. Neurol.* 522, 3960–3977. doi: 10.1002/cne.23602

Sun, W., and May, P. J. (2014b). Central pupillary light reflex circuits in the cat: II. Morphology, ultrastructure and inputs of preganglionic motoneurons. *J. Comp. Neurol.* 522, 3978–4002. doi: 10.1002/cne.23601

Takamori, S., Rhee, J. S., Rosenmund, C., and Jahn, R. (2000). Identification of a vesicular glutamate transporter that defines a glutamatergic phenotype in neurons. *Nature* 407, 189–194. doi: 10.1038/35025070

Takamori, S., Rhee, J. S., Rosemund, C., and Jahn, R. (2001). Identification of differentiation-associated brain-specific phosphate transporter as a second vesicular glutamate transporter (vGlut2). *J. Neurosci.* 21:RC182 (1–6).

Tang, X., Büttner-Ennever, J. A., Mustari, M. J., and Horn, A. K. E. (2015). Internal organization of the medial rectus and inferior rectus neurons in the C-group of the oculomotor nucleus in monkey. *J. Comp. Neurol.* 523, 1809–1823. doi: 10.1002/cne.23760

Torres-Torrelo, J., Rodríguez-Rosell, D., Nunez-Abades, P., Carrascal, L., and Torres, B. (2012). Glutamate modulates the firing rate in oculomotor nucleus motoneurons as a function of the recruitment threshold current. *J. Physiol.* 590, 3113–3127. doi: 10.1113/jphysiol.2011.226985

Torres-Torrelo, J., Torres, B., and Carrascal, L. (2014). Modulation of the input-output function by GABAA receptor-mediated currents in rat oculomotor nucleus motoneurons. *J. Physiol.* 592, 5047–5064. doi: 10.1113/jphysiol.2014.276576

Ugolini, G., Klam, F., Doldan Dans, M., Dubayle, D., Brandi, A.-M., Büttner-Ennever, J. A., et al. (2006). Horizontal eye movement networks in primates as revealed by retrograde transneuronal transfer of rabies virus: Differences in monosynaptic input to "slow" and "fast" abducens motoneurons. *J. Comp. Neurol.* 498, 762–785. doi: 10.1002/cne.21092

Waitzman, D. M., Silakov, V. L., and Cohen, B. (1996). Central mesencephalic reticular formation (cMRF) neurons discharging before and during eye movements. *J. Neurophysiol.* 75, 1546–1572.

Wang, N., Perkins, E., Zhou, L., Warren, S., and May, P. J. (2013). Anatomical evidence that the superior colliculus controls saccades through central mesencephalic reticular formation gating of omnipause neuron activity. *J. Neurosci.* 33, 16285–16296. doi: 10.1523/jneurosci.2726-11.2013

Wasicky, R., Horn, A. K. E., and Büttner-Ennever, J. A. (2004). Twitch and non-twitch motoneuron subgroups of the medial rectus muscle in the oculomotor nucleus of monkeys receive different afferent projections. *J. Comp. Neurol.* 479, 117–129. doi: 10.1002/cne.20296

Wentzel, P. R., De zeeuw, C. I., Holstege, J. C., and Gerrits, N. M. (1993). Colocalization of GABA and Glycine in the rabbit oculomotor nucleus. *Neurosci. Lett.* 164, 25–29. doi: 10.1016/0304-3940(93)90848-f

Wentzel, P. R., De Zeeuw, C. I., Holstege, J. C., and Gerrits, N. M. (1995). Inhibitory synaptic inputs to the oculomotor nucleus from vestibulo-ocular-reflex-related nuclei in the rabbit. *Neuroscience* 65, 161–174. doi: 10.1016/0306-4522(94)00471-g

Wentzel, P. R., Gerrits, N. M., and De Zeeuw, C. I. (1996). GABAergic and glycinergic inputs to the rabbit oculomotor nucleus with special emphasis on the medial rectus subdivision. *Brain Res.* 707, 314–319. doi: 10.1016/0006-8993(95)01389-x

Williams, T. L., Ince, P. G., Oakley, A. E., and Shaw, P. J. (1996). An immunocytochemical study of the distribution of AMPA selective glutamate receptor subunits in the normal human motor system. *Neuroscience* 74, 185–198. doi: 10.1016/0306-4522(96)00117-0

Ying, H. S., Fackelmann, K., Messoudi, A., Tang, X. F., Büttner-Ennever, J. A., and Horn, A. K. (2008). Neuronal signalling expression profiles of motoneurons supplying multiply or singly innervated extraocular muscle fibres in monkey. *Prog. Brain Res.* 171, 13–16. doi: 10.1016/s0079-6123(08)00602-x

Zeeh, C., Hess, B. J., and Horn, A. K. E. (2013). Calretinin inputs are confined to motoneurons for upward eye movements in monkey. *J. Comp. Neurol.* 521, 3154–3166. doi: 10.1002/cne.23337

Zhang, Y., Gamlin, P. D. R., and Mays, L. E. (1991). Antidromic identification of midbrain near response cells projecting to the oculomotor nucleus. *Exp. Brain Res.* 84, 525–528. doi: 10.1007/bf00230964

Zhang, Y., Mays, L. E., and Gamlin, P. D. (1992). Characteristics of near response cells projecting to the oculomotor nucleus. *J. Neurophysiol.* 67, 944–960.

Zhang, F. X., Pang, Y. W., Zhang, M. M., Zhang, T., Dong, Y. L., Lai, C. H., et al. (2011). Expression of vesicular glutamate transporters in peripheral vestibular structures and vestibular nuclear complex of rat. *Neuroscience* 173, 179–189. doi: 10.1016/j.neuroscience.2010.11.013

Zhou, J., Nannapaneni, N., and Shore, S. (2007). Vesicular glutamate transporters 1 and 2 are differentially associated with auditory nerve and spinal trigeminal inputs to the cochlear nucleus. *J. Comp. Neurol.* 500, 777–787. doi: 10.1002/cne.21208

Zimmermann, L., May, P. J., Pastor, A. M., Streicher, J., and Blumer, R. (2011). Evidence that the extraocular motor nuclei innervate monkey palisade endings. *Neurosci. Lett.* 489, 89–93. doi: 10.1016/j.neulet.2010.11.072

Conflict of Interest Statement: The authors declare that the research was conducted in the absence of any commercial or financial relationships that could be construed as a potential conflict of interest.

frontiers in NEUROANATOMY

ORIGINAL RESEARCH ARTICLE
published: 12 February 2014
doi: 10.3389/fnana.2014.00002

Delineation of motoneuron subgroups supplying individual eye muscles in the human oculomotor nucleus

***Emmanuel Che Ngwa*[1†], *Christina Zeeh*[1,2], *Ahmed Messoudi*[1], *Jean A. Büttner-Ennever*[1] *and Anja K. E. Horn*[1,2] ***

[1] Oculomotor Group, Institute of Anatomy and Cell Biology, Department I, Ludwig-Maximilians-University of Munich, Munich, Germany
[2] German Center for Vertigo and Balance Disorders, Ludwig-Maximilians-University of Munich, Munich, Germany

Edited by:
Paul J. May, University of Mississippi Medical Center, USA

Reviewed by:
Joan S. Baizer, University of Buffalo, USA
Fiorenzo Conti, Università Politecnica delle Marche, Italy
L. Craig Evinger, Stony Brook University, USA

***Correspondence:**
Anja K. E. Horn, Oculomotor Group, Institute of Anatomy and Cell Biology, Department I, Ludwig-Maximilians-University of Munich, Pettenkoferstrasse 11, D-80336 Munich, Germany
e-mail: anja.bochtler@med.uni-muenchen.de

†Present address:
Emmanuel Che Ngwa, Medizinische Klinik I, Klinikum Fulda AG, Pacelliallee 4, 36043 Fulda, Germany

The oculomotor nucleus (nIII) contains the motoneurons of medial, inferior, and superior recti (MR, IR, and SR), inferior oblique (IO), and levator palpebrae (LP) muscles. The delineation of motoneuron subgroups for each muscle is well-known in monkey, but not in human. We studied the transmitter inputs to human nIII and the trochlear nucleus (nIV), which innervates the superior oblique muscle (SO), to outline individual motoneuron subgroups. Parallel series of sections from human brainstems were immunostained for different markers: choline acetyltransferase combined with glutamate decarboxylase (GAD), calretinin (CR) or glycine receptor. The cytoarchitecture was visualized with cresyl violet, Gallyas staining and expression of non-phosphorylated neurofilaments. Apart from nIV, seven subgroups were delineated in nIII: the central caudal nucleus (CCN), a dorsolateral (DL), dorsomedial (DM), central (CEN), and ventral (VEN) group, the nucleus of Perlia (NP) and the non-preganglionic centrally projecting Edinger–Westphal nucleus (EWcp). DL, VEN, NP, and EWcp were characterized by a strong supply of GAD-positive terminals, in contrast to DM, CEN, and nIV. CR-positive terminals and fibers were confined to CCN, CEN, and NP. Based on location and histochemistry of the motoneuron subgroups in monkey, CEN is considered as the SR and IO motoneurons, DL and VEN as the B- and A-group of MR motoneurons, respectively, and DM as IR motoneurons. A good correlation between monkey and man is seen for the CR input, which labels only motoneurons of eye muscles participating in upgaze (SR, IO, and LP). The CCN contained LP motoneurons, and nIV those of SO. This study provides a map of the individual subgroups of motoneurons in human nIII for the first time, and suggests that NP may contain upgaze motoneurons. Surprisingly, a strong GABAergic input to human MR motoneurons was discovered, which is not seen in monkey and may indicate a functional oculomotor specialization.

Keywords: central caudal nucleus, nucleus of Perlia, extraocular muscles, motoneurons, calretinin, glycine, GABA, eye movements

INTRODUCTION

Eye movements are essential for vision, because they direct the fovea to a visual target, and stabilize gaze during locomotion to compensate for head and body movements (Leigh and Zee, 2006; Horn and Leigh, 2011). The motor and premotor pathways for several eye movement types, e.g., saccades and the vestibulo-ocular reflex, are well studied in monkey, and they form the basis for assessing the homologous brain structures in humans, for example, in clinical cases of eye movement disorders (Horn and Leigh, 2011; Kennard, 2011). However, different species have different patterns of eye movements, and different arrangements of their oculomotor subgroups (for review: Büttner-Ennever, 2006). In order to analyze the clinical-anatomical studies involving horizontal and vertical, up- or downward eye movements, the knowledge of the localization of the motoneurons of individual extraocular muscles in human is essential. Despite the fact that efforts on this topic have been undertaken since 1897 (Bernheimer, 1897) in human, the current map of individual motoneuronal groups adopted in most textbooks is still that of the monkey (Warwick, 1953a). In non-human primates, the oculomotor nucleus (nIII) and trochlear nucleus (nIV) lie in the mesencephalic tegmentum at the ventral border of the periaquaeductal gray beneath the

Abbreviations: nIII, oculomotor nucleus; nIV, trochlear nucleus; nVI, abducens nucleus; CCN, central caudal nucleus; CEN, central group; ChAT, choline acetyltransferase; CMRF, central mesencephalic reticular formation; CR, calretinin; DL, dorsolateral group; DM, dorsomedial group; DR, dorsal raphe nucleus; EAP, extravidin-peroxidase; EW, Edinger–Westphal nucleus; EWcp, centrally projecting Edinger–Westphal nucleus; EWpg, Edinger–Westphal nucleus containing preganglionic neurons; GABA, gamma-aminobutyric acid; GAD, glutamate decarboxylase; GlyR, glycine receptor; IC, inferior colliculus; INC, interstitial nucleus of Cajal; IO, inferior oblique muscle; IPN, interpeduncular nucleus; IR, inferior rectus muscle; LP, levator palpebrae muscle; LR, lateral rectus muscle; MGB, medial geniculate body; MIF, multiply-innervated non-twitch muscle fibers; ML, medial lemniscus; MLF, medial longitudinal fasciclus; MR, medial rectus muscle; NIII, oculomotor nerve; NP, nucleus of Perlia; NP-NF, non-phosphorylated neurofilaments; PAG, periaqueductal gray; PB, phosphate buffer; PN, pontine nuclei; RIMLF, rostral interstitial nucleus of the medial longitudinal fasciculus; RN, red nucleus; SC, superior colliculus; SCP, superior cerebellar peduncle; SE of mean, standard error of the mean; SIF, singly-innervated twitch muscle fibers; SNc, substantia nigra pars compacta; SNr, substantia nigra pars reticulata; SO, superior oblique muscle; SOA, supraoculomotor area; SR, superior rectus muscle; UCN, urocortin; VEN, ventral group.

aqueduct (for review: Büttner-Ennever, 2006). Since the classical work on the nIII in rhesus monkey by Warwick (1953a) using degeneration techniques, the topographic map has undergone substantial revisions in the primate using retrograde tract-tracing methods (Büttner-Ennever and Akert, 1981; Porter et al., 1983; Büttner-Ennever et al., 2001; Büttner-Ennever, 2006). Neurons supplying the ipsilateral medial rectus muscle (MR) are distributed into three clusters within nIII: the ventral A-group extending into the medial longitudinal fasciclus (MLF), the dorsolateral B-group and the small C-group at the dorsomedial border of nIII (Büttner-Ennever and Akert, 1981). The motoneurons of the ipsilateral inferior rectus muscle (IR) are located dorsally at rostral levels of the nIII, and the motoneurons of the contralateral superior rectus muscle (SR) and ipsilateral inferior oblique muscle (IO) lie partly intermingled within the central nIII of one side (Spencer and Porter, 1981; Porter et al., 1983). The nIV contains only the motoneurons of the contralateral superior oblique muscle (SO; Porter et al., 1983). In primates, a separate midline nucleus at the transition of nIII and nIV, the central caudal nucleus (CCN), contains the motoneurons of the levator palpebrae (LP) muscle, which elevates the upper eyelid (Porter et al., 1989).

The Edinger–Westphal nucleus (EW) lies immediately dorsal to nIII. It is often included in the term "nIII complex," although it does not contain motoneurons of extraocular muscles. However, recent work has shown that the EW contains different functional cell groups, which must be clearly demarcated from each other and from the nIII proper. In monkey, EW houses the preganglionic (pg) neurons of the ciliary ganglion, in accordance with traditional belief, and is now called EWpg (Horn et al., 2008; May et al., 2008). However, in human, the cytoarchitectural EW represents a cell group of non-pg centrally projecting (cp) neurons that contain urocortin (UCN), and it is therefore now termed EWcp (Horn et al., 2008; Kozicz et al., 2011; Büttner-Ennever and Horn, 2014).

Transmitter content can also distinguish between oculomotor subgroups. Previous studies of transmitter content in cat and monkey have shown that the motoneurons of horizontally moving eye muscles are controlled by glycinergic inputs, whereas those of vertically moving eye muscles by GABAergic afferents (Spencer et al., 1989, 1992; Spencer and Baker, 1992). In addition, more recent reports revealed that only the motoneurons of muscles involved in upgaze, including the LP, are selectively targeted by calretinin (CR)-positive afferents (Ahlfeld et al., 2011; Zeeh et al., 2013); this finding proved very useful in the present study for the recognition of IO and SR motoneurons.

In the experiments reported here, we identified the motoneuron groups of individual eye muscles in human. This was based partly on a comparison with the localization of motoneurons derived from tract-tracing experiments in monkey, and partly on the cytoarchitecture and differential histochemical inputs to motoneuron subgroups revealed by immunocytochemical staining for non-phosphorylated neurofilaments (NP-NF) glutamate decarboxylase (GAD), CR, glycine receptor (GlyR) in human midbrain sections. These groups have also been clearly separated from the EW and the nucleus of Perlia (NP) subgroups, and present a new map of the human oculomotor subgroups. A preliminary version of the map has been published previously (Büttner-Ennever and Horn, 2014).

MATERIALS AND METHODS

ANTISERA

Choline acetyltransferase

Cholinergic motoneurons were detected with a polyclonal choline acetyltransferase (ChAT) antibody raised in goat (AB144P, Chemicon) against the whole enzyme isolated from human placenta, which is identical to the brain enzyme (Bruce et al., 1985; **Table 1**). In immunoblots, this antibody recognizes a 68–70 kDa protein. The appearance and distribution of ChAT-positive neurons with this antibody in the present study is identical to the data of previous reports (Ichikawa and Shimizu, 1998).

Non-phosphorylated neurofilaments

Non-phosphorylated neurofilaments were detected using a mouse monoclonal antibody (IgG1), supplied as a high titer mouse ascites fluid (**Table 1**). The antibody was raised against homogenized hypothalami recovered from Fischer 344 rats (Sternberger et al., 1982). It reacts with a non-phosphorylated epitope in neurofilament H and is abolished when the epitope is phosphorylated (clone 02-135; SMI32, Sternberger Monoclonals Inc., Lutherville, MD, USA; Sternberger and Sternberger, 1983). This antibody visualizes two bands (200 and 180 kDa) in conventional immunoblots (Goldstein et al., 1987).

Glutamic acid decarboxylase

GABAergic terminals were detected with a monoclonal antibody against the GABA-synthetizing enzyme glutamic acid

Table 1 | Sources and dilutions of primary antibodies.

Antigen	Antibody	Host	Antibody source	Dilution
Choline acetyltransferase (ChAT)	Polyclonal anti-ChAT	Goat	Chemicon, Temecula, CA, USA, AB144P	1:100
Calretinin (CR)	Polyclonal anti-CR	Rabbit	SWant, Bellinzona, Switzerland, 7669/3H	1:2500
Urocortin 1 (UCN)	Polyclonal anti-UCN	Rabbit	Sigma, St. Louis, USA, U4757	1:8000
GAD	Monoclonal anti-GAD	Mouse	Biotrend, GC3108	1:4000
α and β subunits of glycine receptor (GlyR)	Monoclonal anti-GlyR (clone mAb4a)	Mouse	Synaptic Systems, Göttingen, Germany, 146 011	1:300
Non-phosphorylated neurofilaments (NP-NF)	Monoclonal anti-NP-NF	Mouse	Sternberger, Lutherville, MD, USA, SMI-32P	1:5000

decarboxylase (GAD; $GAD_{65/67}$ GC3108, batch number Z05507, clone 1111, Biotrend, Cologne, Germany; **Table 1**). Two molecular forms of GAD – GAD_{65} and GAD_{67} – are known from different species. There is 65% amino acid sequence homology between the two isoforms. Whereas GAD_{67} is a cytoplasmic protein consisting of 594 amino acid residues, GAD_{65} is an amphiphilic and membrane anchored protein consisting of 585 amino acid residues. The antibody GC 3108 recognizes a linear epitope at the C-terminus of rat GAD, common to both isoforms. The hybridoma secreting the antibody to $GAD_{65/67}$ was generated by fusion of splenocytes from a mouse immunized with fragments of recombinant human GAD_{65} fused to glutathione-*S*-transferase (Ziegler et al., 1996).

Glycine receptor

The GlyR is a ligand gated Cl^- channel, mediating synaptic inhibition in various brain regions. It is a pentamer consisting of α and β subunits. In this study, a monoclonal mouse antibody, clone mAb4a (Cat. No. 146 011, Synaptic Systems, Göttingen, Germany), was used, which recognizes the α and β subunits of the GlyR (**Table 1**). This antibody results in stronger labeling compared to antibodies directed against the α subunit only (Pfeiffer et al., 1984; Waldvogel et al., 2010). The GlyR is present in postsynaptic structures and intracellular sites involved in protein synthesis and transport shown by electron microscopy studies, which explains the diffuse immunostaining of neuronal somata and punctate labeling along the membranes of neurons (Triller et al., 1985; Baer et al., 2009).

Calretinin

A rabbit polyclonal CR antibody (7699/3H, LOT 18299, Swant, Bellinzona, Switzerland) was used to detect CR-containing neuronal profiles (**Table 1**). CR is a calcium-binding protein of the EF-hand family, related to calbindin D-28k and calmodulin, with a widespread distribution within the brain in different species (Andressen et al., 1993; Baizer and Baker, 2006; Baizer and Broussard, 2010). The CR antiserum is produced in rabbits by immunization with recombinant human CR containing a 6-his tag at the N-terminal.

Urocortin

For the identification of UCN-containing neurons a polyclonal antibody (Sigma, U-4757; Sigma, St. Louis, USA) was used. It was raised in rabbit using a synthetic peptide corresponding to the C-terminus of human UCN (amino acids 25–40 with N-terminally added lysine), conjugated to keyhole limpet hemocyanin (KLH) as immunogen. The antibody does not cross-react with human or rat corticotrophin releasing factor or human adrenocorticotropic hormone (Bachtell et al., 2003).

HUMAN TISSUE

The brainstems from seven *postmortem* human cases (case 1 – frozen; cases 2–6 – paraffin embedded) were obtained 24–72 h after death from bodies donated to the Anatomical Institute of the Ludwig-Maximilians-University in accordance with the ethical regulations of the University, and through the Reference Center for Neurodegenerative Disorders of the Ludwig-Maximilians-University with written consent from next of kin, who confirmed the wishes at time of death. All procedures were approved by the Local Research Ethics Committees. The study is in accordance with the ethical standards laid down in the 1964 Declaration of Helsinki. The age of the donators ranged from 54 to 90 years, and there is no history of neurological disease (**Table 2**). The tissue was immersed either in 4% paraformaldehyde in 0.1 M phosphate buffer (PB), pH 7.4, or in 10% formalin for 7 days. Five brainstems were embedded in paraffin, and from each case serial sections of 5, 10, and 20 μm thickness were cut. Sections of 20 μm thickness were used for Nissl- and Gallyas fiber staining, 5 and 10 μm thick sections were immunostained "on-slide" after deparaffination and rehydrating in distilled water. For freeze cutting, one brainstem (case 1) was equilibrated in increasing concentrations of sucrose in 0.1 M PB and cut at 40 μm using a cryostat. Every sixth frozen section (240 μm interval) was defatted, rehydrated, then stained with 0.5% cresyl violet for 5 min. In neighboring sections, the myelin was stained with silver using the physical developing method of Gallyas (Gallyas, 1979). The nomenclature and abbreviations for human brainstem structures are in accordance with the revised new edition of Olszewski and Baxter's "cytoarchitecture of the human brainstem" (Büttner-Ennever and Horn, 2014).

Table 2 | Human post-mortem cases used in the study.

Case	Age	Gender	Post-mortem delay (hour)	Fixation duration (day)	Cutting
1	90	Female	24	2	Frozen
2	69	Male	24	2	Paraffin
3	57	Female	24	6	Paraffin
4	67	Male	24	10	Paraffin
5	75	Male	72	10	Paraffin
6	54	Female	24	8	Paraffin

Single immunostaining for NP-NF, GAD, CR, UCN

Parallel series of adjacent frozen sections (40 μm) were processed "free-floating," whereas the paraffin sections (10 μm) were processed "on-slide" after deparaffination in three changes of xylene and rehydration in decreasing concentration of alcohol (100, 96, 90, and 70%) and a final rinse in distilled water. In addition, for the paraffin sections of formalin-fixed tissue an antigen retrieval procedure preceded the protocol for immunostaining: after deparaffinizing, the sections were incubated in 0.01 M sodium citrate buffer (pH 8.5) in a water bath at 80°C for 15 min, and then for another 15 min at room temperature, before being rinsed and started with the immunostaining protocol (Jiao et al., 1999).

After a short rinse in double distilled water and 0.1 M PB, pH 7.4, the sections were treated with 3% H_2O_2 and 10% methanol for 15 min to eliminate endogenous peroxidase activity and were washed extensively with 0.1 M Tris-buffered saline (TBS; pH 7.4). To block non-specific binding sites, the sections were then incubated with either 2% normal horse (for NP-NF, GAD, GlyR) or 2% normal goat serum (for CR, UCN) in 0.3% Triton-X 100 in 0.1 M TBS for 1 h at room temperature. Parallel 2 mm spaced series of neighboring sections were subsequently treated either with mouse

anti-NP-NF (1:5000; Sternberger) or mouse anti-GAD (1:4000, Biotrend) or mouse anti-GlyR (1:300, Synaptic Systems) or rabbit anti-CR (1:2500, Swant) or rabbit anti-UCN (1:8000; Sigma) for 2 days at 4°C. After washing in 0.1 M TBS, the sections were incubated either in biotinylated horse anti-mouse IgG (1:200; Vector Laboratories) or biotinylated goat anti-rabbit IgG (1:200; Vector Laboratories) at room temperature for 1 h, followed by three washes in 0.1 M TBS. Then, sections were incubated in extravidin-peroxidase (EAP; 1:1000; Sigma) for 1 h at room temperature. After two rinses in 0.1 M TBS, and one rinse in 0.05 M Tris-buffer (TB), pH 8, the EAP complex indicating the antigenic sites was visualized by a reaction in 0.05% diaminobenzidine (DAB) and 0.01% H_2O_2 in 0.05 M TB for 10 min. After several rinses in TBS, "free floating" sections were mounted, air-dried, dehydrated in increasing concentrations of alcohol and xylene, and coverslipped in DePex mounting medium (Serva, Heidelberg, Germany).

Combined immunoperoxidase labeling for ChAT and GAD

In selected paraffin sections, combined immunoperoxidase labeling was used to simultaneously detect ChAT and GAD.

After deparaffination and rehydration, the sections were washed in 0.1 M TBS (pH 7.4), treated with 1% H_2O_2 in TBS for 30 min, were rinsed again, and preincubated with 2% normal rabbit serum in 0.3% Triton-X 100 in TBS for 1 h at room temperature. The sections were then treated with goat anti-ChAT (1:100; Chemicon, AB144P) in TBS with 2% rabbit serum and 0.3% Triton X-100 for 48 h at room temperature. After three washes in 0.1 M TBS, the sections were incubated in biotinylated rabbit anti-goat IgG (1:200, Vector Laboratories) in TBS containing 2% bovine serum albumin for 1 h at room temperature. After three washes in 0.1 M TBS, the sections were treated with EAP (1:1000; Sigma) for 1 h. Then, two rinses with 0.1 M TBS were followed by one wash with 0.05 M TB, pH 8, and the reaction with 0.025% DAB, 0.4% ammonium nickel sulfate, and 0.015% H_2O_2 in 0.05 M TB, pH 8, for 10 min. This results in a black staining of ChAT-positive structures. After a thorough washing and blocking of residual peroxidase activity with 1% H_2O_2 in 0.1 M TBS, the sections were incubated in 2% normal horse serum in 0.3% Triton-X-100 in 0.1 M TBS for 1 h at room temperature before being transferred to mouse anti-GAD (1:4000; Biotrend, GC 3108) in 2% normal horse serum and 0.3% Triton-X-100 in TBS for 24 h at room temperature. After washing in 0.1 M TBS, the sections were incubated in biotinylated horse anti-mouse IgG (1:200; Vector Laboratories, Burlingame, CA, USA) in TBS containing 2% bovine serum albumin for 1 h at room temperature. The antigen binding site was detected by incubating sections in EAP (1:1000; Sigma, St. Louis, MO, USA) for 1 h and a subsequent reaction with 0.025% DAB and 0.015% H_2O_2 in 0.05 M TB (pH 7.6) for 10 min to yield a brown staining of GAD-positive profiles. After washing, the sections were air-dried, dehydrated in alcohol, and coverslipped with DePex mounting medium (Sigma, St. Louis, MO, USA).

ANALYSIS OF STAINED SECTIONS

The slides were examined with a light microscope Leica DMRB (Bensheim, Germany). Brightfield photographs were taken with a digital camera (Pixera Pro 600 ES, Klughammer, Markt Indersdorf, Germany, or Microfire (Optronics, USA) mounted on the microscope. The images were captured on a computer with Pixera Viewfinder software (Klughammer, Markt Indersdorf) or Picture frame 2.2 (Optronics, USA) and processed with Photoshop 7.0 software (Adobe Systems, Mountain View, CA, USA). The sharpness, contrast, and brightness were adjusted to reflect the appearance of the labeling seen through the microscope. The pictures were arranged and labeled with drawing software (Coreldraw 11.0; COREL).

QUANTIFICATION OF CR AND GAD INPUTS

The CR and GAD inputs to all motoneuronal groups in nIII and nIV were quantified by counting immunoreactive puncta along the measured length of the contour of a motoneuron with Image J (public domain, Java-based image processing program developed at the National Institutes of Health). The values were transferred in a spreadsheet table for calculation of the statistics (Microsoft Excel, 2010). The analysis of each chosen group was performed on sections from two different cases. In one focus plane, the immunoreactive puncta along the outlines of at least 35 cells in each subgroup were counted. Simultaneous ChAT-immunolabeling was used to identify the motoneurons. Immunoreactive puncta were considered to contact a motoneuron, when its soma and the CR or GAD-positive terminal were in the same focal plane, and no space was seen between them. The ratio of the number of terminals per micrometer of cell outline was calculated with Excel software (Microsoft 2010). Then, the average and mean terminal density of inputs and the standard error of the mean were calculated for all motoneuronal subgroups, including those of the LP.

Data were analyzed with the PRISM 5 software (GraphPad Prism 5, San Diego, CA, USA). Statistical analysis was performed using a one-way analysis of variance (ANOVA). p Values below 0.0001 were considered statistically significant. Two groups of downgaze motoneurons were identified: those that receive CR-input and those that do not. In addition, those groups of downgaze motoneurons receiving CR-input were separately analyzed and compared with the CR-input of upgaze motoneurons, using the Bonferroni's multiple comparison test. p Values below 0.05 were considered statistically significant.

RESULTS

The cytoarchitecture of the nIV and nIII complex was visualized with Nissl- and Gallyas fiber staining, which revealed eight separate cell groups. All these cell groups differed in their staining pattern for the transmitter-related markers GAD, GlyR, and the calcium binding protein CR. These findings are described in detail in the following sections beginning with caudal levels.

TROCHLEAR NUCLEUS

With Nissl- and immunohistochemical staining for NP-NFs, the nIV can be delineated within the mesencephalic tegmentum. At the level of the inferior colliculus (IC), the nIV is clearly outlined as a round nucleus embedded in the fibers of the MLF (**Figures 1A,B**; corresponds to plate 32 in Olszewski and Baxter's work, 2nd edition, 1982, and 3rd edition by Büttner-Ennever and Horn, 2014). The NP-NF-staining reveals that the dendrites of the motoneurons are interwoven within nIV (**Figure 1C** with inset), and that they

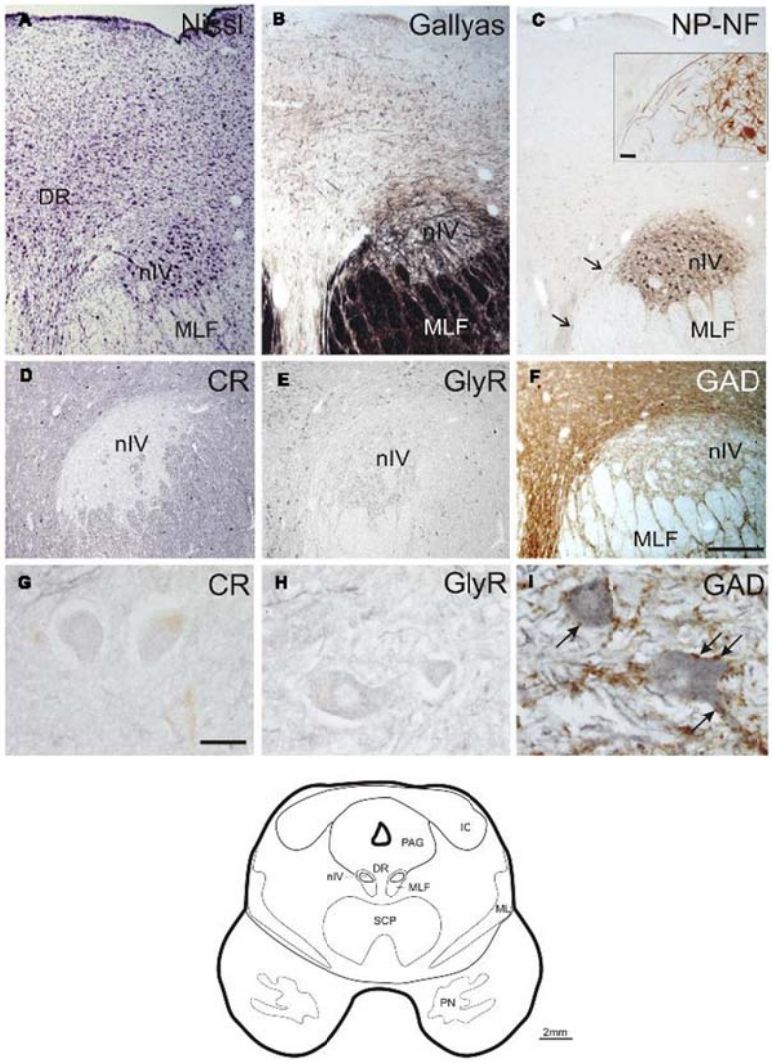

FIGURE 1 | Transverse sections of the human trochlear nucleus (nIV) demonstrating the cytoarchitecture in cresyl violet (A), Gallyas fiber staining (B), and immunostaining for non-phosphorylated neurofilaments (NP-NF) (C). The nIV is devoid of calretinin (CR) expressing neurons and fiber profiles **(D,G)**, and it does not express immunoreactivity for the glycine receptor (GlyR) **(E,H)**. The nIV shows a modest supply by GABAergic punctate profiles revealed with antibodies against glutamate decarboxylase (GAD) **(F)**. Panels **(A–C, F)** show neighboring 40 μm frozen sections of one case, panels **(D,E)** show neighboring 10 μm paraffin sections of another case. Panels **(G–I)** are detailed views from **(D–F)**. A line drawing the midbrain section at this level is given at the bottom. DR, dorsal raphe nucleus; IC, inferior colliculus; ML, medial lemniscus; MLF, medial longitudinal fascicle; PAG, periaqueductal gray; PN, pontine nuclei; SCP, superior cerebellar peduncle. Scale bar: **(A–F)** 500 μm; **(G–I,C)** inset 30 μm.

are confined to the nucleus at the medial and dorsal aspects. The dendrites extend from the nuclear boundaries at the lateral and ventral aspects and intermingle between the fibers of the MLF. The axons travel medial to the MLF (**Figure 1C**, arrows, inset). As reported by others, two completely separate divisions of the nIV are apparent in the caudo-rostral direction (not shown; Pearson, 1943; Büttner-Ennever and Horn, 2014).

No CR-positive neurons or puncta were found within the boundaries of nIV (**Figures 1D,G**). The same observation was made for GlyR-immunostaining (**Figures 1E,H**). GAD-immunostaining did not reveal any labeled somata within nIV, but numerous labeled puncta were detected around cholinergic motoneurons, many of them most likely representing synaptic terminals (**Figures 1F,I**, arrows).

CENTRAL CAUDAL NUCLEUS AND CAUDAL OCULOMOTOR NUCLEUS

The caudal end of nIII appears as a V-shaped nucleus with the CCN dorsally embedded in the V-opening shown on a plane approximately 2 mm further rostral to nIV (**Figures 2A–C**; corresponds to plate 34 in Büttner-Ennever and Horn, 2014). At this plane, a small group of densely packed neurons adjacent to the dorsal rim of nIII becomes apparent in Nissl-stained sections. This cell group consists of UCN-positive neurons (Ryabinin et al., 2005; Horn et al., 2008) and has recently been termed EWcp (**Figure 2A**; Kozicz et al., 2011). As shown earlier, the EWcp does not express NP-NF-immunoreactivity (**Figure 2C**, arrow; Horn et al., 2008). Within the main nIII, four subgroups can be delineated at this level: a ventral (VEN) group outlined dorsomedially by traversing fibers shown by Gallyas fiber staining (**Figure 2B**), and a central (CEN) group dorsal to it (**Figures 2A,C**). A lateral (LAT) group is apparent as cell islands between the rootlets of the third nerve (NIII), separated from the main nucleus by the traversing fibers of the MLF (**Figures 2A–C**). A dorsolateral group (DL) appears as a relatively isolated circular subnucleus, most apparent in Gallyas staining and NP-NF-immunostaining (**Figures 2B,C**).

A strong supply by CR-positive fibers and nerve endings was evident in the CEN group, thereby highlighting it selectively from CR-negative DL and DM groups (**Figures 2D** and **3D**; **Figures 4A,D**). A considerable supply was also found around the LP motoneurons in the CCN (**Figures 2D,G**). Immunostaining for the GlyR revealed a strong signal in the CCN (**Figure 2E**). At high magnification, the GlyR-immunostaining appears as diffuse staining of the neuronal somata and punctate labeling along the neuronal membrane surface of somata and dendrites of LP motoneurons (**Figure 2H**). Within the nIII, the DL and VEN subgroups were highlighted by their strong GlyR-immunostaining (**Figure 2E**). As in nIV, a strong supply by GAD-immunopositive puncta was evident in CCN and in all subgroups of the caudal nIII (**Figures 2F,I**). The DL and VEN subgroups were outlined by their relatively stronger abundance of GAD-positive punctate labeling compared to other subgroups (**Figure 2F**).

MID nIII, NUCLEUS OF PERLIA

At planes through the nIII 2 mm further rostral (corresponding to plate 36, Büttner-Ennever and Horn, 2014), the medial portion of the EWcp appears between the dorsal parts of nIII (**Figures 3A–F**). The NP-NF-negative EWcp is embedded in dorsoventrally traveling fibers (**Figures 3B,C**). At the midline of this level, an unpaired cell group is separated from the main nIII by dorsoventrally traversing fibers. This nucleus is called the nucleus of Perlia (NP) (**Figures 3A–C**; Perlia, 1889). Between EWcp and the DL group, an additional dorsomedial group (DM) appears at this level (**Figures 3A–F**).

Calretinin-immunostaining revealed only a few scattered small CR-positive neurons in nIII, mainly at the dorsomedial and medial border between both nIII. A group of CR-positive neurons is present in the dorsal, medial, and ventral perioculomotor region, in part covering the EWcp (**Figures 3D** and **4M**). The careful analysis of neighboring 5 μm thick paraffin sections, stained either for CR or UCN (**Figures 3G–I**), revealed that both populations do not overlap to any great extent. Only few UCN-positive neurons in EWcp express CR-immunoreactivity (**Figures 3H,I**, arrows). The CR-positive neurons in EWcp may form the origin of at least one portion of the dorsoventrally running fibers that embrace the NP and separate it from the lateral nIII (**Figure 3D**, arrows, insert). As for CCN and CEN, a considerable supply of CR-positive axonal profiles was found around neurons in NP (**Figures 3D** and **4G,J**).

Whereas CEN, NP, and EWcp were largely devoid of GlyR-positive neuronal profiles (**Figures 3E** and **4H,K,N**), the DM expressed some GlyR-immunoreactivity in addition to DL and VEN (**Figures 3E** and **4B,E**). The GlyR-labeling of DM most probably represents dendrites of the adjacent motoneurons of LP and the DL group, which are strongly labeled (**Figures 4B,E**). The close inspection of sections stained for ChAT and GAD revealed that in all nIII subgroups the somata and proximal dendrites of the cholinergic motoneurons were associated with GAD-immunoreactive profiles. A similar strong GAD-input was found in the DL, CEN, VEN subgroups, as in the NP (**Figures 4C,I,L**). The DM, LAT showed the weakest supply from GAD-positive puncta, the non-cholinergic neurons in EWcp the strongest (**Figures 4F,O**).

ROSTRAL nIII

Another 2 mm further forward, at the rostral end of nIII, the DL is the only remaining subgroup. It is bordered by the EWcp, which forms a large cell group dorsally and a small extension ventrally (**Figure 5A**; corresponding to plate 38, Büttner-Ennever and Horn, 2014). Interestingly at this level fibers arising from the nIII of both sides intermingle intensely with each other, apparent from Gallyas staining and NP-NF-immunostaining (**Figures 5B,C,E,F**, arrows). GAD-positive puncta covered the DL and EWcp densely (**Figure 5D**).

QUANTITATIVE ANALYSIS OF GAD AND CR-POSITIVE INPUTS

A summarized view of the histochemical properties is given in **Figure 6**. For verification of the impression received from visual inspection, the GAD- and CR-positive inputs were quantified by counting immunoreactive puncta along the outlines of the perimeter of somata and proximal dendrites in all subgroups of nIII and nIV. The quantitative analysis of GAD-positive puncta confirmed the visual impression, and revealed that the strongest GABAergic input was found to the somata of EWcp neurons (**Figures 6C,E,G,I,K** and **7A**; see also **Figure 4O**) with an averaged density of 0.183 puncta/μm (see **Table 3**). Similar strong GAD-input was found to the motoneurons in nIV, CEN, DL, VEN, NP, and CCN (**Table 3**; **Figures 6A,C,E,G,I,K** and **7A**). The weakest supply was found to involve motoneurons in the DM and LAT subgroups (**Table 3**; **Figures 6A,C,E,G,I,K** and **7A**). The one-way ANOVA revealed a significant difference of the mean values with $p < 0.001$ (**Figure 7A**). GlyR-immunostaining was only found in CCN and the DL and VEN subgroups in nIII, all with a similar intensity (**Figures 6C,E,G,I,K**). All motoneurons including neurons of NP expressed ChAT- and NP-NF-immunostaining, the neurons in EWcp contain UCN, as already shown previously (Horn et al., 2008; **Figures 6B,D,F,H,J,L**).

As is apparent from visual inspection of the immunocytochemical staining, the strongest CR-input is found around neurons of the NP, and around motoneurons in CEN (**Table 3**;

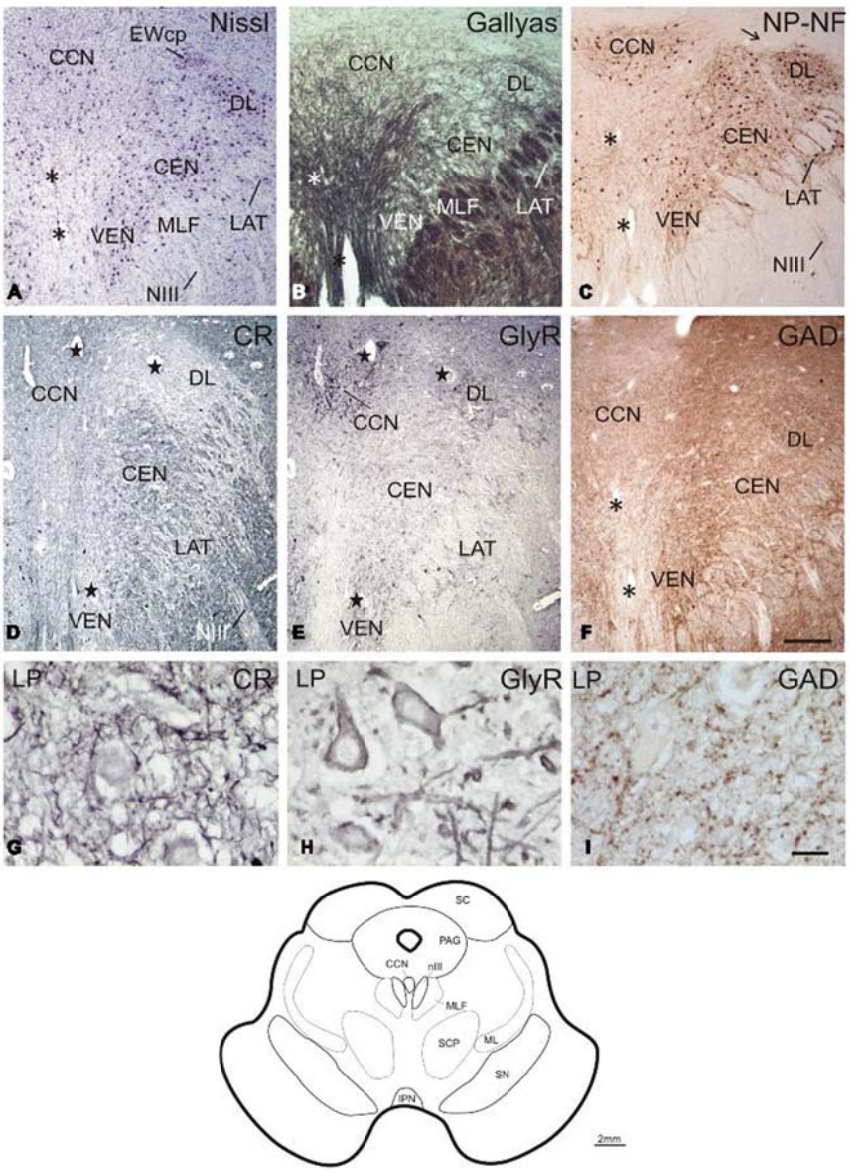

FIGURE 2 | Transverse sections through the caudal plane of the oculomotor nucleus (nIII). Cresyl violet **(A)**, Gallyas fiber staining **(B)**, and immunostaining for non-phosphorylated neurofilaments (NP-NF) **(C)** reveal several subnuclei of the oculomotor nucleus complex that exhibit different staining patterns for calretinin (CR) **(D)**, glycine receptor (GlyR) **(E)**, and glutamate decarboxylase (GAD) **(F)**. The central caudal nucleus (CCN) appears as a separate nucleus embedded in the medially descending fibers **(A–C)**. The CCN is high-lighted by its GlyR expression **(E)** and shows a moderate supply by CR- and GAD-positive profiles **(D,F)**. A dorsolateral group (DL) of nIII is separated by encircling fibers **(A–C)**. DL is devoid of CR-positive profiles **(D)**, but rich in GlyR- and GAD-positive profiles **(E,F)**. A similar pattern is seen for the ventral group (VEN) and lateral group (LAT), which forms an island of cells within the medial longitudinal fascicle (MLF) **(A–F)**. A central group (CEN) is high-lighted by its strong expression of CR **(D)**, but shows less staining for GAD **(F)** and almost none for GlyR **(E)**. Panels **(A–C,F)** show neighboring 40 μm frozen sections of one case, **(D,E)** neighboring 10 μm paraffin sections of another case. Panels **(G–I)** are detailed views from **(D–F)**. Asterisks label corresponding blood vessels in neighboring frozen sections of one case **(A–C,F)**, stars label those in neighboring paraffin sections from a different case **(D,E)**. Detailed views of levator palpebrae (LP) motoneurons in CCN are shown for CR **(G)**, GlyR **(H)**, and GAD-immunoreactivity **(I)**. A line drawing at the bottom shows the midbrain section at this level. IPN, interpeduncular nucleus; ML, medial lemniscus; PAG, periaqueductal gray; SC, superior colliculus; SCP, superior cerebellar peduncle; scale bars: **(A–F)** 500 μm; **(G–I)** 30 μm.

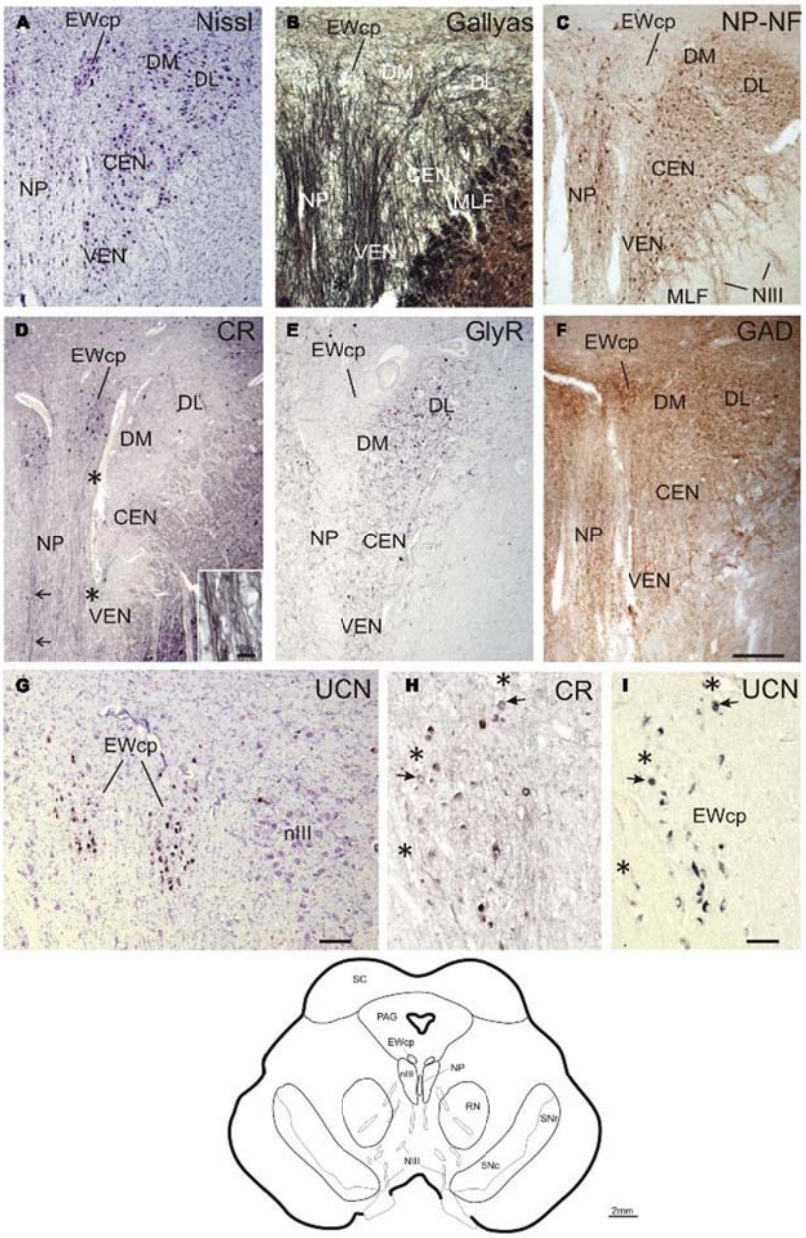

FIGURE 3 | Transverse sections at the level of the mid oculomotor nucleus (line drawing at the bottom). Cresyl violet **(A)**, fiber staining **(B)**, and immunostaining for non-phosphorylated neurofilaments (NP-NF) **(C)** reveal six subnuclei of the nIII complex at this level that exhibit different staining patterns for calretinin (CR) **(D)**, glycine receptor (GlyR) **(E)**, and glutamate decarboxylase (GAD) **(F)**. The nucleus of Perlia (NP) forms an elongated midline cell group separated from the main nucleus by dorsoventrally traversing fibers **(A,B)**, some expressing CR-immunoreactivity (**D**, arrows, inset). At the dorsomedial border of nIII, a compact cell group forms the centrally projecting non-preganglionic part of the Edinger–Westphal nucleus (EWcp), which contain urocortin (UCN)-positive and some scattered CR-positive neurons **(D,G)**. The EWcp does not contain NP-NF **(C)**, is devoid of GlyR **(E)**, but receives a strong GAD input **(F)**. High power magnification of two adjacent 5 μm paraffin sections immunostained for CR and UCN reveal only few UCN-positive neurons expressing CR (**H,I**, arrows). Corresponding blood vessels are indicated by asterisks. PAG, periaqueductal gray; RN, red nucleus; SC, superior colliculus; SN, substantia nigra (reticulata and compacta). Scale bar: **(A–F)** 500 μm; **(G)** 100 μm; **(H,I)** 50 μm.

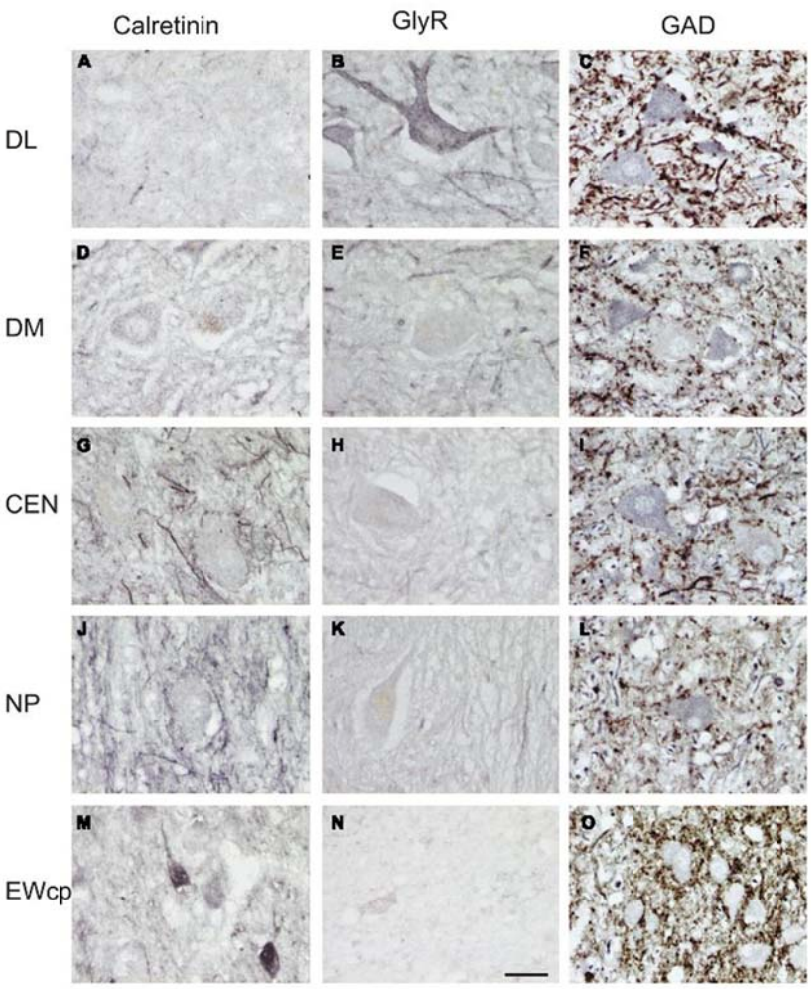

FIGURE 4 | High-power photographs of the staining pattern with different markers in the oculomotor nucleus complex. Numerous calretinin (CR)-positive profiles are found in association with cell bodies only in CEN and NP **(G,J)**, but not in DL, DM **(A,D)**. CR-staining of somata is found in EWcp (**M**; see also **Figure 3**). Strong labeling for glycine receptors (GlyR) is found only in the dorsolateral group (DL) **(B)**, and with some traversing fibers in the dorsomedial group (DM) **(E)**, but none in CEN, NP and EWcp **(H,K,N)**. Different density of glutamate decarboxylase (GAD)-positive puncta is seen around choline acetyltransferase (ChAT)-immunoreactive motoneurons in the dorsolateral (DL) **(C)**, dorsomedial (DM) **(F)**, central groups (CEN) **(I)**, and the nucleus of Perlia (NP) **(L)**. The strongest supply by GAD-positive punctate profiles is present around ChAT-negative non-preganglionic centrally projecting neurons in the Edinger–Westphal nucleus (EWcp) **(O)**. Scale bar **(A–O)** 30 μm.

Figures 6D,F,H,J and **7B**). Furthermore, a high density of CR-positive puncta was noticed in the CCN with 0.051 puncta/μm (**Table 3**; **Figures 6D** and **7B**). In contrast, only a few motoneurons in all other motoneuronal subgroups were associated with CR-positive profiles at an average density of around 0.01 puncta/μm (**Table 3**; **Figure 7B**). A comparative analysis revealed that the density of CR-positive puncta around motoneurons for upgaze in CCN and the CEN subgroup was significantly stronger than those around motoneurons for down- or horizontal gaze ($p < 0.001$). Even those down- and horizontal gaze motoneurons receiving some CR-input were contacted by significantly less CR-positive puncta, when separately analyzed and compared with the CR-input of upgaze motoneurons (Bonferroni's multiple comparison test; $p < 0.05$; not shown).

DISCUSSION

In this study of the histochemical characteristics of the human nIII and nIV, eight cell groups were distinguished from each other. From these results, and those of a previous study on non-human primates (Zeeh et al., 2013), a map of the subgroups of the human

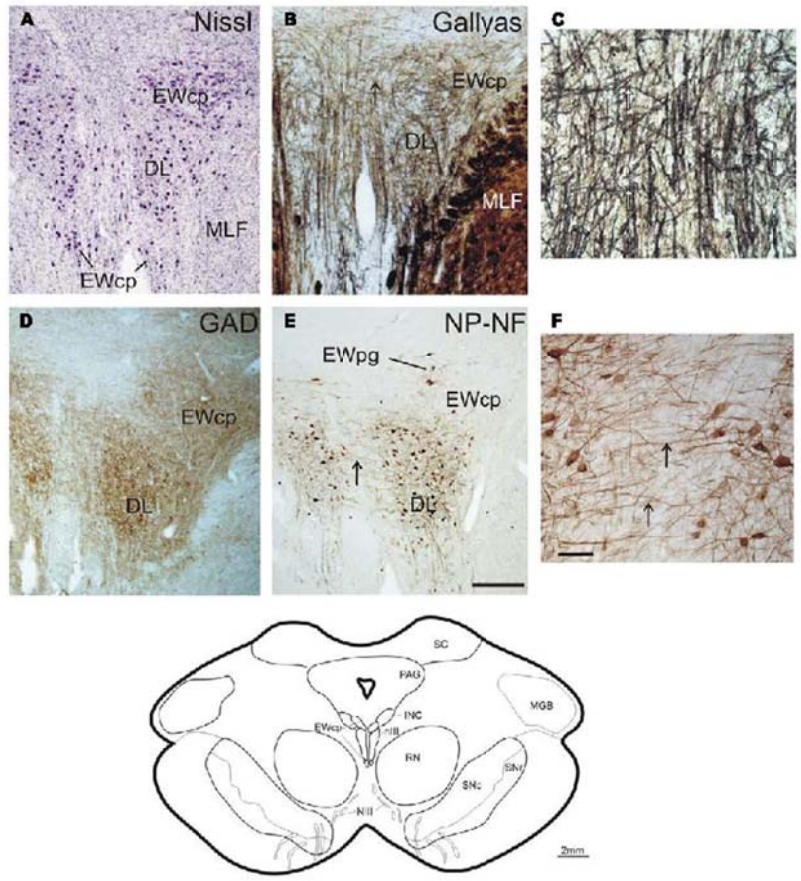

FIGURE 5 | Transverse sections at the level of the rostral oculomotor nucleus (line drawing at the bottom). Cresyl violet **(A)**, Gallyas-fiber staining **(B)** with detail **(C)**, immunostaining for glutamate decarboxylase (GAD) **(D)**, and non-phosphorylated neurofilaments (NP-NF) **(E)** with detail **(F)**. Note, unlike the preganglionic neurons of the Edinger–Westphal nucleus (EWpg), the centrally projecting non-preganglionic neurons of EWcp do not express non-phosphorylated neurofilaments (NP-NF) **(C)**. The strong labeling of GAD-positive puncta in the most rostral group in the nIII speaks for a continuation of the dorsolateral group (DL), which most likely corresponds to the medial rectus B-group in monkey **(D)**. Note the presence of numerous crossing fibers between both nIII at this level (**B,C,E,F**, arrows). INC, interstitial nucleus of Cajal; MGB, medial geniculate body; PAG, periaqueductal gray; RN, red nucleus; SN, substantia nigra (reticulata and compacta). Scale bar: **(A,B,D,E)** 500 μm; **(C,F)** 100 μm.

nIII is drawn up here, proposing the target of innervation, for each individual subgroup. In the following sections, the subgroups will be discussed in terms of their proposed function.

OCULOMOTOR SUBGROUPS INVOLVED IN UPGAZE

Motoneurons of superior rectus and inferior oblique muscles

As in monkey, only selected subgroups within nIII receive a strong input from CR-positive afferents (Zeeh et al., 2013); in human these include the CCN, the CEN group, and NP. Combined tract-tracing and CR-immunostaining experiments in monkey have shown that the CR-positive input was confined to motoneurons participating in upgaze, e.g., SR, IO, and LP in the CCN (Fuchs et al., 1992; Zeeh et al., 2013). Furthermore, tracer injections into the IO or SR muscles in monkey revealed that these two subgroups occupy a similar portion in the central part of the caudal nIII, except for the fact that the SR motoneurons are located contralaterally and tend to lie more medially to the IO motoneurons, which project to the ipsilateral eye muscle. The dendrites of retrogradely labeled IO and SR motoneurons are intimately intermingled and are not confined to any individual cytoarchitectural borders (Spencer and Porter, 1981; Zeeh et al., 2013). Based on the similar anatomical and histochemical features of the CEN group including the selective CR input, the CEN subgroup in the human nIII is considered as the location of SR and IO motoneurons (**Figure 8**).

With combined tract-tracing studies, three sources of the CR input to the nIII complex have been identified in monkey:

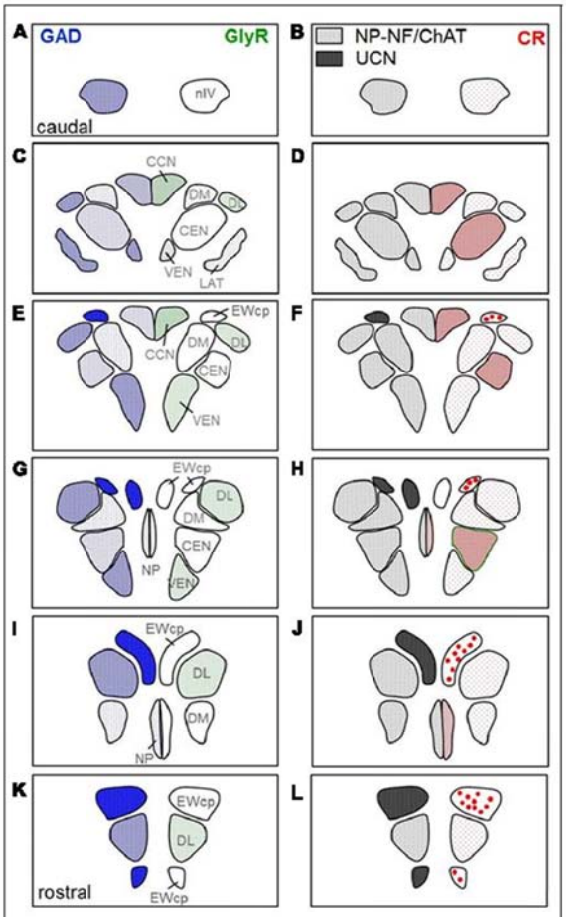

FIGURE 6 | Two parallel series of drawings of transversal sections through the trochlear (nIV) and oculomotor nucleus (nIII) complex arranged from caudal to rostral. Panels **(A,B)** correspond to the level of **Figure 1**, **(C,D)** to the level of **Figure 2**, **(G,H)** to the level of **Figure 3**, and **(K,L)** to the level of **Figure 5**. Panels **(E,F** and **I,J)** correspond to additional intermediate levels. On the left, the density of glutamate decarboxylase (GAD) positive puncta and the intensity of immunostaining for the glycine receptor (GlyR) in the different subgroups is indicated by blue hatching on the left and green hatching on the right, respectively. The right column shows the presence of neurons expressing immunoreactivity for urocortin (UCN, black), non-phosphorylated neurofilaments (NP-NF; gray) and calretinin (CR; red filled circles). The density of CR-positive profiles is indicated by different grades of red hatching.

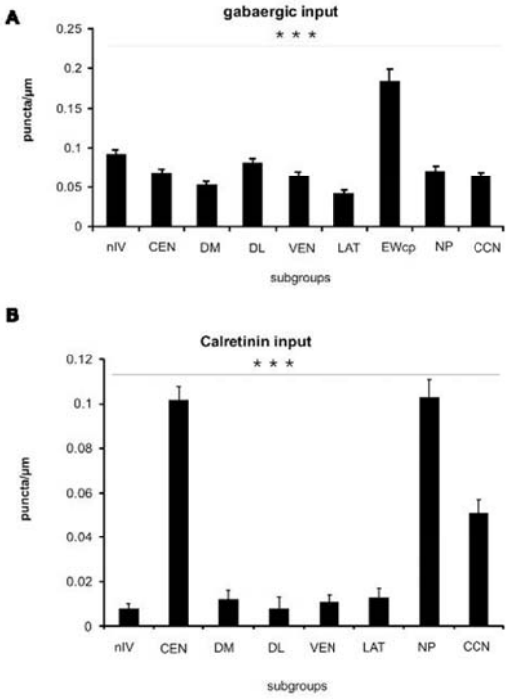

FIGURE 7 | Histogram of the quantitative analysis of GABAergic and calretinin (CR) input to motoneurons in the oculomotor and trochlear nucleus. The values are given in **Table 3**. **(A)** The GABA-input was quantified by counting glutamate decarboxylase-positive (GAD) puncta along the measured length of the contour of a given neuron. The mean terminal density of input and the standard error of the mean values were calculated for each subgroup. The one-way analysis of variance revealed a significant difference ($p < 0.001$). The strongest input is seen to non-preganglionic centrally projecting neurons in the Edinger–Westphal nucleus (EWcp; compare to **Figure 4O**), whereas the neurons of all other subgroups did not show major differences. **(B)** The strongest CR input is seen to neurons of the nucleus of Perlia (NP), the central group in oculomotor nucleus (CEN), and the central caudal nucleus (CCN). The number of counted CR-positive puncta associated with putative upgaze motoneurons is significantly higher compared to those around horizontal – and downgaze motoneurons (***$p < 0.001$).

the rostral interstitial nucleus of the medial longitudinal fascicle (RIMLF), the interstitial nucleus of Cajal (INC) and the y-group of the vestibular nuclei (Ahlfeld et al., 2011). The RIMLF contains premotor neurons of different types; some exhibit a high-frequency burst for upward saccades, others for downward saccades, and they are all intermingled with each other (Büttner et al., 1977; Horn and Büttner-Ennever, 1998). Considering their targets, the CR-positive population probably represents the premotor burst neurons for upward saccades (Ahlfeld et al., 2011). The CR-input from INC to upgaze motoneurons may derive from premotor burst-tonic neurons involved in integration of the velocity signal from RIMLF into the eye-position signal, required for gaze stabilization after a saccade (Fukushima et al., 1992). The lack of GAD in CR-immunopositive neuronal profiles in monkey nIII as revealed by double-immunofluorescence and confocal scanning, indicated that the CR input is excitatory (Zeeh et al., 2013). CR-positive projections from the y-group to SR and IO motoneurons may provide the excitatory drive during smooth pursuit eye movements (Partsalis et al., 1995). The functional significance of the selective CR presence in upgaze pathways remains unclear, it has been discussed in previous publications (Ahlfeld et al., 2011; Zeeh et al., 2013).

Table 3 | Quantification of calretinin and GABAergic input to nIV and nIII subgroups.

	CR		GAD	
Subgroup	**Puncta/μm**	**SE of mean**	**Puncta/μm**	**SE of mean**
nIV	0.008	0.002	0.091	0.006
CEN	0.102	0.006	0.067	0.006
DM	0.012	0.004	0.052	0.005
DL	0.008	0.005	0.08	0.006
VEN	0.011	0.003	0.063	0.006
LAT	0.013	0.004	0.041	0.005
NP	0.103	0.008	0.069	0.008
CCN	0.051	0.006	0.063	0.005
EWcp	0	0	0.183	0.016

Central caudal nucleus

Panegrossi (1898), was the first to describe the CCN in human. Originally he had termed the nucleus on the midline, situated between the oculomotor nuclei at caudal levels, as *nucleus posterior dorso-centralis*. He found this nucleus as a constant feature in human, and noted it also in monkey, dog, and cat. Since this nucleus degenerated after removal of the bulbus in cat, he designated it as part of the nIII (review: Warwick, 1953a,b). Similarly, Tsuchida (1906) described a central medial nucleus between the main cell columns of caudal nIII, but he did not relate it to Panegrossi's findings. He called this medial nucleus the *caudal central nucleus* (Tsuchida, 1906). In spite of the fact that Tsuchida (1906) designated it probably to the dorsal raphe nucleus, his term was later adopted for the midline nucleus containing LP motoneurons. Based on removal of individual eye muscles in monkey, Warwick was the first to show that the CCN contains the LP motoneurons (Warwick, 1953b). This was later confirmed with tract-tracing methods, also showing that the LP motoneurons of both eyes are intermingled within the CCN, with a slight predominance for a contralateral representation (Porter et al., 1989). There are conflicting reports as to whether some LP motoneurons innervate the muscles of both sides (Sekiya et al., 1992; Van der Werf et al., 1997), or whether LP populations are completely separated for each eye (Porter et al., 1989). As in monkey, the CCN in human forms an unpaired nucleus dorsal to the caudal end of nIII (Schmidtke and Büttner-Ennever, 1992; Horn and Adamcyzk, 2011; Büttner-Ennever and Horn, 2014). Furthermore, the present study revealed, that in addition to a significant CR-input, there is a strong input from GABAergic and glycinergic afferents to LP motoneurons, as found in monkey (Horn and Büttner-Ennever, 2008; Zeeh et al., 2013). One possible source of direct or indirect inhibitory GABAergic afferents is the nucleus of the posterior commissure, since lesions of this area result in lid retraction (Schmidtke and Büttner-Ennever, 1992; Averbuch-Heller, 1997). A further direct inhibitory connection was shown from pontine neurons at the rostral and ventral border of the principal trigeminal nucleus to LP motoneurons in the CCN, which presumably provide the inhibition during blinks

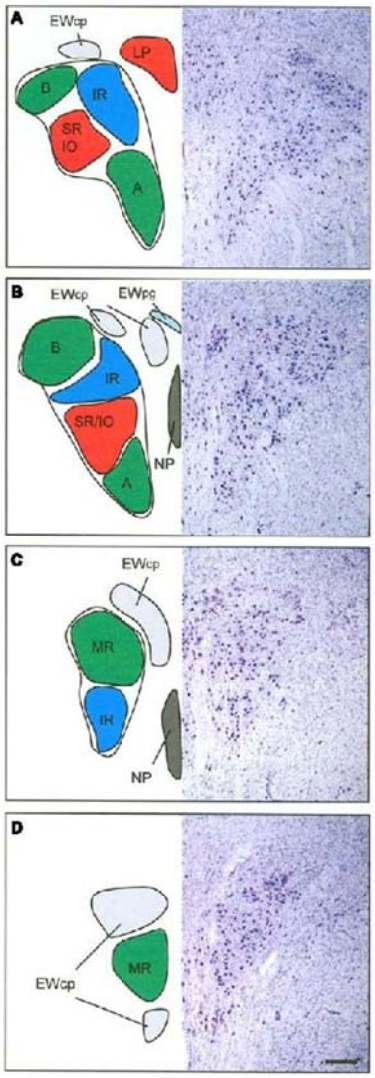

FIGURE 8 | Proposed map of the motoneurons for individual extraocular muscles in human shown at four representative planes from caudal to rostral. The right half shows corresponding sections in Nissl staining to demonstrate the cytoarchitecture. The central caudal nucleus at most caudal planes contains the motoneurons of the levator palpebrae muscle (LP) **(A)**. The medial rectus muscles (MR) is represented in two groups, the dorsolateral B- and the ventral A-group **(A,B)**. The central group represents the motoneurons of the inferior oblique (IO) and superior rectus (SR) muscle **(A,B)**. The nucleus of Perlia (NP) is separated from the main nucleus, but may contain SR motoneurons as well **(B,C)**. The dorsomedial group corresponds to the inferior rectus motoneurons (IR) **(A–C)**. The centrally projecting neurons of the Edinger-Westphal nucleus (EWcp) appear as a single lateral group on caudal levels dorsal to nIII **(A)**, adjoined by a medial group further rostrally **(B)**, which both merge to a single dorsal group **(C)**. Another ventral extension of the EWcp appears on rostral levels **(D)**. Note that the preganglionic neurons in the EWpg do not form a compact nucleus **(B)**. Scale bar: **(A–D)** 500 μm.

(May et al., 2012). The glycinergic input to LP motoneurons may originate from saccadic omnipause neurons, as indicated by tract-tracing studies in monkey (Horn and Büttner-Ennever, 2008). The function of this connection is not clear, yet, but may contribute to pathways involved in blink-saccade interaction (Leigh and Zee, 2006).

Premotor neurons in the medial RIMLF in cat, and in the M-group in monkey, which target LP motoneurons, represent a further possible CR source (Horn et al., 2000; Chen and May, 2002). Furthermore, a monosynaptic excitatory connection from INC to LP motoneurons has been described in cat (Chen and May, 2007). This projection may originate from the same premotor neurons in INC, which target SR and IO motoneurons, thereby coupling vertical eye and lid movements not only during saccades, but also during gaze holding, to provide a larger, and freer upper field of vision.

Nucleus of Perlia

The NP was described by Perlia (1889) and originally considered as a cell group participating in the control of convergence, but up to now, without any proof (Warwick, 1955). In spite of several references describing the presence of the NP in non-human primates as a labeled midline group, after tracer injections into the ciliary ganglion (Burde, 1983, 1988; Burde and Williams, 1989; Ishikawa et al., 1990), its existence is still questioned in these species. The tracer labeled neurons are more likely to represent motoneurons of multiply-innervated muscles fibers (MIF) of the IO and SR, due to superficial contamination of the muscles as discussed previously (Büttner-Ennever et al., 2001; Horn et al., 2008). In fact, the morphology of the neurons of NP and their histochemical properties, e.g., expression of ChAT, cytochrome oxidase, NP-NF, and chondroitin sulfate proteoglycans, suggest that they may present motoneurons of singly-innervated twitch muscle fibers (SIF; Eberhorn et al., 2005; Horn et al., 2008). The present study demonstrated a CR input to NP and thereby indicates a role in upgaze, which supports the hypothesis that NP may represent SR twitch motoneurons that are separated from the main subgroup in nIII by dorsoventrally traveling nerve fibers (Horn et al., 2008; Büttner-Ennever and Horn, 2014).

OCULOMOTOR SUPGROUPS INVOLVED IN DOWNGAZE

Motoneurons of superior oblique and inferior rectus muscles

In addition to the SO motoneurons in nIV, the IR motoneurons in nIII participate in downward eye movements (Leigh and Zee, 2006). In monkey, the IR motoneurons lie within the rostral half of nIII appearing medial to the B group of the MR motoneurons. At the rostral end of nIII they form the dorsal part of nIII (Evinger, 1988; Büttner-Ennever, 2006). Unlike motoneurons of horizontal moving eye muscles, a strong GABAergic input was found to the motoneurons of all vertically pulling eye muscles in monkey, including those for downgaze (Spencer and Baker, 1992). One well known source for GABAergic afferents to the vertically pulling eye muscles arises from the secondary vestibulo-ocular neurons in the superior vestibular nuclei (de la Cruz et al., 1992; Wentzel et al., 1996; Highstein and Holstein, 2006). Electrophysiological and pharmacological studies have shown that stimulation of the vestibular nerve results in inhibitory postsynaptic potentials in the ipsilateral nIV and nIII, which are blocked after administration of GABA antagonists (Obata and Highstein, 1970). Similarly, a lesion of the MLF results in a drastic decrease of GABA in nIII and nIV in cat (Precht et al., 1973).

Another source for GABAergic afferent input to nIII and nIV is the INC. In monkey, tracer injections into nIV or rostral nIII resulted in retrograde labeling of medium-sized GABAergic neurons in the contralateral INC (Horn et al., 2003). This is in line with the recordings of monosynaptic inhibitory postsynaptic potentials in nIV and nIII after INC stimulation (Schwindt et al., 1974). Recent findings in cat confirm these results, and re-emphasize that premotor inhibitory neurons in INC may represent inhibitory burst neurons of the vertical saccadic system (Sugiuchi et al., 2013).

OCULOMOTOR SUBGROUPS INVOLVED IN HORIZONTAL GAZE

Aside from the CCN, the VEN, LAT, and DL subgroups in nIII receive a strong glycinergic input, as indicated by the relatively selective presence of GlyRs. In cat and monkey, glycinergic afferents were found to be associated specifically with motoneurons involved in *horizontal* eye movements, i.e., MR in nIII and lateral rectus muscle (LR) in the abducens nucleus (nVI). This is in contrast to the high concentration of GABAergic input to motoneurons for *vertical* eye movements in nIII and nIV (Spencer et al., 1989; Spencer and Baker, 1992). Tract-tracing experiments in monkey had shown that the MR is represented in two separated groups within nIII (Büttner-Ennever and Akert, 1981; Porter et al., 1983): the A-group occupying the ventral part of nIII and extending through its whole rostro-caudal extents, and the B-group forming a well separated DL group at caudal nIII levels (Büttner-Ennever and Akert, 1981). In addition at caudal levels, the MR population reaches as finger-like extensions into the fibers of the MLF, partly in conjunction with the A-group, partly forming completely separated islands. Based on the similar cytoarchitectural features and the selective glycinergic inputs, we consider the VEN group in human nIII as the homolog to the MR "A-group" in monkey, including the extensions of LAT into the surrounding MLF. Accordingly, the DL group is considered to be the homolog of the MR "B-group" (**Figure 8**): it has the same circular contour as in monkey, and a similar separation from the neighboring subgroups, with no motoneuronal dendrites extending beyond its boundaries. Interestingly, at the rostral nIII pole the dendrites of presumed MR motoneurons reach across the midline to their contralateral counterparts. Whether this is only the consequence of the disappearance of the NP at this level, or whether it has a functional background in the collection of common afferent inputs for controlling vergence, remains unclear.

The inhibitory control of horizontal gaze by glycinergic afferents that is seen for LR and MR motoneurons in cat and monkey is found to be preserved in the human as well (Spencer et al., 1989, 1992; Spencer and Baker, 1992). With anatomical, recording and pharmacological methods, the inhibitory nature of the glycinergic projection from the prepositus nucleus to the nVI has been demonstrated in the cat (Spencer et al., 1989). Up to date, the source of the glycinergic input to MR motoneurons in

nIII is unknown. Although strychnine-sensitive GlyRs are known to mediate synaptic inhibition by activating chloride channels (Dutertre et al., 2012), glycine can also contribute to excitatory transmission by serving as an allosteric modulator for the glutamate N-methyl-D-aspartate receptor (Johnson and Ascher, 1987). Therefore, it is possible that the presence of GlyR seen in the MR subgroups in primates is associated with the glutamatergic inputs from the ipsilateral lateral vestibular nuclei via the ascending tract of Deiters (Nguyen and Spencer, 1999), which may contribute to viewing distance related gain changes of the vestibulo-ocular reflex (Snyder and King, 1992; Chen-Huang and McCrea, 1998).

However, in contrast to cat and monkey, in human all presumed MR subgroups receive an additional strong supply from GABAergic afferents, which even exceeds that of the motoneurons for vertical gaze. This finding is in line with observations from the human nVI, which also receives a strong GABAergic – in addition to a strong glycinergic – input. This observation is, surprisingly, *not* the same as in monkey, where only a moderate GABAergic input is observed (Spencer and Baker, 1992; Waldvogel et al., 2010). Thereby, the GABAergic inputs provided the least useful marker to delineate the motoneuronal subgroups in human nIII, but at the same time they revealed an interesting and unusual neuroanatomical difference between monkey and man, which is seldom observed.

Although the GABA-immunoreactivity in the cat nVI is relatively weak, both motoneurons and internuclear neurons get some GABAergic input (de la Cruz et al., 1989). In cat 20% of retrogradely labeled small internuclear neurons in and around the nIII expressed GABA-immunoreactivity (de la Cruz et al., 1992) and may be one source for the relatively weak GABAergic input to motoneurons and internuclear neurons in nVI (de la Cruz et al., 1992). In cat, tracer-labeled MR motoneurons receive a similar strong supply from glycinergic and GABAergic afferents (de la Cruz et al., 1992).

Up to date, it is generally accepted that horizontal conjugate eye movements are mediated through the nVI, which contains motoneurons and internuclear neurons. The motoneurons innervate the ipsilateral LR, the internuclear neurons activate the contralateral MR motoneurons in nIII via the MLF (for review: Horn and Leigh, 2011). A separate "extra-MLF" vergence pathway involving premotor neurons in the supraoculomotor area (SOA) with pure vergence signals (not conjugate eye movements) provides the command to move the eyes at equal magnitudes, but in opposite direction for alignment of gaze between targets at different depths (Mays, 1984). At the same location in the SOA, divergence neurons have been identified, which showed decreased firing rates with increasing vergence angles (Mays, 1984; Judge and Cumming, 1986). Direct inputs from the SOA to MR motoneurons have been demonstrated (Zhang et al., 1991), and they were shown to be related either to pure vergence or accommodation, or to both (Zhang et al., 1992). Theoretically, divergent eye movements require the activation of LR motoneurons and inhibition of MR motoneurons, which could be mediated through inhibition from GABAergic neurons in the SOA.

Another direct premotor input to motoneurons of the horizontal system was indicated from the central mesencephalic reticular formation (CMRF) after retrograde transsynaptic labeling studies in monkey applying rabies virus injections into LR (Ugolini et al., 2006; Büttner-Ennever, 2008). The CMRF is closely interconnected with the superior colliculus and the paramedian pontine reticular formation including the saccadic omnipause neurons (Cohen and Büttner-Ennever, 1984; Chen and May, 2000; Wang et al., 2013) and has been found to be correlated with horizontal and vertical saccades (Waitzman et al., 2000a,b, 2002). Preliminary data applying small biotin dextran injections into the rostromedial part of the CMRF in monkey revealed monosynaptic inputs to all MR motoneuron subgroups on both sides and pg neurons in the EWpg, indicating a role in vergence and the near triad, at least of this CMRF region (May et al., 2011; Horn et al., 2012). The accompanying ultrastructural analysis revealed that many of the tracer labeled terminals contacting MR motoneurons have features in accordance with inhibitory synapses, some of them expressing GABA-immunolabeling (May et al., 2011). To what extent the GABA-negative afferent terminals may represent glycinergic afferents remains to be studied. Based on the monkey data, the strong GABAergic input seen here in the human nIII may derive at least in part from the adjacent CMRF and/or SOA.

GENERAL ORGANIZATION IN OCULOMOTOR NUCLEUS: PRIMATE

The first anatomical description of the nIII is given by Stilling (1846). The partition into a dorsal and ventral portion, and the presence of numerous decussating axons was first described by von Gudden (1881; for review: Warwick, 1953a). A very precise description of the cytoarchitecture of the nIII was provided by Perlia on fetal human brain, which included the lateral and medial portion of the classical EW and the NP, which he originally had termed "Centralkern" (Perlia, 1889). Based on observations made after the removal of extraocular muscles in various species, different variations of an nIII map had been proposed (reviewed by Warwick, 1953a). The elaborate work of Warwick, who plotted the neurons undergoing chromatolysis after the resection of individual extraocular muscles in monkey, provided a map of the primate nIII, which was widely accepted and used as basis for the human nIII in many textbook illustrations (Warwick, 1953a). The organization of the motoneuronal groups shows a sequence from rostral to caudal of IR, MR, IO, SR, and LP motoneurons. The newly developed tract-tracing method basically confirmed the proposed arrangement of motoneuronal groups of individual muscles in the nIII of monkey, but it revealed for the first time the presence of two motoneuron groups for the MR, the ventral A-group and the DL circular B-group (Büttner-Ennever and Akert, 1981; Porter et al., 1983; Büttner-Ennever, 2006). This twofold representation of the MR within the nIII is most evident in primates and its function remains unclear (Augustine et al., 1981; Sun and May, 1993; Büttner-Ennever, 2006). So far no differences in histochemistry or afferent inputs have been found between the A- and B-group (Spencer et al., 1992; Wasicky et al., 2004; Erichsen et al., 2014).

It has been known for a long time that extraocular muscles exhibit a complex architecture consisting of a global and orbital layer. At least six different types of muscle fibers can be identified, which can be divided into two main categories of SIF and multiply-innervated non-twitch muscle fibers (MIF; for review:

Spencer and Porter, 2006). Tract-tracing experiments in monkey revealed that the motoneurons of MIFs are located in the periphery of the motonuclei. For muscles innervated from the nIII the MIF motoneurons of IR and MR are located in the C-group DM to nIII, and those of IO and SR in the S-group between the both nIII (Büttner-Ennever et al., 2001). Based on their different histochemical properties, SIF motoneurons were identified within nIII and putative MIF motoneurons have been identified around the medial aspects of nIII, also in human (Eberhorn et al., 2005, 2006). However, in the human nIII, the MIF motoneurons could not be allocated to specific extraocular muscles, yet (Horn et al., 2008). Therefore, the proposed map of the human nIII applies only to the SIF motoneurons within nIII, and has yet to be extended in future studies by the location of MIF motoneurons.

The exact knowledge of the location of the subgroups innervating individual eye muscles in human provides an important basis to localize lesions more accurately in MRI scans and relate it to clinical findings. Furthermore, the present work on transmitter inputs to individual eye muscle subgroups will form the basis for postmortem studies of afferent inputs to nIII in cases with known eye-movement deficits

AUTHOR CONTRIBUTIONS

Acquisition of data and analysis was performed by Emmanuel Che Ngwa, Christina Zeeh, and Ahmed Messoudi. Conception of the work was done by Anja K. E. Horn and Jean A. Büttner-Ennever. All authors contributed to the interpretation of data, preparation of the figures, and writing of the manuscript and approved the final version.

ACKNOWLEDGMENTS

This study is part of the medical doctoral thesis of Emmanuel Che Ngwa. The results are published with permission of the Medical Faculty of the Ludwig-Maximilians-University of Munich. We are very grateful to Christine Glombik and Laure Djaleu for their excellent technical assistance. Supported by Deutsche Forschungsgemeinschaft DFG HO 1639/4-3, BMBF (IFB-01EO0901, Brain-Net-01GI0505).

REFERENCES

Ahlfeld, J., Mustari, M., and Horn, A. K. E. (2011). Sources of calretinin inputs to motoneurons of extraocular muscles involved in upgaze. *Ann. N. Y. Acad. Sci.* 1233, 91–99. doi: 10.1111/j.1749-6632.2011.06168.x

Andressen, C., Blümcke, I., and Celio, M. R. (1993). Calcium-binding proteins – selective markers of nerve cells. *Cell Tissue Res.* 271, 181–208. doi: 10.1007/BF00318606

Augustine, J. R., Deschamps, E. G., and Ferguson, J. G. J. (1981). Functional organization of the oculomotor nucleus in the baboon. *Am. J. Anat.* 161, 393–403. doi: 10.1002/aja.1001610405

Averbuch-Heller, L. (1997). Neurology of the eyelids. *Curr. Opin. Ophthalmol.* 8, 27–34. doi: 10.1097/00055735-199712000-00005

Bachtell, R. K., Weitemier, A. Z., Galvan-Rosas, A., Tsivkovskaia, N. O., Risinger, F. O., Phillips, T. J., et al. (2003). The Edinger–Westphal-lateral septum urocortin pathway and its relation to alcohol-induced hypothermia. *J. Neurosci.* 23, 2477–2487.

Baer, K., Waldvogel, H. J., Faull, R. L. M., and Rees, M. I. (2009). Localization of glycine receptors in the human forebrain, brainstem, and cervical spinal cord: an immunohistochemical review. *Front. Mol. Neurosci.* 2:25. doi: 10.3389/neuro.02.025.2009

Baizer, J. S., and Baker, J. F. (2006). Immunoreactivity for calretinin and calbindin in the vestibular nuclear complex of the monkey. *Exp. Brain Res.* 172, 103–113. doi: 10.1007/s00221-005-0318-1

Baizer, J. S., and Broussard, D. M. (2010). Expression of calcium-binding proteins and nNOS in the human vestibular and precerebellar brainstem. *J. Comp. Neurol.* 518, 872–895. doi: 10.1002/cne.22250

Bernheimer, S. (1897). Experimentelle Studien zur Kenntniss der Innervation der inneren und äusseren vom Oculomotorius versorgten Muskeln des Auges. *Albrecht Von Graefes Arch. Ophthalmol.* 44, 481–525. doi: 10.1007/BF02017581

Bruce, G., Wainer, B. H., and Hersh, L. B. (1985). Immunoaffinity purification of human choline acetyltransferase: comparison of the brain and placental enzymes. *J. Neurochem.* 45, 611–620. doi: 10.1111/j.1471-4159.1985.tb04030.x

Burde, R. M. (1983). The visceral nuclei of the oculomotor complex. *Trans. Am. Ophthalmol. Soc.* 81, 532–548.

Burde, R. M. (1988). Direct parasympathetic pathway to the eye: revisited. *Brain Res.* 463, 158–162. doi: 10.1016/0006-8993(88)90540-9

Burde, R. M., and Williams, E. (1989). Parasympathetic nuclei. *Brain Res.* 498, 371–375. doi: 10.1016/0006-8993(89)91119-0

Büttner, U., Büttner-Ennever, J. A., and Henn, V. (1977). Vertical eye movement related unit activity in the rostral mesencephalic reticular formation of the alert monkey. *Brain Res.* 130, 239–252. doi: 10.1016/0006-8993(77)90273-6

Büttner-Ennever, J., and Horn, A. (eds). (2014). *Olszewski and Baxter's Cytoarchitecture of the Human Brainstem*, 3rd Edn. Basel: Karger.

Büttner-Ennever, J. A. (2006). The extraocular motor nuclei: organization and functional neuroanatomy. *Prog. Brain Res.* 151, 95–125. doi: 10.1016/S0079-6123(05)51004-5

Büttner-Ennever, J. A. (2008). Mapping the oculomotor system. *Prog. Brain Res.* 171, 3–11. doi: 10.1016/S0079-6123(08)00601-8

Büttner-Ennever, J. A., and Akert, K. (1981). Medial rectus subgroups of the oculomotor nucleus and their abducens internuclear input in the monkey. *J. Comp. Neurol.* 197, 17–27. doi: 10.1002/cne.901970103

Büttner-Ennever, J. A., Horn, A. K. E., Scherberger, H., and D'Ascanio, P. (2001). Motoneurons of twitch and nontwitch extraocular muscle fibers in the abducens, trochlear, and oculomotor nuclei of monkeys. *J. Comp. Neurol.* 438, 318–335. doi: 10.1002/cne.1318

Chen, B., and May, P. J. (2000). The feedback circuit connecting the superior colliculus and central mesencephalic reticular formation: a direct morphological demonstration. *Exp. Brain Res.* 131, 10–21. doi: 10.1007/s002219900280

Chen, B., and May, P. J. (2002). Premotor circuits controlling eyelid movements in conjunction with vertical saccades in the cat: I. The rostral interstitial nucleus of the medial longitudinal fasciculus. *J. Comp. Neurol.* 450, 183–202. doi: 10.1002/cne.10313

Chen, B., and May, P. J. (2007). Premotor circuits controlling eyelid movements in conjunction with vertical saccades in the cat: II. Interstitial nucleus of Cajal. *J. Comp. Neurol.* 500, 676–692. doi: 10.1002/cne.21203

Chen-Huang, C., and McCrea, R. A. (1998). Viewing distance related sensory processing in the ascending tract of deiters vestibulo-ocular reflex pathway. *J. Vest. Res.* 8, 175–184. doi: 10.1016/S0957-4271(97)00001-3

Cohen, B., and Büttner-Ennever, J. A. (1984). Projections from the superior colliculus to a region of the central mesencephalic reticular formation (cMRF) associated with horizontal saccadic eye movements. *Exp. Brain Res.* 57, 167–176. doi: 10.1007/BF00231143

de la Cruz, R. R., Escudero, M., and Delgado-García, J. M. (1989). Behaviour of medial rectus motoneurons in the alert cat. *Eur. J. Neurosci.* 1, 288–295. doi: 10.1111/j.1460-9568.1989.tb00796.x

de la Cruz, R. R., Pastor, A. M., Martínez-Guijarro, F. J., López-García, C., and Delgado-García, J. M. (1992). Role of GABA in the extraocular motor nuclei of the cat: a postembedding immunocytochemical study. *Neuroscience* 51, 911–929. doi: 10.1016/0306-4522(92)90529-B

Dutertre, S., Becker, C.-M., and Betz, H. (2012). Inhibitory glycine receptors: an update. *Biol. Chem.* 287, 40216–40223. doi: 10.1074/jbc.R112.408229

Eberhorn, A. C., Ardelenanu, P., Büttner-Ennever, J. A., and Horn, A. K. E. (2005). Histochemical differences between motoneurons supplying multiply and singly innervated extraocular muscle fibers. *J. Comp. Neurol.* 491, 352–366. doi: 10.1002/cne.20715

Eberhorn, A. C., Büttner-Ennever, J. A., and Horn, A. K. E. (2006). Identification of motoneurons innervating multiply- or singly-innervated

extraocular muscle fibres in the rat. *Neuroscience* 137, 891–903. doi: 10.1016/j.neuroscience.2005.10.038

Erichsen, J. T., Wright, N. F., and May, P. J. (2014). The morphology and ultrastructure of medial rectus subgroup motoneurons in the macaque monkey. *J. Comp. Neurol.* 522, 626–641. doi: 10.1002/cne.23437

Evinger, C. (1988). Extraocular motor nuclei: location, morphology and afferents. *Rev. Oculomot. Res.* 2, 81–117.

Fuchs, A. F., Becker, W., Ling, L., Langer, T. P., and Kaneko, C. R. (1992). Discharge patterns of levator palpebrae superioris motoneurons during vertical lid and eye movements in the monkey. *J. Neurophysiol.* 68, 233–243.

Fukushima, K., Kaneko, C. R., and Fuchs, A. F. (1992). The neuronal substrate of integration in the oculomotor system. *Prog. Neurobiol.* 39, 609–639. doi: 10.1016/0301-0082(92)90016-8

Gallyas, F. (1979). Silver staining of myelin by means of physical development. *Neurol. Res.* 1, 203–209.

Goldstein, M. E., Sternberger, N. H., and Sternberger, L. A. (1987). Phosphorylation protects neurofilaments against proteolysis. *J. Neuroimmunol.* 14, 149–160. doi: 10.1016/0165-5728(87)90049-X

Highstein, S. M., and Holstein, G. R. (2006). The anatomy of the vestibular nuclei. *Prog. Brain Res.* 151, 157–203. doi: 10.1016/S0079-6123(05)51006-9

Horn, A. K., and Büttner-Ennever, J. A. (2008). Brainstem circuits controlling lid-eye coordination in monkey. *Prog. Brain Res.* 171, 87–95. doi: 10.1016/S0079-6123(08)00612-2

Horn, A. K., Eberhorn, A., Härtig, W., Ardelenanu, P., Messoudi, A., and Büttner-Ennever, J. A. (2008). Perioculomotor cell groups in monkey and man defined by their histochemical and functional properties: reappraisal of the Edinger–Westphal nucleus. *J. Comp. Neurol.* 507, 1317–1335. doi: 10.1002/cne.21598

Horn, A. K., and Leigh, R. J. (2011). The anatomy and physiology of the ocular motor system. *Handb. Clin. Neurol.* 102, 21–69. doi: 10.1016/B978-0-444-52903-9.00008-X

Horn, A. K. E., and Adamcyzk, C. (2011). "Reticular formation - eye movements, gaze and blinks," in *Human Nervous System*, 3rd Edn, eds G. Paxinos and J. K. Mai (San Diego: Academic Press), 328–366.

Horn, A. K. E., Bohlen, M. O., Warren, S., and May, P. J. (2012). Evidence for the central mesencephalic reticular formation playing a role in the near triad. *Soc. Neurosci. Abstr.* 373.12.

Horn, A. K. E., and Büttner-Ennever, J. A. (1998). Premotor neurons for vertical eye-movements in the rostral mesencephalon of monkey and man: the histological identification by parvalbumin immunostaining. *J. Comp. Neurol.* 392, 413–427. doi: 10.1002/(SICI)1096-9861(19980323)392:4<413::AID-CNE1>3.0.CO;2-3

Horn, A. K. E., Büttner-Ennever, J. A., Gayde, M., and Messoudi, A. (2000). Neuroanatomical identification of mesencephalic premotor neurons coordinating eyelid with upgaze in the monkey and man. *J. Comp. Neurol.* 420, 19–34. doi: 10.1002/(SICI)1096-9861(20000424)420:1<19::AID-CNE2>3.0.CO;2-D

Horn, A. K. E., Helmchen, C., and Wahle, P. (2003). GABAergic neurons in the rostral mesencephalon of the Macaque monkey that control vertical eye movements. *Ann. N. Y. Acad. Sci.* 1004, 19–28. doi: 10.1196/annals.1303.003

Ichikawa, T., and Shimizu, T. (1998). Organization of choline acetyltransferase-containing structures in the cranial nerve motor nuclei and spinal cord of the monkey. *Brain Res.* 779, 96–103. doi: 10.1016/S0006-8993(97)01090-1

Ishikawa, S., Sekiya, H., and Kondo, Y. (1990). The center for controlling the near reflex in the midbrain of the monkey: a double labelling study. *Brain Res.* 519, 217–222. doi: 10.1016/0006-8993(90)90080-U

Jiao, Y., Sun, Z., Lee, T., Fusco, F. R., Kimble, T. D., Meade, C. A., et al. (1999). A simple and sensitive antigen retrieval method for free-floating and slide-mounted tissue sections. *J. Neurosci. Methods* 93, 149–162. doi: 10.1016/S0165-0270(99)00142-9

Johnson, J. W., and Ascher, P. (1987). Glycine potentiates the NMDA response in cultured mouse brain neurons. *Nature* 325, 529–531. doi: 10.1038/325529a0

Judge, S. J., and Cumming, B. G. (1986). Neurons in the monkey midbrain with activity related to vergence eye movement and accommodation. *J. Neurophysiol.* 55, 915–930.

Kennard, C. (2011). Disorders of higher gaze control. *Handb. Clin. Neurol.* 102, 379–402. doi: 10.1016/B978-0-444-52903-9.00020-0

Kozicz, T., Bittencourt, J. C., May, P. J., Reiner, A., Gamlin, P. D. R., Palkovits, M., et al. (2011). The Edinger–Westphal nucleus: a historical, structural, and functional perspective on a dichotomous terminology. *J. Comp. Neurol.* 519, 1413–1434. doi: 10.1002/cne.22580

Leigh, R. J., and Zee, D. S. (2006). *The Neurology of Eye Movements*. New York: Oxford University Press.

May, P. J., Horn, A. K. E., Mustari, M. J., and Warren, S. (2011). Central mesencephalic reticular formation projections onto oculomotor motoneurons. *Soc. Neurosci. Abstr.* 699.01

May, P. J., Reiner, A. J., and Ryabinin, A. E. (2008). Comparison of the distributions of urocortin-containing and cholinergic neurons in the perioculomotor midbrain of the cat and macaque. *J. Comp. Neurol.* 507, 1300–1316. doi: 10.1002/cne.21514

May, P. J., Vidal, P.-P., Baker, H., and Baker, R. (2012). Physiological and anatomical evidence for an inhibitory trigemino-oculomotor pathway in the cat. *J. Comp. Neurol.* 520, 2218–2240. doi: 10.1002/cne.23039

Mays, L. E. (1984). Neural control of vergence eye movements: convergence and divergence neurons in midbrain. *J. Neurophysiol.* 51, 1091–1108.

Nguyen, L. T., and Spencer, R. F. (1999). Abducens internuclear and ascending tract of Deiters inputs to medial rectus motoneurons in the cat oculomotor nucleus: neurotransmitters. *J. Comp. Neurol.* 411, 73–86. doi: 10.1002/(SICI)1096-9861(19990816)411:1<73::AID-CNE6>3.0.CO;2-7

Obata, K., and Highstein, S. M. (1970). Blocking by picrotoxin of both vestibular inhibition and GABA action on rabbit oculomotor neurones. *Brain Res.* 18, 538–541. doi: 10.1016/0006-8993(70)90136-8

Olszewski, J., and Baxter, D. (1982). *Cytoarchitecture of the Human Brain Stem*, 2nd Edn. Basel: Karger.

Panegrossi, G. (1898). Contributo allo studio anatomo-fisiologico dei centri dei nerve oculomotori dell'uomo. *Ric. Lab. Anat. norm. Univ. Roma* 6, 103–155.

Partsalis, A. M., Zhang, Y., and Highstein, S. M. (1995). Dorsal Y group in the squirrel monkey. I. Neuronal responses during rapid and long-term modifications of the vertical VOR. *J. Neurophysiol.* 73, 615–631.

Pearson, A. A. (1943). Trochlear nerve in human fetuses. *J. Comp. Neurol.* 78, 29–43. doi: 10.1002/cne.900780103

Perlia, D. (1889). Die Anatomie des Oculomotoriuscentrums beim Menschen. *Albrecht von Graefes Arch. Ophthalmol.* 35, 287–308. doi: 10.1007/BF01695201

Pfeiffer, F., Simler, R., Grenningloh, G., and Betz, H. (1984). Monoclonal antibodies and peptide mapping reveal structural similarities between the subunits of the glycine receptor of rat spinal cord. *Proc. Natl. Acad. Sci. U.S.A.* 81, 7224–7227. doi: 10.1073/pnas.81.22.7224

Porter, J. D., Burns, L. A., and May, P. J. (1989). Morphological substrate for eyelid movements: innervation and structure of primate levator palpebrae superioris and orbicularis oculi muscles. *J. Comp. Neurol.* 287, 64–81. doi: 10.1002/cne.902870106

Porter, J. D., Guthrie, B. L., and Sparks, D. L. (1983). Innervation of monkey extraocular muscles: localization of sensory and motor neurons by retrograde transport of horseradish peroxidase. *J. Comp. Neurol.* 218, 208–219. doi: 10.1002/cne.902180208

Precht, W., Baker, R., and Okada, Y. (1973). Evidence for GABA as the synaptic transmitter of the inhibitory vestibulo-ocular pathway. *Exp. Brain Res.* 18, 415–428. doi: 10.1007/BF00239109

Ryabinin, A. E., Tsivkovskaia, N. O., and Ryabinin, S. A. (2005). Urocortin 1-containing neurons in the human Edinger–Westphal nucleus. *Neuroscience* 134, 1317–1323. doi: 10.1016/j.neuroscience.2005.05.042

Schmidtke, K., and Büttner-Ennever, J. A. (1992). Nervous control of eyelid function – a review of clinical, experimental and pathological data. *Brain* 115, 227–247. doi: 10.1093/brain/115.1.227

Schwindt, P. C., Precht, W., and Richter, A. (1974). Monosynaptic excitatory and inhibitory pathways from medial midbrain nuclei to trochlear motoneurons. *Exp. Brain Res.* 20, 223–238. doi: 10.1007/BF00238314

Sekiya, H., Kojima, Y., Hiramoto, D., Mukuno, K., and Ishikawa, S. (1992). Bilateral innervation of the musculus levator palpebrae superioris by single motoneurons in the monkey. *Neurosci. Lett.* 146, 10–12. doi: 10.1016/0304-3940(92)90159-5

Snyder, L. H., and King, W. M. (1992). Effect of viewing distance and location of the axis of head rotation on the monkey's vestibuloocular reflex. I. Eye movement responses. *J. Neurophysiol.* 67, 861–874.

Spencer, R. F., and Baker, R. (1992). GABA and glycine as inhibitory neurotransmitters in the vestibulo-ocular reflex. *Ann. N. Y. Acad. Sci.* 656, 602–611. doi: 10.1111/j.1749-6632.1992.tb25239.x

Spencer, R. F., and Porter, J. D. (1981). Innervation and structure of extraocular muscles in the monkey in comparison to those of the cat. *J. Comp. Neurol.* 198, 649–665. doi: 10.1002/cne.901980407

Spencer, R. F., and Porter, J. D. (2006). Biological organization of the extraocular muscles. *Prog. Brain Res.* 151, 43–80. doi: 10.1016/S0079-6123(05)51002-1

Spencer, R. F., Wang, S. F., and Baker, R. (1992). The pathways and functions of GABA in the oculomotor system. *Prog. Brain Res.* 90, 307–331. doi: 10.1016/S0079-6123(08)63620-1

Spencer, R. F., Wenthold, R. J., and Baker, R. (1989). Evidence for glycine as an inhibitory neurotransmitter of vestibular, reticular, and prepositus hypoglossi neurons that project to the cat abducens nucleus. *J. Neurosci.* 9, 2718–2736.

Sternberger, L. A., Harwell, L. W., and Sternberger, N. H. (1982). Neurotype: regional individuality in rat brain detected by immunocytochemistry with monoclonal antibodies. *Proc. Natl. Acad. Sci. U.S.A.* 79, 1326–1330. doi: 10.1073/pnas.79.4.1326

Sternberger, L. A., and Sternberger, N. H. (1983). Monoclonal antibodies distinguish phorphorylated and non-phosphorylated forms of neurofilaments in situ. *Proc. Natl. Acad. Sci. U.S.A.* 80, 6126–6130. doi: 10.1073/pnas.80.19.6126

Stilling, B. (1846). Disquisitiones de structure et functionibus cerebri. *Jenae: sumt. F. Maukii. T.* 1, 36.

Sugiuchi, Y., Takahashi, M., and Shinoda, Y. (2013). Input-output organization of inhibitory neurons in the interstitial nucleus of Cajal projecting to the contralateral trochlear and oculomotor nucleus. *J. Neurophysiol.* 110, 640–657. doi: 10.1152/jn.01045.2012

Sun, W. S., and May, P. J. (1993). Organization of the extraocular and preganglionic motoneurons supplying the orbit in the lesser galago. *Anat. Rec.* 237, 89–103. doi: 10.1002/ar.1092370109

Triller, A., Cluzeaud, F., Pfeiffer, F., Betz, H., and Korn, H. (1985). Distribution of glycine receptors at central synapses: an immunoelectron microscopy study. *J. Cell Biol.* 101, 683–688. doi: 10.1083/jcb.101.2.683

Tsuchida, U. (1906). Ueber die Ursprungskerne der Augenbeweguns-Nerven im Mittel- und Zwischenhirn. *Arb. Hirnanat. Inst. Zürich* 1–2, 1–205.

Ugolini, G., Klam, F., Doldan Dans, M., Dubayle, D., Brandi, A.-M., Büttner-Ennever, J. A., et al. (2006). Horizontal eye movement networks in primates as revealed by retrograde transneuronal transfer of rabies virus: differences in monosynaptic input to "slow" and "fast" abducens motoneurons. *J. Comp. Neurol.* 498, 762–785. doi: 10.1002/cne.21092

Van der Werf, F., Aramideh, M., Ongerboer De Visser, B. W., Baljet, B., Speelman, J. D., and Otto, J. A. (1997). A retrograde double fluorescent tracing study of the levator palpebrae superioris muscle in the cynomolgus monkey. *Exp. Brain Res.* 113, 174–179. doi: 10.1007/BF02454155

von Gudden, B. (1881). Über den Tractus peduncularis transversus. *Arch. Psychiatr. Nervenkr.* 2, 364–366.

Waitzman, D. M., Pathmanathan, J., Presnell, R., Ayers, A. S., and Depalma-Bowles, S. (2002). Contribution of the superior colliculus and the mesencephalic reticular formation to gaze control. *Ann. N. Y. Acad. Sci.* 956, 111–129. doi: 10.1111/j.1749-6632.2002.tb02813.x

Waitzman, D. M., Silakov, V. L., Depalma-Bowles, S., and Ayers, A. S. (2000a). Effects of reversible inactivation of the primate mesencephalic reticular formation. I. Hypermetric goal-directed saccades. *J. Neurophysiol.* 83, 2260–2284.

Waitzman, D. M., Silakov, V. L., Depalma-Bowles, S., and Ayers, A. S. (2000b). Effects of reversible inactivation of the primate mesencephalic reticular formation. II. Hypometric vertical saccades. *J. Neurophysiol.* 83, 2285–2299.

Waldvogel, H. J., Baer, K., Eady, E., Allen, K. L., Gilbert, R. T., Mohler, H., et al. (2010). Differential localization of γ-aminobutyric acid type a and glycine receptor subunits and gephyrin in the human pons, medulla oblongata and uppermost cervical segment of the spinal cord: an immunohistochemical study. *J. Comp. Neurol.* 518, 305–328. doi: 10.1002/cne.22212

Wang, N., Perkins, E., Zhou, L., Warren, S., and May, P. J. (2013). Anatomical evidence that the superior colliculus controls saccades through central mesencephalic reticular formation gating of omnipause neuron activity. *J. Neurosci.* 33, 16285–16296. doi: 10.1523/JNEUROSCI.2726-11.2013

Warwick, R. (1953a). Representation of the extraocular muscles in the oculomotor nuclei of the monkey. *J. Comp. Neurol.* 98, 449–495. doi: 10.1002/cne.900980305

Warwick, R. (1953b). The identity of the posterior dorso-central nucleus of Panegrossi. *J. Comp. Neurol.* 99, 599–611. doi: 10.1002/cne.900990307

Warwick, R. (1955). The so-called nucleus of convergence. *Brain* 78, 92–114. doi: 10.1093/brain/78.1.92

Wasicky, R., Horn, A. K. E., and Büttner-Ennever, J. A. (2004). Twitch and non-twitch motoneuron subgroups of the medial rectus muscle in the oculomotor nucleus of monkeys receive different afferent projections. *J. Comp. Neurol.* 479, 117–129. doi: 10.1002/cne.20296

Wentzel, P. R., Gerrits, N. M., and Dezeeuw, C. I. (1996). GABAergic and glycinergic inputs to the rabbit oculomotor nucleus with special emphasis on the medial rectus subdivision. *Brain Res.* 707, 314–319. doi: 10.1016/0006-8993(95)01389-X

Zeeh, C., Hess, B. J., and Horn, A. K. E. (2013). Calretinin inputs are confined to motoneurons for upward eye movements in monkey. *J. Comp. Neurol.* 521, 3154–3166. doi: 10.1002/cne.23337

Zhang, Y., Gamlin, P. D. R., and Mays, L. E. (1991). Antidromic identification of midbrain near response cells projecting to the oculomotor nucleus. *Exp. Brain Res.* 84, 525–528. doi: 10.1007/BF00230964

Zhang, Y., Mays, L. E., and Gamlin, P. D. R. (1992). Characteristics of near response cells projecting to the oculomotor nucleus. *J. Neurophysiol.* 67, 944–960.

Ziegler, B., Augstein, A., Schröder, D., Mauch, L., Hahmann, J., Schlosser, M., et al. (1996). Glutamate decarboxylase (GAD) is not detectable on the surface of rat islet cells examined by cytofluorometry and complement-dependent antibody-mediated cytotoxicity of monoclonal GAD antibodies. *Horm. Metab. Res.* 28, 11–15. doi: 10.1055/s-2007-979121

Conflict of Interest Statement: The authors declare that the research was conducted in the absence of any commercial or financial relationships that could be construed as a potential conflict of interest.

Received: 16 November 2013; accepted: 14 January 2014; published online: 12 February 2014.

*Citation: Che Ngwa E, Zeeh C, Messoudi A, Büttner-Ennever JA and Horn AKE (2014) Delineation of motoneuron subgroups supplying individual eye muscles in the human oculomotor nucleus. Front. Neuroanat. **8**:2. doi: 10.3389/fnana.2014.00002*

This article was submitted to the journal Frontiers in Neuroanatomy.

4 Discussion

The performed studies on the histochemical profile of motoneuron inputs provide a new insight in the different inhibitory control of motoneurons of horizontally and vertically pulling eye muscles, the different calcium control mechanism of up- and downgaze motoneurons as well as the different transmitter input to MIF- and SIF motoneurons of individual eye muscles.
Furthermore, the present work provides new data on the histochemical properties of premotor inputs to motoneuronal groups of the twitch- and non-twitch eye muscle systems in primates. Especially the different calcium control mechanisms in upgaze pathways may provide the possibility for a targeted analysis of this system in human post-mortem studies of clinical cases with impairment of upward eye movements.

4.1 Different inhibitory transmitter input to motoneurons for horizontal and vertical eyemovements

Inhibition in horizontal eye movements is provided by glycine, while GABA is the major inhibitory transmitter of vertical eye movements (Spencer and Baker, 1992). But there are contradictory results about a strong GABAergic input to MR motoneurons mediating horizontal eye movements. No obvious difference is noticed in the density of GABAergic terminals between the different subgroups of nIII in cat, rabbit and monkey (De la Cruz et al., 1992; Wentzel et al., 1996; Zeeh et al., 2015).
In human a strong GABAergic input is found to presumed MR motoneurons, which is not seen in monkey. Here the number of GABAergic terminals contacting putative MR subgroups exceeded even that of motoneuron groups involved in vertical gaze. This may indicate an evolvement of inputs related to vergence, which is particularly prominent in human (Che-Ngwa et al., 2014).
The inhibition of motoneurons involved in horizontal eye movements seems to be a more constant feature in primates (Waitzman et al., 1996). In both primate species a glycinergic input is almost exclusively seen to motoneurons of MR (Spencer et al., 1989; Che-Ngwa et al., 2014; Zeeh et al., 2015). In contrast, glycinergic terminals appear to be distributed to all motoneuron subgroups except the MR subdivision in cats (Spencer et al., 1989; Spencer and Baker, 1992). In rabbit glycine-

immunoreactive boutons are distributed through all subdivisions of nIII including MR region (Wentzel et al., 1996), but may colocalize with GABA (Wentzel et al., 1993).
An overview of possible GABAergic and glycinergic sources projecting to motoneurons mediating horizontal and vertical eye movements is seen in Fig.8 and in Tab.2.

4.2 Up- and downgaze pathways differ in their calcium-binding proteins

The calcium-binding protein calretinin (CR) has been identified in several brainstem regions known to contain premotor neurons involved in vertical eye movements (Horn et al., 2003; Baizer and Baker, 2006). In the vertical system CR is exclusively associated with upgaze pathways in primates (Zeeh et al., 2013). Although motoneurons of up- and downgaze pathways exhibit similar firing characteristics (Vilis et al., 1989; Moschovakis et al., 1991a; Moschovakis et al., 1991b), which may be reflected by the expression of the calcium-binding protein parvalbumin (PV), motoneurons involved in upgaze contain an additional calcium-binding protein CR. Until now the functional significance of CR in upgaze connection is unclear. Whereas PV is present in many fast-firing or highly active neurons, for example in the saccadic burst neurons in the rostral interstitial nucleus of the medial longitudinal fascicle (RIMLF) and interstitial nucleus of Cajal (INC) (Horn and Büttner-Ennever, 1998), no obvious association of CR with specific properties is known. Generally calcium-binding proteins serve as Ca^{2+} buffers, controlling the duration and spread of Ca^{2+} signals, as well as Ca^{2+} sensors, translating changes of Ca^{2+} concentration into intracellular signals (Brini et al., 2014). The suggested functions of CR involve a role in neuroprotection, development and regulation of neuronal excitability (for review: Schwaller, 2014). The specific presence of CR in addition to PV in premotor up-burst neurons of the INC and RIMLF may reflect different calcium control mechanism for upgaze neurons compared to downgaze neurons (Horn et al., 2003).
Up- and downward saccades can be affected in a different manner in several clinical conditions. For example structural lesions induced by infarcts or tumors can affect the efferent pathways of premotor burst neurons selectively (Büttner-Ennever et al., 1982; Pierrot-Deseilligny et al., 1982; Partsalis et al., 1994). The down-burst neurons in RIMLF project ipsilaterally to IR and SO motoneurons, whereas the up-burst

neurons project bilaterally to SR and IO motoneurons in both nIII. The crossing fibers travel through the posterior commissure, a lesion of which results in an upgaze palsy (Partsalis et al., 1994; Zeeh et al., 2013).

There are also neurodegenerative diseases characterized by paresis of vertical saccades, often affecting only one direction, for example Niemann-Pick disease type C (NPC) and progressive supranuclear palsy (PSP) (Chen et al., 2010; Strupp et al., 2014). A disturbance of the Ca^{2+} signaling could be a possible mechanism for the degeneration of only one pathway. With CR as a marker for excitatory premotor up-burst neurons in RIMLF and INC, these populations can be specifically identified for analysis in post-mortem analysis of cases with for example NPC (Ahlfeld et al., 2011).

Fig. 8 and Tab. 2 show sources of CR positive neuronal population projecting to upgaze motoneurons in nIII.

4.3 Different transmitter input to MIF motoneurons and SIF motoneurons

The current concept of a dual control of eye muscles – activation of SIFs for generation of eye movements and activation of MIFs for gaze holding – was initially suggested to be regulated by different premotor pathways (Büttner-Ennever and Horn, 2002). Motoneurons in and around nIII activating MIFs and SIFs do not receive identical afferent inputs. Some afferents are known to target both, such as the abducens area, Y-group or parvocelluar medial vestibular nucleus, whereas others innervate either one or the other (Wasicky et al., 2004). A major input to MIF motoneurons of nIII is the pretectum, the central mesencephalic formation (cMRF) and supraoculomotor area (SOA) (Zhang et al., 1991; Büttner-Ennever et al., 1996; Büttner-Ennever et al., 2002; Graf et al., 2002). In comparison to SIF motoneurons, MIF motoneurons do not receive direct afferents from premotor saccadic regions, for example the paramedian pontine reticular formation (PPRF), the region of inhibitory burst neurons and also not from oculomotor internuclear neurons (Ugolini et al., 2001; Büttner-Ennever et al., 2002; Wasicky et al., 2004).

An overview of afferent inputs to nIII is shown in Fig. 8 and Tab. 2.

The current study extends these findings by demonstrating differences in transmitter inputs to SIF- and MIF motoneurons of individual eye muscles. SIF- and MIF motoneurons do not differ in their GABAergic, glycinergic and vesicular glutamate transporter (vGlut) 2 input, whereas vGlut1 containing terminals covering the supraoculomotor area target only MR MIF motoneurons (Zeeh et al., 2015). Unlike vGlut1, a considerable supply of vGlut2-positive afferents is seen to nIII that are evenly distributed across all subgroups. In general, vGlut1 is densely expressed in regions where the synapses have lower releasing probabilities, while vGlut2 is enriched in areas where synapses have a relatively high release probability (Weston et al., 2011). This corresponds to the findings that SIFs respond to an electrical stimulation with a fast twitch, whereas MIFs respond with a slow tonic contraction (Lennerstrand, 1974; Chiarandini and Stefani, 1979). SIF- and MIF motoneurons of individual eye muscles also differ in their α-amino-3-hydroxy-5-methyl-4-isoxazolepropionic acid (AMPA) receptor and N-methyl-D-aspartate (NMDA) receptor immunoreactivity. NMDA receptors (NMDAR1) and AMPA receptors (Glu4 subunit) are only expressed in SIF motoneurons in monkey (Ying et al., 2008), this may suggest that SIF motoneurons participate in the fast and slow components of postsynaptic response to glutamate. The phasic-tonic firing of larger motoneurons, like SIF mototneurons, is reinforced by glutamate and may provide a strong muscle contraction for eye movements (Torres-Torrelo et al., 2012).

In addition, SIF- and MIF motoneurons display histochemical differences, which may reflect their different physiological properties. SIF motoneurons possess perineuronal nets and contain non-phosphorylated neurofilaments (NP-NF), whereas MIF motoneurons lack both (Eberhorn et al., 2005a; Eberhorn et al., 2006).

Possible sources of GABA, glycine and vGlut1/2 are summarised in Fig. 8 and Tab. 2.

4.3.1 Supraoculomotor area (SOA) as a center for near response

The SOA is located dorsal to nIII in the ventral portion of the periaqueductal gray and was first described by Edwards and Henkel in 1978 (Edwards and Henkel, 1978) and may function as an integration center for near response. The “near response” or “near triad” is defined by the simultaneous activation of vergence, lens

accommodation and pupillary constriction (Myers et al., 1990). Several functional cell groups involved in near response are found within the SOA.

4.3.1.1 Cell groups in SOA

MIF motoneurons of medial rectus:

MIF motoneurons in the C-group form two independent populations (Büttner-Ennever et al., 2001; Tang et al., 2015). IR MIF motoneurons lie adjacent to the dorsomedial border of the oculomotor nucleus and MR motoneurons are located more medially (Tang et al., 2015). One noticeable feature of the C-group is the different pattern of dendrite distribution of MR and IR motoneurons. Dendrites of IR motoneurons spread out into the SOA bilaterally, whereas dendrites of MR motoneurons are restricted to the ipsilateral side. Furthermore, the dendrites of MR MIF motoneurons extend dorsally to the preganglionic neurons of the Edinger-Westphal nucleus (Büttner-Ennever et al., 2001; Lienbacher et al., 2011; Tang et al., 2015). Thereby the C-group motoneurons may receive a synaptic input from the same sources as the preganglionic motoneurons in EW (Erichsen et al., 2014). Since vGlut1 containing terminals densely cover the SOA and target MR MIF motoneurons (Zeeh et al., 2015), it is possible that the vGlut1 input affects the near response system.

Edinger-Westphal nucleus (EW):

Further cell groups of the SOA are represented by the EW, which consists of two separate populations with different projection targets and function: 1. EWpg contains the cholinergic preganglionic neurons of the ciliary ganglion mediating pupillary constriction and lens accommodation and 2. EWcp, a centrally projecting division containing the neuropeptide urocortin 1 (UCN). UCN is considered to play a role in stress modulation and in food and fluid intake (Kozicz et al., 1998; Gaszner and Kozicz, 2003; Vasconcelos et al., 2003; Kübler et al., 2014). There has been some confusion, because the term ‘Edinger-Westphal nucleus’ has been used to describe two different cell groups, which display different arrangements in different species. Kozicz and colleagues introduced a new terminology, EWcp and EWpg, to clarify the population being addressed in a study independent of the location (Kozicz et al.,

2011). In general, either the preganglionic neurons are located in the cytoarchitecturally defined EW, as in monkey and bird, and the UCN-positive cells are distributed around them, or the UCN-positive cells are located in the cytoarchitecturally defined EWcp and the preganglionic neurons are scattered around them (Horn et al., 2009). The latter arrangement is found in most species including rat, cat, ferret, and human (Horn et al., 2008; May et al., 2008; Horn et al., 2009).

Near response cells:
An additional group of neurons is located in the SOA dorsolateral to nIII termed “near response cells”. These cells change their firing rate with disjunctive eye movements, but show no change in activity for conjugate gaze shift (Zhang et al., 1992). Another study showed that the activity of most near response cells is proportional to the angle of convergence of the eyes (Mays, 1984).

4.3.2 The central mesencephalic reticular formation (cMRF) as possible premotor source for near response

Only recently, an area in the mesencephalic reticular formation has drawn researchers´ attention because of a possible involvement in control of the near response. A distinct population of neurons within the central mesencephalic reticular formation (cMRF) was shown to project to the SOA including preganglionic neurons of the ciliary ganglion in primates (Bohlen et al, 2015; May et al., 2015). Originally, the cMRF was considered to be a center for saccades, since electrical stimulation of the cMRF produces horizontal saccades (Cohen and Büttner-Ennever, 1984; Waitzman et al., 1996; Zhou et al., 2008; Wang et al., 2010). The new finding of the specific projection targets of the cMRF suggests that at least a subgroup may be involved in the control of the near triad (Bohlen et al., 2015). A monosynaptic input from cMRF to the MR C-group neurons as well as to preganglionic neurons has been identified in monkey. GABA staining and ultrastructural analysis indicates that projections from cMRF to C-group and preganglionic neurons contain inhibitory and excitatory elements (Horn et al., 2012, May et al, 2011). Thereby these afferents may correspond to vGlut1 and GABA inputs found in the present study (Zeeh et al., 2015). It remains a yet unanswered question, whether it is a coincidence that the modulatory

cell group of EWcp involved in stress reaction and in food intake is located close to neurons responsible for near response. A recent study in monkey demonstrated that a weak input is also found to UCN-positive neurons in the EWcp in addition to those to the EWpg from the cMRF (May et al., 2015). Changes in gaze direction and attention is also necessary in food supply and dangerous situations, when the eyes are turned towards the source of danger (Kübler et al., 2014), which may explain the close spatial relationship of both neuronal groups.

The targets of cMRF projections are summarized in Fig. 8 and Tab. 2.

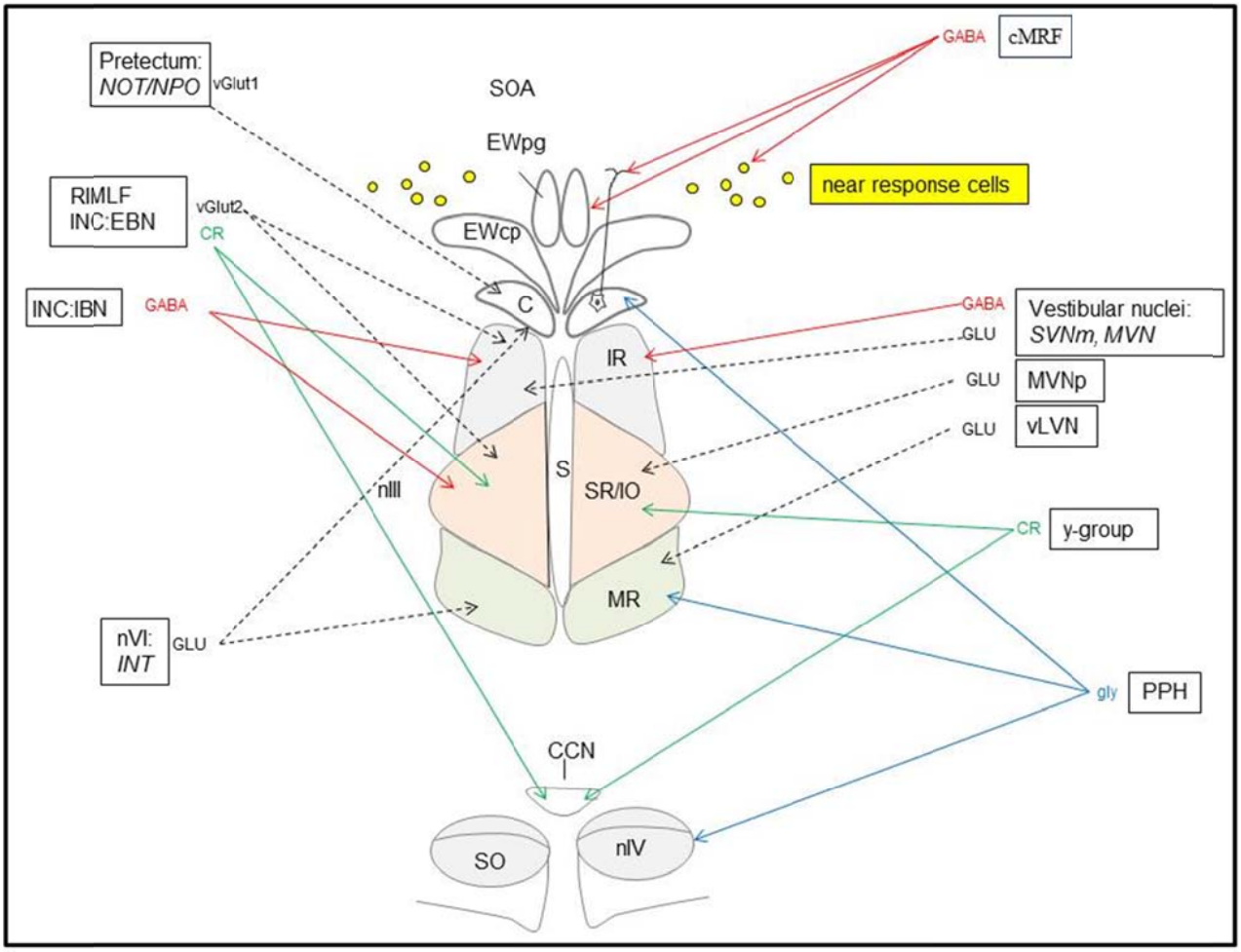

Fig. 8: Summary of afferent inputs to different cell groups in oculomotor (nIII) and trochlear (nIV) nucleus and in the supraoculomotor area (SOA).

nVI - abducens nucleus; CCN - central caudal nucleus; cMRF - central mesencephalic reticular formation; CR - calretinin; EBN - excitatory burst neuron; EWcp - non-preganglionic centrally projecting EW; EWpg - Edinger-Westphal nucleus preganglionic; GLU - Glutamate; IBN - inhibitory burst neuron; INC - interstitial nucleus of Cajal ; INT - internuclear neuron; IO - inferior oblique muscle; IR - inferior rectus muscle; MR - medial rectus muscle; MVN - medial vetibular nuclus; MVNp - MVN parvocellular part; NPO – pretectal olivary nucleus; NOT - Nucleus of the optic tract; PPH - Nucleus prepositus hypoglossi; RIMLF - rostral interstitial nucleus of the medial longitudinal fascicle; SR - superior rectus muscle; SVNm - superior vestibular nucleus magnocellular part; vGlut - vesicular glutamate transporter; vLVN - ventral part of the lateral vestibular nucleus

Region	Transmitter	Target area
Vestibular nuclei SVNm, MVN	GABA, GLU	IR
MVNp	GLU	SR/IO
vLVN	GLU	MR
Y-group	CR	SR/IO, CCN
nVI (INT)	GLU	MR, C-group
Pretectum (NOT/NPO)	vGlut1	C-group
PPH	Glycine	C-group, MR, SO
RIMLF/INC:EBN	vGlut2	IR, SR/IO
	CR	CCN, SR/IO
INC:IBN	GABA	IR, SR/IO
cMRF	GABA, non-GABAergic projections	EWpg, near response cells, dendrites of MIF-motoneuons in C-group

Table 2: Overview of afferent inputs to different cell groups in oculomotor (nIII) and trochlear (nIV) nucleus and in the supraoculomotor area (SOA).
nVI - abducens nucleus; CCN - central caudal nucleus; cMRF - central mesencephalic reticular formation; CR - calretinin; EBN - excitatory burst neuron; EWcp - non-preganglionic centrally projecting EW; EWpg - Edinger-Westphal nucleus preganglionic; GLU - glutamate; IBN - inhibitory burst neuron; INC - interstitial nucleus of Cajal ; INT - internuclear neuron; IO - inferior oblique muscle; IR - inferior rectus muscle; MR - medial rectus muscle; MVN - medial vetibular nuclus; MVNp - MVN parvocellular part; NPO - pretectal olivary nucleus; NOT - Nucleus of the optic tract; PPH - Nucleus prepositus hypoglossi; RIMLF - rostral interstitial nucleus of the medial longitudinal fascicle; SR - superior rectus muscle; SVNm - superior vestibular nucleus magnocellular part; vGlut - vesicular glutamate transporter; vLVN - ventral part of the lateral vestibular nucleus

References

Ahlfeld J, Mustari M, Horn AKE. 2011. Sources of calretinin inputs to motoneurons of extraocular muscles involved in upgaze. Ann N Y Acad Sci 1233:91-99.

Akagi Y. 1978. The localization of the motor neurons innervating the extraocular muscles in the oculomotor nuclei of the cat and rabbit, using horseradish peroxidase. J Comp Neurol 181, 745-761.

Akao T, Kumakura Y, Kurkin S, Fukushima J, Fukushima K. 2007. Directional asymmetry in vertical smooth-pursuit and cancellation of the vertical vestibulo-ocular reflex in juvenile monkeys. Exp Brain Res 182(4): 469-478.

Akert K, Glicksman MA, Lang W, Grob P, Huber A. 1980. The Edinger-Westphal nucleus in the monkey. A retrograde tracer study. Brain Res 184, 491-498.

Alvarado-Mallart RM, Pincon Raymond M. 1979. The palisade endings of cat extraocular muscles: a light and electron microscope study. Tissue Cell 11, 567-584.

Bach-Y-Rita P, Ito F. 1966. In vivo studies on fast and slow muscle fibers in cat extraocular muscles. J Gen Physiol 49, 1177-1198.

Baizer JS, Baker JF. 2006. Immunoreactivity for calretinin and calbindin in the vestibular nuclear complex of the monkey. Exp Brain Res 172:103-113.

Baker R, Gilland E, Green A, Straka H, Suwa H. 1998. Rhombomeric organization of horizontal optokinetic and vestibulo-ocular reflexes in goldfish. Soc Neurosci Abstr 24, 1411.

Becker W. 1989. The neurobiology of saccadic eye movements. Metrics. Rev Oculomot Res 3:13-67.

Bernheimer S. 1897. Experimentelle Studien zur Kenntniss der Innervation der inneren und äusseren vom Oculomotorius versorgten Muskeln des Auges. Arch f Ophthalmol 44, 481-525.

Bohlen MO, Warren S, May PJ. 2015. A central mesencephalic reticular formation projection to the supraoculomotor area in macaque monkeys. Brain Struct Funct. DOI: 10.1007/s00429-015-1039-2.

Bondi AY, Chiarandini DJ. 1983. Morphologic and electrophysiologic identification of multiply innervated fibers in rat extraocular muscles. Invest Ophthal Vis Sci 24, 516-519.

Briggs MM, Schachat F. 2002. The superfast extraocular myosin (MYH13) is localized to the innervation zone in both the global and orbital layers of rabbit extraocular muscle. J Exp Biol 205, 3133-3142.

Brini M, Calì T, Ottolini D, Carafoli E. 2014. Neuronal calcium signaling: function and dysfunction. Cell Mol Life Sci 71(15):2787-814.

Brouwer B. 1918. Klinisch-anatomische Untersuchung über den Oculomotoriuskern. Z Ges Neurol Psychiat 40, 152-193.

Brückner G, Brauer K, Härtig W, Wolff JR, Rickmann MJ, Derouiche A, Delpech B, Girard D, Oertel WH, Reichenbach A. 1993. Perineuronal nets provide a polyanionic, glia-associated form of microenvironment around certain neurons in many parts of the rat brain. Glia 8, 3183-3200.

Brückner G, Schütz A, Härtig W, Brauer K, Paulke BR, Bigl V. 1994. Projection of non-cholinergic basal forebrain neurons ensheathed with perineuronal nets to rat mesocortex. J Chem Neuroanat 8, 11-18.

Brückner G, Hausen D, Härtig W, Drlicek M, Arendt T, Brauer K. 1999. Cortical areas abundant in extracellular matrix chondroitin sulphate proteoglycans are less affected by cytoskeletal changes in Alzheimer`s disease. Neuroscience 92, 791-805.

Brueckner JK, Itkis O, Porter JD. 1996. Spatial and temporal patterns of myosin heavy chain expression in developing rat extraocular muscle. J Muscle Res Cell Motil 17, 297-312.

Büttner U, Büttner-Ennever JA. 2006. Present concepts of oculomotor organization. Prog Brain Res 151, 1-42.

Büttner-Ennever JA, Akert K. 1981. Medial rectus subgroups of the oculomotor nucleus and their abducens internuclear input in the monkey. J Com Neurol 197, 17-27.

Büttner-Ennever JA, Büttner U, Cohen B, Baumgartner G. 1982. Vertical gaze paralysis and the rostral interstitial nucleus of the medial longitudinal fasciculus. Brain 105:125-149.

Büttner-Ennever JA, Cohen B, Horn AKE, Reisine H. 1996. Pretectal projections to the oculomotor complex of the monkey and their role in eye movements. J Comp Neurol 366:348-359.

Büttner-Ennever JA, Horn AKE, Scherberger H, D'Ascanio P. 2001. Motoneurons of twitch and nontwitch extraocular muscle fibers in the abducens, trochlear, and oculomotor nuclei of monkeys. J Comp Neurol 438:318-335.

Büttner-Ennever JA, Horn AKE, Graf W, Ugolini G. 2002. Modern concepts of brainstem anatomy. Ann N Y Acad of Sci 956:75-84.

Büttner-Ennever JA, Horn AKE. 2002. Oculomotor system: a dual innervation of the eye muscles from the abducens, trochlear, and oculomotor nuclei. Mov Disord 17, 2-3.

Büttner-Ennever JA. 2006. The extraocular motor nuclei: organization and functional neuroanatomy. Prog Brain Res 151, 95-125.

Che-Ngwa E, Zeeh C, Messoudi A, Büttner-Ennever JA, Horn AKE. 2014. Delineation of motoneuron subgroups supplying individual eye muscles in the human oculomotor nucleus. Front Neuroanat 8: 2. DOI: 10.3389/fnana.2014.00002.

Chen AL, Riley DE, King SA, Joshi AC, Serra A, Liao K, Cohen ML, Otero-Millan J, Martinez-Conde S, Strupp M, Leigh RJ. 2010. The Disturbance of Gaze in Progressive Supranuclear Palsy (PSP): Implications for Pathogenesis. Front Neurol 1: 147.

Chiarandini DJ, Stefani E. 1979. Electrophysiological identification of two types of fibres in rat extraocular muscles. J Physiol 290:453-465.

Cilimbaris PA. 1910. Histologische Untersuchungen über die Muskelspindeln der Augenmuskeln. Archiv für mikroskopische Anatomie und Entwicklungsgeschichte 75, 692-747.

Clark RA, Demer JL. 2014. Lateral Rectus Superior Compartment Palsy. Am J Ophthalmol 157, 479-487.

Cohen B, Büttner-Ennever JA. 1984. Projections from the superior colliculus to a region of the central mesencephalic reticular formation (cMRF) associated with horizontal saccadic eye movements. Exp Brain Res 57:167-176.

Cooper S, Eccles JC. 1930. The isometric responses of mammalian muscles. J Physiol 69:377.

Da Silva Costa RM, Kung J, Poukens V, Yoo L, Tychsen L, Demer JL. 2011. Intramuscular Innervation of Primate Extraocular Muscles: Unique Compartmentalization in Horizontal Recti. Invest Ophthalmol Vis Sci 52, 2830-2836.

De la Cruz RR, Pastor AM, Martinez-Guijarro FJ, Lopez-Garcia C, Delgado-García JM. 1992. Role of GABA in the extraocular motor nuclei of the cat: a postembedding immunocytochemical study. Neuroscience 51:911-929.

Demer JL, Yeul Oh S, Poukens V. 2000. Evidence for active control of rectus extrocular muscle pulleys. Invest Ophthal Vis Sci 41, 1280-1290.
Denny-Brown D. 1929. The histological features of striped muscle in relation to its functional activity. Proc R Soc Lond B Biol Sci 104:252,1929.
Dogiel AS. 1906. Die Endigungen der sensiblen Nerven in den Augenmuskeln und deren Sehnen beim Menschen und den Säugetieren. Archiv für mikroskopische Anatomie 68, 501-526.
Donaldson IML. 2000. The functions of the proprioceptors of the eye muscles. Phil Trans Soc London B 355, 1685-1754.
Durston JH. 1974. Histochemistry of primate extraocular muscles and the changes of denervation. J Ophthalmol 58, 193-216.
Eberhorn AC, Ardelenanu P, Büttner-Ennever JA, Horn AKE. 2005a. Histochemical differences between motoneurons supplying multiply and singly innervated extraocular muscle fibers. J Comp Neurol 491, 352-366.
Eberhorn AC, Horn AKE, Fischer P, Büttner-Ennever JA. 2005b. Proprioception and palisade endings in extraocular muscles. Ann N . Acad Sci 1039, 1-8.
Eberhorn AC, Büttner-Ennever JA, Horn AKE. 2006. Identification of motoneurons innervating multiply- or singly-innervated extraocular muscle fibres in the rat. Neuroscience 137, 891-903.
Edinger L. 1885. Über den Verlauf der centralen Hirnnervenbahnen mit Demonstrationen von Präparaten. Arch Psychiat Nervenkr 16, 858-859.
Edwards SB, Henkel CK. 1978. Superior colliculus connections with the extraocular motor nuclei in the cat. J Comp Neurol 179:451-467.
Erichsen JT, Wright NF, May PJ. 2014. Morphology and ultrastructure of medial rectus subgroup motoneurons in the macaque monkey. J Comp Neurol. 522(3):626-41.
Evinger C, Graf WM, Baker R. 1987. Extra- and intracellular HRP analysis of the organization of extraocular motoneurons and internuclear neurons in the guinea pig and rabbit. J Comp Neurol 262, 429-445.
Evinger C. 1988. Extraocular motor nuclei: location, morphology and afferents. In: Büttner-Ennever JA. (Ed.), Rev Oculomot Res 81-117, Amsterdam; New York; Oxford: Elsevier.
Fernand VSV, Hess A. 1969. The occurrence, structure and innervation of slow and twitch muscle fibres in the tensor tympani and stapedius of the cat. J Physiol 200, 547-554.
Fraterman S, Khurana TS, Rubinstein NA. 2006. Identification of acetylcholine receptor subunits differentially expressed in singly and multiply innervated fibers of extraocular muscles. Invest Ophthalmol Vis Sci 47, 3828-3834.
Fritzsch B. 1998. Evolution of the vestibulo-ocular system. Otolaryngol Head Neck Surg 119, 182-192.
Fuchs AF, Scudder CA, Kaneko CR. 1988. Discharge patterns and recruitment order of identified motoneurons and internuclear neurons in the monkey abducens nucleus. J Neurophysiol 60, 1874-1895.
Gacek RR. 1977. Location of brain stem neurons projecting to the oculomotor nucleus in the cat. Exp Neurol 57, 725-749.
Gamlin PDR, Reiner A. 1991. The Edinger-Westphal nucleus: sources of input influencing accommodation, pupilloconstriction, and choroidal blood flow. J Com Neurol 306, 425-438.
Gaszner B, Kozicz T. 2003. Interaction between catecholaminergic terminals and urocortinergic neurons in the Edinger-Westphal nucleus in the rat. Brain Res 989:117-121.

Glicksman MA. 1980. Localization of motoneurons controlling the extraocular muscles of the rat. Brain Res 188, 53-62.
Graf W, Baker R. 1985. The Vestibuloocular Reflex of the Adult Flatfish.I. Oculomotor Organization. J Neurophysiol 54(4):887-99.
Graf W, Gerrits N, Yatim-Dhiba N, Ugolini G. 2002. Mapping the oculomotor system: the power of transneuronal labelling with rabies virus. Eur J Neurosci 15:1557-1562.
Han Y, Wang J, Fischman DA, Biller HF, Sanders I. 1999. Slow tonic muscle fibers in the thyroarytenoid muscles of human vocal folds; a possible specialization for speech. Anat Rec 256, 146-157.
Harker DW. 1972. The structure and innervation of sheep superior rectus and levator palpebrae extraocular eye muscles. II: Muscle spindles. Invest Ophthalmol Vis Sci 11, 970-979.
Henn V, Hepp K. 1984. Motoneuron activity around the primary position and in extreme positions of gaze. Proc Fifth Int Orthoptic Congress.
Hess A, Pilar G. 1963. Slow fibres in the extraocular muscles of the cat. J Physiol 169, 780-798.
Highstein SM; Reisine H. 1979. Synaptic and functional organization of vestibulo-ocular reflex pathways. Prog Brain Res 50:431-42.
Hobohm C, Härtig W, Brauer K, Brückner G. 1998. Low expression of extracellular matrix components in rat brain stem regions containing modulatory aminergic neurons. J. Chem Neuroanat 15, 135-142.
Hockfield S, Kalb RG, Zaremba S, Fryer H. 1990. Expression of neural proteoglycans correlates with the acquisition of mature neuronal properties in the mammalian brain. Cold Spring Harbor Symp Quant Biol 55, 505-514.
Hoppeler H, Fluck M. 2002. Normal mammalian skeletal muscle and its phenotypic plasticity. J Exp Biol 205, 2143-2152.
Horn AKE, Büttner-Ennever JA. 1998. Premotor neurons for vertical eye-movements in the rostral mesencephalon of monkey and man: the histological identification by parvalbumin immunostaining. J Comp Neurol 392:413-427.
Horn AKE, Brückner G., Härtig W, Messoudi A. 2003. Saccadic omnipause and burst neurons in monkey and human are ensheathed by perineuronal nets but differ in their expression of calcium-binding proteins. J Comp Neurol 455, 341-352.
Horn AKE, Eberhorn A, Härtig W, Ardelenanu P, Messoudi A, Büttner-Ennever JA. 2008. Perioculomotor cell groups in monkey and man defined by their histochemical and functional properties: reappraisal of the Edinger-Westphal nucleus. J Comp Neurol 507(3):1317-1335.
Horn AKE, Schulze C, Radtke-Schuller S. 2009. The Edinger-Westphal nucleus represents different functional cell groups in different species. Ann N Y Acad Sci 1164:45-50.
Horn AKE, Leigh RJ. 2011. The anatomy and physiology of the ocular motor system. Handb Clin Neurol 102, 21-69.
Horn AKE, Bohlen, MO, Warren S, May PJ. 2012. Evidence for the central mesencephalic reticular formation playing a role in the near triad. Soc Neurosci Abstr 38:371.02.
Huber GC. 1900. Sensory nerve terminations in the tendons of the extrinsic eye-muscles of the cat. J Comp Neurol 10, 152-158.
Isomura G. 1981. Comparative anatomy of the extrinsic ocular muscles in vertebrates. Anat Anz 150, 498-515.

Jacoby J, Chiarandini DJ, Stefani E. 1989. Electrical properties and innervation of fibers in the orbital layer of rat extraocular muscles. J Neurophysiol 61, 116-125.

Jacoby J, Ko K, Weiss C, Rushbrook JI. 1990. Systematic variation in myosin expression along extraocular muscle fibres of the adult rat. J Muscle Res Cell Motil 11, 25-40.

Kaminski HJ, Kusner LL, Block CH. 1996. Expression of acetylcholine receptor isoforms at extraocular muscle endplates. Invest Ophthalmol Vis Sci 37, 345-351.

Kato T. 1938. Über histologische Untersuchungen der Augenmuskeln von Menschen und Säugetieren. Okajimas Folia Anat Jap 16, 131-145.

Kjiellgren D, Thornell LE, Andersen J, Pedrosa-Dömellöf F. 2003. Myosin heavy chain isoforms in human extraocular muscles. Invest Ophthalmol Vis Sci 44:1419-1425.

Kozicz T, Yanaihara H, Arimura A. 1998. Distribution of urocortin-like immunoreactivity in the central nervous system of the rat. J Comp Neurol 391:1-10.

Kozicz T, Bittencourt JC, May PJ, Reiner A, Gamlin PDR, Palkovits M, Horn AKE, Toledo CAB, Ryabinin AE. 2011. The Edinger-Westphal nucleus: A historical, structural, and functional perspective on a dichotomous terminology. J Comp Neurol 519(8):1413-1434.

Kübler TC, Kasneci E, Rosensteil W, Schiefer U, Nagel K, Papgeorgiou E. 2014. Stress- indicators and exploratory gaze forthe analysis of hazard perception in patients with visual field loss. Transport Res (F) 24:231-243.

Leigh RJ, Zee DS. 2006. The Neurology of Eye Movements. New York: Oxford University Press.

Lennerstrand G. 1974. Electrical activity and isometric tension in motor units of the cat's inferior oblique muscle. Acta Physiol Scand 91, 458-474.

Li T, Feng CY, von Bartheld CS. 2011. How to make rapid eye movements "rapid": the role of growth factors for muscle contractile properties. Pflugers Arch 461(3):373-86.

Lienbacher K, Mustari M, Ying HS, Büttner-Ennever JA, Horn AKE. 2011. Do Palisade Endings in Extraocular Muscles Arise from Neurons in the Motor Nuclei? Invest Ophthalmol Vis Sci 52(5):2510-2519.

Lienbacher K, Horn AKE. 2012. Palisade endings and proprioception in extraocular muscles: a comparison with skeletal muscles. Biol Cybern 106, 643-655.

Lisberger SG, Miles FA, Optican LM, Eighmy BB. 1981. Optokinetic response in monkey: underlying mechanisms and their sensitivity to long-term adaptive changes in vestibuloocular reflex. J Neurophysiol 45, 869-890.

Lynch GS, Frueh BR, Williams DA. 1994. Contractile properties of single skinned fibres from the extraocular muscles, the levator and superior rectus, of the rabbit. J Physiol 475, 337-346.

MacLennan C, Beeson D, Buijs A-M, Vincent A, Newsom-Davis J. 1997. Acetylcholine receptor expression in human extraocular muscles and their susceptibility to myasthenia gravis. Ann Neurol 41, 423-431.

Mascarello F, Carpenè E, Veggetti A, Rowlerson A, Jenny E. 1982. The tensor tympani muscle of cat and dog contains IIM and slow-tonic fibres: an unusual combination of fibre types. J Muscle Res Cell Motil 3, 363-374.

May PJ, Reiner AJ, Ryabinin AE. 2008. Comparison of the distributions of Urocortin-containing and cholinergic neurons in the perioculomotor midbrain of the cat and Macaque. J Comp Neurol 507, 1300-1316.

May PJ, Horn AKE, Mustari MJ, Warren S. 2011. Central mesencephalic reticular formation projections onto oculomotor motoneurons. Soc Neurosci Abstr 699.01/PP22.
May PJ, Warren S, Bohlen MO. 2015. A central mesencephalic reticular formation projection to the Edinger-Westphal nuclei. Brain Struct Funct, 1-17.
Mayr R, Gottschall J, Gruber H, Neuhuber W. 1975. Internal structure of cat extraocular muscle. Anat Embryol 148, 25-34.
Mayr R. 1977. Funktionelle Morphologie der Augenmuskeln. In: Kommerell G. (Ed.). Augenbewegungsstörungen: Neurologie und Klinik 1-15, J.F. Bergmann Verlag, Munich.
Mays LE. 1984. Neural control of vergence eye movements: convergence and divergence neurons in midbrain. J Neurophysiol 51:1091-1108.
McCrea RA, Strassman A, Highstein SM. 1986. Morphology and physiology of abducens motoneurons and internuclear neurons intracellulary injected with horseradish peroxidase in alert squirrel monkey. J Comp Neurol 243, 291-308.
McLoon LK, Rios L, Wirtschafter JD. 1999. Complex three-dimensional patterns of myosin isoform expression: differences between and within specific extraocular muscles. J Muscle Res Cell Motil 20, 771-783.
Miller NR. 1998. Embryology of the visual sensory pathway. In: Miller NR, Newman NJ (Eds.), Williams & Wilkins 1st Edition, Vol 5(1); 3-23.
Missias JR, Chu GC, Klocke BJ, Sanes JR, Merlie JP. 1996. Maturation of the acetylcholine receptor in skeletal muscle: regulation of the AChR gamma-to-epsilon switch. Dev Biol 179, 223-238.
Miyazaki S. 1985a. Bilateral innervation of the superior oblique muscle by the trochlear nucleus. Brain Res 348:52-56.
Miyazaki S. 1985b. Location of motoneurons in the oculomotor nucleus and the course of their axons in the oculomotor nerve. Brain Res 348, 57-63.
Morgan DL, Proske U. 1984. Vertebrate slow muscle: its structure, pattern of innervation, and mechanical properties. Physiol Rev 64, 103-138.
Morris NP, Henderson Z. 2000. Perineuronal nets ensheath fast spiking, parvalbumin-immunoreactive neurons in the medial septum/diagonal band complex. Eur J Neurosci 12, 828-838.
Moschovakis AK, Scudder CA, Highstein SM. 1991a. The structure of the primate oculomotor burst generator. I. Medium-lead burst neurons with upward on-directions. J Neurophysiol 65:203-217.
Moschovakis AK, Scudder CA, Highstein SM, Warren JD. 1991b. The structure of the primate oculomotor burst generator. II. Medium-lead burst neurons with downward on-directions. J Neurophysiol 65:218-229.
Murphy EH, Garone M, Tashayyod D, Baker RB. 1986. Innervation of extraocular muscles in the rabbit. J Comp Neurol 254, 78-90.
Myers GA, Stark L. 1990. Topology of near respose triad. Ophthalmic Physiol Opt 10:175-181.
Namba T, Nakamura T, Takahashi A, Grob D. 1968. Motor nerve endings in extraocular muscles. J Comp Neurol 134, 385-396.
Nelson JS, Goldberg SJ, Mcclung JR. 1986. Motoneuron electrophysiological and muscle contractile properties of superior oblique motor units in cat. J Neurophysiol 55, 715-726.
Nguyen LT, Spencer RF 1999. Abducens internuclear and ascending tract of Deiters inputs to medial rectus motoneurons in the cat oculomotor nucleus: neurotransmitters. J Comp Neurol 411, 73-86.

Oda K. 1993. Differences in acetylcholine receptor-antibody interactions between extraocular and extremity muscle fibers. Ann N Y Acad Sci 21681, 238-255.
Okamoto M, Mori S, Endo H. 1994. A protective action of chondroitin sulfate proteoglycans against neuronal cell death induced by glutamate. Brain Res 637, 257-267.
Partsalis AM, Highstein SM, Moschovakis AK. 1994. Lesions of the posterior commissure disable the vertical neural integrator of the primate oculomotor system. J Neurophysiol 71:2582-2585.
Peng M, Poukens V, da Silva Costa R.M, Yoo L, Tychsen L, Demer JL. 2010. Compartmentalized innervation of primate lateral rectus muscle. Invest Ophthalmol Vis Sci 51(9):4612-7.
Pickard GE, Smeraski CA, Tomlinson CC, Banfield BW, Kaufman J, Wilcox CL, Enquist LW, Sollars PJ. 2002. Intravitreal injection of the attenuated pseudorabies virus PRV Bartha results in infection of the hamster suprachiasmatic nucleus only by retrograde transsynaptic transport via autonomic circuits. J Neurosci 22, 2701-2710.
Pierrot-Deseilligny C, Chain F, Gray F, Serdaru M, Escourolle R, Lhermitte F. 1982. Parinaud's syndrome: electro-oculographic and anatomical analyses of six vascular cases with deductions about vertical gaze organization in the premotor structures. Brain 105:667-696.
Pilar G, Hess A. 1966. Differences in internal structure and nerve terminals of the slow and twitch muscle fibres in the cat superior oblique. Anat Rec 154, 243-252.
Pilar G. 1967. Further study of the electrical and mechanical responses of slow fibers in cat extraocular muscles. J Gen Physiol 50, 2289-2300.
Porter JD, Guthrie BL, Sparks DL. 1983. Innervation of monkey extraocular muscles: localization of sensory and motor neurons by retrograde transport of horseradish peroxidase. J Comp Neurol 218, 208-219.
Porter JD, Guthrie BL, Sparks DL. 1985. Selective retrograde transneuronal transport of wheat germ agglutinin-conjugated horseradish peroxidase in the oculomotor system. Exp Brain Res 57, 411-416.
Porter JD, Baker RS, Ragusa RJ, Brueckner JK. 1995. Extraocular muscles: basic and clinical aspects of structure and function. Surv Ophthal 39, 451-484.
Reisine H, Highstein SM. 1979. The ascending tract of Deiters' conveys a head velocity signal to medial rectus motoneurons. Brain Res 170, 172-176.
Richmond FJR, Johnston WSW, Baker RS, Steinbach MJ. 1984. Palisade endings in human extraocular muscle. Invest Ophthal Vis Sci 25, 471-476.
Robinson DA. 1981. Control of eye movements. In: Brooks V. (Ed.). Ha ndbook of Physiology, pp1275-1320, William & Wilkins.
Rubinstein NA, Hoh JF. 2000. The distribution of myosin heavy chain isoforms among rat extraocular muscle fiber types. Invest Ophthal Vis Sci 41, 3391-3398.
Ruff R, Kaminski H, Maas E, Spiegel P. 1989. Ocular muscles: physiology and structure-function correlations. Bull Soc Belge Ophtalmol 237, 321-352.
Ruskell GL. 1978. The fine structure of innervated myotendinous cylinders in extraocular muscles in rhesus monkey. J Neurocytol 7, 693-708.
Ruskell GL. 1999. Extraocular muscle proprioceptors and proprioception. Prog Retin Eye Res 18, 269-291.
Ryabinin AE, Tsivkovskaia NO, Ryabinin SA. 2005. Urocortin 1-containing neurons in the human Edinger-Westphal nucleus. Neuroscience 134, 1317-1323.

Sakurai T. 2007. The neural circuit of orexin (hypocretin): maintaining sleep and wakefulness. Nat Rev Neurosci 8, 171-181.
Schnyder H. 1984. The innervation of the monkey accessory lateral rectus muscle. Brain Res 296:139-144.
Schreyer S, Büttner-Ennever JA, Tang X, Mustari MJ, Horn AKE. 2009. Orexin-A inputs onto visuomotor cell groups in the monkey brainstem. Neuroscience 164(2): 629–640.
Schwaller B. 2014. Calretinin: from a “simple” Ca2+ buffer to a multifunctional protein implicated in many biological processes. Front Neuroanat 8:3. DOI 10.3389/fnana.2014.00003.
Sevel D. 1986. The origins and insertions of the extraocular muscles: development, histologicfeatures, and clinical significance. Trans Am Ophthalmol Soc 24, 488-526.
Siebeck R, Kruger P. 1955. The histological structure of the extrinsic ocular muscles as an indication of their function. Albrecht Von Graefes Arch Ophthalmol 156, 636-652.
Simons B, Büttner U. 1985. The influence of age on optokinetic nystagmus. Eur Arch Psychiatry Neurol Sci 234, 369-373.
Spencer RF, Baker R, Mccrea RA. 1980. Localization and morphology of cat retractor bulbi motoneurons. J Neurophysiol 43, 754-770.
Spencer RF, Porter JD. 1981. Innervation and structure of extraocular muscles in the monkey in comparison to those of the cat. J Comp Neurol 198(4):649-65.
Spencer RF, Porter JD. 1988. Structural organization of the extraocular muscles. In: Büttner-Ennever JA. (Ed.), Rev Oculomot Res 33-79, Amsterdam; New York; Oxford: Elsevier.
Spencer RF, Wenthold RJ, Baker R. 1989. Evidence for glycine as an inhibitory neurotransmitter of vestibular, reticular, and prepositus hypoglossi neurons that project to the cat abducens nucleus. J Neurosci 9, 2718-2736.
Spencer RF, Baker R. 1992. GABA and glycine as inhibitory neurotransmitters in the vestibulo-ocular reflex. Ann N Y Acad Sci 656, 602-611.
Spencer RF, Wang SF. 1996. Immunohistochemical localization of neurotransmitters utilized by neurons in the rostral interstitial nucleus of the medial longitudinal fasciculus (riMLF) that project to the oculomotor and trochlear nuclei in the cat. J Comp Neurol 366, 134-148.
Spencer RF, Porter JD. 2006. Biological organization of the extraocular muscles. Prog Brain Res 151, 43-80.
Straka H, Dieringer N. 1991. Internuclear neurons in the ocular motor system of frogs. J Comp Neurol 312, 537-548.
Straka H, Dieringer N. 2004. Basic organization of the VOR: lessons from frog. Prog Neurobiol 73:259-309.
Strupp M, Kremmyda O, Adamczyk C, Böttcher N, Muth C, Yip CW, Bremova T. 2014. Central ocular motor disorders, including gaze palsy and nystagmus. J Neurol 261:542-58.
Sun W, May PJ. 1993. Organization of the extraocular and preganglionic motoneurons supplying the orbit in the lessor galago. Anat Rec 237, 89-103.
Tang X, Büttner-Ennever JA, Mustari MJ, Horn AKE. 2015. Internal Organization of Medial Rectus and Inferior Rectus Muscle Neurons in the C-Group of the Oculomotor Nucleus in Monkey. J Comp Neurol 523(12):1809-23.
Torres-Torrelo J, Rodríguez-Rosell D, Nunez-Abades P, Carrascal L, Torres B. 2012. Glutamate modulates the firing rate in oculomotor nucleus motoneurons as a function of the recruitment threshold current. J Physiol. 590:3113-27.

Tsang YM, Chiong F, Kuznetsov D, Kasarskis E, Geula C. 2000. Motor neurons are rich in non-phosphorylated neurofilaments: cross-species comparison and alterations in ALS. Brain Res 861, 45-58.

Ugolini G, Büttner-Ennever JA, Doldan M, al. e. 2001. Horizontal eye movement networks in primates: differences in monosynaptic input to slow and fast abducens motoneurons. Soc Neurosci Abstr 27:403-413.

Ugolini G, Klam F, Doldan Dans M, Dubayle D, Brandi A-M, Büttner-Ennever JA, Graf W. 2006. Horizontal eye movement networks in primates as revealed by retrograde transneuronal transfer of rabies virus: Differences in monosynaptic input to "slow" and "fast" abducens motoneurons. J Comp Neurol 498, 762-785.

Vann VR, Atherton SS. 1991. Neural spread of herpes simplex virus after anterior chamber inoculation. Invest Ophthal Vis Sci 32, 2462-2472.

Vasconcelos LAP, Donaldson C, Sita LV, Casatti CA, Lotfi CFP, Wang L, Cadinouche MZA, Frigo L, Elias CF, Lovejoy DA, Bittencourt JC. 2003. Urocortin in the central nervous system of a primate (*Cebus apella*): sequencing, immunohistochemical, and hybridization histochemical characterization. J Comp Neurol 463:157-175.

Vaughan J, Donaldson C, Bittencourt JC, Perrin MH, Lewis K, Sutton S, Chan R, Turnbull A, Lovejoy D, Rivier C, Rivier J, Sawchenko PE, Vale W. 1995. Urocortin, a mammalian neuropeptide related to fish urotensin I and to corticotropin-releasing factor. Nature 378, 287-292.

Veggetti A, Mascarello F, Carpene E. 1982. A comparative histochemical study of fibre types in middle ear muscles. J Anat 135, 333-352.

Vilis T, Hepp K, Schwarz U, Henn V. 1989. On the generation of vertical and torsional rapid eye movements in the monkey. Exp Brain Res 77:1-11.
Vis Sci 51(9):4612-7.

Waitzman DM, Silakov VL, Cohen B. 1996. Central mesencephalic reticular formation (cMRF) neurons discharging before and during eye movements. J Neurophysiol 75:1546-1572.

Wang N, Warren S, May P. 2010. The macaque midbrain reticular formation sends side-specific feedback to the superior colliculus. Exp Brain Res 201(4):701-717.

Warwick R. 1953. Representation of the extraocular muscles in the oculomotor nuclei of the monkey. J Comp Neurol 98(3):449-503.

Wasicky R, Zhya-Ghazvini F, Blumer R, Lukas JR, Mayr R. 2000. Muscle fiber types of human extraocular muscles: a histochemical and immunohistochamical study. Invest Ophthal Vis Sci 41:980-990.

Wasicky R, Horn AKE, Büttner-Ennever JA. 2004. Twitch and non-twitch motoneuron subgroups of the medial rectus muscle in the oculomotor nucleus of monkeys receive different afferent projections. J Comp Neurol 479:117-129.

Wentzel PR, Dezeeuw CI, Holstege JC, Gerrits NM. 1993. Colocalization of GABA and Glycine in the rabbit oculomotor nucleus. Neurosci Lett 164:25-29.

Wentzel PR, Gerrits NM, Dezeeuw CI. 1996. GABAergic and glycinergic inputs to the rabbit oculomotor nucleus with special emphasis on the medial rectus subdivision. Brain Res 707:314-319.

Weston MC, Nehring RB, Wojcik SM, Rosenmund C. 2011.Interplay between VGLUT isoforms and endophilin A1 regulates neurotransmitter release and short-term plasticity. Neuron 69(6):1147-59.

Westphal C. 1887. Über einen Fall von chronischer progressiver Lähmung der Augenmuskeln (Ophtalmopregia externa) nebst Beschreibung von

Ganglienzellen im Bereiche des Okulomotoriuskerns. Arch Psychat Nervenheilk 98, 846-871.

Wieczorek DF, Periasamy M, Butler-Browne GS, Whalen RG, Nadal-Ginard B. 1985. Co-expression of multiple myosin heavy chain genes, in addition to a tissue-specific one, in extraocular musculature. J Cell Biol 101(2):618-29.

Yamamoto H, Maeda T, Fujimura M, Fujimiya M. 1998.Urocortin-like immunoreactivity in the substantia nigra, ventral tegmental area and Edinger-Westphal nucleus of rat. Neurosci Lett 243:21-24.

Ying HS, Fackelmann K, Messoudi A, Tang XF, Büttner-Ennever JA, Horn AK. 2008. Neuronal signalling expression profiles of motoneurons supplying multiply or singly innervated extraocular muscle fibres in monkey. Prog Brain Res 171:13-16.

Zeeh C, Hess BJ, Horn AKE. 2013. Calretinin inputs are confined to motoneurons for upward eye movements in monkey. J Comp Neurol 521:3154-3166.

Zeeh C, Mustari MJ, Hess BJ, Horn AKE. 2015. Transmitter inputs to different motoneuron subgroups in the oculomotor and trochlear nucleus in monkey. Front. Neuroanat. DOI 10.3389/fnana.2015.00095.

Zhang Y, Gamlin PDR, Mays LE. 1991. Antidromic identification of midbrain near response cells projecting to the oculomotor nucleus. Exp Brain Res 84:525-528.

Zhang Y, Mays LE, Gamlin PDR. 1992. Characteristics of Near Response Cells Projecting to the Oculomotor Nucleus. J Neurophysiol 67:944-960.

Zhou L, Warren S, May PJ. 2008. The feedback circuit connecting the central mesencephalic reticular formation and the superior colliculus in the macaque monkey: tectal connections. Exp Brain Res 189:485-496.

Zimmermann L, May PJ, Pastor AM, Streicher J, Blumer R. 2011. Evidence that the extraocular motor nuclei innervate monkey palisade endings. Neurosci Lett 489(2):89-93.